The epithelial cell adhesion molecule (EpCAM) regulates cell motility and cell-cell adhesion by inhibiting PKC signaling

Nadim Maghzal

Department of Biology

McGill University, Montreal

September 2012

A thesis submitted to McGill University in partial fulfillment of the requirements of the degree of Doctor of Philosophy.

Learn the changes, then forget them – Charlie Parker

Table of Contents

Abstract

Tissue cohesion is achieved in part by a large family of plasma membrane-bound cell adhesion molecules (CAMs). During morphogenesis, CAM-mediated interactions provide adhesive forces required for cells to aggregate and form tissues. CAM-mediated adhesions in developing cells are highly dynamic, which provides the fluidity required for cellular movements that drive morphogenesis. *Xenopus laevis* gastrulation is an established model to study morphogenetic movements. During this phase of development, the mesoderm moves inside the embryo through involution, and migrates along the inner surface of the ectoderm while remaining separated from this tissue. Members of the Fagotto lab have identified the *Xenopus* orthologue of the Epithelial Cell Adhesion Molecule (EpCAM) in a gain-of-function screen to find gene products that cause aberrant ectoderm/mesoderm tissue mixing in the gastrula. EpCAM is a well known tumor-associated antigen that is specifically expressed in epithelial tissues, where its overexpression often correlates with malignancy. The initial aim of this thesis was to understand the molecular mechanism through which EpCAM promotes ectoderm/mesoderm tissue mixing. Overexpression of EpCAM in cells at the boundary increases their "invasive" behavior via a signaling property of its cytoplasmic domain (EpTAIL) that inhibits PKC signaling to promote cell motility. The most important findings of this thesis are that 1) EpTAIL inhibits PKC activity to promote cell motility and cell-cell adhesion by acting as a PKC pseudosubstrate domain that binds the enzyme on its catalytic site, and 2) this previously unknown mode of PKC inhibition is not specific to EpCAM as other PKC pseudosubstrate-mimicking plasma membrane proteins were identified and could potentially play important roles in the regulation of PKC activity. The data presented in this thesis further our understanding of EpCAM biology and unravel a new mode of PKC regulation that is valuable as PKCs are one of the major families of cytoplasmic kinases in cells.

Résumé

Les mécanismes de liaison cellulaire sont établis en partie par une vaste famille de protéines d'adhésion cellulaire ou CAMs. Lors de la morphogenèse, les interactions induites par les CAMs créent des forces d'adhésion nécessaires afin que les cellules

puissent s'agréger et former des tissues. Les adhésions induites par les CAMs dans les cellules en développement sont très dynamiques et offrent ainsi la fluidité nécessaire aux mouvements cellulaires qui régissent la morphogenèse. La gastrulation chez la grenouille *Xenopus laevis* sert de modèle d'étude des mouvements morphogéniques. Durant ce stade de développement, le mésoderme se déplace vers l'intérieur de l'embryon via un mouvement d'involution et migre le long de la paroi interne de l'ectoderme tout en maintenant une séparation des deux tissues. Des membres du laboratoire de Dr. Fagotto ont réussi à identifier un orthologue de la protéine «Epithelial Cell Adhesion Molecule (EpCAM) » chez *Xenopus* dans un tri de gain de fonction permettent d'identifier des protéines pouvant être à l'origine d'aberrations au niveau du maintien de la séparation de l'ectoderme et du mésoderme durant la gastrulation. EpCAM est un antigène associé aux tumeurs exprimé dans les cellules épithéliales et dont la surexpression corrèle avec des tumeurs malignes. L'objectif initial de cette thèse était de découvrir les mécanismes moléculaires pouvant expliquer l'effet de EpCAM sur les aberrations entre la séparation des tissues de l'ectoderme et du mésoderme. Une surexpression de EpCAM dans les cellules à la bordure de l'ectoderme et du mésoderme cause une augmentation du comportement « invasif » entre les deux tissues, via la fonction de transduction du signal de son domaine cytoplasmique (EpTAIL), qui inhibe le signal de la protéine PKC afin de promouvoir le mouvement cellulaire. Les principales contributions de cette thèse ont été 1) EpTAIL inhibe l'activité de PKC en jouant le rôle d'un pseudosubstrat de PKC en interagissant avec le site catalytique de l'enzyme, et 2) ce mécanisme d'inhibition jusqu'à présent inconnu pour PKC n'est pas seulement spécifique à EpCAM, car d'autres protéines membranaires possède également cette capacité à imiter le pseudosubstrat de PKC et pourraient potentiellement avoir un rôle important à jouer au niveau de la régulation de l'activité de PKC. Les donnée présentées dans cette thèse contribuent à approfondir davantage notre connaissance d'EpCAM et dévoilent un nouveau mécanisme de régulation de PKC qui pourrait être important puisque les molécules PKC forment l'une des plus importantes familles de kinases cytoplasmiques dans les cellules.

Acknowledgements

I would like to express my great gratitude to my thesis supervisor François Fagotto for being an inspiring mentor who has been generous with his time, ideas and most importantly understanding. Francois's contribution went way beyond this thesis and into my personal development, and I will miss our passionate discussions and debates. I would especially like to thank my girlfriend Zoé Joly-Lopez for her love, continuous support and for direct help with critical reading of my thesis (and also for the great food and drinks that fueled my studies). I would also like to deeply thank my dear friend, band mate, roommate and brother Philippe Manasseh for his support through life and for endless inspiring discussions. Thanks to my lab mates Nazanin Rohani, Laura Canty, Emily Vogt, Hulya Kayali, Anne-Sophie Touret and past/present members for directly helping with experiments and for their critical feedback, with a special thanks to Xiaoyong Liu for guiding me through several biochemical techniques and cell line cultures. Thanks also to my supervisory committee, Laura Nilson and Frieder Schöck for their attention, guidance and suggestions. I'm also very grateful for the support that my dearest friends have given me as I have walked this path, with a special nod to Derek Koziol, Lory Ajamian and Yasmine Abboud. Most of all, I want to thank my parents Jean and Samia Maghzal, my sister Lena (and her family) and brother Tony, without whom this Ph.D. would have never happened. My funding was provided in part by Hydro Québec and the McGill cancer center (Canderel studentship).

Contributions

Chapter I is a comprehensive review of the literature pertinent to my area of research. I researched and wrote this chapter with guidance from my thesis supervisor, Prof. François Fagotto.

Chapter II was published in The Journal of Cell Biology: **Maghzal N**, Vogt E, Reintsch W, Fraser JS, Fagotto F. 2010. The tumor-associated EpCAM regulates morphogenetic movements through intracellular signaling. The Journal of cell biology *191(3)*: 645-59. Co-first authorship is shared with E. Vogt who conducted the roof assays and helped with embryo manipulations. More specifically, E. Vogt conducted the experiments that led to Figure 1D-F; Figure 2; Figure 6; Figure 8K, L and Figure S2. W. Reintsch and F. Fagotto identified EpCAM in the gain-of-function screen that led to the discovery of EpCAM as an inducer of tissue mixing. JS. Fraser was involved in preliminary analyses. F. Fagotto contributed to experimental design, data acquisition and analysis (Figure S1 and Figure S4), and writing. I designed, conducted and analyzed the sandwich assay, acquired and analyzed all immunofluorescence images, conducted and analyzed all western blots, and contributed to writing. More specifically, I contributed to Figure 1B-C, Figure 3, Figure 4, Figure 5, Figure 7, Figure 8A-J, Figure S1 and Figure S3.

Chapter III was recently submitted to Cell for publication: **Maghzal N**, Kayali HA, Kajava AV, Fagotto F. 2012. The tumor associated EpCAM controls Erk signaling, actomyosin contractility, and cell-cell adhesion by directly inhibiting PKC. Submitted to Cell on September 19th 2012. HA. Kayali produced several recombinant proteins used for pulldowns, conducted *in vitro* pulldowns, conducted the SPR affinity experiments and helped with one LEI assay. More specifically, HA. Kayali contributed to Figure 4B, E; Figure 7 and Figure S9. AV. Kajava modelled the PKC-EpCAM interaction and generated the list of plasma membrane candidate proteins with a PKC PS motif. More specifically, AV. Kajava contributed to Figure 7A-B; Figure S8 and Figure S10. F. Fagotto contributed to the experimental design, construction of all plasmids used for recombinant protein production, data acquisition and analysis (Figure S5), analysis/characterization of PS motif on EpCAM, and writing. I designed, conducted and analyzed the large majority of

experiments on this paper with guidance from F. Fagotto, and I contributed to writing. More specifically, I conducted all the experiments that led to the results presented in Figure 1; Figure 2; Figure 3; Figure 4; Figure 5; Figure 6; Figure S1; Figure S2; Figure S3; Figure S4; Figure S6 and Figure S7.

Chapter IV is not intended as a manuscript for publication. It is an addendum to Chapter II in which I investigate other morphogenetic phenotypes resulting from EpCAM manipulations in *Xenopus laevis* development. I designed, conducted and analyzed all experiments and was solely responsible for writing with guidance from F. Fagotto.

CHAPTER I

Literature review and thesis objectives

Introduction

In order to maintain the proper organization of multicellular animals, cells need to be able to adhere, to move relative to each other, to repel and signal to each other. Individual cells fulfill these tasks by communicating across their plasma membranes. These tasks are especially crucial in morphogenesis, where highly dynamic developmental cells adhere to each other, migrate, receive and send cues in an orderly fashion to form a patterned tissue. Such interactions across the plasma membrane are equally important in differentiated adult tissues. For example, in a wounded epithelium, cells must coordinate migration to heal the wound with maintenance of adhesion to their neighbors, as well as absorption and secretion of nutrients. Rapid interactions also occur across the plasma membranes of metastatic cancer cells that detach from a primary tumor, migrate on unfamiliar extracellular substrates and reattach after metastasis.

Cell adhesion, detachment and migration are mediated by a large family of cell adhesion molecules (CAMs), which are plasma membrane receptors capable of promoting cell-cell and cell-matrix adhesion by binding to each other on opposing membranes and/or to extracellular matrix (ECM) substrates. CAM interactions with extracellular components can also provide the cell with important information about its extracellular environment by transducing cytoplasmic signals. Some CAMs simultaneously act as adhesive molecules and sensors while others have evolutionarily co-opted to function predominantly as adhesive factors or signal transducing sensors. The work presented in this thesis explores these concepts in the context of the Epithelial Cell Adhesion Molecule (EpCAM), a long known tumor-associated antigen highly expressed in carcinomas.

Cell Adhesion Molecules

The functions of CAMs are essential and tightly regulated throughout all stages of development and during adulthood. Mutations in CAMs can have dire consequences

ranging from developmental defects and organ malformation to embryonic death (Larue et al., 1994).

To date, a very large number of cell surface proteins have been reported to play important roles in adhesion. "CAMs" are classically defined as cell surface receptors whose interaction with ligand(s) causes a cell to either attach to another cell or to the ECM. For adhesion to occur, the extracellular domain (ECD) of a CAM on one cell must interact with the ECD of another CAM on the other cell, or with an ECM component. ECD-mediated adhesions are regulated by diverse interactions with cytoplasmic factors via CAMs' intracellular domains (ICDs) that affect the longevity and strength of adhesion. Generally, cell adhesion molecules fall into four to six major families based on structural and functional similarities: 1) Cadherins are Ca^{2+}-dependent cell-cell adhesion molecules, 2) The immunoglobulin (Ig) Superfamily members are usually cell-cell adhesion molecules and occasionally bind ECM components as well, 3) Integrins are α/β heterodimers that mediate mostly cell-matrix adhesion by binding ECM components, but are also capable of interacting with Ig Superfamily members, and 4) Selectins are Ca^{2+}-dependent adhesion molecules that bind to carbohydrate-containing ligands (Fig. 1.1A) (Buckley et al., 1998). CAMs are further classified based on how they interact with each other via their ECD. In general, there are two modes of interactions: homophilic (binding to self) and heterophilic (binding to non-self ligands).

Diverse extracellular domain interactions

The structure of a CAM's extracellular domain dictates the types of interactions it is capable of having. The ECDs of CAMs are structurally complex; they are often composed of several domains and repeats, which can promote interactions with various extracellular ligands and render the CAM functionally versatile. For example, the neural cell adhesion molecule (NCAM) is capable of interacting with itself via its Ig-domains and with extracellular matrix (ECM) and other cell surface components via its Fibronectin III (FNIII) repeats (Kiselyov et al., 2005). In this case, the Ig-domains promote homophilic cell-cell interactions whereas the FNIII repeats promote heterophilic cell-ECM interactions. Post-translational modifications of a

CAM's ECD can make the CAM multi-functional by promoting interactions with different extracellular partners. For example, variations in glycosylation of CD44's extracellular domain are thought to dictate which ligands the protein preferentially interacts with (Naor et al., 1997). Another mechanism generating variability in extracellular interactions is the alternative dimerization of receptors. Integrins are α/β heterodimers that function as major receptors for cell adhesion to ECM proteins. 18 α subunits can dimerize with 8 β subunits to form 24 distinct integrins with different ligand specificities, e.g. α1β1, α2β1 and α10β1 act as collagen receptors while α3β1, α6β1 and α7β1 are laminin receptors (Hynes, 2002). Thus, the structural complexity, post-translational modifications and alternative dimerizations of ECDs make CAMs capable of diverse extracellular interactions, which increase their versatility and adaptability to various extracellular environments. Through diverse interactions with extracellular components, CAMs' ECDs act in some cases as extracellular sensors capable of triggering cytoplasmic signals through their intracellular domains. Integrins for instance are well known for their ability to form essential adhesion and "sensing" interactions via their ECD (Fig. 1.1B). The interaction of integrins with extracellular ligands leads to changes in cell differentiation, proliferation, migration and gene expression (Keely et al., 1998; Schlaepfer and Hunter, 1998; Schwartz et al., 1995). This process is referred to as "outside-in" signaling whereby signals sensed by the ECD of integrins are transduced to the cell through cytoplasmic signaling factors, such as PKC, Rho, Rac, Ras and PI3-Kinase. Similarly, it has been shown that classical cadherins function as ligand-activated signaling receptors in addition to their indirect role as modulators of Wnt/β-catenin signaling (Yap and Kovacs, 2003). Binding of cadherin activates Rac signaling via PI3K, and this alters the surface-protrusive activity of the actin cytoskeleton and stabilizes nascent contacts (Kovacs et al., 2002). It is well established that NCAM, LCAM and N-cadherin homophilic/heterophilic extracellular interactions activate various cytoplasmic signaling cascades (Hay et al., 2009; Marambaud et al., 2003; Riedle et al., 2009). The molecular pathways through which these molecules transduce the signals "sensed" by their ECDs via their intracellular domains are discussed in greater detail in the section below (See "Signaling through ICD").

Intracellular cytoskeletal anchorage

For many CAMs, linkage to the cytoskeleton is required for the establishment and maintenance of significant adhesion bonds. ICD-mediated linkage is thought to strengthen adhesion by anchoring the CAM on the plasma membrane, which makes it capable of withstanding pulling forces exerted by the opposing cell. The ICD of a CAM can interact with the cytoskeleton directly, in some cases via cytoskeletal-bound proteins, but also indirectly, where the reorganization of the cytoskeletal is required to mediate CAM adhesion. The ICD of the Carcinoembryonic Antigen cell adhesion molecule (CEA) can directly bind actin (Schumann et al., 2001). On the other hand, integrins and cadherins interact with actin directly via actin-bound proteins. The cytoplasmic domain of integrin β can interact with actin by binding either talin or α-actinin (Takahashi, 2001). Classical cadherins are thought to interact directly with the actin cytoskeleton via cytoplasmic proteins β- and α-catenins (Yap et al., 1998). Two desmosomal cadherins, desmocollin and desmoglein, on the other hand, interact with intermediate filaments (keratin). Cadherin ICDs in desmosomes bind plakophillin and plakoglobin, which recruit IF-bound desmoplakin (Garrod et al., 2002). In the case of desmosomes, linkage to keratin is proven essential as mutations which disrupt the desmosome-keratin complex lead to deficient desmosomal adhesion and result in severe diseases such as Arrhythmogenic right ventricular cardiomyopathy and skin blistering (Mahoney et al., 2010; McKoy et al., 2000) .

While linkage to the cytoskeleton may be important for CAM-mediated adhesion, the mechanism by which linkage occurs in the dynamic environment of a cell and its exact contribution to adhesion remains debatable even for extensively studied CAMs. In the case of classical cadherins, it is long known that α-catenin links the cadherin/β-catenin complex to actin via its ability to bind β-catenin and F-actin, and by doing so, provides a stable mechanical link between the extracellular cadherin bond and the underlying actin network (Gumbiner, 2005; Yap et al., 1997). This direct link between cadherin and actin has recently been challenged by an alternate hypothesis claiming that the cadherin/actin link is indirect. It was proposed that β-catenin inhibits binding of α-catenin to actin and that α-catenin is consequently

incapable of directly binding cadherin/β-catenin and F-actin simultaneously (Abe and Takeichi, 2008; Yamada et al., 2005). Rather, the alternate hypothesis proposed by Nelson's group states that the formation of nascent cadherin contacts at the membrane increases the concentration of β-catenin/cadherin bound to α-catenin at the developing junction. Upon its dissociation from β-catenin, concentrated α-catenin induces a reorganization of F-actin near adhesion sites by inhibiting Arp2/3-stimulated branched actin polymerization and bundling actin into linear cables that promotes stable cell-cell adhesion (Drees et al., 2005). Based on this model, α-catenin does not promote cadherin adhesion directly by linking cadherins to actin, but rather α-catenin's role in stabilizing cadherin contacts occurs via its ability to reorganize F-actin in a way that stabilizes cell-cell contacts when it is unbound to cadherins. It is important to note that the work on which this model is based focuses only on α-E-catenin and may not be true for other α-catenins (α-N and α-T catenin), which could mediate direct actin-cadherin binding. Moreover, most studies have focused on elucidating the E-cadherin/actin link in adherens junctions of epithelial cells. A direct α-catenin link to the cytoskeleton may be crucial for other types of cadherin-mediated adhesions that drive morphogenesis, such as C-cadherin mediated adhesions in developing *Xenopus* embryos which do not form typical epithelial-like adherens junctions. With regards to E-cadherin in adherens junctions, a direct cadherin-actin link may still be required for proper cadherin-mediated adhesion. Lecuit's group identified a pool of actin associated with cadherin clusters but this association is independent of α-catenin (Cavey et al., 2008). The mechanisms by which different cadherins interact with the cytoskeleton via their ICD in different environments (development vs. differentiated epithelium) still need to be elucidated.

Signaling through intracellular domain

Beside its role in linking CAMs to the cytoskeleton, the ICD is capable of other crucial interactions with cytoplasmic proteins that affect the efficiency, longevity and strength of adhesion. ICD- mediated interactions regulating CAM-mediated adhesion are reviewed in the section below (see "regulation by signaling and interactions with cytoplasmic partners"). Through its association with cytoplasmic proteins the ICD of a CAM can also trigger cytoplasmic signals that affect processes other than adhesion.

The binding of integrins to ECM ligands activates multiple signaling cascades similar to those triggered by growth factor receptors (Hynes, 2002). In neural cells, NCAM, LCAM and N-cadherin strongly stimulate neurite outgrowth by signaling (Williams et al., 1994). NCAM homophilic interactions lead to the activation of many cytoplasmic signaling molecules via NCAM's ICD including non-receptor kinases Fyn, the focal adhesion kinase FAK, growth-associated protein-43 and protein kinases A, C and G (Ditlevsen et al., 2008). Upon cleavage of their ICDs, CAMs can interact with proteins in other cellular compartments. For example, the ICD of LCAM translocates to the nucleus upon regulated proteolytic cleavage where it regulates the transcription of oncogenes (Riedle et al., 2009). Similarly, it has been suggested that N-cadherin's ICD, known to interact with β-catenin, LRP5 and axin (Hay et al., 2009), gets cleaved and then regulates gene expression by promoting the degradation of transcriptional co-activator CBP (Marambaud et al., 2003). Alternatively, via their ICD, CAMs can interact with cytoplasmic components that have crucial roles in signaling pathways thus affecting the activities of the signaling pathways where these components function. A good example is the β-catenin/cadherin interaction. Aside from interacting with the cadherin ICD, β-catenin plays a central role in the Wnt pathway signaling. It is possible that by binding β-catenin via their ICDs, cadherins affect Wnt signaling by regulating the amount of "free" β-catenin available for transduction of Wnt signals (Fagotto et al., 1996).

Despite a large number of investigations, the functions of many CAMs remain elusive. In some cases, the relative contribution of ECD and ICD domains to cell adhesion and/or signaling is poorly understood. Grouping adhesion receptors into families based on structural similarities can limit investigative approaches aimed at elucidating their functions at the cell surface. Protocadherins for example, which fall under the major cadherin family, differ structurally and functionally from classical cadherins. Studies have reported that protocadherins undergo from very weak to no homophilic adhesion (Mutoh et al., 2004; Sano et al., 1993). Instead, protocadherins are believed to act as surface signaling receptors that modulate the adhesion activity of classical cadherins. *Xenopus* paraxial protocadherin (PAPC) was shown to mediate cell sorting by down-regulating the adhesion activity of C-Cadherin (Chen and

Gumbiner, 2006). Another study suggested that in *Xenopus* embryos, PAPC interacts and inhibits Sprouty to promote convergent extension movements during gastrulation (Wang et al., 2008). Taken together, the examples cited above indicate that adhesion receptors do more than "glue" cells together or to the ECM. Rather, through ECD-mediated interactions with extracellular ligands and ICD-mediated interactions with ctyoplasmic components, CAMs act as versatile cell surface receptors capable of mediated adhesion and integrating signals to dynamically regulate adhesion and/or other cellular processes in the cell.

Regulation of CAM-mediated adhesion

To understand how CAM-mediated adhesion is regulated, one must first characterize the molecular nature of the adhesive bond. Individual affinity constants for CAM interactions are usually lower than that of growth factors with their receptors. Cell adhesion relies more on avid interactions rather than high affinity interactions. Indeed, in contrast to high affinity interactions, weaker and more short-lived interactions provide the flexibility that cells need to respond to constantly changing extra/intra-cellular conditions by allowing the CAM to interact with different ligands (Pawson, 2004). This is required for the dynamic processes in which CAMs play key roles, such as migration and cell spreading. Because CAM interactions can be fast and rarely irreversible, measuring the affinity of CAM interactions may not be very informative. Rather, the kinetic parameters of "on and off" rates might be more insightful in characterizing CAM-mediated adhesion. The time scale for the formation and breakage of bonds varies significantly between different types of CAMs. Therefore, whether a receptor-ligand pair acts as an adhesion molecule depends on the magnitude of the adhesive force and the time scale over which the adhesive interaction occurs. Selectins, for instance, make carbohydrate bonds with fast "on and off" rates which allow the capture of fast moving leukocytes from the blood circulation (Buckley et al., 1998). Even in the case of integrin-mediated adhesion featuring receptor-cytoskeleton cross linking and cell anchorage, the "on and off" rates, albeit longer than selectins' rates, are short enough to allow for a relatively fast turnover of bonds, which must happen for cells to detach and migrate. In addition to ligand binding and ligand recognition, CAMs must be able to

withstand force. How CAMs respond to force determines their function and can be regulated by mechanisms discussed below. To determine whether a cell surface receptor is capable of adhesion, measuring its ability to withstand force *in vitro* does not always reflect whether this receptor can function as a physiologically relevant CAM *in vivo*. In the latter case, greater forces may be imposed on the receptor, especially if it is present in the vicinity of other adhesion complexes and anchorage points on the membrane.

There are different ways by which CAM-mediated adhesion is regulated. Here, I present only a few examples to illustrate the complexity and dynamic nature of the regulation of CAM adhesion.

1) Inside-out signaling and cytoskeletal linkage:

Inside-out regulation of adhesion refers to situations where the binding of an adhesion receptor to an extracellular ligand is regulated by cytoplasmic signaling events on the cytoplamic side of the receptor. Inside-out regulation of an adhesion receptor results from a modulation of affinity or avidity (Bazzoni and Hemler, 1998). Integrins are a good example of CAMs whose adhesion is regulated by Inside-out signaling. Talin binding to an integrin ICD was shown to induce conformational changes in the integrin ECD, which increases their affinity for ECM ligands such as collagen, fibrinogen and fibronectin (Calderwood and Ginsberg, 2003). Inside-out signaling is also thought to regulate adhesion via other CAMs. There is evidence that cadherins undergo some sort of alteration in physical conformation associated with their activation state (Gumbiner, 2005).

Another way of regulating CAM adhesion is by altering the state of the cytoskeleton linked to the CAM. This is particularly obvious in CAMs that are indirectly linked to the cytoskeleton. As discussed above, it is believed that α-catenin regulates E-cadherin mediated adhesion by promoting the formation of bundled actin filaments over Arp2/3 branched actin network near cadherin adhesion clusters. Several studies have demonstrated the importance of small GTPases in the regulation of CAM adhesion. Particularly, Rho family GTPases (Rho, Rac and Cdc42) as well as Arf GTPases and Rap1 have been shown to regulate cadherin-mediated adhesion by

altering the assembly state of the actin cytoskeleton (Geiger et al., 2000; Price et al., 2004; Van Aelst and Symons, 2002). Actin structures induced by Rac and Cdc42 were found in association with integrin adhesion complexes (Hall, 1998). It is believed that changes in cortical actomyosin contraction affect CAM mediated adhesion: Rho activity and actomyosin contractility have been implicated in the homeostasis of cell-cell junctions in cell culture systems and developing embryos (Baum and Georgiou, 2011; Liu et al., 2010). In *Drosophila*, activated Rho and myosin II contraction have been shown to destabilize adherens junctions over time (Harris and Peifer, 2004). Aside from acting on the cytoskeleton, GTPases were shown to regulate cell adhesion by controlling the trafficking and turnover of receptors. There's even some evidence that GTPases might play a role in the dynamic inside-out regulation of cadherin adhesion (Gumbiner, 2005).

2) Regulation by signaling and interactions with cytoplasmic partners:

Signaling pathways can negatively regulate CAM-mediated adhesion. It is widely accepted that signaling through receptor tyrosine kinases such as the epidermal growth factor receptor (EGFR), hepatocyte growth factor (HGF) and the scatter factor receptor (met) lead to cadherin downregulation (Birchmeier et al., 1997). This regulation relies on phosphorylation of CAM- interacting cytoplasmic proteins which then leads to downregulation of CAM adhesion in several ways. In the case of cadherins, it is hypothesized that phosphorylation of catenins by EGFR or met disrupts the cadherin-catenin complex which leads to the downregulation of cadherin by breaking the linkage of cadherin to actin (Roura et al., 1999). In neuronal cells, the activation of neuronal guidance receptor Robo upon binding to its ligand Slit, recruits the Abl tyrosine kinase to the N-cadherin-catenin complex, where Abl phosphorylates β-catenin and causes its dissociation from N-cadherin thus inhibiting adhesion (Rhee et al., 2002). There are other ways to regulate cadherin adhesion without affecting its cytoskeletal linkage. For instance, activin (TGFβ ligand) stimulation in *Xenopus* causes a downregulation of cadherin-mediated adhesion without disrupting the cadherin-β-catenin complex (Brieher and Gumbiner, 1994).

Another way to negatively regulate CAM adhesion is via ICD-mediated association with signaling molecules that induce CAM internalization or degradation. Recently, with the development of live imaging techniques, the extent to which CAMs, like cadherins, are turned over at junctions has begun to be appreciated. Surface biotinylation of E-cadherin revealed that E-cadherin is actively internalized and recycled back to the plasma membrane via a process that depends on clathrin-mediated endocytosis (Le et al., 1999). Studies on *Drosophila* have also shown that dynamin- dependent endocytosis is required to remove surface E-cadherin and to maintain the position and stability of mature adherens junctions (Georgiou et al., 2008). These data suggest that the turnover of E-cadherin is an important way to regulate cadherin-mediated adhesion and that this regulation is important for proper formation and maintenance of adherens junction. Ubiquitination and degradation of plasma membrane receptors involved in signal transduction are necessary to ensure that cells do not get over stimulated. There is evidence showing that CAMs, similar to plasma membrane signaling receptors, are also regulated by post-translational modification that lead to cytoplasmic degradation. Binding of p120-catenin to E-cadherin's JuxtaMembrane Domain (JMD) is proposed to stabilize cadherin-mediated adhesion by preventing the internalization and degradation of E-cadherin (Davis et al., 2003). An E3-ubiquitin ligase termed "Hakai" has been shown to bind the same JMD domain of E-cadherin upon Src stimulation, resulting in the ubiquitination and degradation of E-cadheirn (Fujita et al., 2002). In a recent report, Hartsock and Nelson have shown that the Hakai-mediated ubiquitination of E-cadherin JMD inhibits p120-catenin binding and targets E-cadherin for degradation. In this report, the authors propose that the E-cadherin JMD regulates the degradation of E-cadherin by competition between binding of p120-catenin and ubiquitination (Hartsock and Nelson, 2012).

Signaling molecules and interacting partners can also positively regulate CAM-mediated adhesion. One way of promoting CAM adhesion is by reversing the biochemical modifications that negatively affect adhesion receptors. Several tyrosine phosphatases have been identified as promoters of cell-cell adhesion. Some of these molecules do so by de-phosphorylating inhibitory phosphorylations on CAMs and

CAM-associated molecules at cell contacts. For example, the protein tyrosine phosphatase Pez is reported to be a major phosphatase of adherens junctions that promotes E-cadherin mediated adhesion by de-phosphorylating β-catenin (Wadham et al., 2003). Another way of promoting adhesion is via Rho-GTPase activity. It has been shown that nectin interactions near adherens junctions activate Cdc42, Rap1 and Rac in a Src-dependent manner. Through activation of IQGAP1, these Rho GTPases have been shown to stabilize E-cadherin at the cell surface by inhibiting its endocytosis (Izumi et al., 2004).

3) Regulation by clustering and membrane localization

Several CAMs are often observed in clusters or spots on the plasma membrane. It has been long known that, in addition to trans-interactions mediating the adhesion bond, many CAMs also nurture cis-interactions, which generate dimerization or multimerization of the receptor at the membrane. Cis-interactions are believed to strengthen the adhesion bond formed at cell contact sites. In the case of NCAM for instance, it was shown that the adhesion receptors accumulate where NCAM bearing cells contact each other. Clustering of NCAM at these sites is thought to be an important step in strengthening intercellular adhesion (Bloch, 1992). When clustered, cadherins were shown to mediate significantly stronger adhesions (Yap et al., 1997). Clustering of adhesion receptors can also modulate their signaling activities: β1 integrin clustering strengthens integrin-mediated adhesion and increases signaling activity downstream of integrins via tyrosine phosphorylation of FAK (Defilippi et al., 1994; Kornberg et al., 1992).

The recruitment of CAMs to microdomains can be essential for their function. Tetraspanins are known to organize adhesion molecules into microdomains via *cis*-interactions. It was shown that tetraspanin CD63 induces clustering of P-selectin, which is required to support leukocyte rolling (Doyle et al., 2011). *Cis*-interactions with membrane receptors can regulate CAM function by recruitment to membrane domains enriched with adhesive/signaling partners. For example, in growth cones, *cis*-interactions localize NCAM in detergent-resistant microdomains (DRMs) specifically enriched with PKC and GAP-43, and this localization is crucial for

NCAM-mediated signaling and growth cone formation (He and Meiri, 2002). Clustering and enrichment of CAMs at adhesion sites can also recruit regulators of adhesion. The endocytic protein GRAF-1 is recruited to integrin-based podosomes in Hela cells, where it modulates the dynamics of integrin adhesion sites via endocytosis affecting cell spreading and migration (Doherty et al., 2011). CAM distribution on the membrane is also known to affect the localization and activity of other plasma membrane receptors and signaling molecules. Kemler's group found that in epithelial cells, E-cadherin is required for EphA2 receptor localization at cell-cell contacts (Orsulic and Kemler, 2000). Disruption of E-cadherin function leads to perinuclear accumulation of EphA2 and affects ephrin-mediated signaling.

While many different mechanisms have been shown to regulate CAM-mediated adhesion, it is challenging to distinguish those that are physiologically relevant in cells that respond to multiple cues during development and tissue formation. It will therefore be crucial to study those regulatory mechanisms in the context of developing systems where, in contrast to simple cell culture systems, the regulation of CAMs not only affects local cell-cell adhesion or adhesion of a single cell to a substrate, but potentially affects major developmental processes, like tissue formation and patterning. Studying the mechanisms of CAM regulation in developing organisms should allow us to distinguish the major regulators of CAMs from the secondary fine-tuners of CAM adhesions by analysis of whole embryo and/or tissue phenotypes.

Regulation of signaling by CAMs

In addition to mediating cell adhesion and acting as membrane bound signaling sensors, some CAMs function as important regulators of intracellular signaling. CAMs are capable of regulating other signaling pathways directly or indirectly. Regulation can occur via direct binding and sequestering/stabilizing of cytoplasmic or via membrane-bound signaling molecules that function in signal transduction pathways. Recently, Echinoid, an Ig-containing CAM was shown to act as an upstream regulator of the Hippo pathway in *Drosophila* by interacting with and stabilizing the Hippo-binding partner Salvador at adherens junctions (Yue et al.,

2012). Similarly, in primary neurons, N-cadherin was shown to regulate p38 MAPK signaling by binding JLP, a scaffolding protein involved in p38 MAPK signaling. N-cadherin binding decreases the JLP-p38 MAPK interaction thus inhibiting p38 MAPK signaling (Ando et al., 2011). The platelet-endothelial cell adhesion molecule-1 (PECAM-1), also an Ig-containing CAM, was shown to bear an immunoreceptor tyrosine-based inhibitory motif through which the molecule dampens signals transduced by immunoreceptor protein tyrosine kinases by directly binding and recruiting protein-tyrosine phosphatase SHP-2 to the membrane (Newton-Nash and Newman, 1999). Aside from its potential effects on Wnt signaling as discussed above (in "Signaling through ICD"), E-cadherin was shown to regulate nuclear translocation and signaling of FGFR1 by promoting FGF-1 induced co-endocytosis of E-cadherin and FGFR1 (Bryant et al., 2005). More recently, Alpha Yap's group discovered that cytokinetic molecule centralspindlin interacts with α-catenin at interphase zonula adherens, where it recruits RhoGEF "ECT2" to activate Rho signaling (Ratheesh et al., 2012). Integrins-mediated adhesion is also known to modulate major signaling pathways. For example, integrin adhesion to fibronectin induces PAK1-dependent phosphorylation of MEK1, which leads to activation of MAPK (Slack-Davis et al., 2003). Without proper integrin-mediated adhesion, growth factor signaling to MAPK and subsequent activation of the Erk pathway is strongly affected.

Alternatively, CAM-mediated adhesion may indirectly promote receptor/ligand signaling by bringing the plasma membranes of opposing cells together and forcing interaction between a ligand on one cell and its receptor on the other cell. This may be the case for ephrin/Eph signalling. In fact, it has been shown that E-cadherin is required for the membrane localization of Eph receptors and their membrane-bound Eph ligands (Orsulic and Kemler, 2000). Consistently, data generated by other members of my lab suggest that cadherin-mediated adhesion may have a key role in regulating ephrin-mediated repulsion at embryonic ectoderm/mesoderm boundaries by promoting cell contacts required for activation of ephrin/Eph signalling (Rohani et al., 2011). Similarly, in neural growth cones, homophilic binding of NCAM, L1 and N-cadherin creates a neuronal CAM aggregate at sites of cell-cell contact which

is thought to indirectly promote clustering and activation of FGFR thus initiating a cascade that leads to neurite outgrowth (Aplin et al., 1998).

In addition to their inherent adhesive and signaling functions, many CAMs act as crucial regulators of cytoplasmic signaling cascades. CAMs may affect signaling directly via physical interaction with signaling molecules, or indirectly by modulating receptor-ligand interactions and activation of signaling receptors at the plasma membrane. In both cases, the distribution and abundance of CAMs at the membrane may have crucial effects on signaling cascades controlling multiple cellular processes such as movement, growth and proliferation.

The epithelial cell adhesion molecule, EpCAM

Identification of a cell surface antigen highly expressed in carcinomas

The epithelial cell adhesion molecule (EpCAM) has been long known as a tumor-associated antigen, highly expressed in a variety of carcinomas. EpCAM was identified by the monoclonal antibody (mAb) (CO) 17-1A, which was amongst the first mAbs ever generated against a frequently expressed antigen at the surface of carcinoma cells in humans. Because this monoclonal antibody cross-reacted specifically with a tumor-associated antigen expressed by most epithelial neoplasias, the 17-1A antigen was quickly considered a valuable target for immunotherapy of human carcinomas (Mellstedt et al., 1991; Riethmuller et al., 1994). Since the early 1990s, the 17-1A mAb has been successfully used as a post-operative adjuvant treatment to chemotherapy and results were particularly promising in patients with little residual disease. A plethora of names have been given to the protein based on the other mAbs raised against it (HEA125, GA733, 323/A3 etc.). In 1994, the 17-1A antigen was proposed to function as an epithelial homophilic CAM, and consequently the name EpCAM, which reflects tissue specificity and function of the protein, was suggested (Litvinov et al., 1994).

Mammalian EpCAM is expressed in embryonic epithelia but not in cells that have reached terminal differentiation. In zebrafish, maternal EpCAM transcripts are

ubiquitously distributed, whereas zygotic expression is restricted to epithelial tissues, including the skin (Slanchev et al., 2009). In mouse and human, high EpCAM expression is first seen in epithelial cells of the primordial lung where it remains expressed in lung epithelia throughout development and adult life albeit at lower levels. In normal human adult tissues, EpCAM is strictly an epithelial molecule based on immunohistochemical data. It is expressed at the basolateral membrane of all simple, pseudo-stratified and transitional epithelia but not in squamous stratified epithelia nor in mesenchymal, muscular and neuro-endocrin tissues (Balzar et al., 1999). *In situ* mRNA hybridization staining in mouse embryos revealed epithelial EpCAM expression in a variety of organs at E14.5 (Nagao et al., 2009a). EpCAM expression levels vary greatly among different adult tissues, being at the highest in small intestine, especially in the colon. Increased or de novo EpCAM expression is normally associated with active proliferation in several epithelial tissues in mammals. This is particularly striking for adult tissues, such as the squamous epithelium, which are EpCAM negative normally and acquire de novo EpCAM expression upon active proliferation (Litvinov et al., 1996). In general, the level of EpCAM expression correlates with the proliferative activity of intestinal cells, and inversely correlates with their differentiation state (Balzar et al., 1999). EpCAM expression at very high levels is specifically seen in most carcinomas, but not in other tumor types.

EpCAM used for diagnosis of carcinomas

Because in human adult tissues EpCAM expression is restricted to normal epithelia and is enhanced in cancerous epithelial tissues, the molecule can be used to distinguish EpCAM-positive epithelial-derived cancers (carcinomas) from EpCAM-negative cancers derived from non-epithelial tissues (Balzar et al., 1999). While EpCAM is typically expressed in a variety of carcinomas, it is not expressed in tumors of mesodermal and ectodermal origins such as melanomas, sarcomas, lymphomas and neurogenic tumors (Trzpis et al., 2007a). This property allows for easier diagnosis and unambiguous identification of tumors. For example, EpCAM is reliably used as a marker to discriminate pulmonary adenocarcinomas from EpCAM-negative mesotheliomas in lungs (Ryan et al., 1997).

Furthermore, the expression levels of EpCAM in certain carcinomas indicate the tumor stage and often, but not always, correlate with poor prognosis. In certain cases, levels of EpCAM expression can indicate how advanced the malignancy is, what the metastatic potential of a tumor is and how well the tumor will respond to the treatment. In transitional cell carcinoma of the bladder, EpCAM is used as a marker of increased malignant potential since the proportion of EpCAM positive cells increases from grade I to grade III tumors (Zorzos et al., 1995). In primary breast tumors, increased EpCAM expression positively correlates with large tumor size and infiltrated lymph nodes (Balzar et al., 1999). Increased EpCAM expression does not always correlate with advanced tumorigenesis. For example, the lack of EpCAM expression in laryngeal carcinomas significantly correlates with nodal metastasis (Takes et al., 1997). Due to its highly reproducible expression patterns in various carcinomas, EpCAM is a useful marker for malignancy potential in the diagnosis of cancer patients, but its contributions to cancer progression remain to be elucidated.

Carcinoma detection using EpCAM antibodies

Novel approaches in epithelial tumor detection were designed based on the abnormally high levels of EpCAM expression in carcinomas. Rare tumor-derived epithelial cells have been identified in peripheral blood from cancer patients (Circulating Tumor Cells, CTCs) and are likely to be the origin of intractable metastatic disease. CTCs represent an alternative to invasive biopsies for the detection, characterization and monitoring of tumors in non-hematologic cancers, but their detection is technically very challenging given their rarity. A recently developed micro fluidic platform (CTC-chip) proved capable of efficient and selective separation of CTCs from peripheral whole blood samples by binding the CTCs in the blood to CTC-chip micro posts coated with EpCAM antibody (Nagrath et al., 2007). This promising new technique, which relies on the robust cell-surface overexpression of EpCAM in carcinomas, has successfully identified CTCs in the peripheral blood of patients with metastatic colon, breast, lung, prostate, and pancreatic cancers in 99% of samples. The EpCAM-based CTC-chip provides a novel and effective tool for accurate identification of CTCs in cancer patients. It has

a positive impact on both clinical cancer management and cancer biology research (Nagrath et al., 2007).

EpCAM as a target for immunotherapy

EpCAM was one of the most immunogenic antigens to which many antibodies were generated in mice immunized with carcinoma cells (Balzar et al., 1999). High cell surface expression of EpCAM in carcinomas makes the protein an attractive target for immunotherapy. Early immunotherapy attempts relied on treatments of carcinoma patients with unconjugated mAbs and had modest anti-tumor effects (Mellstedt et al., 1991; Ragnhammar et al., 1993). However, it was quickly noted that treatments with unconjugated mAbs lacked the ability to eradicate robust tumor masses, possibly due to poor localization of mAbs in larger tumors. Recently, novel trifunctional bispecific monoclonal antibody treatments have been proven very useful for treatment of EpCAM positive cancers. Catumaxomab, for example, is a hybrid antibody with two binding specificities: EpCAM on one side and T cell antigen CD3 on the other. Via its Fc-fragment, catumaxomab additionally recruits accessory cells, including macrophages, dendritic cells and natural killer cells (Fig. 1.2A). This tri-functional approach triggers a strong immune response in the vicinity of EpCAM positive tumor cells, which leads to their eradication. Intraperitoneal treatment with catumaxomab has prolonged puncture-free survival of patients with malignant carcinomas and is now approved in Europe and under clinical trials in the USA (Sebastian, 2010).

Characterization of EpCAM

The EpCAM gene and protein in vertebrates

In mammals, EpCAM is encoded by the gene *GA733-2*. The transcribed mRNA is approximately 1.5 kb long and encodes a 314 long amino-acid polypeptide containing a 265 amino-acid N-terminal extracellular domain, a 23 amino-acid transmembrane domain and a short 26 amino-acid C-terminal cytoplasmic domain (referred to as "EpTAIL", "EpTail" or "tail" in this thesis). In higher vertebrates, another molecule homologous to EpCAM has been identified. It is known as TACSTD-2, EGP-1 or

Trop-2 and is the gene product of *GA733-1*, which is thought to have originated from the retroposition of EpCAM mRNA. The retroposition event, which resulted in the intronless gene *GA733-1*, is thought to have preceded the divergence of avian and mammalian species approximately 300 million years ago (Balzar et al., 1999). EpCAM and TACSTD-2 are 49% identical and, taking into account their conserved substitutions, the two antigens have a similarity of 67% (Linnenbach et al., 1993). There are two regions of maximum homology in the extracellular and transmembrane domains, and strong conservation in the position of hydrophobic and hydrophilic residues in the two antigens. Similar to EpCAM, high expression of TACSTD-2 is seen in the majority of human carcinomas (Ripani et al., 1998).

In lower vertebrates, most diploid species have a single copy of EpCAM in their genomes. In the pseudotetraploid *Xenopus laevis* however, two EpCAM genes are found and are probably the result of the recent genome duplication that gave rise to tetraploidy in this species, approximately 40 million years ago. Amino acid sequence alignment of both "EpCAMa" and "EpCAMb" shows that the two proteins are almost identical, with the exception of a few amino acid substitutions. In contrast, the closely related diploid species *Xenopus tropicalis* has a single EpCAM gene in its genome, supporting the idea that the two genes found in *Xenopus laevis* are pseudoalleles resulting from tetraploidization. Sequence alignment of EpCAM homologues from different vertebrate species (zebrafish to human) revealed a high homology between EpCAM amino acid sequences suggesting that the structure of the EpCAM protein is evolutionary conserved among vertebrates (Trzpis et al., 2007a).

EpCAM extracellular domain

The highly antigenic extracellular domain of EpCAM consists of two consecutive Epidermal Growth Factor-like repeats (EGF I and EGF II) at its cysteine-rich N-terminal half, followed by a cysteine-poor region (Fig. 1.2B). The first and second EGF-like repeats are homologous to EGF repeats on the ECD of Nidogen, EGF precursors, the LDL receptor, L-selectin and PECAM (Balzar et al., 1999). Formation of disulphide bridges between cysteine residues in the N-terminal half of

the ECD possibly results in a folded EGF-like globular conformation (Balzar et al., 2001). The EpECD sequence predicts the presence of three potential N-glycosylation sites. Tunicamycin-mediated inhibition of N-glycosylation results in a single polypeptide chain of 34 kDa. However, cancer cell lines and *Xenopus laevis* embryos seem to produce multiple glycosylated forms of EpCAM as suggested by the presence of multiple bands in the 38-45 kDa range on western blots (Fig. 1.2C). Variation in ECD glycosylation is known to regulate CAM function. For example, the differential glycosylation of CD44 has been shown to affect its function by dictating which ligand the protein preferentially interacts with (Naor et al., 1997). To date, no functional difference between the different EpCAM glycosylated forms have been reported. Aside from glycosylation, there is evidence that EpECD undergoes regulated proteolytic cleavage. Early studies have identified a potential cleavage site for trypsin-related proteolytic enzymes in the second EGF repeat on the N-terminal half of the ECD. More recently, it was reported that TNF-α converting enzyme (TACE) cleaves EpECD near the TM domain in cancer cell lines and that EpECD cleavage plays a key role in promoting cell proliferation (Maetzel et al., 2009).

EpCAM transmembrane and intracellular domains

The EpCAM transmembrane domain is composed of 23 hydrophobic amino acid residues and is followed by a short 26-residue cytoplasmic tail that is highly charged. EpTAIL contains the internalization motif NPXY found in many other cell-surface receptors such as the LDL receptor. EpTAIL was also reported to contain two α-actinin binding sites through which EpCAM is thought to bind α-actinin and consequently bind the actin cytoskeleton (Balzar et al., 1998). The same study that identified the EpECD cleavage also reported that EpTAIL gets cleaved by TACE and presenilin-2 and that this cleavage is required for a signaling property of the EpCAM intracellular domain (Maetzel et al., 2009).

Discovery of EpCAM as a cell adhesion molecule

EpCAM is structurally unrelated to any of the major families of CAMs (Balzar et al., 1999). The first functional study of EpCAM suggested that the protein functions as a homophilic Ca^{2+}-independent cell-cell adhesion molecule, based on observations that

EpCAM overexpression mediated the aggregation of cadherin-negative L cells that otherwise do not aggregate in culture. When overexpressed in L cells, EpCAM localized preferentially at sites of cell-cell contacts where it mediated relatively weak adhesion compared to classical cadherin-mediated adhesion (Litvinov et al., 1994). EpCAM's cytoplasmic domain (EpTAIL) was also required for EpCAM-mediated aggregation of L cells, since transfecting an EpCAM mutant lacking the complete cytoplasmic domain (EpΔC) failed to aggregate L cells. EpΔC was still capable of homophilic binding even in the absence of EpTAIL only when the counter-receptor EpCAM molecule was fixed (EpCAM-coated solid phase) suggesting that it retained homophilic specificity but was incapable of forming stable adhesive bonds. The same group argued that EpCAM associates with the actin cytoskeleton via its cytoplasmic domain. EpTAIL was proposed to interact with the actin cytoskeleton by directly binding α-actinin (Balzar et al., 1998). Disruption of the actin cytoskeleton inhibited EpCAM adhesion and caused the internalization of EpCAM. When coexpressed with cadherins in L cells, both molecules localized at cell-cell contact sites and formed independent adhesions, with no EpCAM present near morphologically distinguishable E-cadherin adhesion junctions. However, increased expression of EpCAM in those cells weakened cadherin-mediated adhesion in favor of EpCAM-mediated adhesions (Litvinov et al., 1997). Overexpression of EpCAM in E-cadherin positive L cells had no effect on total levels of E-cadherin, but decreased the association of the cadherin/catenin complex with the actin cytoskeleton. It was therefore suggested that via its α-actinin-mediated link to the actin cytoskeleton, EpCAM overexpression somehow interferes with cadherin-mediated adhesion by disrupting the link between α-catenin and F-actin (Balzar et al., 1999; Litvinov et al., 1997). The involvement of EpCAM in active proliferation and migration of cells was therefore initially attributed to its ability to weaken cadherin-mediated adhesion. Whether EpCAM-mediated homophilic adhesion is required for epithelial cell support remains unclear at the moment.

EpCAM is capable of intracellular signaling

More recently, Gires' group proposed another hypothesis that accounts for the tumor promoting effects of EpCAM in cancer. They showed that via its cytoplasmic

domain, EpCAM is capable of nuclear signaling, which induces transcription of oncogenes in cancer cell lines and immunodeficient mice (Maetzel et al., 2009). EpTAIL interacts with FHL2 and β-catenin in the cytoplasm and, upon regulated proteolytic cleavage by TACE and presinilin-2, the EpTAIL/FHL2/β-catenin complex translocates to the nucleus, where it interacts with transcription factor Lef-1 to promote oncogene transcription. Nuclear EpCAM signaling is affected by cell density as homotypic aggregation of EpCAM's extracellular domain provides a signal that induces cleavage of EpCAM's extracellular domain EpECD. Shedding of EpECD during activation of EpCAM signaling produces a soluble ligand that promotes cleavage of EpTAIL in a paracrine or autocrine fashion and seems to be a prerequisite for release of EpTAIL and subsequent nuclear signaling (Maetzel et al., 2009). In this model, the authors propose that EpCAM acts as a potent tumor promoting molecule in two ways: 1) via nuclear activity of its EpTAIL domain that induces oncogene transcription and 2) via its association with β-catenin (required for nuclear signaling) where EpCAM possibly weakens cadherin-mediated adhesion by sequestering β-catenin away from cadherins. Interestingly, cleavage and nuclear accumulation of EpTAIL was never observed in normal colonic mucosa. This may be because EpCAM levels are suboptimal for the formation of the signalosome and the cleavage of EpECD. Additionally, expression of crucial factors involved in EpCAM's nuclear signaling complex such as FHL2, TACE and presinilins, differ significantly in normal and malignant tissues, being strongly up regulated in the latter case. Therefore, nuclear EpCAM signaling appears to specifically occur in rapidly dividing malignant cells.

EpCAM levels affect cell motility and migration

Several studies have reported that EpCAM promotes metastasis by increasing cell migration. Silencing EpCAM gene expression in breast cancer cell lines leads to a very strong decrease in cell migration and invasion (Osta et al., 2004). In another study, low metastasizing fibrosarcoma cells metastasized to distal lymph nodes and the lung only upon overexpression of EpCAM in the injected tumor (Wurfel et al., 1999). Very recently the migration-promoting role of EpCAM in *in vitro* cancer cell lines was confirmed in mice where EpCAM knockout disrupted the migration of

epidermal Langerhans cells (Gaiser et al., 2012). Based on these studies, EpCAM seems to promote cell migration in normal and cancerous tissues. Paradoxically, in tumor cells that undergo epithelial to mesenchymal transition (EMT), it was shown that EpCAM gets downregulated transiently to enable cell migration (Jojovic et al., 1998). Similarly, low EpCAM levels are required to promote structural rearrangements and cell migration occurring during nephrogenesis (Trzpis et al., 2007b). The fact that EpCAM acts as a promoter of cell migration or not may depend on whether the molecule's ECD undergoes mainly homophilic cell-cell adhesion interactions, cell-ECM interactions or no interaction due to proteolytic cleavage. Until now, no molecular mechanism has been proposed to account for the effect of EpCAM on cell motility. It is conceivable that EpCAM regulates cell motility via a potential signaling property, an adhesive property or via both and so, it will be important to elucidate the molecular mechanism by which EpCAM affects cell movements.

Localization of EpCAM in tetraspanin-enriched plasma membrane microdomains

EpCAM has been shown to be recruited to tetraspanin-enriched microdomain (TEMs) via its association with D6.1A and CD9 (Claas et al., 2005; Le Naour et al., 2006). Since tetraspanins have been implicated in metastasis, it is believed that the potential prometastatic function of EpCAM occurs through its association with TEMs. In pancreatic tumor cell TEMs, EpCAM was shown to interact directly with the tight junction protein claudin-7 via EpECD and metastasis-promoting CAM CD44v4v7 via EpTAIL (Ladwein et al., 2005; Schmidt et al., 2004). This carcinoma-specific EpCAM/Claudin-7/CD44v4v7 complex is believed to influence cell-matrix adhesion, cell-cell adhesion and apoptosis resistance. Furthermore, the EpCAM-claudin-7 complex is frequently seen in highly metastatic colorectal and pancreatic carcinomas. Claudin-7 is a crucial tight junction plasma membrane receptor that promotes tissue compaction. Consistently, during invasion and metastasis of esophageal and breast carcinomas, the expression levels of claudin-7 are reduced to allow for cells to detach, migrate and invade other tissues. It has been suggested that the EpCAM/claudin-7 interaction in carcinomas is required for the downregulation of claudin-7-mediated adhesion in tight junctions. Importantly, EpCAM's function in

TEMs remains entirely unknown and its potential association with claudin-7 is poorly understood. Further investigations are necessary to understand the importance of EpCAM's association with TEMs complexes.

Limitations of EpCAM studies in cancer systems

Based on studies in cancer cell lines, EpCAM emerges as a versatile homo- and heterophilic CAM capable of modulating cell-cell adhesion, migration and proliferation by interacting with important intra- and extra-cellular factors required for major CAM-mediated adhesion (e.g. cadherins, and claudins) and signaling molecules (e.g. β-catenin). Altogether, these studies suggest that EpCAM is more of a cell-surface signaling sensor than a typical cell adhesion molecule in cancerous cellular environments. The predominant function of EpCAM in normal tissues remains highly elusive at this point because studying EpCAM in cancer cell lines exclusively has its limitations: 1) EpCAM is likely to function differently when it is abnormally overexpressed in cancer cells than when it is not highly abundant at the membrane in non-transformed cells. For instance, EpCAM nuclear signaling seems specific to tissues where the protein is highly expressed and may not account for EpCAM's roles in normal adult tissues and developing embryos. 2) The cell surface and cytoplasmic environments of cancer cells are abnormal, unregulated, highly dynamic and chaotic, which makes it difficult to fully grasp the relative contributions of proteins acting in molecular pathways involving EpCAM. 3) Tissue, organ and organismal phenotypes resulting from EpCAM loss of function cannot be assessed in simple cell culture monolayers. Investigating the effects of EpCAM loss or gain of function on tissues can elucidate important functions of the protein. Studies in developmental systems are therefore necessary to tease apart the "possible" EpCAM interactions/functions that may or may not promote cancer progression from the "vital" ones required for tissue formation and maintenance.

Characterization of EpCAM in development

The analysis of a protein's functions in a developmental context can be highly informative. The typical approach that relies on the phenotypic analysis of a mutation is particularly powerful with highly penetrant "whole embryo" or "whole tissue" phenotypes. For example, analysis of *Xenopus* embryonic "double axis" phenotype following Axin knockdown lead to the discovery of Axin's central role in the canonical Wnt pathway (Zeng et al., 1997). Until a few years ago, little was known about EpCAM's function in development. Attempts at generating EpCAM knockout (KO) mice were not informative. First, heterozygous $EpCAM^{+/-}$ mice did not exhibit any abnormalities probably due to the existence of the paralogous gene product (TACSTD-2/Trop-2) mentioned above. The function of TACSTD-2/Trop-2 is largely unknown but it is thought to possibly overlap in part with that of EpCAM. On the other hand, homozygous $EpCAM^{-/-}$ embryos are non viable and die due to placental insufficiency (Nagao et al., 2009b). However, a mouse study recently circumvented the embryonic lethality associated with homozygous EpCAM-null mutations by generating conditional EpCAM KO mice. This approach allowed for an analysis of EpCAM function in the epidermis of adult mice. Knockout of EpCAM attenuated the migratory ability of epidermal Langerhans cells (LC), a subpopulation of cells that migrate from skin to lymph nodes where they regulate the magnitude and quality of immune responses initiated by epicutaneously applied antigens (Gaiser et al., 2012). To date, there has been no double KO of EpCAM and TACSTD-2 in mice. In the case where both proteins overlap functionally, a double KO might generate a stronger and more informative phenotype.

In 2009, Slanchev and colleagues generated maternal-zygotic zebrafish EpCAM mutants and chimeric embryos, which revealed that EpCAM is required for proper epithelial morphogenesis during epiboly and skin development (Slanchev et al., 2009). A loss of EpCAM in zebrafish lead to a downregulation of E-cadherin, an enrichment of tight junction proteins and a basal extension of apical junction complexes, which consequently disrupted deep cell epiboly. Interestingly, concomitant partial loss of E-cadherin in EpCAM mutants lead to more severe defects in epiboly movements of deep cells while the complete loss of E-cadherin in

EpCAM depleted embryos lead to compromised intercellular adhesion within the epidermis of early gastrulas which caused complete embryo lysis by the mid-gastrula stage. It was therefore suggested that in zebrafish epidermis, EpCAM works in partial redundancy with E-cadherin to maintain the integrity of the epidermis by promoting cell-cell adhesion. The severity of phenotype resulting from an EpCAM knockout in zebrafish may be underestimated since the duplicated genome of tetraploid zebrafish contains a second copy of EpCAM that may still be functional. It is therefore possible that the knockdown of both EpCAMs in zebrafish results in a more intense phenotype similar to those seen upon combined downregulation of both EpCAM and E-cadherin.

Altogether, developmental studies so far seem to point towards a role for EpCAM in regulating adhesion and cell movements *in vivo*. However, the mechanisms by which EpCAM affects cell motility and adhesion *in vivo* remain unknown. Additional *in vivo* studies are therefore necessary to fully elucidate the various functions of EpCAM in embryogenesis and adult tissues.

Development of *Xenopus laevis*

Morphogenetic movements during Xenopus gastrulation

Morphogenesis during *Xenopus* gastrulation is exclusively driven by massive rearrangements of preexisting tissues and cells. Gastrulating tissues undergo very dynamic morphogenetic changes leading to the establishment of a basic body plan. This developmental process is driven by highly regulated changes in cell shape, movement and adhesion (Keller and Winklbauer, 1992). Perhaps the most spectacular events at this stage are 1) the epiboly of the ectoderm, where cell intercalation movements are required to thin a multilayered ectoderm into a two-cell layered tissue, 2) convergent extension of deep cells in the involuting marginal zone, which also features radial and lateral intercalations that drive body axis elongation and induce blastopore closure, and 3) the migration of involuted mesoderm on overlying ectoderm, which gives rise to the embryonic anteroposterior axis (Keller et al., 2000). Newly involuted mesoderm cells come in contact with overlying ectoderm cells while remaining separated, thus creating a boundary between both tissues

known as Brachet's cleft (C1; Fig. 3). It has been shown that ectoderm/mesoderm cell contacts across the boundary trigger a repulsive signal through membrane-bound ephrinB ligands and their receptors EphB. Once separated, the signal decays, cells send out protrusions and re-establish cadherin-mediated contacts (Rohani et al., 2011). Dynamic cycles of attachments and repulsions prevent mesoderm cells from invading the ectoderm but allow them to use the ectoderm as a substrate for migration. Ephrin-mediated repulsion seems to be mediated by activation of GTPases RhoA, Rac and Rho kinase, which modulate the actin cytoskeleton possibly through protein kinase C (PKC) signaling. Parallel to ephrin/Eph, other molecular pathways have been reported to control separation at Brachet's cleft via modulation of cytoskeletal dynamics. It was reported that PAPC/Fz7 interaction at the membrane contributes to the development of separation by activating Rho A possibly via xANR5, a PAPC cytoplasmic interacting partner and FGF target gene product (Chung et al., 2007; Medina et al., 2004). Frizzled-7-mediated cell sorting was shown to depend on PKC signaling (Winklbauer et al., 2001).

Xenopus as an experimental model in cell/developmental biology

We use *Xenopus laevis* embryos as a model to study morphogenetic movements. There are several advantages of using this system as a developmental model organism. First, large sizes of embryos, tissues and cells allow for efficient tissue explanting, isolation of tissues in culture and reconstitution of embryonic boundaries/structures by apposition of different tissues *in vitro*. Second, gene expression can be easily modulated by morpholino-mediated transcript silencing and/or injection of mRNA transcripts for gene expression, or by application of specific cell permeable chemical activators and inhibitors on whole tissues or isolated explants. Morpholino-mediated knockdown as well as mRNA overexpression can be easily targeted to specific tissues by microinjection at early stages. It is thus possible to investigate gene function in specific tissues by combining targeted up/down regulation of gene expression with dissection and isolation of the tissue where gene expression has been modulated. Third, for a vertebrate system, embryos develop fast and therefore phenotypes resulting from modulation of gene expression can be analyzed at early and late developmental stages within 8-72 hours post-fertilization.

Identification of Xenopus EpCAM as an inducer of tissue mixing

Previous members of the lab have identified the *Xenopus* ortholog of human EpCAM in a gain-of-function screen for genes that cause aberrant ectoderm/mesoderm tissue mixing at Brachet's cleft. Overexpression of EpCAM in the ectoderm, mesoderm or both tissues disrupted the boundary by inducing cells from both tissues to mix. As mentioned above, a combination of ephrin, frizzled-7 (Fz-7) and PAPC signaling events triggered by ectoderm and mesoderm contacts at the boundary are thought to control the migration of mesoderm on the ectoderm wall while keeping both tissues separated. Importantly, ephrin-mediated signals and Fz-7/PAPC at the membrane seem to impinge on PKC signaling in the cytoplasm to control tissue separation at the boundary.

The following section describes the superfamily of PKCs, their structures, modes of activation and various functions, with emphasis on the roles they play at cell-cell contacts.

Protein Kinase C biology

Protein Kinase C structure and function

The PKC family is a class of highly regulated membrane-localized Ser/Thr protein kinases (Rosse et al., 2010). PKCs play important roles in the dynamic regulation of homotypic and heterotypic cell-cell and cell-matrix interactions mediating adhesion and migration. PKCs are well conserved in eukaryotes, ranging in diversity from a single isoform in budding yeast, to five isoforms in *Drosophila* and 12 isoforms in mammals. The various PKC isoforms in higher vertebrates can be grouped roughly into three subfamilies, based on their divergent regulatory domains and the requirements for activation: 1) the conventional PKCs (cPKCs) comprise PKCα, PKCβ and PKCγ. This family is activated by a combinatorial binding of phospholipid and diacylglycerol (DAG) to their C1 domains and Ca^{2+}-dependent phospholipid binding to their C2 domains. 2) the novel PKCs (nPKCs), which include PKCδ, PKCε, PKCη and PKCθ, are also activated by phospholipids and

DAG but do not respond directly to Ca^{2+}, and 3) the atypical PKCs (aPKCs; PKCλ and PKCζ) are irresponsive to both Ca^{2+} and DAG, but are rather activated allosterically by interacting with cell polarity components in the PAR complex (Suzuki et al., 2001). Despite their different requirements for activation, all PKC isoforms share a highly conserved C-terminal kinase domain, which is linked by a hinge region to a more divergent N-terminal regulatory domain (Fig. 1.4A). When inactive, PKCs are auto-inhibited by a pseudosubstrate sequence (PS) present in their N-terminal regulatory domains, which binds to the substrate binding pockets in the C-terminal kinase domains. By doing so, inactive PKCs are retained in a closed head-to-tail conformation in the cytoplasm. Three phosphorylation priming events on key residues in the kinase domains of cPKCs and nPKCs occur in the cytoplasm and are important for ensuring optimal catalytic activities of PKCs following complete de-inhibition (Rosse et al., 2010). The latter happens when PKCs get fully activated by second messengers at the plasma membrane, such as DAG and phospholipid, and/or allosteric effectors binding to their regulatory domains also at the membrane. These bindings displace the bound PS domains from the active sites and "open up" the PKC molecules in a conformation favorable for substrate interaction with the phospho-primed and active kinase domains (Fig. 1.4B).

There are various ways by which PKC activity can be regulated. A certain degree of regulation occurs by post-translational modifications in the cytoplasm during the "priming" step. As mentioned above, the phosphorylation events that take place on "closed" inactive PKCs are necessary for subsequent full activation at the membrane via interactions with second messengers. These phosphorylation events require kinases PDK1 and mTORC2 as well as autophosphorylation on a single Thr residue (Suzuki et al., 2001). The abundances and activities of PDK1 and mTORC2 can affect the rates at which PKCs get primed into their mature forms for full membrane activation. PKC activity is also regulated by the availability and abundance of second messengers required for full activation of the kinase at the membrane. In the absence of sufficient second messengers, the full activation of PKCs does not occur. Aside from activating second messengers (e.g. DAG and phospholipids), inhibitory second messengers have been identified as negative regulators of PKC activity at the plasma

membrane. Compounds participating in sphingolipid metabolism, such as sphingosine and ceramides, have been demonstrated to act as inhibitory second messengers (Liu and Heckman, 1998). High abundance of such inhibitory second messengers can negatively regulate PKC activity. Another important PKC regulatory process relies on its binding to scaffold proteins and subcellular localization. Although PKCs typically translocate to the plasma membrane upon activation, their residence on membranes would be transient if not stabilized by other interactions. Several PKC receptors/scaffolding proteins have been identified. For example, the Receptor for Activated C-kinases (RACKs), are anchoring proteins that bind active PKCs and are thought to stabilize them at the membrane. Binding of PKCs to RACK1 is maximal in the presence of phospholipids, DAG and Ca^{2+}. RACK binding PKC's regulatory domain is therefore thought to stabilize PKC activity at the membrane without interfering with its activity (Mochly-Rosen and Gordon, 1998). Another type of anchoring protein known to regulate PKC activity is the family of cAMP-dependent A-kinase anchoring proteins (AKAPs). AKAPs are thought to bind and inhibit the catalytic sites of PKCs (Faux et al., 1999). Due to the cytoplasmic localization of AKAPs, AKAP-bound PKCs are sequestered in the cytoplasm far from their substrates (Fig. 1.4B). Lastly, PKCs can be regulated by constitutive activation and proteolytic degradation. It has been shown that proteolytic cleavage by trypsin or calpains I and II generates two distinct fragments of the enzyme: the regulatory domain and the kinase domain. This domain separation leads to constitutively active PKC (Schaap and Parker, 1990). The kinase fragment thus produced was shown capable of affecting several cellular functions. It is possible that the subcellular localization of PKC affects this cleavage, as it was shown that membrane recruitment of PKC protects it partially from the activities of such proteases. Conversely, ubiquitination and proteasomal degradation is a well established mode of PKC downregulation. It is well known that prolonged PKC activity at the membrane, resulting for example from a long exposure to phorbol esters (PMA, TPA) and/or DAG, causes an almost complete depletion of certain PKC isoforms from cells (Lu et al., 1998). In summary, PKC activity seems to be regulated by a variety of mechanisms including kinase-mediated phosphorylation, adaptor binding, interaction with second messengers and proteolytic cleavage. The

diverse modes of PKC regulation ensure that this family of kinases is capable of modulating its activity in response to various cellular and extracellular cues.

PKC activity at cell-cell contacts controls cell migration and cell adhesion

PKC members are key regulatory enzymes involved in processes like cell polarity, differentiation, growth, apoptosis, cytoskeletal reorganization, migration and adhesion. There are many studies implicating PKC signaling in the regulation of cell migration and cell-cell adhesion. In this section, I will discuss a few of those reports. Classical and novel PKCs have been implicated in a number of migratory models because of their implications in regulating cytoskeletal dynamics as well as the function of numerous cell surface proteins involved in cell-ECM interactions and migration (Rosse et al., 2010). The PKC-mediated modulation of the MAPK pathway downstream of the Met receptor is probably the best characterized pathway by which cPKCs and nPKCs regulate cell migration. Following HGF activation of Met, the receptor-ligand pair gets internalized and signals from early endosomes where, among other things, Met signaling promotes cell-ECM migration. It is thought that Met regulates cellular processes by impinging mainly on the Erk pathway. nPKCs exert a positive influence on Met signaling by promoting the recruitment of Erk1 and Erk2 to focal adhesion complexes, where they induce cell migration through phosphorylation of paxillin and other focal adhesion components (Ivaska et al., 2002; Roberts et al., 2003).

In many cases, such as metastatic carcinomas, cell migration also requires a downregulation of cell-cell adhesion; cells must loosen contacts with their neighbors and strengthen their focal contacts with ECM. This is observed in Met-mediated cell scattering induced by HGF, where E-cadherin-mediated adhesion is well known to be strongly reduced prior to scattering of epithelial cells. Two studies have shown that nPKCs, particularly PKCδ, mediate the functional suppression of E-cadherin in response to HGF to promote cell motility (Chen and Chen, 2009; Singh et al., 2009). It was shown that PKCδ is targeted to cell-cell junctions in MDCK cells via its hinge region that links its catalytic domain to its regulatory domain. PKCδ activity at those junctions weakened cell-cell adhesion and facilitated cell scatter induced by HGF

(Chen and Chen, 2009). It was also suggested that upon phosphorylation by EGF at Y-311, PKCδ binds to E-cadherin (Singh et al., 2009), although the mechanism by which PKCδ disrupts E-cadherin-mediated cell-cell adhesion to promote cell scattering and migration remains largely unknown.

There have been a few models proposed to explain how nPKCs negatively regulate E-cadherin-mediated cell-cell adhesion in different systems, where it is likely that similar mechanisms come into play for HGF/EGF-mediated cell scattering. Stow's group has shown that nPKC activation strongly increased the rate of E-cadherin endocytosis in MDCK cells. nPKC activation in those cells lead to changes in the actin cytoskeleton, facilitating E-cadherin endocytosis (Le et al., 2002). Another study has shown that in C4-2 prostate cancer cells, nPKC substrate PKD/PKCμ directly phosphorylates E-cadherin upon activation by nPKCs, which leads to an increase in cell aggregation and decrease in cell motility, although the mechanism by which E-cadherin phosphorylation leads to those changes remains elusive (Jaggi et al., 2005).

In addition to regulating E-cadherin-mediated cell-cell adhesion, PKC activity is thought to regulate other junctional components. In the case of EGF-induced cell scattering, it was shown that EGF stimulation also reduced the expression of tight junction protein, occludin, and that this effect was also mediated by PKCδ through Src (Singh et al., 2009). Another study has shown that PKC inhibition increased gap junction formation and cell adhesion in human neuroblastomas (Morley et al., 2010). On the other hand, CD151, a member of the tetraspanin family of proteins tightly associated with integrin α3β1, was shown to regulate epithelial cell-cell adhesion through PKC-dependent actin cytoskeletal reorganizations. In this study, the authors propose that by impinging on PKC signaling, CD151 promotes E-cadherin-mediated cell-cell adhesion by inducing actin cytoskeletal reorganizations (Shigeta et al., 2003).

PKC is known to regulate cell motility by influencing the contractile state of the actomyosin network. It was shown that EGF induces fibroblast contractility and motility via PKCδ-dependent pathway. Specific inhibition of PKCδ activation by various means abrogated EGF-induced myosin light chain (MLC) phosphorylation

and subsequent cell contractile force generation and motility (Iwabu et al., 2004). This study did not provide a molecular pathway linking PKCδ activation to MLC phosphorylation and contraction. However, other studies have identified PKC substrates capable of activating actomyosin contraction by promoting MLC phosphorylation. For example, phosphorylation of substrate CPI-17 by PKCα/δ inhibits myosin phosphatase activity, resulting in phosphorylation of MLC and increased actomyosin contractility (Eto et al., 2004). Another actomyosin regulatory pathway downstream of PKC involves phosphorylation of actin/myosin binding protein Caldesmon. The latter is a thin-filament associated protein capable of stabilizing actin filaments, inhibiting actomyosin ATPase activity, as well as actin-myosin interactions, thereby reducing contractility. It has been shown that via Raf-1 phosphorylation, active PKCα/ε stimulates Erk1/2 which phosphorylates Caldesmon causing its dissociation from actin and resulting in actomyosin interaction and contraction (Kim et al., 2008).

In addition to its effect on cell motility, PKC-mediated activation of actomyosin contraction was shown to regulate cell-cell adhesion. A recent study reported that PKC activation disrupts epithelial apical junctions via a ROCK-II dependent stimulation of actomyosin contractility (Ivanov et al., 2009). In this study, PKC-dependent activation of actomyosin contraction lead to loss of tight junction proteins occludin and ZO-1 as well as adherens junctions' proteins E-cadherin and β-catenin from cell-cell contact sites and their accumulation in cytosolic dot-like structures.

Taken together, these studies show that PKCs can modulate cell-cell adhesion and cell migration by altering the state of the actin cytoskeleton through induction of actomyosin contraction.

Thesis Objectives

Main objective

The initial objective of this thesis was to understand the molecular mechanism by which EpCAM promotes ectoderm/mesoderm tissue mixing in the *Xenopus* gastrula. Observations made while investigating EpCAM function during gastrulation broadened my interest and geared it towards characterizing the role of EpCAM in gastrulation and later developmental stages. Thus, the main objective of this thesis is to understand the predominant function of EpCAM in development of *Xenopus laevis* embryos and to determine whether this function is conserved in human carcinomas where EpCAM is thought to promote cancer progression.

Chapter II objective

The objective of this chapter is to elucidate the mechanism by which EpCAM induces ectoderm/mesoderm tissue mixing in the *Xenopus* gastrula. Data presented in Chapter II shows that EpCAM induces tissue mixing by increasing cell motility via a signaling property of its cytoplasmic domain that inhibits PKC activity.

Chapter III objective

The first goal of this chapter is to characterize EpCAM function later in development, at the neureula stage, where EpCAM is required to maintain epithelial cell-cell adhesion. I show that EpCAM-mediated inhibition of PKC activity (described in Chapter II) is necessary for maintenance of cell-cell adhesion in post-gastrulation stages. The second main objective of this chapter is to fully understand the molecular mechanism by which EpCAM inhibits PKC signaling to promote motility and cell-cell adhesion. I found that PKC is inhibited by a short segment of the EpCAM cytoplasmic tail that directly binds activated PKCs with high affinity. This motif is 1) highly conserved in all vertebrate EpCAMs, 2) it resembles and acts similarly to the intramolecular pseudosubstrate inhibitory domains of PKCs, and 3) is shared by other plasma membrane proteins which are also able to bind PKCs. Based data presented in this chapter, direct inhibition of PKC by EpCAM represents the

prototype of a novel mode of regulation of signal transduction by cell surface proteins.

Chapter IV objective

This short chapter focuses on further characterizing the expression and function of EpCAM in morphogenesis of non-epithelial *Xenopus* tissues. In this chapter, I show that EpCAM is required for proper patterning of mesoderm-derived notochord tissue. The interest of this short chapter is that it shows for the first time that EpCAM expression is crucial in non-epithelial tissues.

Chapter V objective

The objective of this last chapter is to discuss how the findings made in this thesis reconcile with previous models of EpCAM function in development and cancer. In this chapter, I also summarize the contributions of this body of work to the EpCAM and PKC fields and discuss the impact of my contributions.

References

Abe, K., and Takeichi, M. (2008). EPLIN mediates linkage of the cadherin catenin complex to F-actin and stabilizes the circumferential actin belt. Proceedings of the National Academy of Sciences of the United States of America *105*, 13-19.

Ando, K., Uemura, K., Kuzuya, A., Maesako, M., Asada-Utsugi, M., Kubota, M., Aoyagi, N., Yoshioka, K., Okawa, K., Inoue, H.*, et al.* (2011). N-cadherin regulates p38 MAPK signaling via association with JNK-associated leucine zipper protein: implications for neurodegeneration in Alzheimer disease. The Journal of biological chemistry *286*, 7619-7628.

Aplin, A.E., Howe, A., Alahari, S.K., and Juliano, R.L. (1998). Signal transduction and signal modulation by cell adhesion receptors: the role of integrins,

cadherins, immunoglobulin-cell adhesion molecules, and selectins. Pharmacological reviews *50*, 197-263.

Balzar, M., Bakker, H.A., Briaire-de-Bruijn, I.H., Fleuren, G.J., Warnaar, S.O., and Litvinov, S.V. (1998). Cytoplasmic tail regulates the intercellular adhesion function of the epithelial cell adhesion molecule. Molecular and cellular biology *18*, 4833-4843.

Balzar, M., Briaire-de Bruijn, I.H., Rees-Bakker, H.A., Prins, F.A., Helfrich, W., de Leij, L., Riethmuller, G., Alberti, S., Warnaar, S.O., Fleuren, G.J.*, et al.* (2001). Epidermal growth factor-like repeats mediate lateral and reciprocal interactions of Ep-CAM molecules in homophilic adhesions. Molecular and cellular biology *21*, 2570-2580.

Balzar, M., Winter, M.J., de Boer, C.J., and Litvinov, S.V. (1999). The biology of the 17-1A antigen (Ep-CAM). J Mol Med (Berl) *77*, 699-712.

Baum, B., and Georgiou, M. (2011). Dynamics of adherens junctions in epithelial establishment, maintenance, and remodeling. The Journal of cell biology *192*, 907-917.

Bazzoni, G., and Hemler, M.E. (1998). Are changes in integrin affinity and conformation overemphasized? Trends in biochemical sciences *23*, 30-34.

Birchmeier, W., Brinkmann, V., Niemann, C., Meiners, S., DiCesare, S., Naundorf, H., and Sachs, M. (1997). Role of HGF/SF and c-Met in morphogenesis and metastasis of epithelial cells. Ciba Foundation symposium *212*, 230-240; discussion 240-236.

Bloch, R.J. (1992). Clusters of neural cell adhesion molecule at sites of cell-cell contact. The Journal of cell biology *116*, 449-463.

Brieher, W.M., and Gumbiner, B.M. (1994). Regulation of C-cadherin function during activin induced morphogenesis of Xenopus animal caps. The Journal of cell biology *126*, 519-527.

Bryant, D.M., Wylie, F.G., and Stow, J.L. (2005). Regulation of endocytosis, nuclear translocation, and signaling of fibroblast growth factor receptor 1 by E-cadherin. Molecular biology of the cell *16*, 14-23.

Buckley, C.D., Rainger, G.E., Bradfield, P.F., Nash, G.B., and Simmons, D.L. (1998). Cell adhesion: more than just glue (review). Molecular membrane biology *15*, 167-176.

Calderwood, D.A., and Ginsberg, M.H. (2003). Talin forges the links between integrins and actin. Nature cell biology *5*, 694-697.

Cavey, M., Rauzi, M., Lenne, P.F., and Lecuit, T. (2008). A two-tiered mechanism for stabilization and immobilization of E-cadherin. Nature *453*, 751-756.

Chen, C.L., and Chen, H.C. (2009). Functional suppression of E-cadherin by protein kinase Cdelta. Journal of cell science *122*, 513-523.

Chen, X., and Gumbiner, B.M. (2006). Crosstalk between different adhesion molecules. Current opinion in cell biology *18*, 572-578.

Chung, H.A., Yamamoto, T.S., and Ueno, N. (2007). ANR5, an FGF target gene product, regulates gastrulation in Xenopus. Current biology : CB *17*, 932-939.

Claas, C., Wahl, J., Orlicky, D.J., Karaduman, H., Schnolzer, M., Kempf, T., and Zoller, M. (2005). The tetraspanin D6.1A and its molecular partners on rat carcinoma cells. The Biochemical journal *389*, 99-110.

Davis, M.A., Ireton, R.C., and Reynolds, A.B. (2003). A core function for p120-catenin in cadherin turnover. The Journal of cell biology *163*, 525-534.

Defilippi, P., Bozzo, C., Volpe, G., Romano, G., Venturino, M., Silengo, L., and Tarone, G. (1994). Integrin-mediated signal transduction in human endothelial cells: analysis of tyrosine phosphorylation events. Cell adhesion and communication *2*, 75-86.

Ditlevsen, D.K., Povlsen, G.K., Berezin, V., and Bock, E. (2008). NCAM-induced intracellular signaling revisited. Journal of neuroscience research *86*, 727-743.

Doherty, G.J., Ahlund, M.K., Howes, M.T., Moren, B., Parton, R.G., McMahon, H.T., and Lundmark, R. (2011). The endocytic protein GRAF1 is directed to cell-matrix adhesion sites and regulates cell spreading. Molecular biology of the cell *22*, 4380-4389.

Doyle, E.L., Ridger, V., Ferraro, F., Turmaine, M., Saftig, P., and Cutler, D.F. (2011). CD63 is an essential cofactor to leukocyte recruitment by endothelial P-selectin. Blood *118*, 4265-4273.

Drees, F., Pokutta, S., Yamada, S., Nelson, W.J., and Weis, W.I. (2005). Alpha-catenin is a molecular switch that binds E-cadherin-beta-catenin and regulates actin-filament assembly. Cell *123*, 903-915.

Eto, M., Kitazawa, T., and Brautigan, D.L. (2004). Phosphoprotein inhibitor CPI-17 specificity depends on allosteric regulation of protein phosphatase-1 by regulatory subunits. Proceedings of the National Academy of Sciences of the United States of America *101*, 8888-8893.

Fagotto, F., Funayama, N., Gluck, U., and Gumbiner, B.M. (1996). Binding to cadherins antagonizes the signaling activity of beta-catenin during axis formation in Xenopus. The Journal of cell biology *132*, 1105-1114.

Faux, M.C., Rollins, E.N., Edwards, A.S., Langeberg, L.K., Newton, A.C., and Scott, J.D. (1999). Mechanism of A-kinase-anchoring protein 79 (AKAP79) and protein kinase C interaction. The Biochemical journal *343 Pt 2*, 443-452.

Fujita, Y., Krause, G., Scheffner, M., Zechner, D., Leddy, H.E., Behrens, J., Sommer, T., and Birchmeier, W. (2002). Hakai, a c-Cbl-like protein, ubiquitinates and induces endocytosis of the E-cadherin complex. Nature cell biology *4*, 222-231.

Gaiser, M.R., Lammermann, T., Feng, X., Igyarto, B.Z., Kaplan, D.H., Tessarollo, L., Germain, R.N., and Udey, M.C. (2012). Cancer-associated epithelial cell adhesion molecule (EpCAM; CD326) enables epidermal Langerhans cell motility and migration in vivo. Proceedings of the National Academy of Sciences of the United States of America *109*, E889-897.

Garrod, D.R., Merritt, A.J., and Nie, Z. (2002). Desmosomal adhesion: structural basis, molecular mechanism and regulation (Review). Molecular membrane biology *19*, 81-94.

Geiger, C., Nagel, W., Boehm, T., van Kooyk, Y., Figdor, C.G., Kremmer, E., Hogg, N., Zeitlmann, L., Dierks, H., Weber, K.S.*, et al.* (2000). Cytohesin-1 regulates beta-2 integrin-mediated adhesion through both ARF-GEF function and interaction with LFA-1. The EMBO journal *19*, 2525-2536.

Georgiou, M., Marinari, E., Burden, J., and Baum, B. (2008). Cdc42, Par6, and aPKC regulate Arp2/3-mediated endocytosis to control local adherens junction stability. Current biology : CB *18*, 1631-1638.

Gumbiner, B.M. (2005). Regulation of cadherin-mediated adhesion in morphogenesis. Nature reviews Molecular cell biology *6*, 622-634.

Hall, A. (1998). Rho GTPases and the actin cytoskeleton. Science *279*, 509-514.

Harris, T.J., and Peifer, M. (2004). Adherens junction-dependent and -independent steps in the establishment of epithelial cell polarity in Drosophila. The Journal of cell biology *167*, 135-147.

Hartsock, A., and Nelson, W.J. (2012). Competitive regulation of E-cadherin juxtamembrane domain degradation by p120-catenin binding and Hakai-mediated ubiquitination. PloS one *7*, e37476.

Hay, E., Laplantine, E., Geoffroy, V., Frain, M., Kohler, T., Muller, R., and Marie, P.J. (2009). N-cadherin interacts with axin and LRP5 to negatively regulate Wnt/beta-catenin signaling, osteoblast function, and bone formation. Molecular and cellular biology *29*, 953-964.

He, Q., and Meiri, K.F. (2002). Isolation and characterization of detergent-resistant microdomains responsive to NCAM-mediated signaling from growth cones. Molecular and cellular neurosciences *19*, 18-31.

Hynes, R.O. (2002). Integrins: bidirectional, allosteric signaling machines. Cell *110*, 673-687.

Ivanov, A.I., Samarin, S.N., Bachar, M., Parkos, C.A., and Nusrat, A. (2009). Protein kinase C activation disrupts epithelial apical junctions via ROCK-II dependent stimulation of actomyosin contractility. BMC cell biology *10*, 36.

Ivaska, J., Whelan, R.D., Watson, R., and Parker, P.J. (2002). PKC epsilon controls the traffic of beta1 integrins in motile cells. The EMBO journal *21*, 3608-3619.

Iwabu, A., Smith, K., Allen, F.D., Lauffenburger, D.A., and Wells, A. (2004). Epidermal growth factor induces fibroblast contractility and motility via a

protein kinase C delta-dependent pathway. The Journal of biological chemistry *279*, 14551-14560.

Izumi, G., Sakisaka, T., Baba, T., Tanaka, S., Morimoto, K., and Takai, Y. (2004). Endocytosis of E-cadherin regulated by Rac and Cdc42 small G proteins through IQGAP1 and actin filaments. The Journal of cell biology *166*, 237-248.

Jaggi, M., Rao, P.S., Smith, D.J., Wheelock, M.J., Johnson, K.R., Hemstreet, G.P., and Balaji, K.C. (2005). E-cadherin phosphorylation by protein kinase D1/protein kinase C{mu} is associated with altered cellular aggregation and motility in prostate cancer. Cancer research *65*, 483-492.

Jojovic, M., Adam, E., Zangemeister-Wittke, U., and Schumacher, U. (1998). Epithelial glycoprotein-2 expression is subject to regulatory processes in epithelial-mesenchymal transitions during metastases: an investigation of human cancers transplanted into severe combined immunodeficient mice. The Histochemical journal *30*, 723-729.

Keely, P., Parise, L., and Juliano, R. (1998). Integrins and GTPases in tumour cell growth, motility and invasion. Trends in cell biology *8*, 101-106.

Keller, R., Davidson, L., Edlund, A., Elul, T., Ezin, M., Shook, D., and Skoglund, P. (2000). Mechanisms of convergence and extension by cell intercalation. Philosophical transactions of the Royal Society of London Series B, Biological sciences *355*, 897-922.

Keller, R., and Winklbauer, R. (1992). Cellular basis of amphibian gastrulation. Current topics in developmental biology *27*, 39-89.

Kim, H.R., Appel, S., Vetterkind, S., Gangopadhyay, S.S., and Morgan, K.G. (2008). Smooth muscle signalling pathways in health and disease. Journal of cellular and molecular medicine *12*, 2165-2180.

Kiselyov, V.V., Soroka, V., Berezin, V., and Bock, E. (2005). Structural biology of NCAM homophilic binding and activation of FGFR. Journal of neurochemistry *94*, 1169-1179.

Kornberg, L., Earp, H.S., Parsons, J.T., Schaller, M., and Juliano, R.L. (1992). Cell adhesion or integrin clustering increases phosphorylation of a focal adhesion-associated tyrosine kinase. The Journal of biological chemistry *267*, 23439-23442.

Kovacs, E.M., Goodwin, M., Ali, R.G., Paterson, A.D., and Yap, A.S. (2002). Cadherin-directed actin assembly: E-cadherin physically associates with the Arp2/3 complex to direct actin assembly in nascent adhesive contacts. Current biology : CB *12*, 379-382.

Ladwein, M., Pape, U.F., Schmidt, D.S., Schnolzer, M., Fiedler, S., Langbein, L., Franke, W.W., Moldenhauer, G., and Zoller, M. (2005). The cell-cell adhesion molecule EpCAM interacts directly with the tight junction protein claudin-7. Experimental cell research *309*, 345-357.

Larue, L., Ohsugi, M., Hirchenhain, J., and Kemler, R. (1994). E-cadherin null mutant embryos fail to form a trophectoderm epithelium. Proceedings of the National Academy of Sciences of the United States of America *91*, 8263-8267.

Le Naour, F., Andre, M., Greco, C., Billard, M., Sordat, B., Emile, J.F., Lanza, F., Boucheix, C., and Rubinstein, E. (2006). Profiling of the tetraspanin web of human colon cancer cells. Molecular & cellular proteomics : MCP *5*, 845-857.

Le, T.L., Joseph, S.R., Yap, A.S., and Stow, J.L. (2002). Protein kinase C regulates endocytosis and recycling of E-cadherin. American journal of physiology Cell physiology *283*, C489-499.

Le, T.L., Yap, A.S., and Stow, J.L. (1999). Recycling of E-cadherin: a potential mechanism for regulating cadherin dynamics. The Journal of cell biology *146*, 219-232.

Linnenbach, A.J., Seng, B.A., Wu, S., Robbins, S., Scollon, M., Pyrc, J.J., Druck, T., and Huebner, K. (1993). Retroposition in a family of carcinoma-associated antigen genes. Molecular and cellular biology *13*, 1507-1515.

Litvinov, S.V., Balzar, M., Winter, M.J., Bakker, H.A., Briaire-de Bruijn, I.H., Prins, F., Fleuren, G.J., and Warnaar, S.O. (1997). Epithelial cell adhesion molecule (Ep-CAM) modulates cell-cell interactions mediated by classic cadherins. The Journal of cell biology *139*, 1337-1348.

Litvinov, S.V., van Driel, W., van Rhijn, C.M., Bakker, H.A., van Krieken, H., Fleuren, G.J., and Warnaar, S.O. (1996). Expression of Ep-CAM in cervical squamous epithelia correlates with an increased proliferation and the disappearance of markers for terminal differentiation. The American journal of pathology *148*, 865-875.

Litvinov, S.V., Velders, M.P., Bakker, H.A., Fleuren, G.J., and Warnaar, S.O. (1994). Ep-CAM: a human epithelial antigen is a homophilic cell-cell adhesion molecule. The Journal of cell biology *125*, 437-446.

Liu, W.S., and Heckman, C.A. (1998). The sevenfold way of PKC regulation. Cellular signalling *10*, 529-542.

Liu, Z., Tan, J.L., Cohen, D.M., Yang, M.T., Sniadecki, N.J., Ruiz, S.A., Nelson, C.M., and Chen, C.S. (2010). Mechanical tugging force regulates the size of

cell-cell junctions. Proceedings of the National Academy of Sciences of the United States of America *107*, 9944-9949.

Lu, Z., Liu, D., Hornia, A., Devonish, W., Pagano, M., and Foster, D.A. (1998). Activation of protein kinase C triggers its ubiquitination and degradation. Molecular and cellular biology *18*, 839-845.

Maetzel, D., Denzel, S., Mack, B., Canis, M., Went, P., Benk, M., Kieu, C., Papior, P., Baeuerle, P.A., Munz, M*., et al.* (2009). Nuclear signalling by tumour-associated antigen EpCAM. Nature cell biology *11*, 162-171.

Mahoney, M.G., Muller, E.J., and Koch, P.J. (2010). Desmosomes and desmosomal cadherin function in skin and heart diseases-advancements in basic and clinical research. Dermatology research and practice *2010*.

Marambaud, P., Wen, P.H., Dutt, A., Shioi, J., Takashima, A., Siman, R., and Robakis, N.K. (2003). A CBP binding transcriptional repressor produced by the PS1/epsilon-cleavage of N-cadherin is inhibited by PS1 FAD mutations. Cell *114*, 635-645.

McKoy, G., Protonotarios, N., Crosby, A., Tsatsopoulou, A., Anastasakis, A., Coonar, A., Norman, M., Baboonian, C., Jeffery, S., and McKenna, W.J. (2000). Identification of a deletion in plakoglobin in arrhythmogenic right ventricular cardiomyopathy with palmoplantar keratoderma and woolly hair (Naxos disease). Lancet *355*, 2119-2124.

Medina, A., Swain, R.K., Kuerner, K.M., and Steinbeisser, H. (2004). Xenopus paraxial protocadherin has signaling functions and is involved in tissue separation. The EMBO journal *23*, 3249-3258.

Mellstedt, H., Frodin, J.E., Masucci, G., Ragnhammar, P., Fagerberg, J., Hjelm, A.L., Shetye, J., Wersall, P., and Osterborg, A. (1991). The therapeutic use of

monoclonal antibodies in colorectal carcinoma. Seminars in oncology *18*, 462-477.

Mochly-Rosen, D., and Gordon, A.S. (1998). Anchoring proteins for protein kinase C: a means for isozyme selectivity. FASEB journal : official publication of the Federation of American Societies for Experimental Biology *12*, 35-42.

Morley, M., Jones, C., Sidhu, M., Gupta, V., Bernier, S.M., Rushlow, W.J., and Belliveau, D.J. (2010). PKC inhibition increases gap junction intercellular communication and cell adhesion in human neuroblastoma. Cell and tissue research *340*, 229-242.

Mutoh, T., Hamada, S., Senzaki, K., Murata, Y., and Yagi, T. (2004). Cadherin-related neuronal receptor 1 (CNR1) has cell adhesion activity with beta1 integrin mediated through the RGD site of CNR1. Experimental cell research *294*, 494-508.

Nagao, K., Ginhoux, F., Leitner, W.W., Motegi, S., Bennett, C.L., Clausen, B.E., Merad, M., and Udey, M.C. (2009a). Murine epidermal Langerhans cells and langerin-expressing dermal dendritic cells are unrelated and exhibit distinct functions. Proceedings of the National Academy of Sciences of the United States of America *106*, 3312-3317.

Nagao, K., Zhu, J., Heneghan, M.B., Hanson, J.C., Morasso, M.I., Tessarollo, L., Mackem, S., and Udey, M.C. (2009b). Abnormal placental development and early embryonic lethality in EpCAM-null mice. PloS one *4*, e8543.

Nagrath, S., Sequist, L.V., Maheswaran, S., Bell, D.W., Irimia, D., Ulkus, L., Smith, M.R., Kwak, E.L., Digumarthy, S., Muzikansky, A.*, et al.* (2007). Isolation of rare circulating tumour cells in cancer patients by microchip technology. Nature *450*, 1235-1239.

Naor, D., Sionov, R.V., and Ish-Shalom, D. (1997). CD44: structure, function, and association with the malignant process. Advances in cancer research *71*, 241-319.

Newton-Nash, D.K., and Newman, P.J. (1999). A new role for platelet-endothelial cell adhesion molecule-1 (CD31): inhibition of TCR-mediated signal transduction. J Immunol *163*, 682-688.

Orsulic, S., and Kemler, R. (2000). Expression of Eph receptors and ephrins is differentially regulated by E-cadherin. Journal of cell science *113 (Pt 10)*, 1793-1802.

Osta, W.A., Chen, Y., Mikhitarian, K., Mitas, M., Salem, M., Hannun, Y.A., Cole, D.J., and Gillanders, W.E. (2004). EpCAM is overexpressed in breast cancer and is a potential target for breast cancer gene therapy. Cancer research *64*, 5818-5824.

Pawson, T. (2004). Specificity in signal transduction: from phosphotyrosine-SH2 domain interactions to complex cellular systems. Cell *116*, 191-203.

Price, L.S., Hajdo-Milasinovic, A., Zhao, J., Zwartkruis, F.J., Collard, J.G., and Bos, J.L. (2004). Rap1 regulates E-cadherin-mediated cell-cell adhesion. The Journal of biological chemistry *279*, 35127-35132.

Ragnhammar, P., Fagerberg, J., Frodin, J.E., Hjelm, A.L., Lindemalm, C., Magnusson, I., Masucci, G., and Mellstedt, H. (1993). Effect of monoclonal antibody 17-1A and GM-CSF in patients with advanced colorectal carcinoma--long-lasting, complete remissions can be induced. International journal of cancer Journal international du cancer *53*, 751-758.

Ratheesh, A., Gomez, G.A., Priya, R., Verma, S., Kovacs, E.M., Jiang, K., Brown, N.H., Akhmanova, A., Stehbens, S.J., and Yap, A.S. (2012). Centralspindlin

and alpha-catenin regulate Rho signalling at the epithelial zonula adherens. Nature cell biology *14*, 818-828.

Rhee, J., Mahfooz, N.S., Arregui, C., Lilien, J., Balsamo, J., and VanBerkum, M.F. (2002). Activation of the repulsive receptor Roundabout inhibits N-cadherin-mediated cell adhesion. Nature cell biology *4*, 798-805.

Riedle, S., Kiefel, H., Gast, D., Bondong, S., Wolterink, S., Gutwein, P., and Altevogt, P. (2009). Nuclear translocation and signalling of L1-CAM in human carcinoma cells requires ADAM10 and presenilin/gamma-secretase activity. The Biochemical journal *420*, 391-402.

Riethmuller, G., Schneider-Gadicke, E., Schlimok, G., Schmiegel, W., Raab, R., Hoffken, K., Gruber, R., Pichlmaier, H., Hirche, H., Pichlmayr, R.*, et al.* (1994). Randomised trial of monoclonal antibody for adjuvant therapy of resected Dukes' C colorectal carcinoma. German Cancer Aid 17-1A Study Group. Lancet *343*, 1177-1183.

Ripani, E., Sacchetti, A., Corda, D., and Alberti, S. (1998). Human Trop-2 is a tumor-associated calcium signal transducer. International journal of cancer Journal international du cancer *76*, 671-676.

Roberts, M.S., Woods, A.J., Shaw, P.E., and Norman, J.C. (2003). ERK1 associates with alpha(v)beta 3 integrin and regulates cell spreading on vitronectin. The Journal of biological chemistry *278*, 1975-1985.

Rohani, N., Canty, L., Luu, O., Fagotto, F., and Winklbauer, R. (2011). EphrinB/EphB signaling controls embryonic germ layer separation by contact-induced cell detachment. PLoS biology *9*, e1000597.

Rosse, C., Linch, M., Kermorgant, S., Cameron, A.J., Boeckeler, K., and Parker, P.J. (2010). PKC and the control of localized signal dynamics. Nature reviews Molecular cell biology *11*, 103-112.

Roura, S., Miravet, S., Piedra, J., Garcia de Herreros, A., and Dunach, M. (1999). Regulation of E-cadherin/Catenin association by tyrosine phosphorylation. The Journal of biological chemistry *274*, 36734-36740.

Ryan, P.J., Oates, J.L., Crocker, J., and Stableforth, D.E. (1997). Distinction between pleural mesothelioma and pulmonary adenocarcinoma using MOC31 in an asbestos sprayer. Respiratory medicine *91*, 57-60.

Sano, K., Tanihara, H., Heimark, R.L., Obata, S., Davidson, M., St John, T., Taketani, S., and Suzuki, S. (1993). Protocadherins: a large family of cadherin-related molecules in central nervous system. The EMBO journal *12*, 2249-2256.

Schaap, D., and Parker, P.J. (1990). Expression, purification, and characterization of protein kinase C-epsilon. The Journal of biological chemistry *265*, 7301-7307.

Schlaepfer, D.D., and Hunter, T. (1998). Integrin signalling and tyrosine phosphorylation: just the FAKs? Trends in cell biology *8*, 151-157.

Schmidt, D.S., Klingbeil, P., Schnolzer, M., and Zoller, M. (2004). CD44 variant isoforms associate with tetraspanins and EpCAM. Experimental cell research *297*, 329-347.

Schumann, D., Chen, C.J., Kaplan, B., and Shively, J.E. (2001). Carcinoembryonic antigen cell adhesion molecule 1 directly associates with cytoskeleton proteins actin and tropomyosin. The Journal of biological chemistry *276*, 47421-47433.

Schwartz, M.A., Schaller, M.D., and Ginsberg, M.H. (1995). Integrins: emerging paradigms of signal transduction. Annual review of cell and developmental biology *11*, 549-599.

Sebastian, M. (2010). Review of catumaxomab in the treatment of malignant ascites. Cancer management and research *2*, 283-286.

Shigeta, M., Sanzen, N., Ozawa, M., Gu, J., Hasegawa, H., and Sekiguchi, K. (2003). CD151 regulates epithelial cell-cell adhesion through PKC- and Cdc42-dependent actin cytoskeletal reorganization. The Journal of cell biology *163*, 165-176.

Singh, R., Lei, P., and Andreadis, S.T. (2009). PKC-delta binds to E-cadherin and mediates EGF-induced cell scattering. Experimental cell research *315*, 2899-2913.

Slack-Davis, J.K., Eblen, S.T., Zecevic, M., Boerner, S.A., Tarcsafalvi, A., Diaz, H.B., Marshall, M.S., Weber, M.J., Parsons, J.T., and Catling, A.D. (2003). PAK1 phosphorylation of MEK1 regulates fibronectin-stimulated MAPK activation. The Journal of cell biology *162*, 281-291.

Slanchev, K., Carney, T.J., Stemmler, M.P., Koschorz, B., Amsterdam, A., Schwarz, H., and Hammerschmidt, M. (2009). The epithelial cell adhesion molecule EpCAM is required for epithelial morphogenesis and integrity during zebrafish epiboly and skin development. PLoS genetics *5*, e1000563.

Suzuki, A., Yamanaka, T., Hirose, T., Manabe, N., Mizuno, K., Shimizu, M., Akimoto, K., Izumi, Y., Ohnishi, T., and Ohno, S. (2001). Atypical protein kinase C is involved in the evolutionarily conserved par protein complex and plays a critical role in establishing epithelia-specific junctional structures. The Journal of cell biology *152*, 1183-1196.

Takahashi, K. (2001). The linkage between beta1 integrin and the actin cytoskeleton is differentially regulated by tyrosine and serine/threonine phosphorylation of beta1 integrin in normal and cancerous human breast cells. BMC cell biology *2*, 23.

Takes, R.P., Baatenburg de Jong, R.J., Schuuring, E., Hermans, J., Vis, A.A., Litvinov, S.V., and van Krieken, J.H. (1997). Markers for assessment of nodal metastasis in laryngeal carcinoma. Archives of otolaryngology--head & neck surgery *123*, 412-419.

Trzpis, M., McLaughlin, P.M., de Leij, L.M., and Harmsen, M.C. (2007a). Epithelial cell adhesion molecule: more than a carcinoma marker and adhesion molecule. The American journal of pathology *171*, 386-395.

Trzpis, M., Popa, E.R., McLaughlin, P.M., van Goor, H., Timmer, A., Bosman, G.W., de Leij, L.M., and Harmsen, M.C. (2007b). Spatial and temporal expression patterns of the epithelial cell adhesion molecule (EpCAM/EGP-2) in developing and adult kidneys. Nephron Experimental nephrology *107*, e119-131.

Van Aelst, L., and Symons, M. (2002). Role of Rho family GTPases in epithelial morphogenesis. Genes & development *16*, 1032-1054.

Wadham, C., Gamble, J.R., Vadas, M.A., and Khew-Goodall, Y. (2003). The protein tyrosine phosphatase Pez is a major phosphatase of adherens junctions and dephosphorylates beta-catenin. Molecular biology of the cell *14*, 2520-2529.

Wang, Y., Janicki, P., Koster, I., Berger, C.D., Wenzl, C., Grosshans, J., and Steinbeisser, H. (2008). Xenopus Paraxial Protocadherin regulates morphogenesis by antagonizing Sprouty. Genes & development *22*, 878-883.

Williams, E.J., Furness, J., Walsh, F.S., and Doherty, P. (1994). Activation of the FGF receptor underlies neurite outgrowth stimulated by L1, N-CAM, and N-cadherin. Neuron *13*, 583-594.

Winklbauer, R., Medina, A., Swain, R.K., and Steinbeisser, H. (2001). Frizzled-7 signalling controls tissue separation during Xenopus gastrulation. Nature *413*, 856-860.

Wurfel, J., Rosel, M., Seiter, S., Claas, C., Herlevsen, M., Weth, R., and Zoller, M. (1999). Metastasis-association of the rat ortholog of the human epithelial glycoprotein antigen EGP314. Oncogene *18*, 2323-2334.

Yamada, S., Pokutta, S., Drees, F., Weis, W.I., and Nelson, W.J. (2005). Deconstructing the cadherin-catenin-actin complex. Cell *123*, 889-901.

Yap, A.S., Brieher, W.M., and Gumbiner, B.M. (1997). Molecular and functional analysis of cadherin-based adherens junctions. Annual review of cell and developmental biology *13*, 119-146.

Yap, A.S., and Kovacs, E.M. (2003). Direct cadherin-activated cell signaling: a view from the plasma membrane. The Journal of cell biology *160*, 11-16.

Yap, A.S., Niessen, C.M., and Gumbiner, B.M. (1998). The juxtamembrane region of the cadherin cytoplasmic tail supports lateral clustering, adhesive strengthening, and interaction with p120ctn. The Journal of cell biology *141*, 779-789.

Yue, T., Tian, A., and Jiang, J. (2012). The cell adhesion molecule echinoid functions as a tumor suppressor and upstream regulator of the Hippo signaling pathway. Developmental cell *22*, 255-267.

Zeng, L., Fagotto, F., Zhang, T., Hsu, W., Vasicek, T.J., Perry, W.L., 3rd, Lee, J.J., Tilghman, S.M., Gumbiner, B.M., and Costantini, F. (1997). The mouse Fused locus encodes Axin, an inhibitor of the Wnt signaling pathway that regulates embryonic axis formation. Cell *90*, 181-192.

Zorzos, J., Zizi, A., Bakiras, A., Pectasidis, D., Skarlos, D.V., Zorzos, H., Elemenoglou, J., and Likourinas, M. (1995). Expression of a cell surface antigen recognized by the monoclonal antibody AUA1 in bladder carcinoma: an immunohistochemical study. European urology *28*, 251-254.

Figure legends

Figure 1.1. Cell adhesion molecules, structures and functions. (A) Diagram showing four major classes of cell adhesion molecules (CAMs), and the type of extracellular interactions they engage in, e.g. homophilic (with self) or heterophilic (with other adhesion molecules or with extracellular matrix components such as fibronectin). **(B)** Diagram showing the types of cytoplasmic interactions that occur downstream of cadherins and integrins.

Figure 1.2. EpCAM structure, glycosylation and EpCAM-based therapeutic antibody. (A) Catumaxomab is a rat-mouse hybrid monoclonal antibody that binds antigens EpCAM and CD3. Catumaxomab binds overexpressed EpCAM on tumor cells and CD3 on T-cells and, by doing so, triggers an immune response against the EpCAM-positive tumor cell. **(B)** Diagram showing structure of EpCAM. The extracellular domain (EpECD) contains 2 epidermal growth factor-like repeats (EGF I and EGF II) as well as 3 potentially N-glycosylation sites (N-Gly). "TM" refers to the transmembrane domain, and "EpTAIL" indicates the cytoplasmic domain/tail of the molecule. **(C)** EpCAM western blots from different species and cell lines indicated on top. Except for *Xenopus* EpCAM, which was detected using an antibody raised by the Fagotto lab against EpTAIL, EpCAMs in the three other cell lines were detected using mAb 323/A3 that targets the extracellular domain of the protein. *Xenopus* and Caco-2 blots were performed by me while blots for EpCAM in HCA and L-Ep cells were taken from Litvinov *et al.,* 1997. Arrows indicate possible glycosylated forms of EpCAM that migrate higher than the molecular weight of the protein.

Figure 1.3. *Xenopus laevis* gastrula. Sagittal cut of stage 10.5 embryo. The ectoderm, endoderm and mesoderm are shown. Brachet's cleft (black arrow) refers to the ectoderm/mesoderm boundary that forms on the dorsal side between involuting mesoderm (highlighted area) that is migrating animally (black curved arrow) and overlying ectoderm.

Figure 1.4. PKC structure and mode of activation. (A) Diagrams representing the different domains of classical PKCs (cPKC), novel PKCs (nPKC) and atypical PKCs (aPKC). "PS" refers to the pseudosubstrate domain, "C1" and "C2" to the conserved cysteine-rich zinc finger domains and "Kinase" indicates the catalytic domain of the protein. Collectively, "PS" "C1" and "C2" domains constitute the regulatory region of PKCs. **(B)** Diagram showing the mechanism of activation and regulation of PKC activity. In the cytoplasm PKC is kept inactive in a closed conformation mediated by an intramolecular interaction between the PS domain and the kinase domain. Autophosphorylation and phosphorylation by other cytoplasmic kinases "primes" PKC. PKCs are only fully activated upon translocation to the plasma membrane and interaction with co-activating factors (such as diacylglycerol "DAG" and other lipid activators "LA"). Binding of co-factors tethers the kinases to the plasma membrane and opens them up exposing the kinase domains to their substrates. Signaling of active "opened" PKCs can be negatively regulated by cytoplasmic proteins, such as AKAP, that bind to the catalytic sites of PKCs in the cytoplasm and keep them inactive.

Figure 1.1

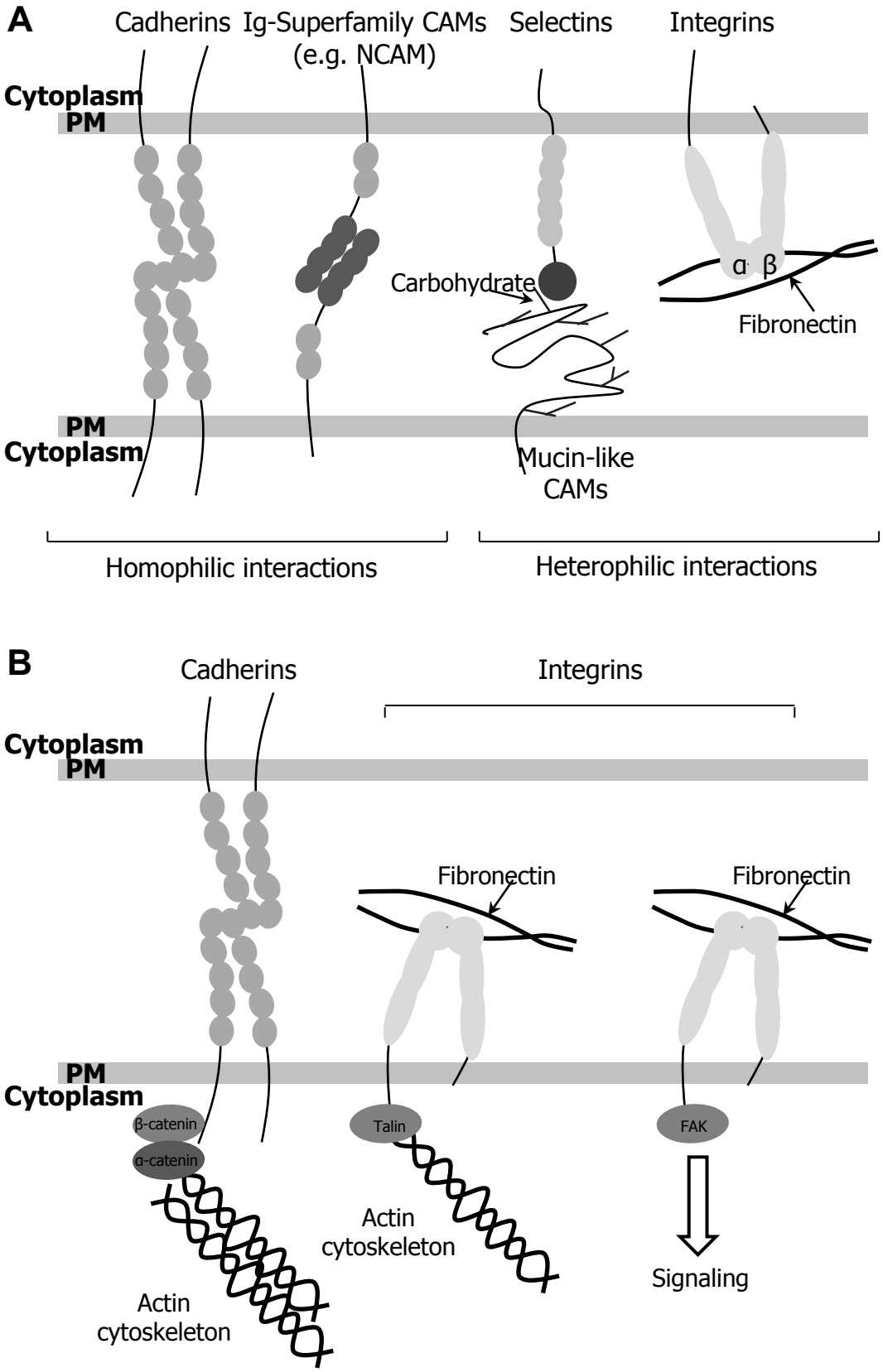
A
Cadherins
Ig-Superfamily CAMs
(e.g. NCAM)
Selectins
Integrins
Cytoplasm
PM
Carbohydrate
α β
Fibronectin
PM
Cytoplasm
Mucin-like
CAMs
Homophilic interactions
Heterophilic interactions
B
Cadherins
Integrins
Cytoplasm
PM
Fibronectin
Fibronectin
PM
Cytoplasm
β-catenin
α-catenin
Talin
FAK
Actin
cytoskeleton
Actin
cytoskeleton
Signaling

Figure 1.2

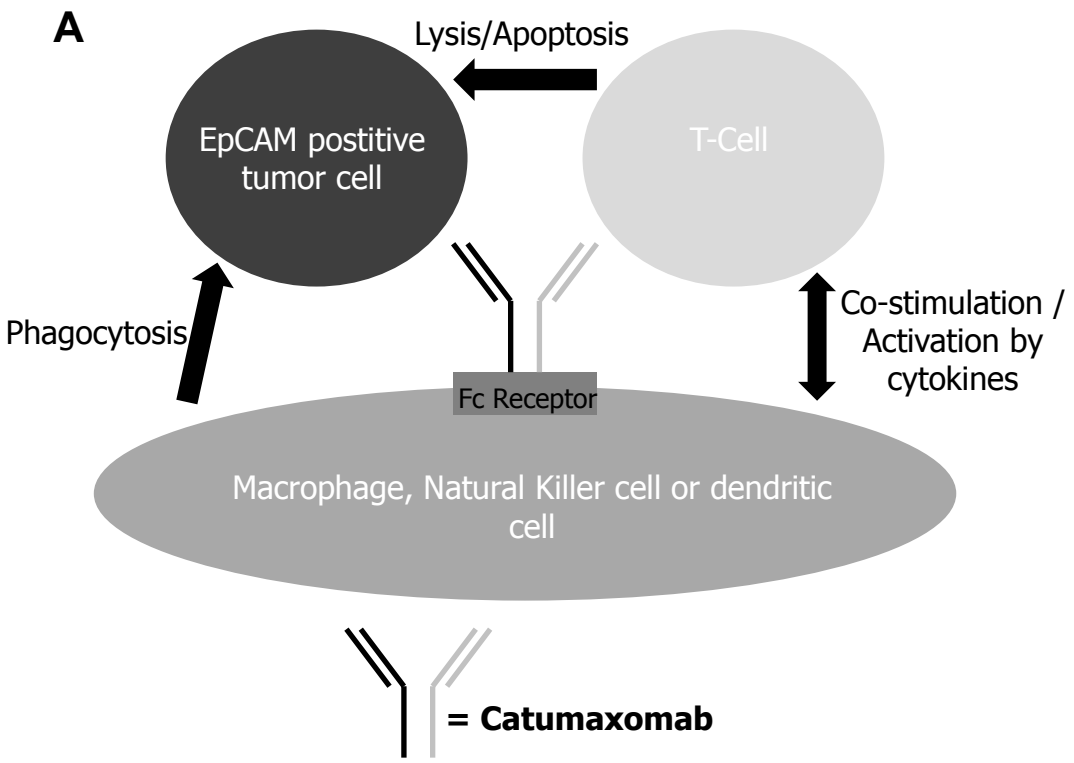
A
Lysis/Apoptosis
EpCAM postitive tumor cell
T-Cell
Phagocytosis
Co-stimulation / Activation by cytokines
Fc Receptor
Macrophage, Natural Killer cell or dendritic cell
= Catumaxomab

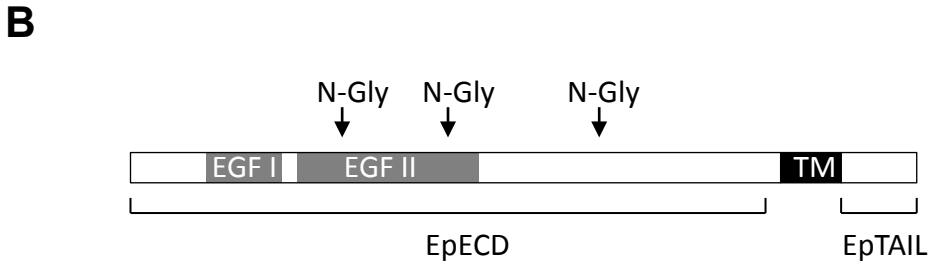
B
N-Gly
N-Gly
N-Gly
EGF I
EGF II
TM
EpECD
EpTAIL

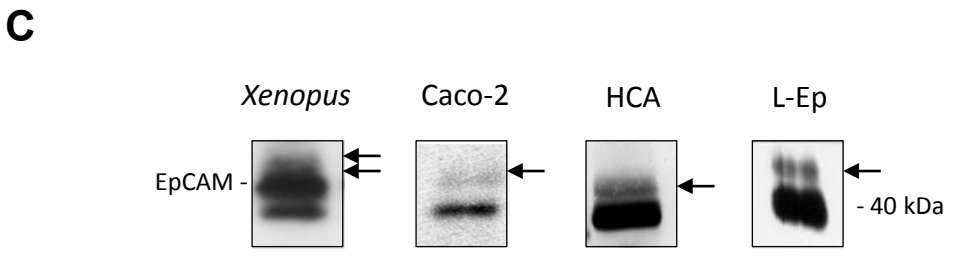
C
Xenopus
Caco-2
HCA
L-Ep
EpCAM -
- 40 kDa

Figure 1.3

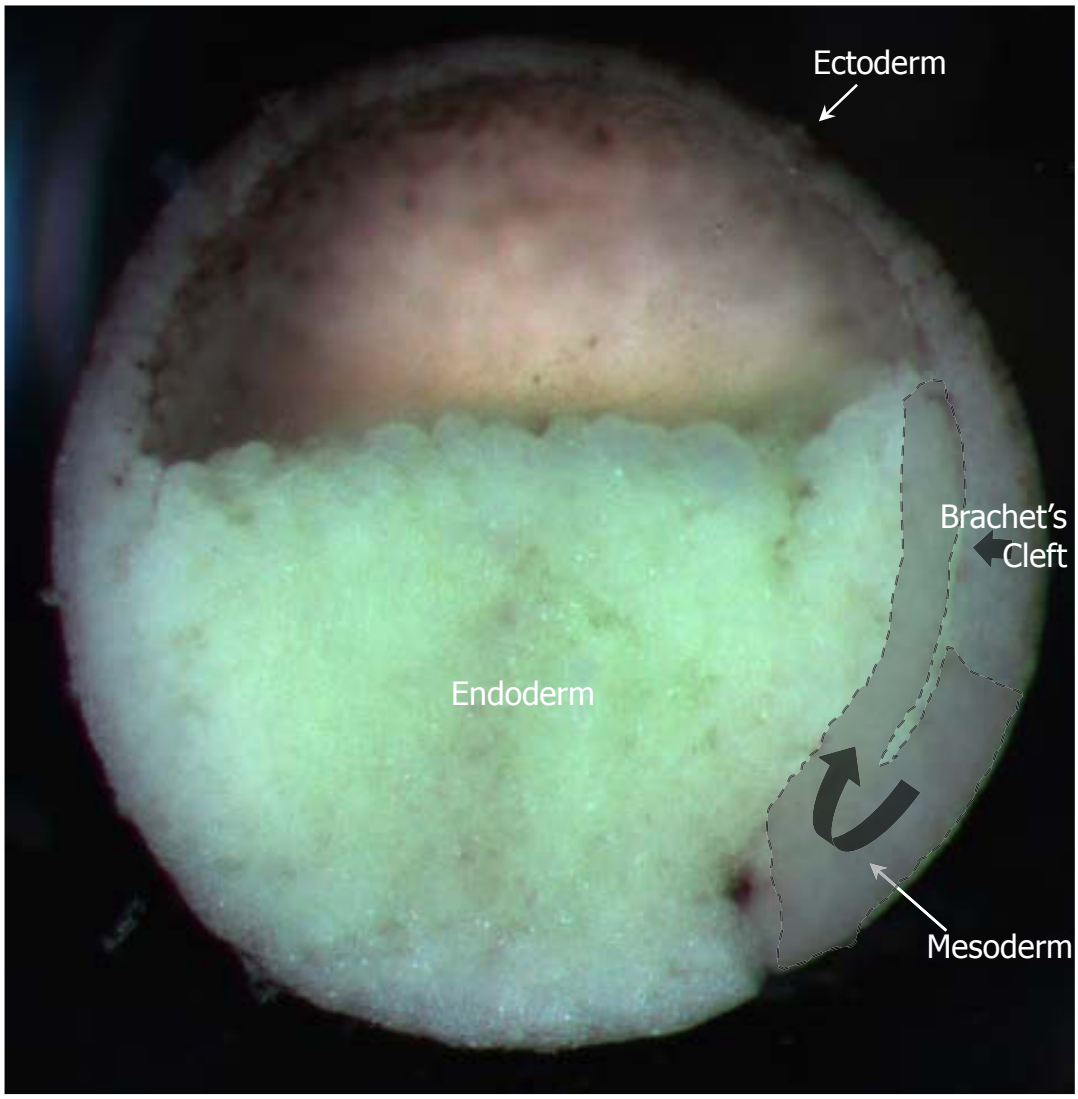

Figure 1.4

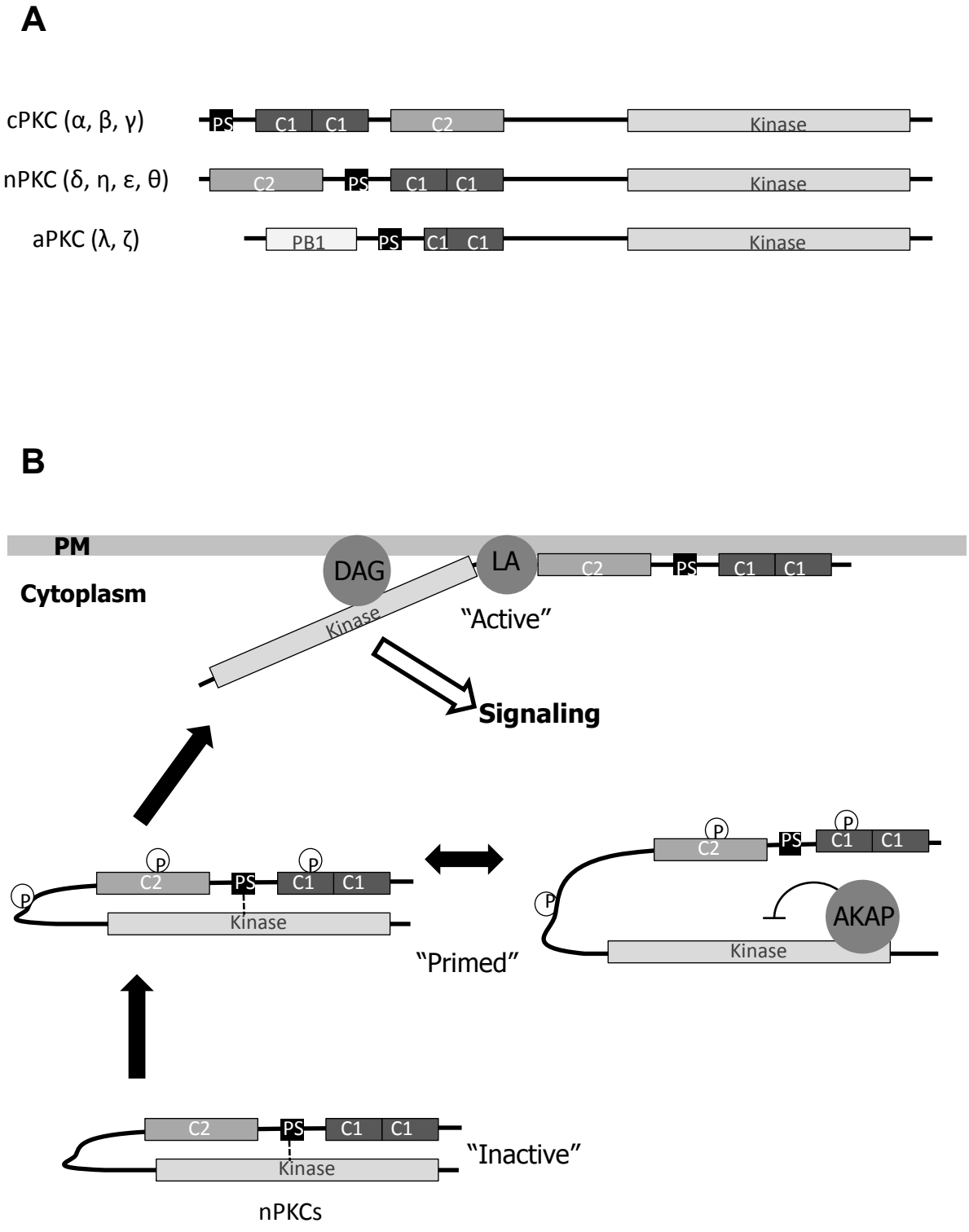
A
cPKC (α, β, γ)
PS
C1
C1
C2
Kinase
nPKC (δ, η, ε, θ)
C2
PS
C1
C1
Kinase
aPKC (λ, ζ)
PB1
PS
C1
C1
Kinase
B
PM
Cytoplasm
DAG
LA
C2
PS
C1
C1
Kinase
"Active"
Signaling
P
C2
PS
C1
C1
Kinase
"Primed"
AKAP
C2
PS
C1
C1
Kinase
"Inactive"
nPKCs

Bridge to Chapter II

In Chapter I, I reviewed the literature on cell adhesion molecules, EpCAM biology and briefly touched upon morphogenetic processes taking place during gastrulation in *Xenopus laevis* embryos. I also mentioned the gain-of-function screen that led to the identification of EpCAM as an ectoderm/mesoderm tissue mixing promoter in the frog. Chapter II focuses on characterizing the molecular mechanism by which EpCAM induces tissue mixing. The data presented in this chapter unravels a key role for EpCAM in gastrulation of *Xenopus*. At this developmental stage, EpCAM regulates cell motility within tissues. Chapter II is a reproduction of the following published article: **Maghzal N**, Vogt E, Reintsch W, Fraser JS, Fagotto F. 2010. The tumor-associated EpCAM regulates morphogenetic movements through intracellular signaling. The Journal of cell biology *191(3)*: 645-59.

CHAPTER II

The tumor associated EpCAM regulates morphogenetic movements through intracellular signaling

Abstract

Epithelial Cell Adhesion Molecule (EpCAM) is best known as a tumor associated protein highly expressed in carcinomas. The function of this cell surface protein during embryonic development and its potential role in cancer are still poorly understood. We identified EpCAM in a gain-of-function screen for inducers of abnormal tissue mixing during gastrulation. Elevated EpCAM levels in either the ectoderm or the mesoderm confer "invasive" properties to cells in both populations. We found that this phenotype represents an "over-stimulation" of an essential activity of EpCAM in controlling cell movements during embryonic development. Surprisingly, this property is independent of the putative adhesive function of EpCAM, and rather relies on a novel signaling function that operates through down-regulation of PKC activity. We show that inhibition of novel PKCs accounts entirely for the invasive phenotype induced by abnormally high levels of EpCAM as well as for its normal function in regulating cell rearrangement during early development.

Introduction

EpCAM has been long known as a tumor-associated antigen highly expressed in a variety of carcinomas (Koprowski et al., 1979). It is used as a marker for aggressive tumors, and has been considered as a potential target for immunotherapy (Osta et al., 2004) . In human and mouse, EpCAM is expressed in embryonic epithelia, but the levels usually drop as cells reach terminal differentiation (Trzpis et al., 2007). Enhanced expression of EpCAM is associated with active proliferation of neoplastic or normal tissues (Boer et al., 1999). The protein can act as a homophilic Ca^{2+}-independent cell-cell adhesion molecule (Litvinov et al., 1994). It is not structurally related to any of the major families of CAMs, but a potential link to the actin cytoskeleton via α-actinin has been documented (Balzar et al., 1998). Thus, it was initially proposed that enhanced proliferation and migration in cells expressing high levels of EpCAM resulted from sequestering α-catenin away from E-cadherin (Litvinov et al., 1997). However a recent study has shown that EpCAM is required

to maintain the integrity and plasticity of the Zebrafish developing epidermis where it works in partial redundancy with E-Cadherin to promote cell-cell adhesion (Slanchev et al., 2009). Another study indicates that the enhancing effect of EpCAM on proliferation rates of carcinoma may in fact largely rely on a signaling activity of its intracellular domain (Munz et al., 2004; Maetzel et al., 2009). This short segment can be cleaved and is then able to form a complex with FHL2, β-catenin and Lef-1 that induces gene transcription of oncogenes such as C-myc and cyclins A/E. Thus, the role of EpCAM in cell-cell adhesion and the relative contributions of its potential adhesive and signaling activities in morphogenesis and proliferation remain unclear.

Xenopus gastrulation is an established model to study morphogenetic movements. During this phase of development, the embryo undergoes massive reorganization. Since there is very little cell division and no increase in total cell mass at this stage, the whole process relies purely on rearrangement of preexisting tissues. In particular, the ectoderm thins and expands to eventually cover the whole embryo (epiboly), while the mesoderm moves inside the embryo through involution, and migrates along the inner surface of the ectoderm (blastocoel roof, BCR). We are particularly interested in the mechanisms that maintain the mesoderm separated from the overlying BCR, which is essential for proper gastrulation to proceed. This system is also more of interest as it deals with interactions between prototypical forms of epithelial and mesenchymal tissues. The ectoderm/mesoderm boundary can be particularly well studied in *Xenopus*, where it can be reconstituted in an in vitro assay using tissue explants (Winklbauer and Keller, 1996; Wacker et al., 2000). On the mesodermal side, the control of separation seems to depend in part on a still poorly characterized non-canonical Wnt pathway leading to PKC activation (Winklbauer et al., 2001). An interaction between the Wnt receptor Frizzled-7, the protocadherin PAPC, and the ankyrin repeat domain protein 5 xANR5, as well as downstream RhoA and Rho Kinase appear to be involved (Hukriede et al., 2003; Medina et al., 2004; Chung et al., 2007). Information is lacking about the mechanisms regulating separation on the ectodermal side.

We have identified the *Xenopus* orthologue of EpCAM in a gain-of-function screen to identify gene products that cause aberrant ectoderm/mesoderm tissue

mixing at gastrula stages. We show that the overexpression of EpCAM in either the ectoderm or the mesoderm causes both tissues to mix. More generally, we show that EpCAM levels crucially regulate movements of cells in embryonic tissues. Interestingly, this property is not restricted to the epithelium as EpCAM levels affect cell movements in the mesoderm-derived notochord (refer to addendum: Chapter IV). We demonstrate that this effect is not due to an adhesive function of EpCAM, but to a signaling activity involving novel PKC isoforms.

RESULTS

Identification of Xenopus EpCAM as a promoter of cell mixing between ectoderm-mesoderm

We identified a *Xenopus* orthologue of human EpCAM in a gain-of-function screen for gene products perturbing the ectoderm-mesoderm boundary, called Brachets' cleft. When EpCAM mRNA was injected in the dorsal region (Fig. 2.1A', green area), the embryos displayed a significant reduction of the posterior part of cleft (Fig. 2.1B-B'). BLAST search revealed that *Xenopus laevis* has two closely related EpCAM genes. Their amino-acid sequences are highly similar to each other and to EpCAM from other vertebrate species (Fig. 2.S1). All subsequent experiments were performed using constructs based on the EpCAMa clone originally identified in our screen.

To analyze the effect of EpCAM on tissue mixing, we used a well-established *in vitro* assay (Wacker et al., 2000), where dissected explants are pressed against a blastocoel roof (BCR), which is constituted of ectoderm (Fig. 2.2A). Explants of ectodermal origin readily mix in the BCR, while wild type mesoderm explants stay out. Note that compared to the original assay, we introduced an intermediate "fused" category corresponding to a partial loss of separation behavior (blurred boundary, yet explants still bulging out of the BCR). This phenotype is observed at low frequency with wild type mesoderm.

Consistent with the cleft phenotype observed in whole embryos, we found significant mixing upon EpCAM overexpression. Remarkably, EpCAM caused the

same phenotype when expressed either in the BCR or in the mesoderm (Fig. 2.2B-C). Simultaneous expression in both tissues did not strengthen the phenotype (data not shown). The effect appeared dose dependent, peaking around an mRNA dose of 250-300pg/injection.

We also examined reconstituted boundaries obtained by juxtaposition of dissected BCRs and mesoderm by cryosectioning and immunofluorescence (Fig. 2.1D). Compared to control boundaries (Fig. 2.1E), the interface between EpCAM-overexpressing BCRs and mesoderm was more irregular (Fig. 2.1E'), and cells from one tissue could be found to intrude into the other tissue (Fig. 2.1E''). In a few cases single ectodermal cells were even found isolated in the middle of the mesoderm explants (not shown), which is never observed for wild type tissues. Quantitative analysis of "rectilinearity" confirmed that upon EpCAM overexpression the interface departed very significantly from the relative straightness measured in controls (Fig. 2.1F).

Endogenous EpCAM is expressed in both ectoderm and mesoderm

EpCAM transcripts are present maternally and throughout development (data not shown). We determined EpCAM protein localization by immunofluorescence on cryosections using an antibody raised against its cytoplasmic tail. Unlike the epithelial-specific expression reported in mammalian embryos and adult tissues, *Xenopus* EpCAM is ubiquitously expressed in the gastrulating embryo (Fig. 2.1C). Some regional differences were observed, levels being highest in the ectoderm and lowest in the endoderm, but such differences may mostly reflect the default distribution of maternally-inherited components, as a graded distribution is also observed for C-cadherin (Fig. 2.1B) and for a variety of other proteins (unpublished results). Interestingly, EpCAM was slightly but reproducibly enriched at the cleft (arrowheads). EpCAM staining was strongly decreased in embryos injected with morpholino antisense nucleotides targeting both EpCAM alleles (EpCAM MO), demonstrating the specificity of the antibody (Fig. 2.1C'-C'').

EpCAM-induced mixing is mediated by its cytoplasmic domain.

To determine which EpCAM domains were required for induction of mixing, deletion mutants of EpCAM lacking the extracellular domain (ΔE) or the cytoplasmic tail (ΔC) were tested, both in the BCR and in the mesoderm (Fig. 2.2D). ΔE, but not ΔC, induced mixing as efficiently as wild type EpCAM, in both tissues. The mixing activity of the ΔE mutant was also observed on sections of reconstituted boundaries (Fig. 2.1F). These surprising results showed that the homophilic binding and adhesive function of EpCAM were dispensable for the mixing phenotype and suggested that signal transduction might be involved.

We further dissected the sequence requirements for this activity using a series of ΔE mutants (Fig. 2.S2). We determined that a short basic segment (RRKKGKYR) is sufficient for EpCAM function, and mutations within this cluster point to a requirement for specific residues (Fig. 2.S2). The same segment of human EpCAM has been reported to bind α-actinin (Balzar et al., 1998). However, we failed to reproduce this interaction with the cytoplasmic tail of *Xenopus* EpCAM (data not shown).

Tissue mixing does not correlate with cadherin stabilization

In Zebrafish embryos mutant for EpCAM, E-cadherin expression in ectodermal cells is decreased (Slanchev et al., 2009). We similarly found that EpCAM overexpressing cells had strongly increased levels of C-cadherin, the major cadherin expressed in *Xenopus* gastrulating embryos (Fig. 2.3). Importantly, this increase was observed in both ectoderm (Fig. 2.3A,B,G) and mesoderm (Fig. 2.3E,F). ΔE expression had a different effect: although total levels were not affected (Fig. 2.3G), two different anti-cadherin antibodies showed significant reduction of the cell membrane staining (Fig. 2.3D and D'). We have not been able to determine the cause of this lower signal, possibly due to more diffused membrane distribution, increased internalization, or decreased antibody accessibility. Note that the decreased cadherin staining is consistent with the fact that, unlike wild type, ΔE caused cell dissociation at later stages (data not shown). Despite these differences, wild type and ΔE EpCAM could both induce mixing, when expressed in either tissue, suggesting that the effect on

tissue separation was uncoupled from the effect on cadherin levels. This is inconsistent with a cell sorting mechanism based on classical differential adhesion.

EpCAM stimulates "intra-tissular" cell movements

We wondered whether EpCAM might regulate a different property common to both ectodermal and mesodermal cells, perhaps the ability of cells to move among other cells. To address this question, we looked at "intra-tissular" movements (Fig. 2.4A) in a "sandwich" prepared by pressing against each other two BCRs, one of which was manipulated, the other one wild type. After a two hour incubation, the sandwich was fixed and the position of the cells analyzed on cryosections. The rationale was that if cells move relative to their neighbors, the initial straight interface created by the apposition of the two BCRs would become progressively more irregular, and a mosaic pattern could eventually appear. The position of the manipulated cells at this interface was scored using a scale of increasing mobility, from 'non-protruding' (i.e. straight boundary) to 'single cells' (i.e. mosaic distribution) (Fig. 2.4E). Because EpCAM-induced ectoderm/mesoderm mixing had shown to peak around 250pg/injection, we tested two concentrations, 200 and 600pg. The patterns observed were striking (Fig. 2.4B-D): Compared to GFP controls, many more cells mildly overexpressing EpCAM had moved away and were found as single cells in the wild type half of the sandwich (Fig. 2.4E). Single and protruding cells added together were also significantly more numerous. The highest amount of EpCAM, however, had the opposite effect: the boundary remained straighter than in the controls (Fig. 2.4D,E). Thus EpCAM displays a bimodal activity, stimulating cell movements at moderate levels, but decreasing it at higher levels, fully consistent with the results of the mesoderm-BCR assays.

We found that the ΔE mutant could also stimulate migratory activity (Fig. 2.4E) when expressed at levels that induced efficient tissue mixing (40pg, Fig. 2.2). However, stronger expression did not lead to compaction as observed with wild type EpCAM: On the contrary, migration increased at 200pg mRNA (Fig. 2.4E). Higher levels caused the disaggregation of ectoderm cells (not shown).

Depletion of endogenous EpCAM interferes with ectoderm cell rearrangement

EpCAM depletion did not cause obvious defects in ectoderm-mesoderm boundary formation (not shown), but the BCR of the early gastrula was significantly thicker than normal (Fig. 2.5A-D, H), indicating that epiboly, a process that involves radial intercalation and leads to expansion and thinning of the tissue (Keller, 1980), was impaired. The phenotype was fully rescued by co-injection of mRNA coding for full-length EpCAM but lacking 5'UTR recognized by the morpholinos (Fig. 2.5E, H). In Zebrafish, a similar phenotype has been reported, and has been mostly discussed based on the presumed adhesive function of EpCAM (Slanchev et al., 2009). Here, we directly addressed this issue by testing the ability of ΔE to rescue epiboly in the EpCAM MO-injected embryos. ΔE could fully rescue a normal BCR (Fig. 2.5F, H), demonstrating that the extracellular domain, and thus homophilic binding, are dispensable for this function.

EpCAM depletion also inhibited cell movement in the BCR sandwich assay: EpCAM-depleted BCRs remained significantly more compact, maintaining a sharp boundary with the apposing wild type BCR (Fig. 2.4H).

EpCAM-induced tissue mixing is independent of β-catenin signaling

Since the EpCAM cytoplasmic tail can act as a signal transducer together with β-catenin and Lef1/TCF (Maetzel et al., 2009), we tested the ability of a dominant-negative xTCF3 construct (dnTCF) to interfere with EpCAM-induced mixing. The efficiency of dnTCF to block β-catenin/TCF-Lef signaling was verified using the well established axis-duplication assay (e.g. Molenaar et al., 1996; Fagotto et al., 1997; Zeng et al., 1997). At doses that completely blocked β-catenin-induced axis duplication (Fig. 2.6B), dnTCF had no effect on EpCAM-induced tissue mixing (Fig. 2.6A), demonstrating that β-catenin/TCF signaling is not involved in this phenotype.

EpCAM operates via downregulation of PKC activity

PKC signaling in the mesoderm has been implicated at the ectoderm-mesoderm boundary downstream of frizzled 7 (Winklbauer et al., 2001). Specifically, frizzled 7 depletion in the mesoderm caused tissue mixing, which could be rescued by overexpression of PKCα (and thus presumably PKC over-activation). We therefore sought to determine whether EpCAM-induced mixing may be related to PKC. We first attempted to rescue separation by directly activating PKC using the phorbol ester phorbol-12-myristate-13-acetate (PMA). A short pre-treatment of EpCAM-expressing mesoderm explants with a low concentration of PMA efficiently rescued separation (Fig. 2.6C). Similarly, PMA treatment of EpCAM-overexpressing BCRs also rescued separation (Fig. 2.6E). Furthermore, inhibition of PKC in wild type tissues by pre-treatment of either mesoderm explants or the BCR with Bisindolylmaleimide (Bis1), a specific inhibitor of classical (α, β, γ) and novel PKC isoforms (δ, ε) phenocopied EpCAM-induced mixing (Fig. 2.6D, E). We asked whether the epiboly phenotype observed upon EpCAM depletion may also be related to PKC activation: Normal epiboly was fully rescued by treating EpCAM MO embryos with Bis1 (Fig. 2.5G, H). Moreover, PMA treatment of wild type embryos induced a thicker BCR (Fig. 2.5I). Thus, the role of endogenous EpCAM in early development can be entirely accounted for by regulation of PKC activity.

That EpCAM negatively regulates PKC activity was directly assessed using an antibody recognizing phosphorylated PKC substrates (Fig. 2.7). This antibody stained multiple structures in ectoderm cells, with prominent signals at the cell periphery, at the nuclear membrane and inside the nuclei (Fig. 2.7A). EpCAM MO-injected BCRs (Fig. 2.7B) showed a much more intense staining than controls, which was drastically decreased by treatment with Bis1 (not shown) or Chelerythrine Chloride (another general PKC inhibitor, Fig. 2.7C). The effect of EpCAM depletion on p-PKC substrates was confirmed on Western blots, with a strong increase in several major bands (data shown in Chapter III).

To determine which PKC isoforms acted downstream of EpCAM, we used a panel of specific inhibitors to rescue EpCAM MO-induced epiboly defects. Since

Bis1 and PMA inhibit/activate both classical (α,β,γ) and novel (δ,ε), but not atypical isoforms, we focused mainly on the first two classes. Each inhibitor was titrated, and the data from the most effective concentration (mostly about 2 folds above the IC50) are shown. The results clearly pointed to novel PKC isoforms, since two specific inhibitors, a PKCε inhibitor peptide and a dominant negative PKCδ, both caused ectoderm-mesoderm mixing (Fig. 2.6E) and rescued normal epiboly as efficiently as Bis1 or Chelerythrine Chloride (Fig. 2.5J). Calphostin C, which has a preference for novel over classical PKCs, also fully rescued epiboly (Fig. 2.S3). Inhibitors of classical PKC, PKC-20-28, Gö 6976 and Ro-32-0432, had only weak effects, suggesting a minor contribution from the classical isoforms (Figs. 2.5J and 2.S3), and an inhibitor of atypical PKCs had no effect (Figs. 2.5J). The role of novel PKCs was further demonstrated by the fact that Coleon U, a specific activator of novel PKCs (Coutinho et al., 2009), induced BCR thickening, phenocopying EpCAM depletion (Fig. 2.5J). Novel PKCs also appeared crucial for ectoderm-mesoderm separation: The PKCε inhibitor and the dominant negative PKCδ induced mixing, while Gö6976 had no effect (Fig. 2.6F). Furthermore, Coleon U treatment of EpCAM-overexpressing BCRs fully rescued tissue separation (Fig. 6D).

We also examined the effect of the various inhibitors on the enhanced phospho-PKC substrate staining observed in EpCAM-depleted BCRs. The signal was reduced to various degrees by inhibitors of both classical and novel PKCs (Fig. 2.7C-F). Different inhibitors preferentially decreased the signal at specific subcellular locations, confirming that various PKC isoforms have distinct sets of targets. For instance, Gö6976 eliminated most of the nuclear membrane signal, but had little effect on the signal at the cell periphery. Globally, however, PKCδ and ε inhibitors had the strongest effect, lowering the signal close to the levels of wild type cells. These results indicate that EpCAM depletion causes a general increase in both classical and novel PKC activities. Nevertheless, the novel isoforms seem to play a major functional role in tissue separation and epiboly. We stained sections of whole embryos, and observed a weak but reproducible enrichment at contacts between ectoderm and mesoderm cells, scattered along the boundary (Fig. 2.7G), suggesting a potential locally controlled activation.

EpCAM levels affect the actin cytoskeleton

We hypothesized that the phenotypes observed may at least partly relate to changes in the actin-myosin cytoskeleton. For instance, one may expect that increased contractility would favor a stable tissue organization and ectoderm-mesoderm separation, while decreased contractility would be permissive for cell movements, including tissue rearrangement such as epiboly, and cell mixing.

The influence of EpCAM levels on the actin cytoskeleton organization was examined by phalloidin staining of whole BCRs (Fig. 2.8A-D), and the results confirmed by actin immunostaining on cryosections and live imaging of BCR expressing RFP-utrophin (data not shown): in wild type BCRs, we observed a thin irregular staining along the cell periphery, with larger patches located at corners between three cells (Fig. 2.8A, C). These patches became more prominent in EpCAM-depleted BCR, while the rest of the staining decreased (Fig. 2.8B). The lateral punctuate pattern was restored, and the large patches at corners disappeared upon treatment with novel PKC inhibitor (Fig. 2.8C), but not inhibitors of classical or atypical PKCs (data not shown). In EpCAM-overexpressing BCRs, the patches were largely absent, and the cells became outlined by a smooth continuous staining (Fig. 2.8D). Levels of phosphorylated myosin light chain detected by Western blot were reproducibly stronger in EpCAM-depleted tissues (Fig. 2.8J), although only very partially rescued by dominant negative PKCδ.

We examined cell protrusive activity by live confocal microscopy BCRs expressing membrane-targeted GFP (mGFP). Consistent with the pattern reported from phalloidin-stained Zebrafish embryos (Slanchev et al., 2009), the basal surface of BCR cells showed wide protrusions, which were globally less and more frequent in EpCAM MO and EpCAM overexpressing BCRs, respctively (Fig. 2.8E-H). A closer look at these protrusions (Fig. 2.8E-H) and at their dynamics (Fig. 2.S4, quantification presented in Fig. 2.8I) revealed that EpCAM-depleted cells formed in fact many protrusions, but these were generally shorter, thinner and most significantly short lived, as opposed to the extremely large and stable extensions produced by EpCAM-overexpressing cells.

We have recently analyzed the role of RhoA in the BCR assay and showed that blocking its activity on either side of the boundary by expression of a dominant negative form causes mixing (Rohani et al., submitted). We found here that activated RhoA could fully rescue the BCR-mesoderm boundary when co-expressed with EpCAM, either in the BCR or in the mesoderm (Fig. 2.8K,L), a result consistent with a role of EpCAM in antagonizing contractility.

Discussion

Our results reveal important aspects of EpCAM biology and also provide interesting insights into the mechanisms of morphogenesis.

It had been so far difficult to reconcile the proposed role of EpCAM as an adhesion molecule (Trzpis et al., 2007) with the observed cell phenotypes, in particular its stimulatory effect on in vitro cell migration (Osta et al., 2004) and its requirement in vivo to enable cells to rearrange during epiboly (Slanchev et al., 2009). Our data provide a different view of EpCAM function in morphogenesis. Indeed, the observed loss- and gain-of function phenotypes (epiboly phenotype, increased migration within the ectoderm, ectoderm-mesoderm mixing in both directions) can all be attributed to a single activity of EpCAM, which does not require its extracellular domain. This activity appears to impinge on a PKC-dependent pathway: 1) PKC inhibition fully rescues the loss-of-function epiboly phenotype and mimics the gain-of-function tissue mixing phenotype, 2) PKC activation interfered with epiboly and rescued rescues the ability of an over-expressing EpCAM tissue to maintain a boundary, and 3) EpCAM levels negatively affect endogenous PKC activity. We have established that novel PKCs play a major role in tissue separation and epiboly. Together with data implicating PKCδ in convergence extension (Kinoshita et al., 2003), novel PKCs emerge as crucial regulators of morphogenesis. We found no evidence for a role of classical, calcium-activated PKCα/β at the cleft, at least in the most downstream events activated/inhibited during our short pre-treatments. It is thus possible that PKCs are involved at two levels: classical PKCs in an upstream frizzled-calcium-dependent pathway (Sheldahl et al., 1999; Medina et al., 2004), and novel PKCs in regulating more proximally the actin cytoskeleton. Note

however that neither the role of classical PKC nor a direct requirement for calcium in PKC activation have been demonstrated in the context of tissue separation. Previous rescues have used PKCα overexpression (Winklbauer et al., 2001), which may have resulted from global, non-specific PKC over-activation. Yet, considering the many potential activities of PKCs, it is even possible that each isoform has multiple roles, of which we detect only the ones related to the most obvious phenotypes and/or to those most sensitive to modulation of PKC activity.

We show that PKC function is not restricted to the mesoderm, as previously assumed, and may in fact repress a general property of embryonic cells to move actively among other cells. Presumably, the establishment of a boundary requires this motile activity to be tamed. The widespread localization of PKC phosphorylated substrates and the global deregulation observed in EpCAM-depleted ectoderm explants suggest that this control is in place in all cells/tissues, although the enhanced signal detected along the cleft hint at an additional local activity specifically at the boundary, an interesting possibility to be addressed in the future.

Despite EpCAM being expressed at significant levels in the mesoderm and enriched at the cleft, loss of EpCAM function did not cause obvious defects in mesoderm involution or in tissue separation (data not shown). Whether the low levels left at this stage in MO-injected embryos are sufficient or whether EpCAM is not required in this context remains to be solved. Clearly however, a tight regulation of EpCAM levels is crucial for gastrulation: decreasing levels in the BCR lead to impaired cell mobility and block epiboly, while higher levels stimulate cell mobility and even cause neighboring tissues to mix. Note that EpCAM is also required for mesoderm morphogenesis at a slightly later stage (neurula), as we have observed failure of notochord cells to adopt their final arrangement in EpCAM-depleted embryos (unpublished results).

EpCAM appears to regulate cell movement via re-organization of the actin cytoskeleton, enabling cells to "flow" more freely within the tissue. Note that we still do not understand how cells "move" within these tissues. In our preliminary live images ectoderm cells seem to slide smoothly past each other (unpublished results),

and we do not think that the protrusions formed along the inner surface of the ectoderm (Slanchev et al., 2009 and our results) are necessarily involved in epiboly. However, these superficial structures are striking and represent a useful source of information about the dynamic state of the cytoskeleton: In the absence of EpCAM, cells appear to be frozen in a rigid, contracted state, unable to extend but very small and transient extensions. Filamentous actin accumulates in clusters and, although we do not know their nature (the phospho-myosin signal was too weak at this stage to confirm with confidence its presence at these sites), it is tempting to speculate by analogy with other systems (Cavey et al., 2008), that they represent structures under tension involved in restricting cell rearrangements. The increased total levels of phospho-myosin in EpCAM-depleted tissues and the fact that RhoA activation rescues separation (Fig. 2.8) are consistent with this hypothesis. With high EpCAM levels this tight actin organization is lost and large protrusions can extend, a process classically counteracted by Rho-induced contraction. Altogether, these observations suggest an antagonism between EpCAM-dependent signaling and actin-myosin contractility.

The chemical activators and inhibitors showed effects on tissue mixing within minutes, demonstrating that this is a rather direct response to PKC modulation. Even though, the downstream events are likely to be complex, considering the many targets of PKC. None of the other clones isolated in our screen had any obvious connection to PKC signaling (unpublished). It should be noted, however, that the initial round of this relatively small screen (~6000 clones), involved pools of 50-60 clones, which limited the amount of mRNA injected to 100pg per clone. Thus, only molecules particularly active at interfering with tissue separation could be picked, a fact that emphasizes the remarkable properties of EpCAM.

Classical models of sorting at early embryonic boundaries have assumed asymmetric properties of the two apposing tissues: one of the tissues would display stronger adhesion or stronger cortical tension (Steinberg and McNutt, 1999; Krieg et al., 2008), or each tissue would express a different set of adhesion molecules (Steinberg and Takeichi, 1994). While such differences might indeed contribute to the ectoderm/mesoderm boundary, our data show that cells from either tissue can

be induced to mix in a manner that appears perfectly symmetric according to several criteria (extracellular domain not required, PKC dependence, and RhoA rescue). Furthermore, mixing occurs irrespectively of changes in cadherins surface expression in the ectoderm or in the mesoderm, indicating that the process is largely insensitive to differences in cell-cell adhesion. This surprising observation is in fact quite consistent with our previous results on the notochord-somitic boundary, where cells could sort on either side of the boundary independently of the strength of cadherin-mediated adhesion (Reintsch et al., 2005).

A physiological role for EpCAM as a bona fide cell adhesion molecule remains to be established. In our experimental model, a "compacting" phenotype consistent with such function is observed only with highest levels of expression, and could also result from strong cadherin stabilization rather than direct EpCAM adhesion. In addition to its role in epiboly, EpCAM is required to maintain epithelial tissue integrity in Zebrafish (Slanchev et al., 2009), which has been interpreted as a result of EpCAM adhesive properties. We have observed a similar requirement for EpCAM in late (post-gastrulation) *Xenopus* embryos (unpublished data). Further studies are necessary to discriminate between direct roles in adhesion, or other possible function of the extracellular domains, dependent or independent of homophilic binding (e.g. localization to membrane subdomains). EpCAM is structurally unique among CAMs. It rather resembles Notch in its general extracellular domain organization and has some distant homology with the plasminogen activator (Cirulli et al., 1998), thus molecules functioning in signaling and cell migration. In this context, EpCAM has been found to co-purify with glycolipid-enriched lipid micro-domains (Schmidt et al., 2004; Claas et al., 2005; Ladwein et al., 2005), which have the potential to organize signaling complexes at the cell surface.

From the available data, EpCAM rather emerges as a crucial signaling molecule, controlling two independent pathways, one regulating cell proliferation via nuclear activities, which involve β-catenin-dependent transcripton (Maetzel et al., 2009), and this novel PKC-dependent role in morphogenetic processes. The remarkable "invasive" phenotype is obviously of interest for the understanding of EpCAM function in the context of adult tissues and metastasis. It is indeed tempting to

speculate that high levels of EpCAM may similarly provide cancer cells with the ability to move more actively within a tissue (and/or a tumor), help to escape the tissue of origin, and perhaps even invade other tissues.

Material and Methods

Embryo manipulations

Embryos were obtained as described previously (Danilchick et al., 1991). The culture, dissection and injection media used are the same as in Fagotto and Schohl (2003). Embryos were injected animally at the 2-cell stage (once in each blastomere) for BCR targeting, equatorially at the 4-cell stage (once in each dorsal blastomere) for mesoderm targeting and ventrally at the 4-cell stage (in one blastomere only) for the double-axis induction experiment. Embryonic staging was performed according to Nieuwkoop and Faber 1967. Dissections and assays were performed in MBS-H (Modified Barth Solution containing: 88mM NaCl, 1mM KCl, 2.4mM $NaHCO_3$, 0.82mM $MgSO_4$, 0.33mM $Ca(NO_3)_2$, 0.41mM $CaCl_2$, 10mM Hepes and 10μg/ml Streptomycin Sulfate and Penicillin, pH 7.4 adjusted with NaOH).

Plasmids, mRNAs and oligonucleotides

The following EpCAM cDNAs were cloned into pCS2+: EpCAM encodes full-length EpCAM (aa1-315). EpCAM-MT corresponds to full length EpCAM C-terminally fused to 6x myc tag, cloned into pCS2+MT. EpCAM-ΔC (aa1-278) had the cytoplasmic tail replaced by the 6xmyc-tag of pCS2+myc. ΔE-EpCAM was constructed by fusing the signal sequence and the 5th extracellular repeat of C-cadherin (gift from P. Hausen, Max-Planck-Institut fur Entwicklungsbiologie, Tuebingen, Germany) to a fragment of EpCAM lacking most of its extracellular domain (aa 265-315), cloned into pCS2+MT, containing a C-terminal 6xmyc-tag; ΔEΔ247 and ΔEΔ253 (deletion of the cytoplasmic tail after aa247 and aa 253) and ΔE-EpCAM-NQ (point mutations K243N and K244Q) and ΔE- QQ (R242Q and K244Q) were generated from ΔE-EpCAM by site directed mutagenesis. Other plasmids used: dnXTCF in pT7Ts (Molenaar et al., 1996), Myc-eGFP (Reintsch et al.,

2005) and β-galactosidase in pCS2+ (Rupp et al., 1994), dominant negative PKCδ (Kinoshita et al., 2003), and membrane-targeted GAP43-eGFP.

All pCS-EpCAM plasmids were linearized with Not I and mRNAs were synthesized in vitro using SP6 RNA polymerase.

Morpholino oligonucleotides: Control MO, 5'-CCTCTTACCTCAGTTACAATTTATA-3' (human β-globin mutant sequence); EpCAM1 MO, 5'-CTTCATCCTCCAACAGACGGAACCC-3'. EpCAM2 MO, 5'-GCCTCAGAGCTGTAACGAGCTGCAT-3'; Injected doses were 2x40ng control MO or 2x 20ng EpCAM MO1 + 20ng EpCAM MO2 per embryo.

Antibodies

Antibodies used in this study were rabbit anti-EpCAM antibody (raised against the cytoplasmic tail of EpCAM fused to GST), mouse anti-C-cadherin mAb 5G5 and rabbit anti-C-cadherin (generous gifts of B.M. Gumbiner, University of Virginia), mouse anti-myc tag mAb 9E10, , mouse anti-β-catenin mAb H102 (Santa Cruz), mouse anti-α-actinin antibody and rabbit anti-actin (Abcam) rabbit anti-phospho-myosin light chain and anti-phospho-PKC substrates (Cell signaling), and mouse anti-GFP mAb 3E6 (Molecular Probes).

PKC agonists and antagonists

Concentrations used and suppliers: Phorbol-12-myristate-13-acetate (PMA), 32nM; Bisindolylmaleimide I (Bis1), 500nM; Calphostin C, Chelerythrine Chloride (ChelCl), 1μM; Gö6976, 20nM; PKC-20-28, 20μM; Ro-32-0432, 30nM; all from Calbiochem. PKCε inhibitor peptide, 5μg/ml, Santa Cruz Biotech. PKC zeta peptide inhibitor, 2.5μM, Enzo Life Sciences. Coleon U was a generous gift from Dr. M.F. Simões, University of Lisbon. It was used at 5μM for epiboly and 10μM for mixing assays. They were all prepared from > 400x stock solutions in DMSO.

Explants

Tissue separation assays

The tissue separation assay were performed largely as described in Wacker et al., (2000). One modification from the original protocol was the source of mesoderm. To insure that the exact same region of the mesoderm would be dissected, independent of potential effects of exogenously expressed proteins on involution we

used, rather than involuted mesoderm, earlier pre-involuted mesoderm dissected from stage 10+ embryos (Winklbauer et al., 2001). Non-involuted mesoderm already displays strong separation behavior in the assay (Wacker et al., 2000). Statistical significance was determined using the Student's t-test, each experiment (2-3 BCRs and 8-15 explants) being treated as the experimental unit.

Sandwich assays and inner cell explants

Embryos were injected animally at the 2 cell stage. BCRs and mesoderm pieces were dissected from stage 10+ embryos. Sandwiches were gently pressed with a coverslip and cultured for 2 hours in 1x MBS-H, then fixed in 4% paraformaldehyde, embedded in 2% low-melting-agarose, permeabilized in 1 X PBS + 1% Triton, infiltrated with fish gelatin, and processed for cryosectioning and immunostaining as described (Fagotto and Brown, 2008). Explants of inner ectodermal cells were prepared from stage 10 BCRs by peeling off the inner cell layer using an eyelash. The explants were placed in 1 X MBS-H in 1% agarose coated dishes and cultured for 2 hours before fixation, agarose embedding, cryosectioning and immunostaining.

Cell migration in sandwich assays were repeated in three independent experiments. The % of cells in each category was calculated for each explants, and averaged for each experiment. The values were calculated as average of the three experiments (the average from all explants combined gave virtually identical values). Statistical significance was determined using the Student's t-test, using each sandwich as the experimental unit.

Immunofluorescence

Cryosectioning and immunofluorescence were performed as described previously (Schohl and Fagotto, 2002; Fagotto and Brown, 2008). Images were obtained using either an Axiovert TV135 micorscope (Carl Zeiss) equipped with a 25 X N.A. 0.8 water immersion objective (Carl Zeiss MicroImaging, Inc.) and a Retiga 2000R CCD camera (Quantitative Imaging Corporation), or a DM IRE2 microscope (Leica) equipped with a 20 X/0.70 IMM Corr CS oil immersion objective and a Hamamatsu ORCA-ER camera. Images were acquired using AnalySIS (Soft Imaging System GmbH) and MetaMorph (Molecular Devices) softwares. Large fields were reconstituted by collating pictures of adjacent regions (Schohl and Fagotto, 2002). Images of explants were acquired using a MZ16F stereomicroscope (Leica), a

QImaging camera (MicroPublisher 3.3 RTV) and QCapture image acquisition software (Quantitative Imaging Corporation).

Quantification of rectilinearity of reconstituted boundaries

Images of the interface between BCR and mesoderm explants were divided in segments of about 8 cell diameter. For each segment, the length of the interface, measured using the R software (http://www.r-project.org/), was divided by the length of the straight line connecting its ends. This ratio provided a measurement for straightness of the boundary. Data collected from three independent experiments, with a total of 11-12 sandwiches per condition, were analyzed using ANOVA.

Phalloidin staining

Dissected BCRs were put inner layer facing down on the glass of a FluoroDish chamber (World Precision Instruments), then covered with a small piece of a Minicell-CM 0.4μm membrane and a piece of coverglass secured with silicone grease and flattened by gently pressing the coverglass down. The membrane was inserted to improve diffusion during staining. BCRs were fixed in 4% formaldehyde in MBSX for 10min, followed by 5 min permeabilization in 1% formaldehyde, 0.1% TritonX100, 1 hr incubation with blocking buffer (10% sheep serum), and overnight incubation with 2U/ml Alexa488-phalloidin (Invitrogen) in 10% sheep serum. Images from planes about 3-5 μm inside the inner BCR surface were taken with a Zeiss LSM510 with a 40x Neofluar NA=1.3 oil objective.

Fluorescence live imaging

All experiments were performed at room temperature. Dissected BCRs were flattened on glass coated for 30min with 1μg/ml fibronectin (Sigma) and blocked for 10 min with 1% bovine serum albumin. The inner BCR surface was imaged with a Quorum technologies WaveFX spinning disc confocal mounted on an automated DMI6000B Leica microscope, with a 20x HC PL APO CS NA=0.7oil objective. Images were collected every 6 min with EM CCD 512X512 BT camera and controlled with Improvision Volocity 3DM software. For each condition, 5-6 cells were picked randomly in each image (4-5 images, from different BCRs, per condition, repeated in 3 independent experiments, with a total of 70 cells per

condition), and protrusions were followed over 10 frames to determine their life span. Statistical significance was determined using the Student's t-test.

Acknowledgements

This work was supported by CCSRI grant #017162 to F.F. N.M. is recipient of a Canderell McGill Cancer Centre award and a HydroQuebec fellowship. We thank Dr. Patrick Lemaire for generous gift of cDNA library, Dr. Barry Gumbiner for antibodies, and Dr. Noriyuki Kinoshita for dnPKCδ construct. We thank Caolan Kovach-Orr for writing codes and help with statistical analysis. We thank members of the lab and Dr. Rudi Winklbauer for critical reading of the manuscript.

References

Balzar, M., Bakker, H.A.M., Briaire-de-Bruijn, I.H., Fleuren, G.J., Warnaar, S.O., and S.V. Litvinov. 1998. Cytoplasmic Tail Regulates the Intercellular Adhesion Function of the Epithelial Cell Adhesion Molecule. *Mol. Cell Biol.*18(8): 4833-4843.

Balzar, M., Prins, F.A., Bakker, H.A.M., Fleuren, G.J., Warnaar, S.O., and S.V. Litvinov. 1999. The Structural Analysis of Adhesions Mediated by Ep-CAM. *Exp. Cell Res*. 246: 108-121.

de Boer, C.J., van Krieken, J.H., Janssen-van Rhijn, C.M., and S.V. Litvinov. 1999. Expression of Ep-CAM in normal, regenerating, metaplastic, and neoplastic liver. *J. Pathol.* 188: 201-206.

Cavallaro, U.. and G. Christofori. 2004. Cell adhesion and signalling by cadherins and Ig-CAMs in cancer. Nat. Rev. *Cancer* 4(2): 118-132.

Cavey, M., Rauzi, M., Lenne, J.F., and T. Lecuit. 2008. A two-tiered mechanism for stabilization and immobilization of E-cadherin. *Nature* 453:751-756.

Chen, X., and B.M. Gumbiner. 2006. Paraxial protocadherin mediates cell sorting and tissue morphogenesis by regulating C-cadherin adhesion activity. *J. Cell Biol.*174: 301-313.

Chung, H.A., Yamamoto, T.S., and N. Ueno. 2007. ANR5, an FGF Target Gene Product, Regulates Gastrulation in Xenopus. *Curr. Biol.* 17: 932-939.

Cirulli, V., Crisa, L., Beattie, G.M., Mally, M.I., Lopez, A.D., Fannon, A., Ptasznik, A., Inverardi, L., Ricordi, C., Deerinck, T., Ellisman, M., Reisfeld, R.A., and A. Hayek. 1998. KSA antigen Ep-CAM mediates cell-cell adhesion of pancreatic epithelial cells: morphoregulatory roles in pancreatic islet development. *J. Cell Biol.* 140: 1519-34.

Claas, C., Wahl, J., Orlicky, D.J., Karaduman, H., Schnölzer, M., Kempf, T., and M. Zöller. 2005. The tetraspanin D6.1A and its molecular partners on rat carcinoma cells. *Biochem J.* 389: 99-110.

Coutinho, I., Pereira, G., Simoes, M.F., Corte-Real, M., Goncalves, J. and Saraiva, L. 2009. Selective activation of protein kinase C-delta and -epsilon by 6,11,12,14-tetrahydroxy-abieta-5,8,11,13-tetraene-7-one (coleon U). *Biochem. Pharmacol.* 78: 449-459.

Danilchick, M., Peng, H.B., and B.K. Kay. 1991. Xenopus laevis: Practical uses in cell and molecular biology. Pictorial collage of embryonic stages. *Methods Cell Biol.* 36: 679-681.

Fagotto, F., and C.M. Brown. 2008. Detection of nuclear β-catenin in Xenopus embryos. *Methods Mol. Biol.* 469: 363-380.

Fagotto, F., Guger, K., and B.M. Gumbiner. 1997. Induction of the primary dorsalizing center in Xenopus by the Wnt/GSK/beta-catenin signaling pathway, but not by Vg1, Activin or Noggin. *Development.* 124:453-460.

Gumbiner, B.M. 2005. Regulation of cadherin-mediated adhesion in morphogenesis. *Nat. Rev. Mol. Cell Biol.*6: 622-634.

Halbleib, J.M., and W.J. Nelson. 2006. Cadherins in development: cell adhesion, sorting, and tissue morphogenesis. *Genes Dev.* 20: 3199-3214.

Hukriede, N.A., Tsang, T.E., Habas, R., Khoo, P.L., Steiner, K., Weeks, D.L., Tam, P.P., and I.B. Dawid. 2003. Conserved requirement of Lim1 function for cell movements during gastrulation. *Dev. Cell* 4(1): 83-94.

Keller, R.E. 1980. The cellular basis of epiboly: An SEM study of deep-cell rearrangement during gastrulation in Xenopus laevis. *J. Embr. Exper. Morphol.* 60(1): 201-234.

Kinoshita, N., Iioka, H., Miyakoshi, A., and N. Ueno. 2003. PKCδ is essential for Dishevelled function in a noncanonical Wnt pathway that regulates Xenopus convergent extension movements. *Genes Dev.* 17: 1663-1676.

Koprowski, H., Steplewski, Z., Mitchell, K., Herlyn, M., Herlyn, D., and P. Fuhrer. 1979. Colorectal carcinoma antigens detected by hybridoma antibodies. *Somatic Cell Genet.* 5(6): 957-971.

Krieg, M., Arboleda-Estudillo, Y., Puech, P.H., Kafer, J., Graner, F., Muller, D.J., and C.P. Heisenberg. 2008. Tensile forces govern germ-layer organization in zebrafish. *Nat. Cell Biol.*10(4): 429-436.

Ladwein, M., Pape, U.F., Schmidt, D.S., Schnölzer, M., Fiedler, S., Langbein, L., Franke, WW., Moldenhauer, G., and M. Zöller. 2005. The cell-cell adhesion molecule EpCAM interacts directly with the tight junction protein claudin-7. *Exp. Cell Res.* 309: 345-357.

Litvinov, S.V., Bakker, H.A., Gourevitch, M.M., Velders, M.P., and S.O. Warnaar. 1994. Evidence for a role of the epithelial glycoprotein 40 (Ep-CAM) in epithelial cell-cell adhesion. *Cell Adhes. Commun.* 2(5): 417-428.

Litvinov, S.V., Balzar, M., Winter, M.J., Bakker, H.A.M., Briaire-de Bruijn, I.H., Prins, F., Fleuren, G.J., and S.O. Warnaar. 1997. Epithelial Cell Adhesion Molecule (Ep-CAM) Modulates Cell-Cell Interactions Mediated by Classic Cadherins. *J. Cell Biol.* 139(5): 1337-1348.

Maetzel, D., Denzel, S., Mack, B., Canis, M., Went, P., Benk, M., Kieu, C., Papior, P., Baeuerle, P.A., and M. Munz. 2009. Nuclear signalling by tumour-associated antigen EpCAM. *Nat. Cell Biol.* 11(2): 162-171.

Medina, A., Swain, R.K., Kuerner, K-M., and H. Steinbeisser. 2004. Xenopus paraxial protocadherin has signaling functions and is involved in tissue separation. *EMBO J.* 23: 3249-3258.

Molenaar, M., van de Wetering, M., Oosterwegel, M., Peterson-Maduro, J., Godsave, S., Korinek, V., Roose, J., Destree, O., and H. Clevers. 1996. XTcf-3 transcription factor mediates beta-catenin-induced axis formation in Xenopus embryos. *Cell.* 86: 391-399.

Munz, M., Kieu, C., Mack, B., Schmitt, B., Zeidler, R., and O. Gires. 2004. The carcinoma-associated antigen EpCAM upregulates c-myc and induces cell proliferation. *Oncogene.* 23(34): 5748-5758.

Nieuwkoop, P.D., and J. Faber. 1967. Normal table of Xenopus laevis (Daudin). A systematical and chronological survey of the development from the fertilized egg till the end of metamorphosis. North-Holland Pub. Co., Amsterdam.

Osta, W.A., Chen, Y., Mikhitarian, K., Mitas, M., Salem, M., Hannun, Y.A., Cole, D.J., and W.E. Gillanders. 2004. EpCAM Is Overexpressed in Breast Cancer and Is a Potential Target for Breast Cancer Gene Therapy. *Cancer Res.* 64(16): 5818-5824.

Philippova, M., Joshi, M.B., Kyriakakis, E., Pfaff, D., Erne, P., and T.J. Resink. 2009. A guide and guard: The many faces of T-cadherin. *Cell Signal.* 21(7): 1035-1044.

Reintsch, W.E., Habring-Mueller, A., Wang, R.W., Schohl, A., and F. Fagotto. 2005. β-Catenin controls cell sorting at the notochord-somite boundary independently of cadherin-mediated adhesion. *J. Cell Biol.* 170(4): 675-686.

Rupp, R.A., Snider, L., and H. Weintraub. 1994. Xenopus embryos regulate the nuclear localization of XMyoD. *Genes Dev.* 8(11): 1311-1323.

Schmidt, D.S, Klingbeil, P., Schnölzer, M., and M. Zöller. 2004. CD44 variant isoforms associate with tetraspanins and EpCAM. *Exp. Cell Res.* 297: 329-347.

Schohl, A., and F. Fagotto. 2002. β-catenin, MAPK and Smad signaling during early Xenopus development. *Development*. 129(1): 37-52.

Schohl, A., and F. Fagotto. 2003. A role for maternal beta-catenin in early mesoderm induction in Xenopus. *EMBO J.* 22(13): 3303-3313.

Sheldahl, L.C., Park, M., Malbon, C.C., and R.T. Moon. 1999. Protein kinase C is differentially stimulated by Wnt and Frizzled homologs in a G-proteindependent manner. *Curr. Biol.* 9:695–698.

Slanchev, K., Carney, T.J., Stemmler, M.P., Koschorz, B., Amsterdam, A., Schwarz, H., and M. Hammerschmidt. 2009. The Epithelial Cell Adhesion Molecule EpCAM Is Required for Epithelial Morphogenesis and Integrity during Zebrafish Epiboly and Skin Development. *PLoS Genet.* 5(7): e1000563.

Steinberg, M., and P. McNutt. 1999. Cadherins and their connections: adhesion junctions have broader functions. *Curr. Op. Cell Biol.*11: 554-560.

Steinberg, M.S., and M. Takeichi. 1994. Experimental specification of cell sorting, tissue spreading, and specific spatial patterning by quantitative differences in cadherin expression. *Proc. Natl. Acad. Sci. USA*. 91(1): 206-209.

Trzpis, M., McLaughlin, P.M., de Leij, L.M., and M.C. Harmsen. 2007. Epithelial Cell Adhesion Molecule: More than a Carcinoma Marker and Adhesion Molecule. *Am. J. Pathol.* 171(2): 386-395.

Wacker, S., Grimm, K., Joos, T., and R. Winklbauer. 2000. Development and Control of Tissue Separation at Gastrulation in Xenopus. *Dev. Biol.* 224(2): 428-439.

Winklbauer, R. and R.E. Keller. 1996. Fibronectin, mesoderm migration, and gastrulation in Xenopus. *Dev. Biol.* 177(2): 413-426.

Winklbauer, R., Medina, A., Swain, R.K., and H. Steinbeisser. 2001. Frizzled-7 signalling controls tissue separation during Xenopus gastrulation. *Nature.* 413(6858): 856-860.

Zeng, L., Fagotto, F., Zhang, T., Hsu, W., Vasicek, T.J., Perry, W.L., Lee, J.J., Tilghman, S.M., Gumbiner, B.M., and F. Costantini. 1997. The mouse Fused locus encodes Axin, an inhibitor of the Wnt signaling pathway that regulates embryonic axis formation. *Cell.* 90:181-192.

Figure legends

Figure 2.1. Identification of EpCAM as inhibitor of the ectoderm-mesoderm boundary. (A) Diagram of an early *Xenopus* gastrula (stage 10.5). Curved arrow indicates direction of mesoderm involution. **(A')** Test for disruption of the ectoderm-mesoderm boundary (Brachet's cleft) by dorsal injection of mRNA (green). (**B, B'**) Sagittal views of the dorsal region of embryos injected with control GFP mRNA (B) or EpCAM mRNA (B'). The boundary (arrowheads) is disrupted in the posterior region (arrow) of EpCAM-overexpressing embryos. Cryosections were stained with anti-C-cadherin antibody. Note that exposure has been increased for controls to match the staining intensity of EpCAM-expressing samples. For proper comparison of C-cadherin levels, see figure 3. (**C**) Ubiquitous expression of endogenous EpCAM in all three germ layers, ectoderm (ecto), mesoderm (meso) and endoderm (endo) of the early gastrula. Arrowheads point to Brachet's cleft. (**C'-C"**) Detail of ectoderm from cryosections of control MO (COMO) and EpCAM MO-injected embryos stained with anti-EpCAM antibody, demonstrating antibody specificity. **(D-F)** Reconstituted boundaries made of dissected wild type mesoderm sandwiched between two injected BCRs, analyzed by cryosectioning and immunofluorescence. **(D)** Diagram of the assay. **(E-E")** Examples of a control boundary (E) and of the irregular interfaces observed between wild type mesoderm and EpCAM-overexpressing BCR (E', E"). Membrane GFP was co-expressed as tracer. Cell contours were visualized using an anti-β-catenin (red) and injected ectodermal cells with anti-GFP ab (green). **(F)** Quantification of boundary straightness (see Materials and Methods), represented in box plots (50% of the data are within the box, the median is represented by a horizontal line, the whiskers indicate the maximum and minimum value, without outliers, and the single dots the outliers). 1 corresponds to a perfectly rectilinear boundary, high values to convoluted lines, reflecting tissue mixing. EpCAM and its ΔE mutant caused significant mixing compared to controls ($p<0.001$, Tukey-HSD test). Numbers on top represent # fields/ # sandwiches (from 3 independent experiments).

Figure 2.2. EpCAM induces ectoderm/mesoderm tissue mixing. **(A)** Diagram of the *in vitro* tissue separation assay. mRNA is injected animally at the 2 cell stage for BCR expression and dorsally at the 4-cell stage for mesoderm expression. At stage 10+, explants and BCRs are dissected and combined, and the degree of separation is scored as "out" (complete separation), "fused" or "mixed". **(B)** Roof assay of control GFP-expressing and EpCAM- overexpressing mesoderm on wt BCRs. The three EpCAM-overexpressing mesoderm, distinguishable thank to their lighter color, have mixed with the BCR, while control explants have remained out. **(C)** Quantification of tissue mixing induced by EpCAM in the BCRs or in the mesoderm. mRNA amounts/injection are indicated. β-gal and membrane GFP mRNAs were used as controls. **(D)** The extracellular domain of EpCAM is dispensable for induction of tissue mixing. Quantification of tissue mixing upon expression in the BCR (C) or the mesoderm (D) of full length EpCAM (FL), or mutant constructs lacking the cytoplasmic tail (ΔC) or the extracellular domain (ΔE). In both tissues, the cytoplasmic tail is required for activity, but the extracellular domain is dispensable. Numbers on top indicate total # explants/# experiments. * and ** indicate respectively $p<0.05$ and $p<0.01$ compared to controls (Student's t-test).

Figure 2.3. C-Cadherin levels are increased by wild type EpCAM but not by ΔE EpCAM. (**A-F**) Sections of control membrane GFP, wild type EpCAM, or ΔE EpCAM-expressing tissues (200pg mRNA/injection) stained for C-cadherin. C,D: double staining using mouse monoclonal 5G5 (C,D) or rabbit polyclonal CE antibodies (C',D'). Note that exposure has been increased in C,D compared to A,B. (**E**) Western Blot comparing C-Cadherin levels in control GFP- and EpCAM or ΔE-expressing ectoderm explants.

Figure 2.4. EpCAM stimulates cell migration within the ectodermal tissue. **(A)** Schematic representation of a migration assay in ectoderm explants. Sandwiches were produced by combining wild type uninjected BCRs with BCRs injected with various mRNAs coding for membrane GFP, EpCAM-MT (see Suppl. fig. 2) or ΔE, or with EpCAM MO or COMO (co-injected with membrane GFP mRNA to trace injected cells). The degree of mixing was scored by determining the relative position of individual injected cells, immunostained for GFP or Myc, at the interface with wild type cells. **(B-D)** Examples of sandwiches with BCRs expressing control membrane GFP, and low and high levels of EpCAM. **(E)** Illustration of the four categories used to score cell migration: cells protruding less than ½ cell diameter relative to their neighbors (non-protr.), cells protruding between ½ and 1 diameter (0.5-1), or more than one cell diameter (>1), and cells entirely surrounded by wild type cells (single cells). **(F-H)** Quantification. Cells moderately overexpressing EpCAM tended to migrate significantly more, while cells with high EpCAM levels remained more compacted. Cells expressing ΔE also showed increased migration, for both mRNA doses tested. On the contrary, cells depleted of EpCAM (EpCAM MO) remained significantly more compact. Numbers on top indicate total # explants/# experiments. * and ** indicate respectively $p<0.05$ and $p<0.01$ compared to controls (Student's t-test, see Material and Methods).

Figure 2.5. Block of BCR epiboly upon EpCAM depletion and rescue by ΔE EpCAM or by PKC inhibition. **(A-B)** Cross-sections of early gastrula BCRs from embryos injected with control MO (COMO) and EpCAM MO. Sections were stained with anti-C-cadherin antibody. **(C-F)** Higher magnification views of BCRs from controls, EpCAM MO, and rescue by full length EpCAM or ΔE mRNA co-injection. Arrows indicate the outer and inner surfaces of the BCRs. Control BCRs were 2-3 cell layers thick, including the outer layer, which does not undergo radial intercalation. EpCAM MO BCRs were much thicker. Normal morphology was rescued by EpCAM or ΔE. **(G)** BCR of an embryo injected with EpCAM MO and incubated for 2 hrs with the PKC inhibitor Bis1 before fixation. **(H)** Quantification of BCR thickness (counted as # of inner cell layers, excluding the outer layer). ** indicate $p<0.01$ compared to EpCAM MO (Student's t-test). **(I)** Impaired epiboly upon treatment with PMA or Coleon U (Col U), a specific inhibitor of novel PKCs. ** indicate $p<0.01$ compared to controls. **(J)** Effect of selective PKC inhibitors on epiboly of EpCAM MO-injected embryos. ** indicate $p<0.01$ compared to EpCAM MO. Activator/inhibitor concentrations are listed in Material and Methods. Numbers on top indicate total # explants/# experiments.

Figure 2.6. EpCAM-induced tissue mixing is independent of β-cat/TCF signaling but involves downregulation of PKC signaling. **(A)** Effect of dominant negative xTCF (dnTCF) co-expression. dnTCF does not rescue EpCAM-induced cell mixing. **(B)** Effect of dnTCF on secondary axis induction by β-catenin. dnTCF completely abolished double-axis induction. **: $p<0.01$, Student's t-test. **(C)** Rescue of EpCAM-induced mixing by PMA and Coleon U (ColU). EpCAM overexpressing BCRs or mesoderm explants were incubated in the presence of PMA/Coleon U for 15 min prior to the assay. * and ** indicate respectively $p<0.05$ and $p<0.01$ compared to EpCAM alone. **(D)** PKC inhibition interferes with tissue separation. Wild-type BCRs or mesoderm explants were pre-incubated for 15 min in the presence of 500nM Bis1. The assay was then performed in the absence (2nd column) or in the presence (3rd column) of Bis1. * and ** indicate respectively $p<0.05$ and $p<0.01$ compared to controls. **(E)** Effect of PKC isoform-specific inhibitors on tissue separation. Inhibitors were added to the BCRs 15 min prior assembling the assay. In the case of Gö6976, the assay was also then performed in the continuous presence of the inhibitor (last column). * and ** indicate respectively $p<0.05$ and $p<0.01$ compared to controls. Numbers on top indicate total # explants/# experiments.

Figure 2.7. PKC over-activation in EpCAM-depleted embryos, and enhanced activation at the ectoderm-mesoderm boundary. **(A-F)** Cryosections of ectoderm explants stained with an antibody recognizing phosphorylated PKC substrates. **(A)** Control, with weak signal at the cell periphery (large arrows), in the nucleus (small arrow), and at the nuclear membrane (arrowheads). Note that not all nuclei are visible on one section. **(B)** Bright signal in EpCAM depleted cells, including a prominent signal at the periphery (large arrows) and at the nuclear membrane (arrowheads). **(C-E)** Strong decrease after treatment of EpCAM-depleted explants with Chelerythrine Chloride (ChelCl, inhibitor of classical and novel PKCs), PKCε peptide inhibitor, or expression of dominant negative PKCδ. **(F)** Partial selective decrease (mostly cytoplasm and nuclear membrane) after treatment with Gö6976 (classical PKCs). **(G, G')** Dorsal region of stage 10.5 whole embryo section double-stained for C-cadherin (red channel, G), and phospho-PKC substrates (green channel, G', including enlarged areas and corresponding pseudocolors). Nuclei were counterstained with Hoechst (not shown). Exposure is higher than for panels A-F. The signal tends to be enriched along parts of Brachet's cleft (arrowheads). Other bright signals correspond mainly to nuclei and mitotic structures (small arrows).

Figure 2.8. Effects of EpCAM depletion on actin cytoskeleton organization, myosin phosphorylation and protrusive activity. **(A-D)** Confocal images of phalloidin stained BCR explants. **(A)** Typical punctate phalloidin pattern (arrowheads) in control cells (COMO) with prominent accumulation at tricellular corners (large arrows). **(B)** Concentration at corners in EpCAM MO cells (large arrows), and decrease of the signal along the membranes. **(C)** Rescue of membrane staining and disappearance of the signal at corners upon co-injection of dominant negative PKCδ mRNA. **(D)** Homogenous membrane staining of EpCAM-overexpressing cells. **(E-H)** Live confocal images of the surface of membrane GFP-expressing BCR cells. Arrows: large protrusion. Arrowheads: small protrusions. **(I)** Quantitation of protrusive activity from time lapse movies (see selected frames in Suppl. Fig. S4). EpCAM MO-injected cells showed much fewer long lasting protrusions than controls ($p = 2{,}5E^{-07}$, Student's t-test) but many more short live extensions ($p = 5{,}4E^{-07}$). Most protrusions emanating from EpCAM-overexpressing cells were long lived ($p = 6{,}9E^{-06}$ compared to GFP controls). **(J)** Increased myosin light chain (MLC) phosphorylation in EpCAM MO BCRs, and partial rescue by co-expression of dominant negative PKCδ. **(K-L)** Rescue of tissue separation by co-expression of constitutively active RhoA. EpCAM mRNA (200pg) was injected alone or with V14RhoA mRNA (25pg). Numbers on top indicate total # explants/# experiments. * indicate $p<0.05$ compared to EpCAM alone (Student's t-test).

Supplementary figure legends

Figure 2.S1. Amino acid sequences of *Xenopus laevis* EpCAMa and b pseudoalleles and alignement with EpCAMs of representative Vertebrate species.

Figure 2.S2 (A) Diagram of the EpCAM constructs used in this study. The transmembrane (TM) and cytoplasmic (Ctail) domains and the 6xmyc tag, but not the extracellular domain (ECD), are presented on scale. **(B)** C-terminally myc-tagged EpCAM has the same tissue mixing activity as wild type EpCAM. **(C)** The mixing activity resides in specific residues of the cytoplasmic tail proximal to the transmembrane domain.

Figure 2.S3. Epiboly rescue experiments using the following PKC inhibitors: ChelCl, Chelerythrine Chloride; Calph, Calphostin C; 20-28, PKC-20-28; Gö, Gö6976; Ro32, Ro32-0432; dnPKCδ, dominant negative PKCδ; PKCεi, PKCε inhibitor; PKCζi, inhibitor of atypical PKCs. Numbers on top indicate total # explants/# experiments. * and ** indicate respectively $p<0.05$ and $p<0.01$ compared to controls, and NS indicates "not statistically significant (Student's t-test).

Figure 2.S4. Selected frames from live time lapse movies of BCRs expressing membrane GFP. Every second frames is shown (12 min time interval). Numbers: Examples of cells with long lived protrusions (arrows), or short lived protrusions (small arrowheads indicate the beginning and the end, large arrow heads the peak of protrusion extension). Note that large extensions often appear to be constituted of 2 or more parts that behaved independently (thin and large arrows in the last colum (EpCAM mRNA). In those cases, each part was scored as separate protrusions.

Figure 2.1

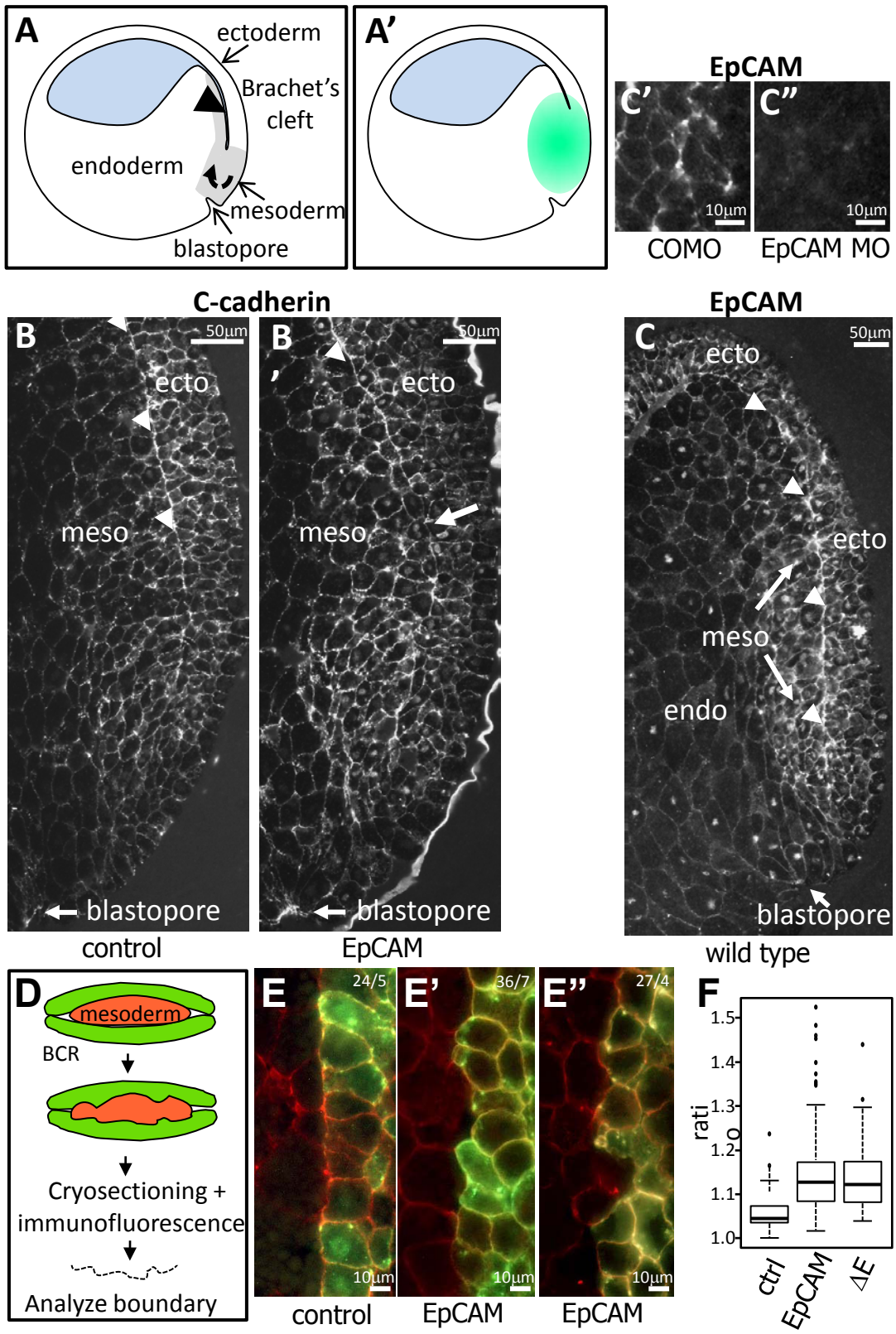
A
ectoderm
Brachet's cleft
endoderm
mesoderm
blastopore
A'
EpCAM
C'
C"
10µm
COMO
EpCAM MO
C-cadherin
B
50µm
ecto
meso
blastopore
control
B'
EpCAM
C
endo
wild type
D
mesoderm
BCR
Cryosectioning + immunofluorescence
Analyze boundary
E
24/5
E'
36/7
E"
27/4
F
ratio
ctrl
EpCAM
ΔE

Figure 2.2

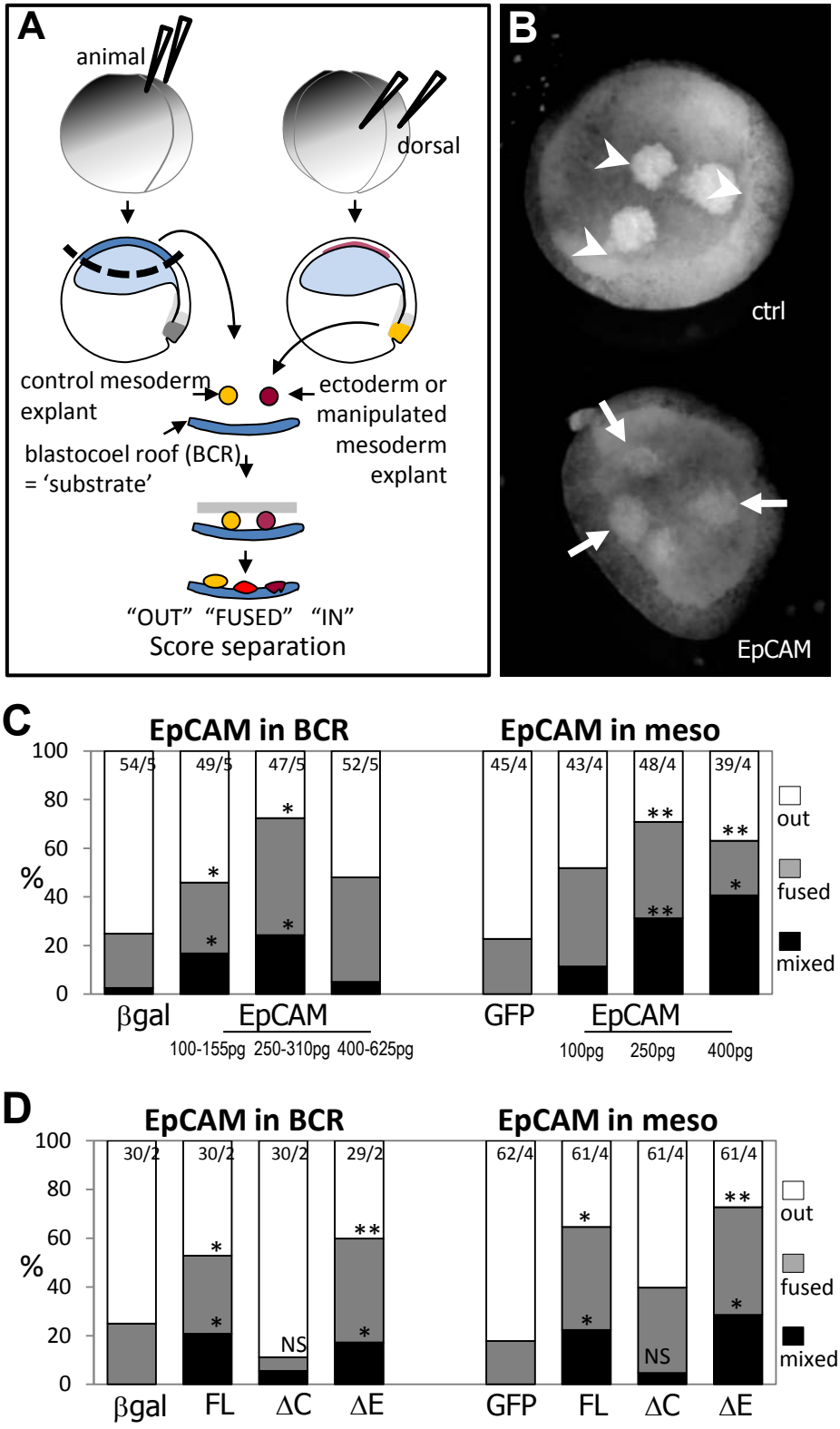
A
animal
dorsal
control mesoderm explant
ectoderm or manipulated mesoderm explant
blastocoel roof (BCR) = 'substrate'
"OUT" "FUSED" "IN"
Score separation
B
ctrl
EpCAM
C
EpCAM in BCR
EpCAM in meso
%
out
fused
mixed
βgal
EpCAM
100-155pg 250-310pg 400-625pg
GFP
EpCAM
100pg 250pg 400pg
D
EpCAM in BCR
EpCAM in meso
βgal
FL
ΔC
ΔE
GFP
FL
ΔC
ΔE
NS

Figure 2.3

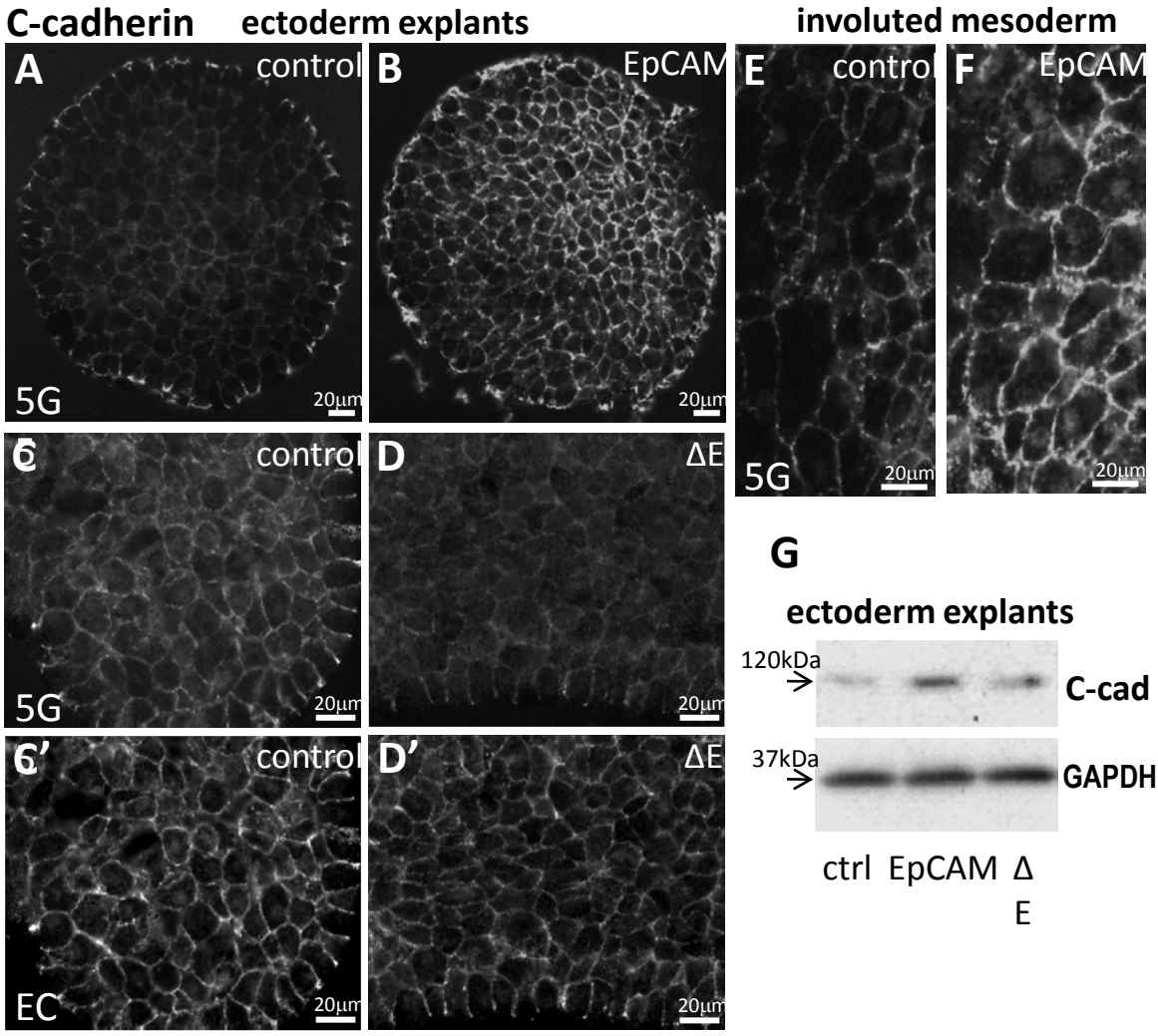
C-cadherin
ectoderm explants
involuted mesoderm
A
control
5G
20µm
B
EpCAM
20µm
E
control
5G
20µm
F
EpCAM
20µm
C
control
5G
20µm
D
ΔE
20µm
C'
control
EC
20µm
D'
ΔE
20µm
G
ectoderm explants
120kDa
C-cad
37kDa
GAPDH
ctrl
EpCAM
Δ E

Figure 2.4

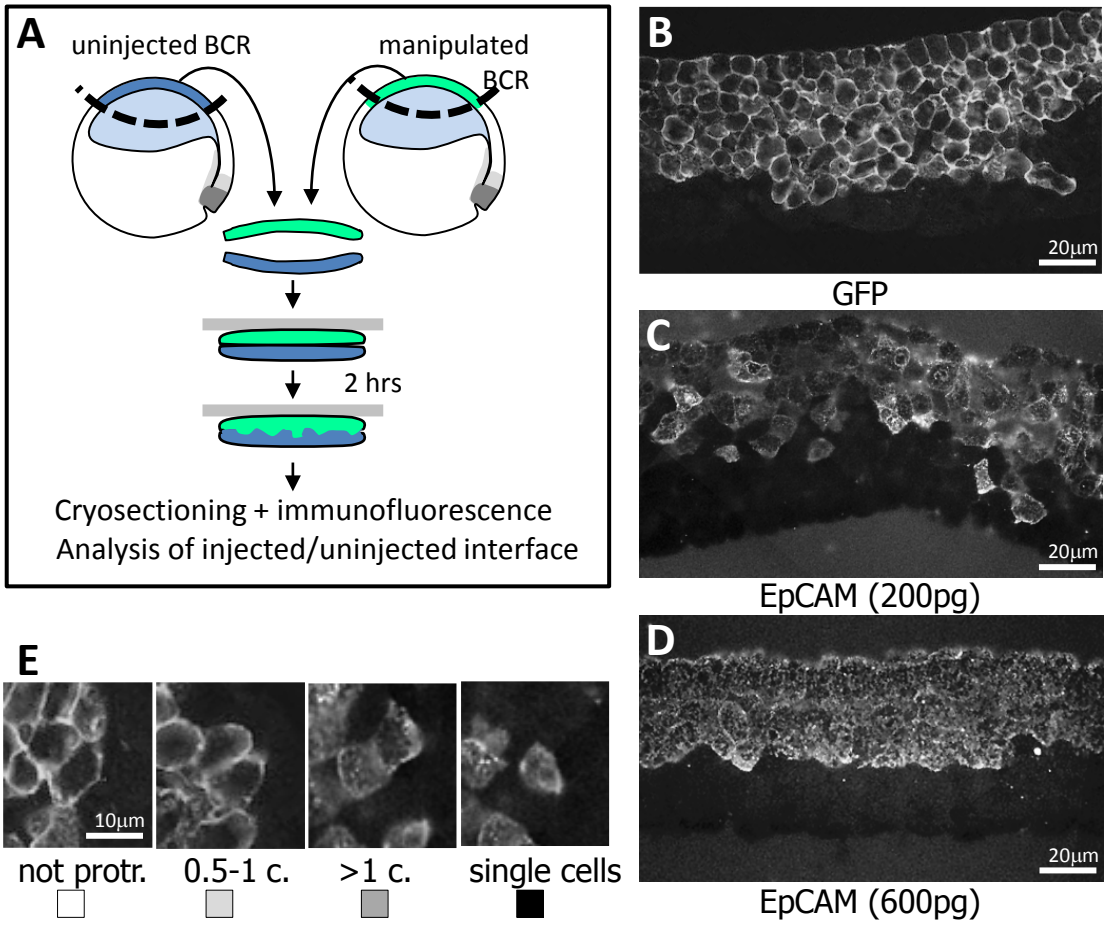
A
uninjected BCR
manipulated BCR
2 hrs
Cryosectioning + immunofluorescence
Analysis of injected/uninjected interface
B
20µm
GFP
C
20µm
EpCAM (200pg)
D
20µm
EpCAM (600pg)
E
10µm
not protr.
0.5-1 c.
>1 c.
single cells
F
cells/ explants:
825 /13
598/ 15
576/ 10
%
GFP
EpCAM (200pg)
EpCAM (600pg)
G
636/ 12
583/ 12
549/ 12
GFP
ΔE (40pg)
ΔE (200pg)
H
584/ 12
514/ 10
COMO
EpCAM MO

Figure 2.5

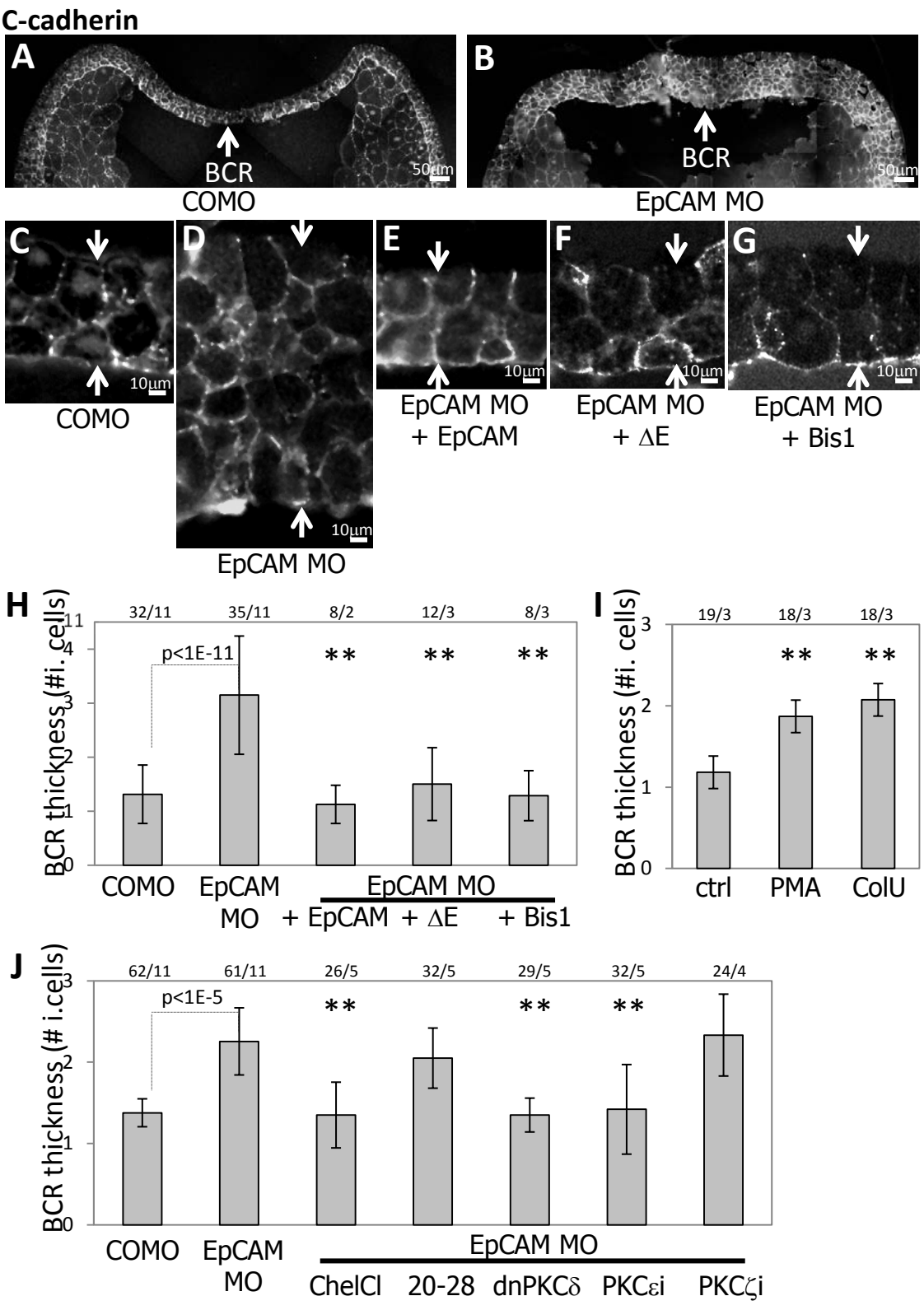
C-cadherin
A
BCR
50µm
COMO
B
BCR
50µm
EpCAM MO
C
10µm
COMO
D
10µm
EpCAM MO
E
10µm
EpCAM MO
+ EpCAM
F
10µm
EpCAM MO
+ ΔE
G
10µm
EpCAM MO
+ Bis1
H
BCR thickness (#i. cells)
32/11
35/11
8/2
12/3
8/3
p<1E-11
**
**
**
COMO
EpCAM MO
EpCAM MO
+ EpCAM
+ ΔE
+ Bis1
I
BCR thickness (#i. cells)
19/3
18/3
18/3
**
**
ctrl
PMA
ColU
J
BCR thickness (# i.cells)
62/11
61/11
26/5
32/5
29/5
32/5
24/4
p<1E-5
**
**
**
COMO
EpCAM MO
EpCAM MO
ChelCl
20-28
dnPKCδ
PKCεi
PKCζi

Figure 2.6

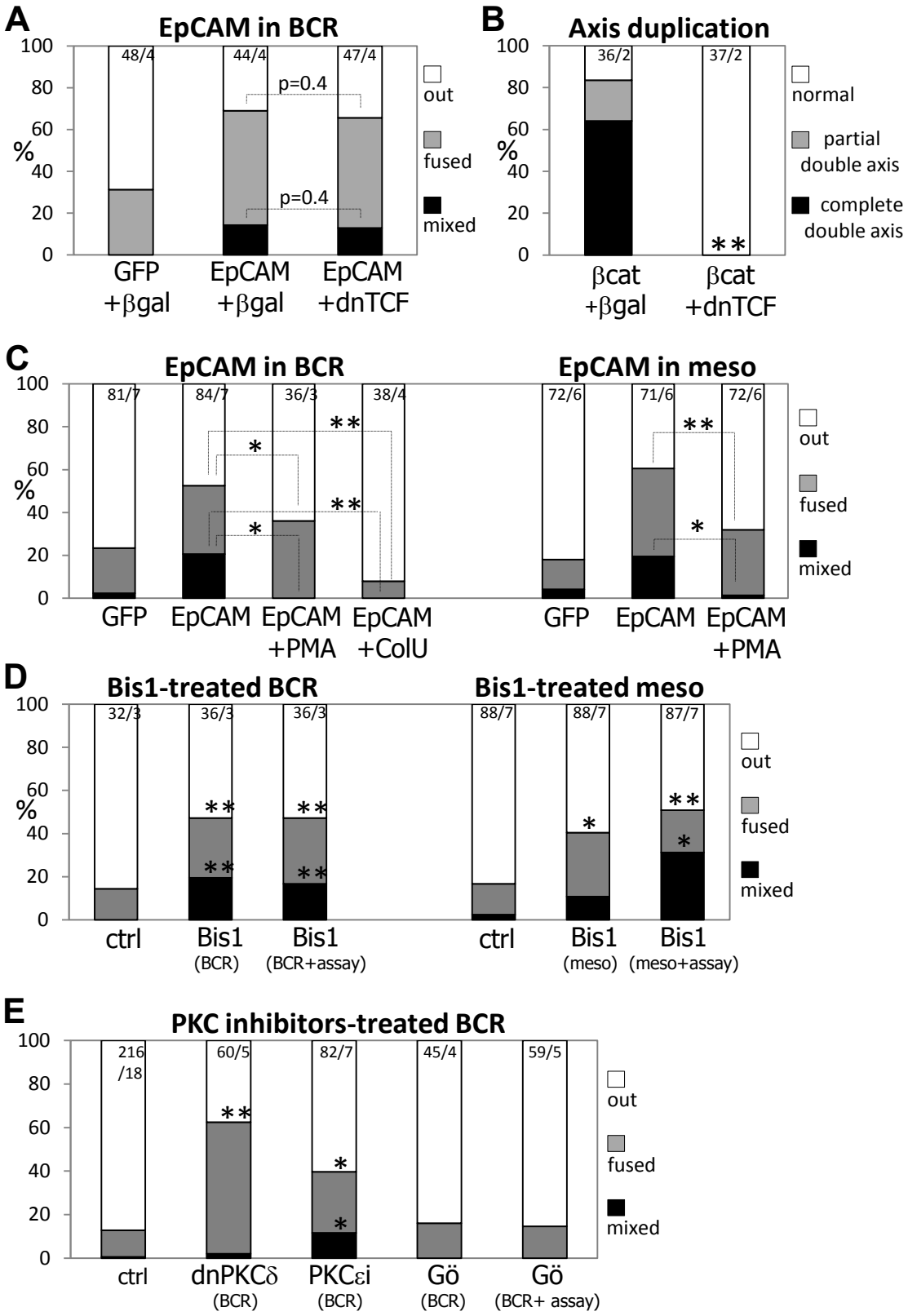
A
EpCAM in BCR
100
80
60
40
20
0
%
48/4
44/4
47/4
p=0.4
p=0.4
out
fused
mixed
GFP +βgal
EpCAM +βgal
EpCAM +dnTCF
B
Axis duplication
36/2
37/2
**
normal
partial double axis
complete double axis
βcat +βgal
βcat +dnTCF
C
EpCAM in BCR
EpCAM in meso
81/7
84/7
36/3
38/4
72/6
71/6
72/6
*
**
out
fused
mixed
GFP
EpCAM
EpCAM +PMA
EpCAM +ColU
GFP
EpCAM
EpCAM +PMA
D
Bis1-treated BCR
Bis1-treated meso
32/3
36/3
36/3
88/7
88/7
87/7
ctrl
Bis1 (BCR)
Bis1 (BCR+assay)
ctrl
Bis1 (meso)
Bis1 (meso+assay)
E
PKC inhibitors-treated BCR
216 /18
60/5
82/7
45/4
59/5
ctrl
dnPKCδ (BCR)
PKCεi (BCR)
Gö (BCR)
Gö (BCR+ assay)

Figure 2.7

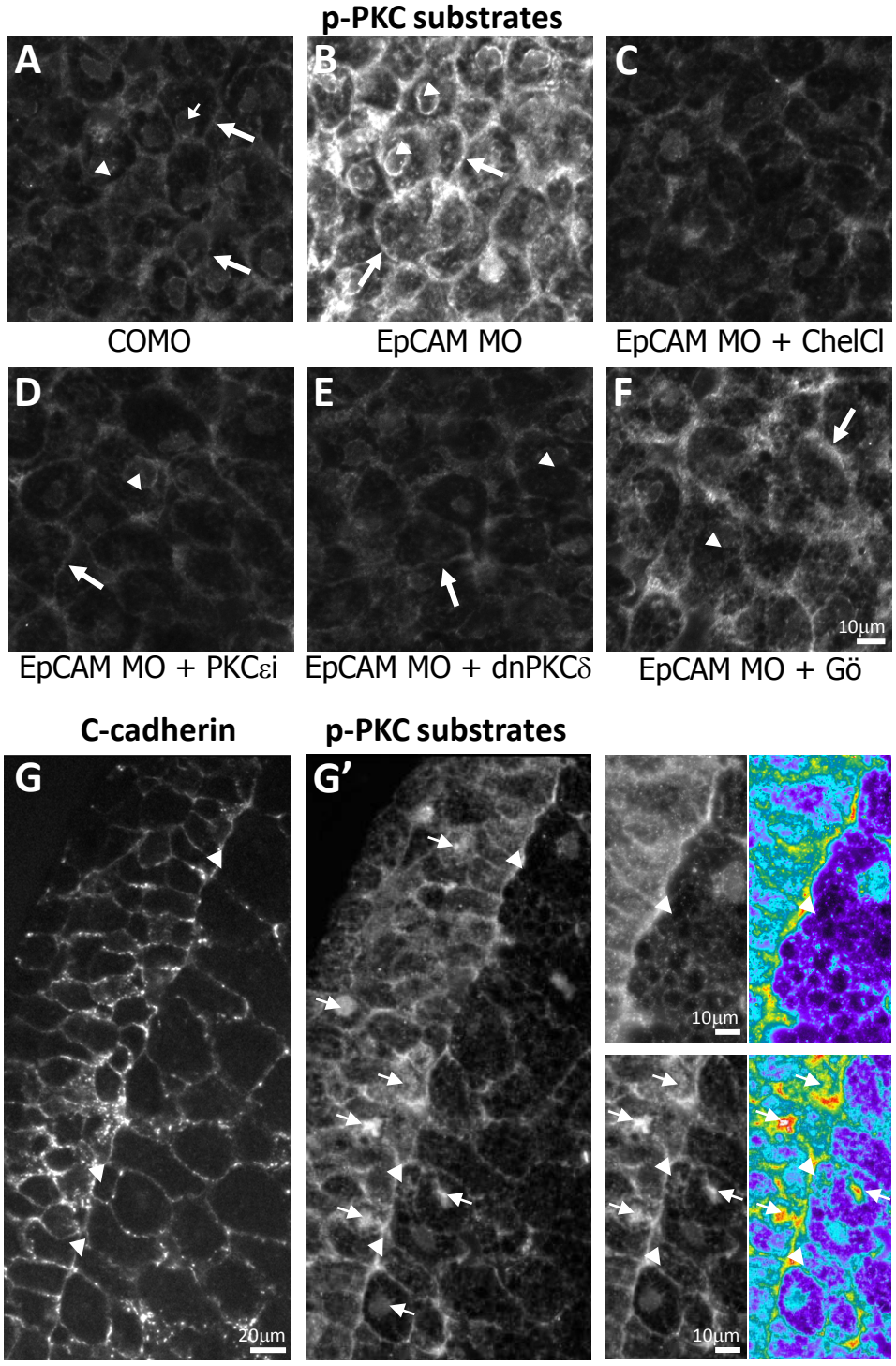
p-PKC substrates
A
B
C
COMO
EpCAM MO
EpCAM MO + ChelCl
D
E
F
10µm
EpCAM MO + PKCεi
EpCAM MO + dnPKCδ
EpCAM MO + Gö
C-cadherin
p-PKC substrates
G
G'
20µm
10µm
10µm

Figure 2.8

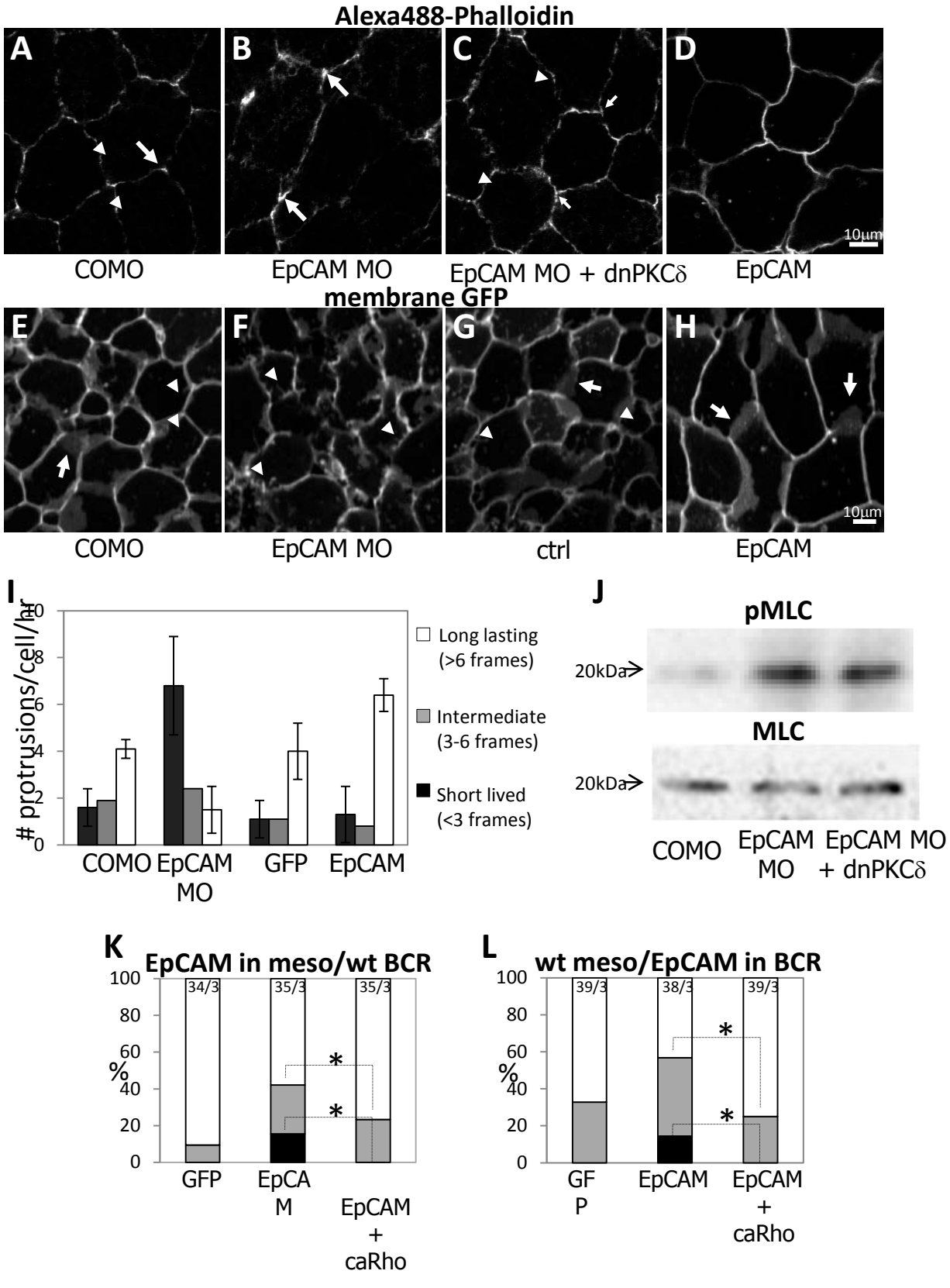
Alexa488-Phalloidin
A
B
C
D
10µm
COMO
EpCAM MO
EpCAM MO + dnPKCδ
EpCAM
membrane GFP
E
F
G
H
10µm
COMO
EpCAM MO
ctrl
EpCAM
I
protrusions/cell/hr
0
2
4
6
8
10
Long lasting (>6 frames)
Intermediate (3-6 frames)
Short lived (<3 frames)
COMO
EpCAM MO
GFP
EpCAM
J
pMLC
20kDa
MLC
20kDa
COMO
EpCAM MO
EpCAM MO + dnPKCδ
K
EpCAM in meso/wt BCR
%
100
80
60
40
20
0
34/3
35/3
35/3
*
*
GFP
EpCAM
EpCAM + caRho
L
wt meso/EpCAM in BCR
%
100
80
60
40
20
0
39/3
38/3
39/3
*
*
GFP
EpCAM
EpCAM + caRho

Figure 2.S1

EpCAM Multiple Sequence Alignment Xenopus & vertebrates

CLUSTAL 2.0.12 multiple sequence alignment

```
xEmCAMa         --------------------MCLVLVAQVQSQGCKCRTHYMGKCDNSGASSDCQCTLTIG 40
xEmCAMb         MKFVSVLRLG-------AALMCLVLVTRAQNPGCKCKTHYLGKCDNSGASSDCQCALSIG 53
xtEpCAM         MHLSTVLRLG-------AALLCFALVAQAQSPGCTCSTLYMGKCDNSGAG-GCQCTLAIG 52
hEpCAM1         MAPPQVLAF-------GLLLAAATATFAAAQEECVCENYKLAVNCFVNNNRQCQCT-SVG 52
mEpCAM1         MAGPQALAF-------GLLLAVVTATLAAAQRDCVCDNYKLATSCSLNEYGECQCT-SYG 52
cEpCAM          MELLRGAAL-------LLLLCAA----ACAQDSCTCTKNKRVTNCRLIDN-VCHCN-SIG 47
hEpCAM2         MARGPGLAPPPLRLPLLLLVLAAVTGHTAAQDNCTCPTNKMTVCSPDGPGGRCQCR-ALG 59
mEpCAM2         MARGLDLAP------LLLLLLAMATRFCTAQSNCTCPTNKMTVCDTNGPGGVCQCR-AMG 53
zEpCAM1         MK--------------VLVALFVVALVD-VTSQCTCKTMKWANCDD-----SCSCSLTLT 40
zEpCAM2         MK--------------VLVALFVVALVDVVTSQCACKTMKWANCDD-----SCSCSLTLT 41
                                           * *  .          * *  :

xEmCAMa         P-DSQPVNCSKLIPKCWLMKRESL---GTKAGR-RVKP-AQALIDNDGLYNPECDTNGVF 94
xEmCAMb         P-ASQAVDCTKLIPKCWLMKRESL---GTKAGR-RVKP-VQALIDNDGLYDPECETNGVF 107
xtEpCAM         T-ATQSINCSALIPKCWLMKRESL---GTKAGR-RVKP-VQALVDNDGLYDPECDVNGVF 106
hEpCAM1         --AQNTVICSKLAAKCLVMKAEMN---GSKLGR-RAKP-EGALQNNDGLYDPDCDESGLF 105
mEpCAM1         --TQNTVICSKLASKCLAMKAEMT---HSKSGR-RIKP-EGAIQNNDGLYDPDCDEQGLF 105
cEpCAM          --SSVPVNCEILTSKCLLMKAEMA---NTKSGR-REKP-KDALQDTDGLYDPECENNGLF 100
hEpCAM2         --SGMAVDCSTLTSKCLLLKARMS---APKNARTLVRPSEHALVDNDGLYDPDCDPEGRF 114
mEpCAM2         --SQVLVDCSTLTSKCLLLKARMS---ARKSGRSLVMPSEHAILDNDGLYDPECDDKGRF 108
zEpCAM1         ESSKQTLDCSKLVPKCFLMKAEMYRARHNLGTRKTGKPDENAFVDNDGIYDPECQSDGKF 100
zEpCAM2         ESSTQTLNCSKLVPKCFLMQAEMYRACNHQDTRSGGKPVETAFVDNDGIYDPVCESDGKF 101
                      : *  * .**  :: .          *    *   *: :.**:*:* *: .* *

xEpCAMa         KARQCNNTDTCWCVNTAGVRRTDKGDKNWKCPELVRTNWVYVEMKRNNTDS-VNDDDLKK 153
xEpCAMb         KARQCNNTDTCWCVNTAGVRRTDKGDKNWKCPELVRTNWVIVEMKRNNSDS-VNDDVLIQ 166
xtEpCAM         KARQCNNTDTCWCVNSAGVRRTDKGDKNWKCPELVKTNWVIVEMKRNGTES-VSDADLIQ 165
hEpCAM1         KAKQCNGTSTCWCVNTAGVRRTDK-DTEITCSERVRTYWIIIELKHKAREKPYDSKSLRT 164
mEpCAM1         KAKQCNGTATCWCVNTAGVRRTDK-DTEITCSERVRTYWIIIELKHKERESPYDHQSLQT 164
cEpCAM          KAKQCNGT-TCWCVNTAGVRRTDKHDTDLKCNQLVRTTWIIIEMRHAERKTPLNAESLTR 159
hEpCAM2         KARQCNQTSVCWCVNSVGVRRTDKGDLSLRCDELVRTHHILIDLRHRPTAGAFNHSDLDA 174
mEpCAM2         KARQCNQTSVCWCVNSVGVRRTDKGDQSLRCDEVVRTHHILIELRHRPTDRAFNHSDLDS 168
zEpCAM1         KAVQCNNTEVCWCVNSAGVRRSDKKDKNIKC-EPAETYWVRAEMTHKSVDVPIDVANLRM 159
zEpCAM2         KAVQCNNTEVCWCVNSAGVRRSDKKDKNIKC-EPAETYWVRVEMKHKSVDVPIDATKLRT 160
                ** *** * .*****:.****:** * .  * : ..*  :  :: :       .   *

xEmCAMa         ALKTTIVNRYGLPEKCVSVELEGPS--LIYVDLKQNGSQKLPGEVDITDVAYYMEKDIKG 211
xEmCAMb         ALKTTILNRYGLPEKYVSVELEGSS--FIYIDLKQNGTQKLPGEVDITDVGYYMEKDIKG 224
xtEpCAM         ALKTTITNRYGLPDKYISVELETP---LIYIDLKQNTSQKLPGEVDITDVAYYMEKDVKG 222
hEpCAM1         ALQKEITTRYQLDPKFITSILYENN--VITIDLVQNSSQKTQNDVDIADVAYYFEKDVKG 222
mEpCAM1         ALQEAFTSRYKLNQKFIKNIMYENN--VITIDLMQNSSQKTQDDVDIADVAYYFEKDVKG 222
cEpCAM          YLKDTITSRYMLDGRYISGVVYENP--TITIDLKQNSSDKTPGDVDITDVAYYFEKDVKD 217
hEpCAM2         ELRRLFRERYRLHPKFVAAVHYEQP--TIQIELRQNTSQKAAGDVDIDDAAYYFERDIKG 232
mEpCAM2         ELRRLFQERYKLHPSFLSAVHYEEP--TIQIELRQNASQKGLRDVDIADAAYYFERDIKG 226
zEpCAM1         GIENALQQRYFLDKNFVSEVQYDKDARLIVVDVKKDKNDR---TTDLSLMTYYLEKDIKV 216
zEpCAM2         GIENVLQQRYGLDKKLVSEVQYDKDGRLIVVDVKKDKDDR---TTDLSLMTYYMEKDIKV 217
                 :.  :  ** *    :           * ::: ::  ::    .*:    **:*:*:*

xEmCAMa         DSLFHPDEKFEILVNGNNFAVKEP--IIYYIDEKPHEISMKHLTPGVIAVIVVVVLAIVA 269
xEmCAMb         DPLFHPDEKFEILVNGKNFGVKEP--VIYYVDEKPHEITMKHLTPGVIAVIVVVVLAVVA 282
xtEpCAM         DSLFPANNQFQILANGNKISVKEP--MIYYIDEKPHEISMRHLTPGVIAVIVVVVLAVVA 280
hEpCAM1         ESLFHS-KKMDLTVNGEQLDLDPGQTLIYYVDEKAPEFSMQGLKAGVIAVIVVVVIAVVA 281
mEpCAM1         ESLFHSSKSMDLRVNGEPLDLDPGQTLIYYVDEKAPEFSMQGLTAGIIAVIVVVSLAVIA 282
cEpCAM          DSIFLN-NKLNMNIDNEELKFDN--MMVYYVDEVPPEFSMKSLTAGVIAVIVIVVLAIVA 274
hEpCAM2         ESLFQGRGGLDLRVRGEPLQVER--TLIYYLDEIPPKFSMKRLTAGLIAVIVVVVVALVA 290
mEpCAM2         ESLFMGRRGLDVQVRGEPLHVER--TLIYYLDEKPPQFSMKRLTAGVIAVIAVVSVAVVA 284
zEpCAM1         KPLFSDEKPFVLSVQGKNVTMEN--VLIYYVDDKAPTFTMQKLTGGIIAVIVVVSLIVIG 274
zEpCAM2         LPLFWNGQPFEVDVPGTKVSMEN--VLIYYVDDRAPTFTMQKLTGGIIAVIVVVSLIVIG 275
                 .:*     : :   .  . ..    ::**:*: .  ::*: *. *:****.:* : ::.

xEmCAMa         LIAVLIFTRRKR-GKYQKAEMKELNEMQQEAST 301
xEmCAMb         LIAVLIFTRRKK-GKYQKAEMKELNEMQKEVST 314
xtEpCAM         LIAVLIFTRRKK-ARYQKAEMKELNEMQKEVST 312
hEpCAM1         GIVVLVISRKKRMAKYEKAEIKEMGEMHRELNA 314
mEpCAM1         GIVVLVISTRKKSAKYEKAEIKEMGEIHRELNA 315
cEpCAM          GIIGLVLSRRRK-GKYVKAEMKEMNEMHRGLNA 306
hEpCAM2         GMAVLVITNRRKSGKYKKVEIKELGELRKEPSL 323
mEpCAM2         GVVVLVVTKRRKSGKYKKVELKELGEMRSEPSL 317
zEpCAM1         GFLVLFFLARRQKAHYSKAQAREMETIS----- 302
zEpCAM2         GFLVLFFLARRQKAQYSKAQAREMETIS----- 303
                 .  *..  ::: .:* *.: :*:  :
```

Accession Numbers

- xEmCAMa: *Xenopus laevis* NP_001086975
- xEmCAMb: *Xenopus laevis* AAN86618
- xtEpCAM: *Xenopus tropicalis* AAH84898
- hEpCAM1: *Homo sapiens* AAH14785
- hEpCAM2: *Homo sapiens* CAG47056
- mEpCAM1: *Mus musculus* NP_032558
- mEpCAM2: *Mus musculus* NP_064431
- cEpCAM: *Gallus gallus* NP_001012582
- zEpCAM1: *Danio rerio* NP_998340
- zEpCAM2: *Danio rerio* NP_001017593

Figure 2.S2

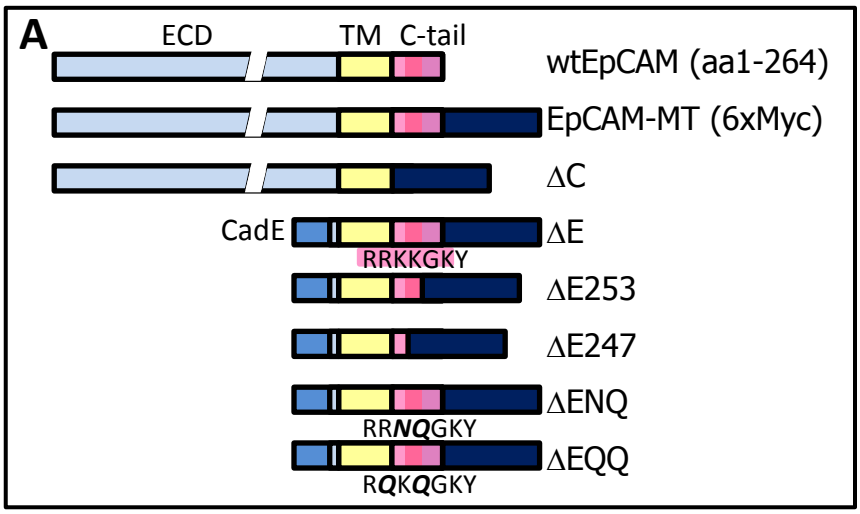
A
ECD
TM
C-tail
wtEpCAM (aa1-264)
EpCAM-MT (6xMyc)
ΔC
CadE
ΔE
RRKKGKY
ΔE253
ΔE247
ΔENQ
RRNQGKY
ΔEQQ
RQKQGKY

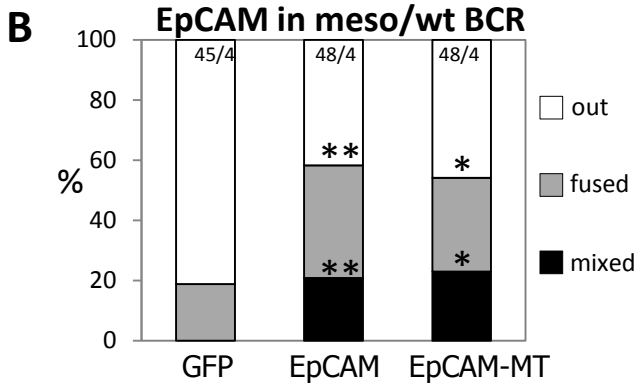
B
EpCAM in meso/wt BCR
100
80
60
40
20
0
%
45/4
48/4
48/4
**
**
*
*
out
fused
mixed
GFP
EpCAM
EpCAM-MT

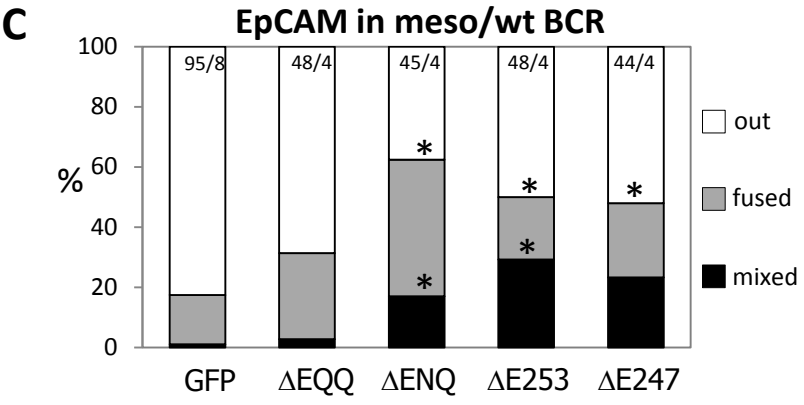
C
EpCAM in meso/wt BCR
100
80
60
40
20
0
%
95/8
48/4
45/4
48/4
44/4
*
*
*
*
out
fused
mixed
GFP
ΔEQQ
ΔENQ
ΔE253
ΔE247

Figure 2.S3

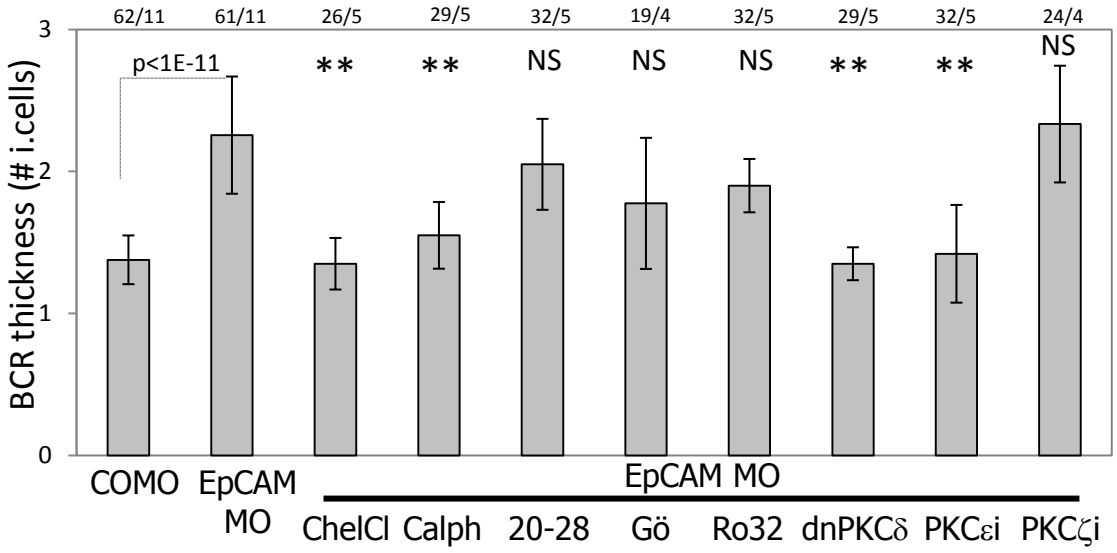
62/11
61/11
26/5
29/5
32/5
19/4
32/5
29/5
32/5
24/4
p<1E-11
**
**
NS
NS
NS
**
**
NS
BCR thickness (# i.cells)
3
2
1
0
COMO
EpCAM MO
EpCAM MO
ChelCl
Calph
20-28
Gö
Ro32
dnPKCδ
PKCεi
PKCζi

Figure 2.S4

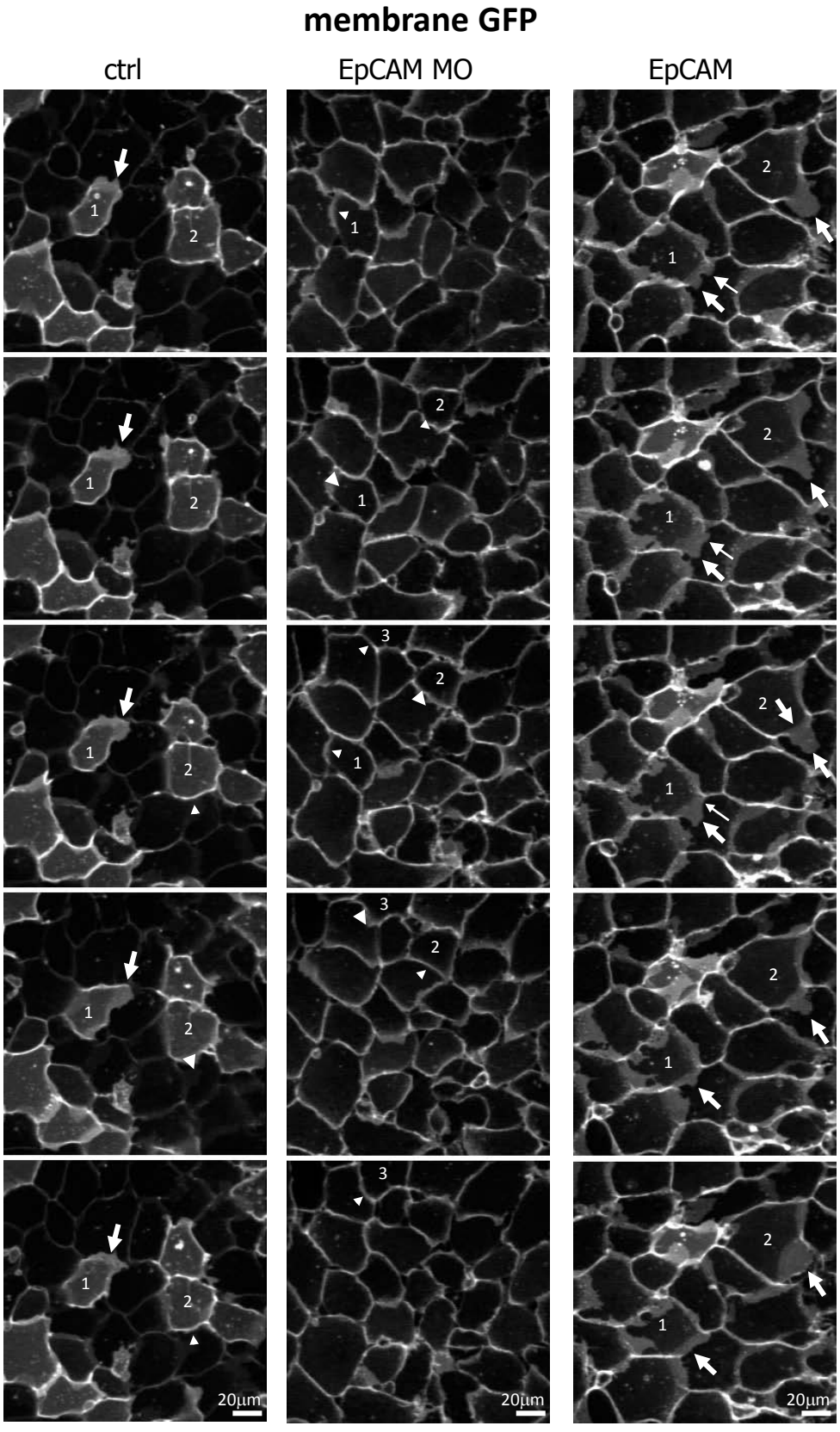

Bridge to Chapter III

In Chapter II, I established that EpCAM causes aberrant ectoderm/mesoderm tissue mixing in the gastrula by inhibiting novel PKCs via its cytoplasmic domain. Overexpression of EpCAM at this stage makes cells more invasive by inhibiting PKC activity, while that loss of EpCAM results in a surge of PKC activity which restricts cell movements within tissues by increasing actomyosin contractility. In Chapter III, I extend my analysis of EpCAM loss of function to a later developmental stage in *Xenopus* embryos. In the neureula, EpCAM depletion causes a strong loss of cell-cell adhesion which results in dissociation of the skin and embryonic death. Similar to the motility defects described in Chapter II, I show that loss of cell-cell adhesion in EpCAM depleted embryos is also due to increased nPKC activity. I further described the molecular consequences of elevated PKC activity in the absence of EpCAM: increased myosin contractility by PKC-dependent overstimulation of the Erk pathway, causes loss of cadherin-mediated adhesion, tissue dissociation and ultimately cell death. In Chapter III, I fully describe the molecular mechanism by which EpCAM inhibits PKC activity: PKC inhibition is due to a short segment of the EpCAM cytoplasmic tail that directly binds activated PKCs with high affinity. This motif, highly conserved in all vertebrate EpCAMs, resembles and acts similarly to the intramolecular pseudosubstrate inhibitory domains of PKCs. Other plasma membrane proteins containing similar pseudosubstrate-like motifs were found by a bioinformatics search. Preliminary data suggests that these proteins can bind PKCs and could therefore be important negative regulators of PKC activity. Chapter III has recently been submitted to Cell for publication.

CHAPTER III

Tumor-associated EpCAM controls Erk signaling, actomyosin contractility and cell adhesion by direct PKC inhibition

Abstract

EpCAM is a cell surface protein highly expressed in malignant carcinomas, important in cancer diagnostic and as target for immunotherapy. We report that EpCAM acts as a potent inhibitor of novel PKCs, both in embryos and in cancer cells. This repression is required to maintain tissue integrity during embryonic development. The consequences of deregulation of PKC activity upon loss of EpCAM are sequentially: overstimulation of the Erk pathway and myosin contractility, loss of cadherin-mediated adhesion, tissue dissociation and ultimately cell death. We show that PKC inhibition is due to a short segment of the EpCAM cytoplasmic tail. This motif resembles the own pseudosubstrate inhibitory domains of PKCs and binds indeed nPKCs with high affinity. A bioinformatics search reveals the existence of similar motifs in other plasma membrane proteins, most of which are cell-cell adhesion molecules. Thus direct inhibition of PKC by EpCAM represents a novel mode of regulation of signal transduction by cell surface proteins.

Introduction

EpCAM was initially discovered as a cell surface antigen highly expressed in a variety of carcinomas. It is currently considered to be an important carcinoma marker and a promising target for immunotherapy of several malignancies (Munz et al., 2009; Patriarca et al., 2012; Seimetz et al., 2010; Visvader and Lindeman, 2008). EpCAM stands for "Epithelial Cell Adhesion Molecule", a name that relates to its restricted expression in adult human and mice epithelia and its ability to bind homophilically (Litvinov et al., 1994). EpCAM and the closely related EpCAM-2/EGP-1/Trop-2 (Cubas et al., 2009) have thus been classified as unique Ca^{2+}-independent cell-cell adhesion molecules unrelated to any of the major families of CAMs. They are characterized by an extracellular domain with two EGF domains, a single transmembrane domain and by a very short (24 amino acids) cytoplasmic tail. EpCAM has been highly conserved in Vertebrates, but no obvious homologues are found outside of this subphylum. Single EpCAM knock out in mice and EpCAM null mutants in Zebrafish give relatively weak embryonic phenotypes (Lei *et al.*, 2012;

Slanchev et al., 2009; Villablanca et al., 2006), although in one report it seemed to cause mouse embryonic lethality through placental defects (Nagao et al., 2009). It is likely that the second EpCAM gene present in both species (Q568H0 in Zebrafish, called here EpCAM-2) functions redundantly, however phenotypes for complete loss-of-function of both EpCAMs have yet to be reported.

High EpCAM levels have been long suspected to play an important role in cancer development and invasion, and it has been indeed found to increase proliferation and migration of tumor cell lines (Munz et al., 2004; Osta et al., 2004). The proliferative action of EpCAM has been attributed to the ability of its short cytoplasmic tail to form a transcription activator complex with FHL2 and β-Catenin (Maetzel et al., 2009). This association occurs in the nucleus, and is thus conditional to the release of the cytoplasmic domain as a soluble proteolytic fragment by the sequential action of TNF-α converting enzyme (TACE) and presenilin-2 (Maetzel et al., 2009). This mechanism, however, may not be general but rather restricted to some cancer cells, depending perhaps on EpCAM levels and expression of the relevant proteolytic enzymes (Denzel et al., 2009).

As for its role in migration, *in vivo* supporting data have been scarce, except for a report of impaired migration of skin Langerhans cells in conditionally knocked out mice (Gaiser et al., 2012). In both Zebrafish and *Xenopus* embryos, EpCAM depletion affects epiboly, a morphogenetic process through which the ectoderm thins and expands during gastrulation (Slanchev et al., 2009). That cell migration and/or tissue re-arrangement would be promoted by a protein assumed to function as cell-cell adhesion is quite counterintuitive. The fact that EpCAM expression caused increased cadherin levels (Maghzal et al., 2010; Slanchev et al., 2009) further added to the puzzle. It comes to no surprise that in the absence of a mechanistic understanding of EpCAM function the various proposed models have been inconsistent and contradictory. While we confirmed and strengthened the observations that EpCAM positively regulates both cell movements and cadherin levels, we demonstrated that regulation of cell motility occurred independently of the stabilization of cadherins (Maghzal et al., 2010). Most strikingly, it also appeared to be independent of the presumed adhesive function of EpCAM: Indeed, motility and normal epiboly could be fully rescued in EpCAM-depleted tissues/embryos by

expression of an EpCAM construct lacking the whole extracellular domain (Maghzal et al., 2010). These results implied that EpCAM had a signaling activity, which we confirmed by showing that EpCAM controlled novel PKC activity and actomyosin-based contractility.

How EpCAM regulated cadherin levels and cell-cell adhesion, in particular whether this function also relied on repression of PKC activity was an important issue that remained to be established. The mechanism that led to PKC inhibition was certainly the most puzzling and exciting question, especially considering how dramatic was the impact of EpCAM levels on total cellular PKC activity, which positioned EpCAM as a major regulator of intracellular signaling.

Results

EpCAM is required for tissue integrity

Global depletion of EpCAM by injection of antisense Morpholino oligonucleotides (EpCAM MO) caused *Xenopus* embryonic lethality with strong penetrance (>90%, Fig. 3.S1). Tailbud stage embryos showed numerous morphological defects, including a shortened body axis, head malformations (Fig. 3.1B), but the most dramatic effect of EpCAM depletion was the appearance at the early tailbud stage of large superficial lesions of the epidermis (Fig. 3.1B, arrows), which eventually led in all cases to its full disintegration (Fig. 3.1B, lower embryo). Co-injection of EpCAM mRNA lacking the 5' UTR region recognized by EpCAM MO rescued epidermal integrity and largely restored normal morphology, demonstrating the specificity of these oligonucleotides (Fig. 3.1C). Analysis of mosaic embryos showed that the phenotype was cell autonomous (Fig. 3.1E-G): EpCAM MO-injected cells were rounder (Fig. 3.1F, G) and had a much weaker C-Cadherin staining (Fig. 3.1G') than neighboring wild type cells or cells injected with control morpholinos (COMO) (Fig. 3.1D, E, E'). Many EpCAM-depleted cells were fully detached and had been expelled from the tissue (Fig. 3.1F, G, arrowheads), which correlated with a nearly complete loss of cadherin (arrowheads in G'). The decrease in cadherin was detected before overt changes in cell shape and dissociation (Fig. 3.1H, H'), suggesting that the former may be causal to the latter. Other tissues (neuroderm, mesoderm derivatives, and endoderm) were similarly affected, although dissociation of the ectoderm

occurred earlier and was more complete. Thus, EpCAM appeared to be crucially required for tissue integrity.

Because EpCAM-depletion affected to different degree the development of the various tissues, we used ectoderm explants as a simpler system to further investigate the cellular function of EpCAM (Fig. 3.2A): When the prospective ectoderm is explanted out of a blastula embryo, it heals into a ball made of the outer pigmented layer surrounding an inner mass of unpigmented cells. As these explants are now isolated from patterning signals, they remain pure ectoderm, and can be maintained *in vitro* in this state for up to three days, i.e. past the time of hatching of control embryos. Quite remarkably, ectoderm explants from EpCAM MO-injected embryos started to burst at the same time as lesions appeared on whole embryos (Fig. 3.2A"). EpCAM depletion affected equally outer and inner cells (supplementary Fig. 3.S2A-C). Further consistent with the whole embryo phenotype, C-Cadherin protein levels were strongly decreased in EpCAM MO explants (Fig. 3.2C). The "loss of epithelial integrity" phenotype (LEI) could thus be readily quantified by counting the number of bursting ectoderm explants. Typically, the incidence of LEI in EpCAM-depleted explants in our standard procedure was around 80% (Fig. 3.2B). It was rescued by co-injection of *Xenopus* or human EpCAM mRNA (Fig. 3.2B). We then asked whether the downregulation of C-Cadherin was sufficient to explain the LEI in EpCAM-depleted ectoderm. C-Cadherin overexpression was indeed sufficient to fully rescue LEI (Fig. 3.2B), consistent with LEI being a simple direct consequence of C-Cadherin depletion.

The control of cadherin levels by EpCAM is post-transcriptional and involves endocytosis

While EpCAM depletion caused a dramatic decrease in C-cadherin protein levels, it did not affect its mRNA levels (nor any of the tested related molecules, E-cadherin, α- and β-catenin, supplementary Fig. 3.S2D), indicating that the regulation occurs at a post-transcriptional level. Once dissociated, EpCAM-depleted cells showed typical signs of apoptosis (caspase 3 activation, Fig. 3.S2E, and DNA cleavage, data not shown). However, C-cadherin overexpression was sufficient to rescue cell-cell adhesion (Fig. 3.2B) and to block caspase activation (Fig.S2E), indicating that

apoptosis was not the cause for cadherin loss and cell dissociation, but rather their consequence. C-cadherin disappearance from EpCAM-depleted cells appeared to be preceded by massive internalization (Fig. 3.2E, arrows). Consistent with degradation via the endocytic-lysosomal pathway, C-Cadherin levels and tissue integrity could be fully restored and LEI rescued by inhibiting dynamin (supplementary Fig. 3.S2F, G).

EpCAM promotes cadherin mediated adhesion by repressing PKC signaling

We had previously showed that EpCAM depletion caused an increase in PKC activity, which was responsible for the observed defective epiboly (Maghzal et al., 2010). We confirmed that the levels of phosphorylated PKC substrates (p-PKCsub) were abnormally elevated in EpCAM-depleted ectoderm explants (Fig. 3.3A). We thus hypothesized that cadherin downregulation and loss of adhesion at later stages may similarly result from PKC overactivation. Indeed, treatment of EpCAM-depleted explants with bisindolylmaleimide (Bis1), an inhibitor of classical and novel PKCs, rescued LEI and C-cadherin levels (Fig. 3.3D, E). Out of a panel of PKC inhibitors, those with specificity for novel PKCs tended to rescue LEI better than inhibitors of classical PKCs (Fig. 3.3D). Thus, similar to the effect on early morphogenetic movements, repression of novel PKCs by EpCAM appears to be required for stabilization of cell-cell adhesion. Note that general PKC inhibitors such as Bis1 or Calphostin C gave weaker rescues than more specific novel PKC inhibitors, probably because interfering globally with such a central cellular function as PKC signaling provoked other deleterious effects. In fact, we had to titrate each inhibitor used in this work in order to compromise with their "toxicity" effects.

We also examined the link between EpCAM, PKCs and cadherins in Caco-2 cells, a human colon cancer cell line that expresses high levels of EpCAM (Trebak et al., 2001; Ammons et al., 2003; Maaser and Borlak, 2008). We similarly detected a large increase in p-PKCsub in EpCAM-depleted Caco-2 cells (Fig. 3.3B and C), and a concomitant decrease in E-cadherin levels (supplementary Fig. 3.S3), which could be rescued by PKC inhibition. Thus stabilization of cell adhesion by repression of PKC activity seems to be a conserved function of EpCAM.

LEI is due to increased actomyosin contractility

EpCAM depletion led to increased myosin activation and cortical contractility (Fig. 3.4A). This effect was conserved in Caco-2 cells (Fig. 3.4A). We therefore hypothesized that exacerbated stiffening of the cortical actin cytoskeleton could be the cause of LEI. High cortical tension would destabilize adhesions, which in turn would indirectly cause internalization of disengaged cadherins and their degradation. Artificial stimulation of contractility with a constitutively active RhoA construct indeed phenocopied EpCAM MO-induced loss of adhesion and cadherin depletion (Fig. 3.4D, E, F). Consistently, adhesion and cadherin levels were fully rescued in EpCAM-depleted explants upon inhibition of Rho, ROK, MLCK, or direct inhibition of myosin II ATPase activity with blebbistatin (Fig. 3.4B, C, and supplementary Fig. 3.S4).

We finally confirmed in the whole embryo that inhibition of novel PKCs, C-cadherin overexpression or myosin inhibition were each on its own fully sufficient to compensate for loss of EpCAM, efficiently restoring tissue integrity (Fig. 3.4G,H). Quite amazingly, the embryos rescued by dominant negative PKCδ and C-cadherin developed almost normally (Fig. 3.4G). Embryos rescued with blebbistatin had more severe morphological defects (data not shown), as expected from downregulating myosin activity, yet no epithelial disruption was observed, and the embryos hatched (Fig. 3.4H). We conclude that upregulation myosin activity by nPKCs is responsible for cadherin depletion, and can fully account for the defects caused by loss of EpCAM.

Increased contractility and LEI result from Erk overactivation

While there wasn't any obvious reported link between PKC and the Rho-ROK-MLCK pathway, a clear connection existed with another well-established parallel branch of myosin activation through Erk (Nguyen et al., 1999). This pathway can indeed be stimulated by PKD/PKCμ, a direct target of nPKCs (Rozengurt et al., 2005; Wong and Jin, 2005). We found that EpCAM depletion led indeed to nPKC-dependent overactivation of the PKD/PKCμ-Raf1-MAPK-Erk cascade (Fig. 3.5A): We observed in EpCAM MO explants a strong increase of phosphorylation of PKD/PKCμ at a PKC-specific site, which was blocked by inhibiting PKCδ (Fig.

3.5B). Erk phosphorylation was similarly boosted in EpCAM-depleted *Xenopus* explants and Caco-2 cells (Fig. 3.5C; supplementary Fig. 3.S5A, C), while basal p-Erk levels were strongly reduced by EpCAM overexpression (supplementary Fig. 3.S5B). Again the reaction was sensitive to PKC inhibition (Fig. 3.5C), as well as to inhibition of Raf-1 (Fig.3.5C), which is the direct target of PKD/PKCμ along the MAPK-Erk pathway. We then showed that Erk activation can account for increased myosin phosphorylation, loss of cadherin and LEI in EpCAM MO ectoderm: treatment of explants with a Raf or an Erk-1 (pep1) inhibitor rescued p-MLC and cadherin levels (Fig.3.5D and E) and tissue integrity (Fig. 3.5F).

The cytoplasmic tail of EpCAM binds directly nPKCs and acts as a pseudosubstrate inhibitor.

Optimal PKC substrate consensus sequences are all characterized by a cluster of basic residues positioned N-terminus to the Ser/Thr, although other feature vary between PKC isoforms (Newton, 2001; Nishikawa et al., 1997). PKCs themselves display a short motif resembling a substrate sequence, but lacking the phosphorylatable Ser/Thr (Newton, 2001). In their inactive conformation, PKCs are folded in such a way that this motif binds to the catalytic domain and acts as an internal pseudosusbtrate inhibitor. Upon activation, the conformational change produced by phospholipids and diacylglycerol DAG binding relieves the autoinhibition.

We discovered that the highly conserved 24-amino acid cytoplasmic tail of EpCAM (EpTail) contains residues adjacent to the transmembrane domain (designated as the juxtamembrane domain or JM, Fig. 3.6A) resembling quite strikingly a typical pseudosusbtrate motif, more specifically the motifs of two novel PKCs, PKCδ and PKCη (Fig. 3.6A). This surprising feature suggested that EpTail may directly bind and inhibit nPKCs. Coimmunoprecipitation experiments in Caco-2 cells showed that endogenous PKCδ and EpCAM physically interact *in vivo* (Fig. 3.6B) and recombinant GST-EpTail could pull down at least two PKC isoforms, one of which identified as PKCδ, from *Xenopus* extracts (Fig. 3.6C). To demonstrate that

the interaction was direct, we repeated the pulldown experiments using pure lipid-activated recombinant PKCs. GST-EpTail bound efficiently PKCδ and PKCη but not classical PKCβ (Fig. 3.6D). PKCδ and PKCη could also bind to GST fusions of the juxtamembrane domain alone, as well as to peptides corresponding to the equivalent human and Zebrafish JM sequences (Fig. 3.6D). The interaction could be efficiently competed by an excess of PKCη pseudosubstrate peptide (Fig. 3.6E), fully consistent with EpCAM tail interacting with the substrate binding surface of the PKC catalytic domain.

We thus expected that EpTail would similarly inhibit PKC activity. We assayed PKC phosphorylation *in vitro* using recombinant PKCδ and a recombinant form of its classical substrate, myelin basic protein (Kishimoto et al., 1985). We found that the addition of GST-EpTail strongly inhibited PKCδ activity (Fig. 3.6F). We used surface plasmon resonance spectroscopy (SPR) to obtain quantitative data on EpCAM-PKC interactions. Xenopus and human EpCAM JMs bound PKCδ and PKCη with affinity constants of about 30-50 nanomolar, in the same range as for the PKCδ pseudosubstrate. These results demonstrate that EpCAM functions as a direct and strong pseudosubstrate inhibitor of novel PKCs.

We also modeled the 3D structure of active PKCδ bound to the human EpCAM JM (Fig. 3.7A). The model predicts an intimate and extended association of the JM to the groove of the catalytic site, readily explaining the high affinity of this interaction. The model also predicts EpCAM-bound PKCs to be tightly apposed to the lipid bilayer, thus further impairing substrate accessibility. This clearly suggests that the EpCAM JM has been optimized for efficient inhibitory activity toward nPKCs.

The juxtamembrane domain of EpCAM defines a new group of PKC-binding transmembrane proteins

Charged amino acids are systematically found on both sides of the transmembrane domains of membrane proteins, where they serve to "clamp" the hydrophobic helix into its correct position. On the cytoplasmic side, these residues are most frequently

basic. Since basic residues are essentially the hallmark of PKC substrates, we wondered whether cell surface proteins other than EpCAM may similarly bind PKCs. Our molecular model indicated that a cluster of 3-4 basic consecutive residues constituted part of the PKC-interacting domain of the EpCAM JM, but also suggested additional specific interactions, consistent with the strict conservation of most residues of the JM motif from Xenopus to Mammals (Fig. 3.6A and supplementary Table 3.S1). To get some indication about the stringency of the requirements, we tested a series of GST-EpTail point mutation variants by *in vitro* pull down and surface plasmon resonance. While no single mutation abolished PKC binding, some features appeared to be important for strong interaction (see supplementary Fig. 3.S6 and supplementary Table 3.S2).

Based on both the EpCAM sequence conservation, on predictions from the molecular modeling and on our experimental results, we defined an approximate consensus sequence, which we used to interrogate the human proteome sequence database. Since we were more specifically interested in cell surface proteins, we narrowed the search to sequences that would closely follow a transmembrane helix, thus corresponding to bona fide JMs. The search identified several JMs with high similarity to the nPKC-binding consensus motif (supplementary Table 3.S3). Quite strikingly most of the top ranked sequences belonged to known or hypothesized cell-cell adhesion molecules. We tested experimentally three of the candidate JMs, EphA4, ICAM1 and NrCAM, in the *in vitro* pull down assay (Fig. 3.7C), and found that all three sequences bound PKCδ and PKCη. EphA4 was the best interactor, consistent with its high similarity score relative to the EpCAM consensus sequence. We conclude that EpCAM is the first member of a group of evolutionary unrelated plasma membrane proteins that can sequester PKCs via a short pseudosubstrate-like juxtamembrane motif.

Discussion

EpCAM been reported to promote cell adhesion as well as cell migration, but in the absence of a molecular explanation the apparent opposition of these effects has remained a puzzle. We provide here a mechanism that satisfactorily reconciles all observed phenotypes: by impinging on Erk signaling via novel PKCs and PKD, EpCAM represses actomyosin contractility. Stimulation of migration is an obvious consequence of tempering contractility. On the other hand, one does not always appreciate that, while some actomyosin activity is required for cell-cell and cell-matrix adhesion, high cortical contractility rather negatively affects adhesion (see e.g. Sahai and Marshall, 2002). We have shown here that stimulation of p-MLC up to the levels reached upon EpCAM knock down is sufficient to cause cadherin downregulation and tissue dissociation in our embryonic system. EpCAM is thus a remarkable regulator of cell behavior: by stimulating cell movement while insuring at the same time tissue coherence, it creates ideal conditions for high tissue dynamism. The fact that the same principles link contractility to cell-cell and to cell-matrix adhesion explains the positive role of EpCAM on both (Gostner et al., 2011; Maghzal et al., 2010; Osta et al., 2004; Slanchev et al., 2009; Tsukahara et al., 2011; Villablanca et al., 2006, our present results and unpublished observations). Considering the general importance of these processes, EpCAM is likely to be crucial in a wide range of situations, in embryos, in adult tissues, and in cancer.

The agreement of our data in *Xenopus* and human cells demonstrate that repression of PKC, Erk and MLC and the consequent stabilization of cadherins are conserved functions of EpCAM. Decreased cadherin levels were also observed in Zebrafish EpCAM-1 -/- embryos (Slanchev et al., 2009), even though in that case the phenotype was milder, most likely due to redundancy with EpCAM-2: Two pseudo-alleles are also present in *Xenopus laevis* (Maghzal et al., 2010), both of which were targeted in our loss-of-function experiments, while single depleted embryos developed almost normally (data not shown). Deregulation of myosin activity and cadherin levels may similarly explain the defects observed in the intestinal epithelium of mouse EpCAM-1 knock out (Lei et al., 2012).

Our results show that nPKC repression alone is sufficient to account for EpCAM regulation of cell behavior, although EpCAM may certainly have additional functions. Similarly, while nPKCs and downstream components are known to regulate other relevant targets (including cadherin, a direct substrate for PKD, (Jaggi et al., 2005)), the observed rescues are robust enough to indicate that by identifying Erk and myosin we have unraveled the major route of regulation. One particularly striking observation was the extent of PKC and Erk overactivation in EpCAM-depleted cells, which clearly positions EpCAM as a major regulator of intracellular signaling. Our immunoblots detected an effect on multiple PKC substrates (Fig.3A, B), and Erk activation was widespread, including in the nucleus. Thus, the lack of EpCAM must have affected cell homeostasis well beyond myosin phosphorylation and increased contractility. Note however that experimental depletion is a rather artificial situation, and the actual physiological functions of EpCAM may not necessarily be as pleiotropic as this massive PKC upregulation may suggest. In normal embryonic ectoderm, most p-Erk signal concentrates along the plasma membrane and EpCAM overexpression seems to inhibit preferentially this pool, leaving the weaker cytoplasmic and nuclear signals unchanged (supplementary Fig. 3.S5B). We believe that EpCAM primary function is probably to create at the membrane a mechanism that locally controls Erk, and probably other regulators downstream of nPKC. This would be consistent with the abundant literature presenting novel PKCs as regulators of the actin cytoskeleton and of cell adhesion (Newton, 2001; Le et al., 2002; Kinoshita et al., 2003; Steinberg, 2004; Iwabu et al., 2004; Chen and Chen, 2009; Singh et al., 2009; Rosse et al., 2010). It is however quite conceivable that regulation of p-Erk may affect also the nuclear pool and thus cell proliferation, which could represent an alternative mechanism to the previously reported interaction of the cleaved tail with β-catenin (Slanchev et al., 2009).

One should note that while EpCAM has clearly a crucial influence on cell migration and adhesion, its precise impact is expected to also depend on a variety of other parameters, including for example the degree of PKC activation by other pathways, or basal cell contractility/rigidity. In the embryo, for instance, the fact that ectoderm is intrinsically stiffer than mesoderm could well explain why the former is

particularly sensitive to EpCAM loss despite EpCAM ubiquitous expression in the early embryo. It is thus likely that the extent to which EpCAM controls migration and adhesion, even at equivalent levels of expression, will probably vary significantly between cell types as well as at different stages of cancer progression.

Mechanistically, EpCAM regulates signaling in a unique way. To our knowledge this is the first example of a plasma membrane protein that can directly bind and inhibit a kinase's catalytic site. It can be viewed as a remarkable case of convergent evolution toward the optimal pseudosubstrate sequence of novel PKCs (Fig. 3.6A and supplementary Table 3.S1). Consistent with the sequence similarity, our *in vitro* measurements demonstrate a clear specificity of EpCAM for the novel isoforms PKCδ and η compared to PKCβ. Note that in our binding experiments the PKCδ and η did not show the strict specificity for their own pseudosubstrate that is generally assumed. As for EpCAM, it binds nPKCs about as efficiently as the pseudosubstrates, and its affinity in the nanomolar range is consistent with a powerful inhibitory capacity. The 3D structure of PKC bound to EpCAM deduced through molecular modeling (Fig. 3.7A) is consistent with local efficient scavenging of membrane-bound activated PKCs. The tight sequestration of the catalytic site, which may be additionally constrained by the vicinity to the lipid bilayer, is expected to further hamper access to protein substrates, thus reinforcing the efficiency of the competitive inhibition. Potential mechanisms regulating this interaction will be the next obvious question to address in the future. Another interesting related question would be to determine whether an EpCAM-bound PKC may still be eventually released in the active form. Alternatively, PKCs may remain sequestered until eventually inactivated by loss of their lipid anchors, then released and potentially degraded. This latter possibility could then represent some sort of "catalytic" function of EpCAM in PKC de-activation, in which case one EpCAM may repress more than one PKC molecule, thus contributing to the observed massive repression.

We have found that EpCAM is probably not the only plasma membrane protein that can bind PKCs, but rather the first example of a novel group of regulators. The top list of the candidates identified by our search includes a variety of gene families evolutionary unrelated to each other. However, the list includes many functionally

related candidates (see annotations of supplementary Table S3). The largest group consists of CAMs. It includes at least 16 cell-cell or cell-matrix adhesion molecules (annotated as "CAM"), as well as several predicted CAMs of "CAM-like" (annotated as "(CAM)"). Altogether CAMs represent more than half of the 37 proteins with scores above 5. A second over-represented category (seven candidates) groups transmembrane proteins typically involved in cell guidance (including Eph receptors, plexin, DCC, slit-like proteins). A potential role in sequestering specifically novel PKC may be again consistent with the fact that they all interact in one way or the other with the actin cytoskeleton. Also, at least in the case of Eph receptors, these have been shown to function as cell-cell adhesion molecules under certain circumstances (Halloran and Wolman, 2006; Noren and Pasquale, 2004), further adding to the surprising coherence of this list. We speculate that these various molecules locally regulate PKC, each in a particular subcellular niche, and that there may be then a particular need to dampen PKC activity at sites of contact, a fascinating avenue to be pursued. The relative impact of each regulator will certainly vary widely, e.g. according to the relative affinity to PKCs, levels of expression and cell type, but we believe that our findings open a potential important new field of investigation in signal regulation. Because the sequence requirements of PKC phosphorylation targets are somewhat flexible (Marais et al., 1990; Kennelly and Krebs, 1991), it is likely that our search has missed additional nPKC binding candidates among the hundreds of juxtamembrane domains that contain basic residues. Furthermore, there isn't *a priori* any reason to exclude the existence of other related motifs specific for the two other classes of PKCs, thus further expanding the potential regulatory events occurring at such sites.

These results have uncovered a novel aspect of EpCAM biology, which stands as an unexpectedly important regulator of intracellular signaling. The discovery of this mechanism of PKC repression should now lead to new paths to understand the exact impact of EpCAM levels on cancer progression, and to explore new therapeutic strategies.

Material and methods

Embryo manipulations

Medium used was MBS-H (modified Barth solution containing: 88 mM NaCl, 1 mM KCl, 2.4 mM NaHCO3, 0.82 mM MgSO4, 0.33 mM Ca(NO3)2, 0.41 mM CaCl2, 10 mM Hepes, and 10 μg/ml streptomycin sulfate and penicillin, pH 7.4 adjusted with NaOH are described in Maghzal et al. (2010). Embryos were cultured in 1/10 MBS-H. Embryos were injected animally at the 2-cell stage (once in each blastomere) for global targeting, and animally at the 16-cell stage in 4 blastomeres (once in each blastomere) for mosaic embryos. Embryonic staging was performed according to Nieuwkoop and Faber (Nieuwkoop and Faber, 1967).

Plasmids, mRNAs, morpholino oligonucleotides and siRNAs

The following EpCAM cDNAs were cloned into pCS2+: xEpCAM encodes full-length *Xenopus laevis* EpCAM (aa1-315) C-terminally fused to 6x myc-tag (cloned into PCS2+MT) and hEpCAM encodes untagged full-length human EpCAM (Gostner et al., 2011). Other plasmids used: C-Cadherin in SP64 (Brieher et al, 1994), dominant negative PKCδ (Kinoshita et al., 2003), constitutively active V14RhoA, dominant negative N19RhoA and dominant negative N17Rac, membrane-targeted GAP43-eGFP (Rohani et al., 2011), and dominant negative dynamin (Jarrett et al., 2002). All plasmids were linearized with NotI and mRNAs were synthesized *in vitro* using SP6 RNA polymerase except for dominant negative dynamin which was linearized with KpnI and constitutively active V14RhoA which was linearized with KpnI and its mRNA synthesized using T3 polymerase.

cDNAs encoding full cytoplasmic domains of *Xenopus* EpCAM (aa290-314), the juxtamembrane sequences of *Xenopus* (aa290-302), human EpCAM-2/Trop-2 (aa298-312) and Zebrafish EpCAM-2 (Uniprot # Q568H0_DANRE) (aa283-295), human EphA4 (aa568-580), ICAM (aa504-517) and NrCAM (aa 1191-1203), and the pseudosubstrate sequences of human PKCδ (aa139-151) and PKCη (aa149-161) were all cloned into pGEX-4T3 to generate GST fused recombinant proteins for pulldown experiments. Single point mutations of Xenopus juxtamembrane are summarized in supplementary Fig.S6.

Control morpholino (COMO) and EpCAM morpholino (EpCAM MO)

(Maghzal et al., 2010) were injected at 40ng/blastomere at 2 cell stage and 10ng at 16 cell stages.

Control siRNA-A (siCTL) and human EpCAM siRNA (siEpCAM) were purchased from Santa Cruz Biotechnology, Inc. (Cat# sc-43032 and sc-37007).

Antibodies

Mouse anti-C-Cadherin mAb 5G5 was a generous gift of Barry Gumbiner, University of Virginia, Charlottesville, VA). The antibodies were purchased from the following source: Mouse anti-myc tag mAb 9E10 (Santa Cruz Biotechnology); rabbit anti-c-myc (Sigma Aldrich); mouse anti-EpCAM (323/A3) (Santa Cruz Biotechnology). Rabbit anti-PKC (H-300), rabbit anti-PKCη, rabbit anti-PKCδ, rabbit anti-PKCβII, rabbit anti-GAPDH and rabbit anti-α-Tubulin (all Santa Cruz Biotechnology); rabbit anti-phospho-myosin light chain 2 (Ser19), rabbit anti-phospho-(Ser) PKC substrates, rabbit anti-phospho-PKD/PKCμ (Ser744/748), rabbit anti-PKD/PKCμ and rabbit anti-E-Cadherin (24E10) (Cell Signaling Technology); mouse anti-Myosin light chain mAb T14-s (Developmental Studies Hybridoma Bank); mouse anti-phospho-Erk1/2 (T183+Y185) and rabbit anti-active caspase 3 (Abcam); mouse anti-Erk2 (BD Biosciences). Mouse anti-GSK3β (Beckton Dickenson, Transduction Laboratories).

Soluble inhibitors

Concentrations used and suppliers: bisindolylmaleimide I (Bis1), 500 nM; calphostin C (Calph C), 0.2 μM; Gö6976, 20 nM; PKC 20-28, 20 μM; Raf1 Kinase Inhibitor I (5-Iodo-3-[(3,5-dibromo-4-hydroxyphenyl)methylene]-2-indolinone), 5 nM; Erk Activation Inhibitor Peptide I (pep1), 500 nM; Blebbistatin, 100 μM; ML7, 20 μM, all from EMD. PKCη pseudo-substrate inhibitor, 25 ng/μl; Dynamin Inhibitor I, Dynasore, 10 μM (Santa Cruz Biotechnology). Y-27632 dihydrochloride, 25 μM (Sigma-Aldrich).

Loss of epithelial integrity assay and explant protein extraction

Ectoderm caps were dissected at stage 10 and cultured in 1x MBS-H overnight at 14^0C. Inhibitors were added in culture media before overnight incubation of explants

(7 h post-dissection). LEI phenotype was scored ~ 30 h post-dissection when the control embryos reached stage 18-20. For immunoblot analysis, explants were extracted ~ 23 h post-dissection (stage 16-17), i.e. before any incidence of lesions. Protein extraction was performed as follows: 6 explants were homogenized in 15µl Extraction Buffer (10 mM HEPES/NaOH pH 7.4, 150 mM NaCl, 2mM EDTA pH 8.0, 1% IGEPAL, 50 mM NaF, 10 mM Na-molybdate, 2 mM Na-vanadate). Homogenates were centrifuged at 15000g for 5 minutes, 15µl supernatants were collected to which 15µl of 2x SDS-PAGE sample buffer.

Cell culture and siRNA transfection

Caco-2 cells were cultured in Minimum Essential Medium 1X (MEM), [+] Earle's Salts, [+] L-Glutamine, with 10% fetal bovine serum and 5ml Non-essential amino acids (Gibco). Cells at ~60-80% confluency were seeded in six well tissue culture plates and transfected with 80 pmols of either siCTL or siEpCAM duplex in serum-free medium (Opti-MEM I, Invitrogen) using LipofectAMINE 2000 reagent (Invitrogen). After 8 h at 37^0C, the medium was replaced by 1X MEM, [+] Earle's Salts, [+] L-Glutamine, with 20% fetal bovine serum and 5ml NEAA and the cells were grown for further 24-72 h. Inhibitors were added in the culture medium 24h post-transfection, cells were then grown overnight in the presence of the inhibitor (~16 h) before fixation or extraction. For immunoblot analysis, cells in each well were lysed by scraping directly in 250µl of boiling 2x Laemmli sample buffer. Collected supernatants were sonicated and heated for 5 minutes at 98^0C.

Immunofluorescence and microscopy

Cryosectioning and immunofluorescence of *Xenopus* embryos and explants were performed as previously described (Fagotto and Brown, 2008; Schohl and Fagotto, 2002). Caco-2 cells grown on coverslips were fixed with 4% paraformaldehyde, 0.5% Triton X-100 in phosphate-buffered saline for 10 min, followed by a 30min incubation in blocking buffer (0.2% gelatin, 0.5% bovine serum albumin in phosphate-buffered saline) and a 2hrs incubation with primary antibody in blocking buffer. Secondary antibodies were Alexa488 and Alexa594 (Molecular Probes/Invitrogen). Samples were observed under a DM IRE2 microscope (Leica)

equipped with a 20 X/0.70 IMM Corr CS oil immersion objective and a Hamamatsu ORCA-ER camera. Images were acquired using MetaMorph (Molecular Devices) software. Images of whole embryos and explants were acquired using a stereomicroscope (model MZ16F; Leica), a Qimaging camera (Micropublisher 3.3 RTV) and QCapture image acquisition software (Quantitative Imaging Corporation).

Pull downs

In vivo. 20 embryos were lysed in buffer containing 50 mM Tris HCl pH 7.4, 50 mM NaCl, 2mM $MgCl_2$, 0.1 mM EDTA, 1mM DTT, 0.5% IGEPAL (Sigma Aldrich), 1/500 of protease inhibitor cocktails 1 (50 mM PMSF, 0.1 mg/ml TLCK solution in isopropanol) and 2 (1 mg/ml leupeptin, 2 mg/ml aprotinin, 0.2 M benzamidine, 0.5 mg/ml soybean trypsin inhibitor, 0.25 M iodacetamide solution in double-distilled H_2O). Lysates were spun at 15000 g for 15 minutes at 4^0C, supernatents were collected and spun under the same conditions for a second time. Spun extracts were pre-cleared using empty glutathione sepharose 4B beads (GE Healthcare). 20µl of GST or GST-TAIL bound beads were added to pre-cleared lysates and pulldown was performed at 4^0C with end-over-end rocking for 3 h. Beads were then washed 4 times in lysis buffer at 4^0C with end-over-end rocking for 3 minutes, eluted in 20µl 2x Laemmli sample buffer and boiled for 5 minutes at 100^0C.

In vitro. 20µl of GST and GST-TAIL beads were blocked with 100µl of 5% bovine serum albumin (BSA) by end-over-end rocking at 4^0C. Beads were then washed 2x in Pull-down buffer, "PDB" (150 mM NaCl, 50 mM Tris-HCl pH 7.4, 1 mM $CaCl_2$, 2 mM $MgCl_2$, pH 7.4). 10 ng of recombinant N-terminal 6His-tagged PKCs η, δ or β_{II} (Millipore) were added to a tube containing: 20µl of GST or GST-TAIL beads, 39.75µl of PDB, 4µl of PKC lipid activator (Millipore), 2.5µl of 10x ATP regenerating system (10mM adenosine-5'-triphosphate, pH 7.5, 100mM creatine phosphate, 10U creatine kinase, Roche), 3µl of 5% BSA, 0.75µl of 20% IGEPAL and 1/500 of protease inhibitor cocktail. Pulldown were then performed by rocking the tubes end-over-end for 1h at room temperature. Beads were washed as follows: 500µl PDB were added to beads and wash was performed by end-over-end rocking at 4^0C for 5 minutes. The washes were then overlaid carefully on a 185µl 1 M sucrose cushion and spun at 1000g for 1 minute at 4^0C. The wash buffer and sucrose were

carefully removed and replaced by PDB for another round of wash. 3 rounds of washes were performed in total. Proteins were eluted in 20µl 2x Laemmli sample buffer and boiled for 5 minutes at 100^0C.

Immunoprecipitation

3x10cm^2 dishes of confluent Caco-2 cells were washed in 1X Dulbecco's Phosphate Buffered Saline [+] calcium chloride [+] magnesium chloride (GIBCO). Cells in each dish were lysed by scraping with 150µl lysis buffer containing 80 mM NaCl, 10 mM HEPES-NaOH, 2mM $MgCl_2$, 1mM EDTA, 2mM vanadate, 0.5% IGEPAL and 1/500 of protease inhibitor cocktails 1 and 2. Lysates were spun at 15000 g for 10 minutes at 4^0C and supernatents were pre-cleared by end-over-end rocking at 4^0C with protein G agarose (Pierce) for 30mins. 500µl of pre-cleared lysates were immunoprecipitated with 5 µg of mouse anti-Ep-CAM 323/A3 (Santa Cruz Biotechnology, Inc.) or 5 µg of mouse IgG (Jackson ImmunoResearch Laboratories, Inc.) by end-over-end rocking at 4^0C for 2 h. Immunoprecipitates were spun at 15000 g for 10 minutes at 4^0C and supernatents were rocked end-over-end with 20µl of protein G agarose for 45 minutes at 4^0C. Beads were then washed 4 X in lysis buffer at 4^0C and proteins were eluted using 20µl of DTT free 2x Laemmli sample buffer.

Kinase assay

Each 25µl reaction contained 1µl (0.5 mM) Myelin Basic Protein; "MBP" (Santa Cruz Biotechnology, Inc.); 3µl (9ng) of recombinant N-terminal 6His-tagged PKCδ (Millipore); 11µl of reaction master mix containing 2.5µl of 10 X reaction buffer (200mM HEPES/NaOH pH7.4, 0.3% Triton X-100, 1mM $CaCl_2$), 2.5µl PKC lipid activator (Millipore), 2.5µl 1 mM $CaCl_2$, 2.5µl 10x ATP regenerating system, 1µl (1µg) of phorbol 12-myristate 13-acetate (EMD); and varying amounts of GST or GST-TAIL (1.5 – 6 mM). The reaction was started with the addition of PKCδ, and was carried out for 10 minutes at 30^0C for 10 minutes. It was stopped by adding 12.5µl of 4 X Laemmli sample buffer. Samples were analyzed by immunoblot with anti–phospho-(Ser) PKC substrate antibody (Cell Signaling Technology).

Surface Plasmon Resonance (SPR)

Binding of GST-EpCAM fusions (26 kDa GST + 4 kDa short EpCAM tail = ~30 kDa for wild type or mutants) to His-tagged PKCδ and η (~79 kDa each) was examined using label-free, real-time BIACORE 3000 instrumentation (GE Healthcare Bio-Sciences AB, Upsala, Sweden). Experiments were performed on research-grade NTA sensor chips at 25°C using filtered (0.2 μm) and degassed PDB supplemented with 0.05% (v/v) Tween-20). Protein-grade detergents (Tween-20, Empigen) were from Anatrace (Maumee, USA) and Pierce Gentle Elution buffer was from Thermo Scientific (Illinois, USA); all other chemicals were reagent grade quality.

PKC recombinant proteins were centrifuged just before immobilization to remove precipitates. As recommended by the manufacturer, the NTA sensors were pre-conditioned with EDTA (350 mM x 1 min), activated with $NiCl_2$ (500μM x 1 min), and PKC (diluted to 200 nM in running buffer) was captured at low (~500 RU) or high (~3000 RU) density; corresponding reference surfaces were prepared in the absence of any ligand. To assess binding specificity in multi-cycle mode, negative controls (GST, BSA) and the EpCAM fusions were injected over reference and high-density PKC surfaces at 50μl/min (1 min association + 5 min dissociation; 500 nM fixed). Between sample injections, the sensors were regenerated at 50μl/min using two 30-second pulses of solution I (1M NaCl in running buffer) and II (Pierce Gentle Elution buffer containing 0.05% (v/v) Empigen), successfully removing any residually-bound analyte without disturbing the immobilized PKC surfaces. To assess dose-dependent binding in single-cycle mode, samples were then injected over reference and low-density PKC surfaces at 50μl/min (1 min association + 30 – 300 sec dissociation; 2-fold dilution series = 62.5 – 1000 nM); between titration series, surfaces were regenerated as noted above.

Data was doubled-referenced and is representative of duplicate injections acquired from at least two independent trials. During multi- and single-cycle series, replicate injections of an internal standard (xJM= Xenopus EpCAM juxtamembrane

domain, placed at start, middle, and end of runs) verified that consistent PKC surface activity was maintained throughout each assay. Apparent equilibrium dissociation constants (K_D) for the single-cycle titrations were determined by global fitting of the data to the "1:1 Titration" model in the BIAevaluation v4.1 software. Individual dissociation rate constants for the single-cycle titrations were determined using the "Fit separate k_a/k_d" tool in the BIAevaluation software.

Bioinformatics search for additional binding partners of PKCδ.

The generalized sequence profile method and the *pftools* package (Bucher et al., 1996) were used. The initial profile was constructed based on the alignment of the homologous sequences of human tumor-associated calcium signal transducer 2 that was shown to bind PKCδ. This 15 residue binding region was preceded by a transmembrane helix, yielding a 41 residue-long final profile. The profiles were matched against human proteome downloaded from NCBI database (ftp.ncbi.nih.gov). In the later stages of iterative profile refinement, the previous-round profile was used as a template to align the newly accepted sequences. Manual alignment corrections where applied whenever necessary. The newly detected sequences were then examined individually to select candidates for subsequent experimental tests. The probability that the matches are a product of chance alone was calculated by analyzing the score distribution obtained from a profile search against a regionally randomized version of the protein database, assuming an extreme value distribution (Hofmann and Bucher, 1995).

Molecular modeling

Homology-based molecular modeling of human PKCδ kinase catalytic domain (SwissProt accession number Q05655, positions 342 to 674) in complex with ATP and peptide ITNRRKSGKYKKVE from human EpCAM/Trop-2/tumor-associated calcium signal transducer 2 was performed as follows. The PKCδ kinase sequence was aligned by CLUSTALW program (http://www.ebi.ac.uk/Tools/msa/clustalw2/) with several other homologous kinase sequences, for which crystal structures with bound peptide substrates have been already resolved: (human PKC-theta kinase, PDB code 1XJD; mouse cAMP-

dependent protein kinase, PDB code 1ATP ; and human Akt-1 kinase, PDB code 3CQU). Subsequently, the homology modeling option of Insight II program (Dayring et al., 1986) was used. The model was further refined by the energy minimization procedure that was based on the steepest descent algorithm (100 steps) followed by the conjugate gradients algorithm (500 steps). The consistent valence force field and the distance dependent dielectric constant were used. Fig.7A was generated with Pymol (http://pymol.org/).

References

Ammons, W.S., Bauer, R.J., Horwitz, A.H., Chen, Z.J., Bautista, E., Ruan, H.H., Abramova, M., Scott, K.R., and Dedrick, R.L. (2003). In vitro and in vivo pharmacology and pharmacokinetics of a human engineered monoclonal antibody to epithelial cell adhesion molecule. Neoplasia *5*, 146-154.

Bucher, P., Karplus, K., Moeri, N., and Hofmann, K. (1996). A flexible motif search technique based on generalized profiles. Computers & chemistry *20*, 3-23.

Chen, C.L., and Chen, H.C. (2009). Functional suppression of E-cadherin by protein kinase Cdelta. J Cell Sci *122*, 513-523.

Cubas, R., Li, M., Chen, C., and Yao, Q. (2009). Trop2: a possible therapeutic target for late stage epithelial carcinomas. Biochim Biophys Acta *1796*, 309-314.

Dayring, H.E., Tramonato, A., Sprang, S.R., and Fletterick, R.J. (1986). Interactive program for visualization and modeling of proteins, nucleic acids. J Mol Graph *4*, 82-87.

Denzel, S., Maetzel, D., Mack, B., Eggert, C., Barr, G., and Gires, O. (2009). Initial activation of EpCAM cleavage via cell-to-cell contact. BMC Cancer *9*, 402.

Fagotto, F., and Brown, C.M. (2008). Detection of nuclear beta-catenin in Xenopus embryos. Methods Mol Biol *469*, 363-380.

Gaiser, M.R., Lammermann, T., Feng, X., Igyarto, B.Z., Kaplan, D.H., Tessarollo, L., Germain, R.N., and Udey, M.C. (2012). Cancer-associated epithelial cell adhesion molecule (EpCAM; CD326) enables epidermal Langerhans cell motility and migration in vivo. Proc Natl Acad Sci U S A *109*, E889-897.

Gostner, J.M., Fong, D., Wrulich, O.A., Lehne, F., Zitt, M., Hermann, M., Krobitsch, S., Martowicz, A., Gastl, G., and Spizzo, G. (2011). Effects of EpCAM overexpression on human breast cancer cell lines. BMC Cancer *11*, 45.

Halloran, M.C., and Wolman, M.A. (2006). Repulsion or adhesion: receptors make the call. Curr Opin Cell Biol *18*, 533-540.

Hofmann, K., and Bucher, P. (1995). The FHA domain: a putative nuclear signaling domain found in protein kinases and transcription factors. Trends in biochemical sciences *20*, 347-349.

Iwabu, A., Smith, K., Allen, F.D., Lauffenburger, D.A., and Wells, A. (2004). Epidermal growth factor induces fibroblast contractility and motility via a protein kinase C delta-dependent pathway. J Biol Chem *279*, 14551-14560.

Jaggi, M., Rao, P.S., Smith, D.J., Wheelock, M.J., Johnson, K.R., Hemstreet, G.P., and Balaji, K.C. (2005). E-cadherin phosphorylation by protein kinase D1/protein kinase C{mu} is associated with altered cellular aggregation and motility in prostate cancer. Cancer Res *65*, 483-492.

Jarrett, O., Stow, J.L., Yap, A., and Key, B. (2002). Dynamin-dependent endocytosis is necessary for convergentextension movements in Xenopus animal cap explants. Int J Dev Biol *46*, 467-473.

Kennelly, P.J., and Krebs, E.G. (1991). Consensus sequences as substrate specificity determinants for protein kinases and protein phosphatases. J Biol Chem *266*, 15555-15558.

Kinoshita, N., Iioka, H., Miyakoshi, A., and Ueno, N. (2003). PKC delta is essential for Dishevelled function in a noncanonical Wnt pathway that regulates Xenopus convergent extension movements. Genes Dev *17*, 1663-1676.

Kishimoto, A., Nishiyama, K., Nakanishi, H., Uratsuji, Y., Nomura, H., Takeyama, Y., and Nishizuka, Y. (1985). Studies on the phosphorylation of myelin basic protein by protein kinase C and adenosine 3':5'-monophosphate-dependent protein kinase. J Biol Chem *260*, 12492-12499.

Le, T.L., Joseph, S.R., Yap, A.S., and Stow, J.L. (2002). Protein kinase C regulates endocytosis and recycling of E-cadherin. American journal of physiology Cell physiology *283*, C489-499.

Lei, Z., Maeda, T., Tamura, A., Nakamura, T., Yamazaki, Y., Shiratori, H., Yashiro, K., Tsukita, S., and Hamada, H. (2012). EpCAM contributes to formation of functional tight junction in the intestinal epithelium by recruiting claudin proteins. Dev Biol.

Litvinov, S.V., Velders, M.P., Bakker, H.A., Fleuren, G.J., and Warnaar, S.O. (1994). Ep-CAM: a human epithelial antigen is a homophilic cell–cell adhesion molecule. J Cell Biol *125*, 437–446.

Maaser, K., and Borlak, J. (2008). A genome-wide expression analysis identifies a network of EpCAM-induced cell cycle regulators. British journal of cancer *99*, 1635-1643.

Maetzel, D., Denzel, S., Mack, B., Canis, M., Went, P., Benk, M., Kieu, C., Papior, P., Baeuerle, P.A., Munz, M.*, et al.* (2009). Nuclear signalling by tumour-associated antigen EpCAM. Nat Cell Biol *11*, 162-171.

Maghzal, N., Vogt, E., Reintsch, W., Fraser, J.S., and Fagotto, F. (2010). The tumor-associated EpCAM regulates morphogenetic movements through intracellular signaling. J Cell Biol *191*, 645-659.

Marais, R.M., Nguyen, O., Woodgett, J.R., and Parker, P.J. (1990). Studies on the primary sequence requirements for PKC-alpha, -beta 1 and -gamma peptide substrates. FEBS letters *277*, 151-155.

Munz, M., Baeuerle, P.A., and Gires, O. (2009). The emerging role of EpCAM in cancer and stem cell signaling. Cancer Res *69*, 5627-5629.

Munz, M., Kieu, C., Mack, B., Schmitt, B., Zeidler, R., and Gires, O. (2004). The carcinoma-associated antigen EpCAM upregulates c-myc and induces cell proliferation. Oncogene *23*, 5748-5758.

Nagao, K., Zhu, J., Heneghan, M.B., Hanson, J.C., Morasso, M.I., Tessarollo, L., Mackem, S., and Udey, M.C. (2009). Abnormal placental development and early embryonic lethality in EpCAM-null mice. PLoS One *4*, e8543.

Newton, A.C. (2001). Protein kinase C: structural and spatial regulation by phosphorylation, cofactors, and macromolecular interactions. Chem Rev *101*, 2353-2364.

Nguyen, D.H., Catling, A.D., Webb, D.J., Sankovic, M., Walker, L.A., Somlyo, A.V., Weber, M.J., and Gonias, S.L. (1999). Myosin light chain kinase functions downstream of Ras/ERK to promote migration of urokinase-type plasminogen activator-stimulated cells in an integrin-selective manner. The Journal of cell biology *146*, 149-164.

Nieuwkoop, P., and Faber, P. (1967). Normal table of Xenopus laevis. (Amsterdam, North-Holland Publ.).

Nishikawa, K., Toker, A., Johannes, F.J., Songyang, Z., and Cantley, L.C. (1997). Determination of the specific substrate sequence motifs of protein kinase C isozymes. J Biol Chem *272*, 952-960.

Noren, N.K., and Pasquale, E.B. (2004). Eph receptor-ephrin bidirectional signals that target Ras and Rho proteins. Cell Signal *16*, 655-666.

Osta, W.A., Chen, Y., Mikhitarian, K., Mitas, M., Salem, M., Hannun, Y.A., Cole, D.J., and Gillanders, W.E. (2004). EpCAM is overexpressed in breast cancer and is a potential target for breast cancer gene therapy. Cancer Res *64*, 5818-5824.

Patriarca, C., Macchi, R.M., Marschner, A.K., and Mellstedt, H. (2012). Epithelial cell adhesion molecule expression (CD326) in cancer: a short review. Cancer Treat Rev *38*, 68-75.

Rohani, N., Canty, L., Luu, O., Fagotto, F., and Winklbauer, R. (2011). EphrinB/EphB signaling controls embryonic germ layer separation by contact-induced cell detachment. PLoS biology *9*, e1000597.

Rosse, C., Linch, M., Kermorgant, S., Cameron, A.J., Boeckeler, K., and Parker, P.J. (2010). PKC and the control of localized signal dynamics. Nature reviews Molecular cell biology *11*, 103-112.

Rozengurt, E., Rey, O., and Waldron, R.T. (2005). Protein kinase D signaling. J Biol Chem *280*, 13205-13208.

Sahai, E., and Marshall, C.J. (2002). ROCK and Dia have opposing effects on adherens junctions downstream of Rho. Nat Cell Biol *4*, 408-415.

Schohl, A., and Fagotto, F. (2002). Beta-catenin, MAPK and Smad signaling during early Xenopus development. Development *129*, 37-52.

Seimetz, D., Lindhofer, H., and Bokemeyer, C. (2010). Development and approval of the trifunctional antibody catumaxomab (anti-EpCAM x anti-CD3) as a targeted cancer immunotherapy. Cancer Treat Rev *36*, 458-467.

Singh, R., Lei, P., and Andreadis, S.T. (2009). PKC-delta binds to E-cadherin and mediates EGF-induced cell scattering. Exp Cell Res *315*, 2899-2913.

Slanchev, K., Carney, T.J., Stemmler, M.P., Koschorz, B., Amsterdam, A., Schwarz, H., and Hammerschmidt, M. (2009). The epithelial cell adhesion molecule EpCAM is required for epithelial morphogenesis and integrity during zebrafish epiboly and skin development. PLoS Genet *5*, e1000563.

Steinberg, S.F. (2004). Distinctive activation mechanisms and functions for protein kinase Cdelta. Biochem J *384*, 449-459.

Suzuki, T., Elias, B.C., Seth, A., Shen, L., Turner, J.R., Giorgianni, F., Desiderio, D., Guntaka, R., and Rao, R. (2009). PKC eta regulates occludin phosphorylation and epithelial tight junction integrity. Proc Natl Acad Sci U S A *106*, 61-66.

Trebak, M., Begg, G.E., Chong, J.M., Kanazireva, E.V., Herlyn, D., and Speicher, D.W. (2001). Oligomeric state of the colon carcinoma-associated glycoprotein GA733-2 (Ep-CAM/EGP40) and its role in GA733-mediated homotypic cell-cell adhesion. J Biol Chem *276*, 2299-2309.

Tsukahara, Y., Tanaka, M., and Miyajima, A. (2011). TROP2 expressed in the trunk of the ureteric duct regulates branching morphogenesis during kidney development. PLoS One *6*, e28607.

Villablanca, E.J., Renucci, A., Sapede, D., Lec, V., Soubiran, F., Sandoval, P.C., Dambly-Chaudiere, C., Ghysen, A., and Allende, M.L. (2006). Control of cell migration in the zebrafish lateral line: implication of the gene "tumour-associated calcium signal transducer," tacstd. Dev Dyn *235*, 1578-1588.

Visvader, J.E., and Lindeman, G.J. (2008). Cancer stem cells in solid tumours: accumulating evidence and unresolved questions. Nature reviews Cancer *8*, 755-768.

Wong, C., and Jin, Z.G. (2005). Protein kinase C-dependent protein kinase D activation modulates ERK signal pathway and endothelial cell proliferation by vascular endothelial growth factor. J Biol Chem *280*, 33262-33269.

Wong, E.V., Schaefer, A.W., Landreth, G., and Lemmon, V. (1996). Involvement of p90rsk in neurite outgrowth mediated by the cell adhesion molecule L1. J Biol Chem *271*, 18217-18223.

Figure legends

Figure 3.1. EpCAM is required for maintenance of tissue integrity during Xenopus development.

(A-C) External embryo phenotype, tailbud stage. Compared to embryos injected with control morpholinos (A, COMO), EpCAM-depleted embryos (B, EpCAM MO) were generally shorter, which can be attributed to impaired morphogenetic movements. Most of them (>90%) displayed epidermal lesions out of which loose cells leaked out (arrows and inserts B', B"). The lesions invariably expanded and the entire embryo disintegrated (B, last embryo to the bottom). C. Normal development was largely rescued by co-injection of mRNA coding for EpCAM with an upstream coding sequence not recognized by the morpholinos. **(D-H)** Analysis of the inner structure of mosaic embryos. Mosaics were obtained by MO injection in one blastomere at the 16 cell stage. mRNA coding for membrane-targeted GFP (mGFP) was co-injected to trace the injected cells. Sagittal sections were stained for GFP (green) and for C-cadherin (red). (**D, E)** Control cells (COMO). (**F, G, H)** EpCAM-depleted cells. (**D, F)** dorsal side, tailbud stage. (**E, G)** Detail of the ventral side, tailbud stage. **(H)** dorsal side, neurula stage. At tailbud stage, most EpCAM-depleted cells were round. Many were expelled out of the tissues and even out of the embryo (arrowheads). Those remaining in the tissues appeared poorly integrated (arrows). **(G')** EpCAM MO-injected cells displayed a conspicuous loss of C-cadherin compared to adjacent wild type cells or to COMO-injected cells **(E')**. **(H, H')** At an earlier stage (neurula), EpCAM MO- injected cells still maintained contacts with neighboring wild-type cells, but already showed decreased cadherin staining, in all types of tissues (on this section neuroderm, mesoderm, endoderm). Arrows indicate limits between EpCAM MO and wild type groups. ar: archenteron roof; ec: ectoderm; en: endoderm; me: mesoderm; ne: neuroderm; som: somites.

Figure 3.2. Loss of integrity of EpCAM-depleted ectoderm explants.

(A) Animal explants were dissected at the early gastrula stage. Such explants typically heal into balls of undifferentiated ectoderm tissue constituted of an outer pigmented layer of polarized epithelial cells surrounding an inner mass of non-polarized cells. After overnight culture (corresponding to tailbud stage in control embryos), control explants were all still intact **(A')**, but EpCAM MO-injected explants systematically burst **(A")**. **(B)** Quantification of "loss of epithelial integrity" (LEI), i.e. percentage of bursting explants. Integrity could be rescued by co-injection of mRNA coding for Xenopus or human EpCAM, as well as by C-cadherin overexpression. ** indicate $p<0.001$ compared to EpCAM MO (Student's *t* test). Numbers on top indicate total number of explants displaying LEI/total number of injected explants. **(C)** EpCAM and C-cadherin levels in explants extracted at neurula stage, i.e. before visible bursting. EpCAM MO caused almost complete loss of EpCAM, and concurrent strong decrease in cadherin levels. **(D-F)** Cadherin immunostaining on sections of control and EpCAM-depleted explants. **(D)** In control explants, plasma membranes are typically decorated with cadherin "puncta". **(E)** Already at stage 16 (early neurula), cadherin, EpCAM depletion caused strong reduction of plasma membrane cadherin signal and appearance of intracellular spots (arrows). **(F)** By the late neurula (stage 19), the cadherin signal had almost disappeared.

Figure 3.3. EpCAM regulates PKC activity in embryos and in cancer cells. **(A)** Immunoblot detection of PKC activity in embryo extracts, using an antibody recognizing phosphorylated PKC substrates. The signal was increased for a subset of bands upon EpCAM depletion (examples shown with arrows), which was rescued by a co-injection of an mRNA coding for PKCδ pseudosusbtrate (dnPKCδ). Arrowheads point to bands that remained unchanged. Asterisk: band responding to EpCAM MO/dnPKCδ, but saturated in this image. Coommassie staining was used as loading control. **(B)** Immunoblot detection of PKC activity in Caco-2 cells. Caco-2 cells were transfected with anti-EpCAM siRNA, and extracted 2 days later. A massive increase in p-PKC substrate signal is observed (arrows). **(C)** Immunofluorescence detection of PKC activity in Caco-2 cells. siRNA-transfected cells were double stained for EpCAM and p-PKC substrates. EpCAM depletion led to a general increase in p-PKC substrate signal, including in the nucleus and at the plasma membrane. The signal was completely abrogated by a 2 hr treatment with the PKC inhibitor calphostin C. Relative intensities of p-PKC sub are represented as pseudocolors in the lower panels. **(D)** LEI depends on non-classical PKCs. Explant integrity could be rescued by a generic PKC inhibitor (Bis1) and most efficiently by inhibitors specific to non-classical PKCs (δ and η). Calphostin (PKCγ+δ) and Gö6976 (PKCα,β,γ) had moderate effects and PKC 20-28 (PKCα,β) none. **(E)** PKC and Erk inhibitors rescue cadherin levels in EpCAM-depleted explants. EpCAM MO-injected explants were treated with Bis1 (PKC) and pep1 (Erk) inhibitors.

Figure 3.4. LEI in EpCAM-depleted tissues is due to increased myosin contractility downstream of PKC.

(A) EpCAM depletion causes increased myosin light chain phosphorylation (p-MLC). **(B)** Cadherin levels are rescued by treatment of EpCAM-depleted explants with the myosin inhibitor blebbistatin. **(C, D)** Expression of constitutively active RhoA (carhop) stimulates MLC phosphorylation and reduces cadherin levels. **(E-F)** Rescue of tissue integrity by inhibitors of myosin light chain kinase (ML-7) and myosin ATPase (blebbistatin), and induction of LEI by constitutively active Rho. **(G-H)** *In vivo* rescue of tissue integrity by expression of dominant negative PKCδ, by cadherin overexpression, or by treatment with blebbistatin. Embryos were injected in the animal ventral side with control (COMO), EpCAM MO, or EpCAM MO and mRNA coding for C-cadherin of for dominant negative PKCδ. Some EpCAM MO-injected embryos were also treated from early gastrula onwards with blebbistatin. The formation of lesions was completely blocked in each of the three rescues. General development was largely normal for dnPKCδ-inhibited and C-cadherin rescued embryos **(G)**. Blebs near the head are injection artifacts. For blebbistatin-treated embryos, the embryo morphology was rather severely perturbed (not shown), but no epithelial lesion was observed, and the embryos hatched. * and ** indicate respectively $p<0.01$ and $p<0.001$ compared to EpCAM MO (Student's *t* test).

Figure 3.5. LEI upon EpCAM depletion involves activation of the Erk pathway via PKD/PKCμ.

(A) Summary diagram of the pathway: EpCAM inhibits novel PKCs, which otherwise activate PKD/PKCμ, which in turns stimulate the Erk pathway. Phosphorylated Erk phosphorylates/activates MLCK, and thus MLC. Overactivated myosin destabilizes adhesion and causes decrease in cadherin levels. **(B)** Increased PKD/PKCμ phosphorylation in EpCAM MO explants and rescue by dnPKCδ. **(C)** Stimulation of Erk phosphorylation in EpCAM-depleted Xenopus explants and Caco-2 cells, rescued by dnPKCδ and by Raf inhibitor. **(D, E)** Raf inhibition rescues p-MLC and cadherin levels in EpCAM-depleted tissues. **(F)** Rescue of tissue integrity by Raf or Erk (pep1) inhibition.

Figure 3.6. The juxtamembrane region of EpCAM cytoplasmic tail corresponds to a pseudosubstrate-like motif that binds directly and inhibits PKCs.

(A) Alignment of the juxtamembrane region of *Xenopus* (x), human (h) and Zebrafish (z) EpCAMs, non-classical PKC substrate consensus and pseudosubstrate sequences (Steinberg, 2004). Residues replacing the phosphorylated Ser/Thr at position P=0 are underlined. Conserved tyrosine in EpCAM and corresponding phenylalanine at P+1 of PKC substrates are highlighted in yellow, and basic residues on both sides of P=0 in blue. "...TM" indicates the end of the transmembrane domain in the EpCAM sequences. **(B)** EpCAM and PKCδ interact *in vivo*. EpCAM was immunoprecipitated from Caco-2 cell extracts, and the precipitate was probed for PKCδ. **(C)** *In vitro* interaction between endogenous PKCs from a Xenopus embryo extract and recombinant EpCAM cytoplasmic tail fused to GST (xTAIL). Bound PKCs were detected by immunoblot: A pan-PKC antibody recognized three bands in extracts, two of which were recovered in the xTAIL bound fraction (arrowheads). The presence of PKCδ in this fraction was demonstrated using an isoform specific antibody. **(D)** Direct *in vitro* binding of recombinant PKCδ and PKCη to cytoplasmic tails of Xenopus, human and Zebrafish EpCAM. Purified activated PKCs were incubated with GST fusions of the complete Xenopus EpCAM tail (xTAIL), of the 13 amino acids of its juxtamembrane domain (JM), or the equivalent sequence from human and Zebrafish EpCAM2 (see panel A). GST was used negative control. **(E)** EpCAM-PKC interaction is competed by PKC pseudosubstrate. Direct *in vitro* pull down was performed in the presence of 100x excess of a peptide corresponding to the pseudosubstrate region of PKCη. **(F)** The EpCAM cytoplasmic tail directly inhibits PKC activity. *In vitro* kinase activity of PKCδ was determined by monitoring the phosphorylation levels of myelin basic protein (MBP) on immunoblots using the p-PKC substrate antibody. Addition of increasing amounts of recombinant xTAIL, but not of control GST, inhibited MBP phosphorylation in a dose-dependent fashion.

Figure 3.7. Model of EpCAM-PKCδ interaction, and identification of other similar juxtamembrane sequences with PKC binding properties.

(A, A') A model of activated human PKCδ kinase bound to ATP and to the juxtamembrane region ITNRRKSGKYKKVE of human EpCAM2/EGL-1/Trop-2/tumor-associated calcium signal transducer 2. **(A)** Overall structure of the known kinase domains: C2, C1A, C1B and catalytic domain of the kinase linked to each other by flexible cross-linkers. C2, C1A and C1B domains interact with the lipid bilayer through association with diacylglycerol and phospholipids (not represented). The pseudosubstrate region of PKCδ located upstream of C1A domain is shown in ball-and-stick representation. The catalytic domain is shown with the bound peptide region (ball-and-stick representation) and transmembrane (TM) helix (ribbon) of EpCAM. Positively and negatively charged residues on the surface of the kinase are shown by blue and salmon colors correspondingly. The modeling reveals that the positively charged residues (in blue) of the bound peptide are surrounded by the clusters of negatively charged residues (salmon color) of the kinase. The model suggests a positioning and orientation of the kinase catalytic domain relative to EpCAM TM helix that would hold it in tight apposition to the membrane. **(A')** A close-up view of the bound peptide (carbon atoms in green) in the binding pocket of PKCδ catalytic domain (in blue). Oxygen, nitrogen and phosphate atoms are in red, blue and orange, respectively. Ionic or hydrogen bonds between peptide and kinase are denoted by a red broken line. Note the tyrosine of position P+1 intimately fitting into a hydrophobic pocket. The atomic coordinates of the model are available upon request. **(B)** Alignment of the *Xenopus* and human EpCAM juxtamembrane domains (JM) with EphA4, ICAM and NrCAM JMs. The top row indicates a generic nPKC substrate consensus motif. **(C)** JMs of EphA4, ICAM and NrCAM bind novel PKCs. Representative example of *in vitro* interaction pulldowns of PKCδ and PKCη with GST fusions of EphA4, ICAM and NrCAM JMs. Coommassie staining showing levels of GST is used as loading control.

Supplementary figure legends and table legends

Table 3.S1. Related to figure 3.1

Quantification of whole embryo disaggregation phenotype upon EpCAM depletion.

Embryos injected at the two cell stage with control or EpCAM MO were scored for open epithelial wounds at the tailbud stage (see figure 1). All embryos with wound eventually died.

Figure 3.S2. Related to figure 3.2.

(A-C) EpCAM knockdown disrupts adhesion in both inner and outer ectoderm. (A) Diagram of the dissection and *in vitro* culture of inner and outer ectoderm layers. **(B) Examples of explants from control and bursting EpCAM MO-injected outer and inner layer ectoderm explants. (C)** Quantification of three independent experiments. Numbers on top indicate total number of explants displaying LEI/total number of injected explants. P values correspond to Student's *t* test. **(D) Cadherin and catenin mRNA levels are not affected by EpCAM.** Extracts from control (uninjected and COMO-injected), EpCAM-depleted (EpCAM MO) and EpCAM-expressing (EpCAM mRNA) explants were analyzed by RT-PCR for C-cadherin, α-catenin, β-catenin, and E-cadherin. ODC was used as loading control. Explants injected with C-cadherin mRNA were analyzed to compare endogenous and exogenous levels used for rescue experiments. **(E) Apoptosis occurs downstream of PKC/ Erk activation and of cadherin downregulation**. Decreased C-cadherin levels and increased Erk phosphorylation in EpCAM MO ectoderm were accompanied by a strong increase in cleaved activated caspase 3. Forced C-cadherin expression by co-mRNA injection blocked caspase 3 cleavage in EpCAM MO explants. Caspase 3 activation was also inhibited by treatment with the PKC inhibitor Bis1 or the Erk inhibitor pep. Coommassie staining was used to control for loading. **(F, G) Inhibition of dynamin-mediated endocytosis rescues EpCAM MO-induced LEI. (F)** C-cadherin loss in EpCAM MO-injected ectoderm was rescued by dominant negative dynamin (dnDyn). GSK3β was used as a loading control. **(G)** Expression of dominant negative dynamin or incubation with the soluble inhibitor dynasore rescued EpCAM MO-induced LEI. ** = $p<0.001$ compared to EpCAM MO (Student's *t* test). Numbers on top indicate total number of explants displaying LEI/total number of injected explants.

Figure 3.S3. Related to figure 3.3.

E-cadherin is downregulated in EpCAM-depleted Caco-2 cells in a PKC-dependent manner.

Double EpCAM and E-cadherin immunostaining of siCTL (control) and siEpCAM-transfected Caco-2 cells. EpCAM and E-cadherin signals are at plasma membranes of control cells (top panels, arrows). EpCAM depletion reduces membrane E-cadherin staining and causes an accumulation of E-cadherin puncta in the cytoplasm (middle panels, arrowheads). Treatment with the nPKC inhibitor Calphostin C rescues membrane E-cadherin in EpCAM-depleted Caco-2 cells.

Figure 3.S4. Related to figure 3.4.

LEI in EpCAM MO ectoderm is rescued by inhibition RhoA/ROK.

(A) Inhibitions of Rho either by coexpression of dominant negative RhoA or treatment with ROCK inhibitor Y-27632 rescued EpCAM MO-induced LEI. Coexpression of dominant negative Rac failed to rescue LEI. ** indicates $p<0.001$ compared to EpCAM MO (Student's *t* test). Numbers on top indicate total number of explants displaying LEI/total number of injected explants. **(B)** Decreased C-cadh levels in EpCAM MO ectoderm are rescued by ROCK inhibition (Y-27632).

Figure 3.S5. Related to figure 3.5.

Increased Erk activation in EpCAM-depleted *Xenopus* and Caco-2 cells.

(A) p-Erk1/2 immunostaining of siCTL and siEpCAM-transfected Caco-2 cells. Erk1/2 phosphorylation was increased in EpCAM-depleted Caco-2 cells. Corresponding pseudocolors are shown in the lower panels. **(B)** p-Erk1/2 immunostaining in *Xenopus* ectoderm explant. EpCAM overexpression in *Xenopus* ectoderm inhibits Erk activity; GAP-GFP expression was used as control. **(C)** Western blots of EpCAM, p-Erk1/2 and total Erk1/2 in *Xenopus* ectoderm explants at different stages. An equal number of explants were loaded in each lane. Total Erk1/2, used as loading control, remain constant in control explants, but progressively decreased in EpCAM-depleted explants. In control embryos, p-Erk signal was high at the start of gastrulation (stage 10), due to FGF signaling involved in patterning (Schohl and Fagotto, 2002), then progressively disappeared at later stages. In EpCAM-depleted explants, levels were similar to control at stage 10, but then remained high. Proportionally to total erk levels, phosphorylation in EpCAM-MO tissues appeared in fact extreme at late stages.

Figure 3.S6. Identification of EpCAM residues involved in PKC binding. Related to figure 6.

(A) Alignment of a generic novel PKC substrate consensus sequence, *Xenopus*, human and Zebrafish EpCAM juxtamembrane domains, and the series of Xenopus JM variants used for pull down experiments. Variants names are based on the position of the substitutions/deletions (highlighted in orange) compared to P=0. The last two columns provide a semi-quantitative comparison of PKCδ /PKCη binding obtained from *in vitro* pull down experiments (see panel B). Last two rows indicate respectively the consensus motif based on conservation of EpCAM sequence (see supplementary table S2) and a consensus nPKC-binding motif based on *in vitro* interaction experiments. For simplicity, the consensus represents an average of the results for PKCδ and PKCη. **(B)** *In vitro* pulldowns of PKCδ and PKCη with various GST-fused peptides. Nomenclature of peptides is according to panel A. GST levels were compared by Coommassie staining. Results are representative of three to four independent experiments, which all yielded identical results. Note the strong binding of the PKCη pseudosubstrate to both PKCδ and η. Note also that EpCAM and EphA4 peptides bind about as efficiently as the pseudosubstrates.

(C) Surface Plasmon Resonance. PKCδ and PKCη were immobilized on SPR sensors to characterize the binding kinetics of EpCAM JMs and the pseudo substrates (PS). Initially, GST and BSA (negative controls) were injected over reference and high-density PKCδ or PKCη (similar outcomes, data not shown) surfaces, yielding no binding responses as expected. Relative to the wild type Xenopus fusion (xJM), an equimolar injection of wild type human (hJM) exhibited a faster dissociation rate and increased binding capacity for PKCδ; in contrast, wild type Zebrafish (zJM) exhibited a similar dissociation rate and decreased binding capacity. Both PKCδ and η pseudosubstrates generated a binding response lower than human and Xenopus JMs. Among the mutant xJMs, S-6A was similar to wild type, G-1L, Y+1F and E+5Q exhibited larger binding responses, while K0A, K0Q, K-3Q, R-4Q, and R-5S exhibited decreased binding responses (not shown). See supplementary Table S2 for affinity measurements by kinetic titrations in single-cycle mode.

Supplementary Table 3.S1. Related to figure 3.6.

Sequence alignment of PKC substrate consensus, human and Xenopus PKC pseudosubstrate and EpCAM proximal sequences.

Sequences are aligned relative to phosphorylated Ser/Thr (position P=0) of PKC substrates. Conserved phenylalanine at P+1 of PKC substrates and the corresponding tyrosine of EpCAM tails are highlighted in yellow. Basic residues of the pseudosubstrate and EpCAM sequences highlighted in pink correspond to residues conserved in EpCAMs. The color intensity relates to the relative importance in PKC binding, as inferred from pull down with the corresponding mutants (supplementary Fig.S9). Green and blue highlights for Ser/Thr residues at P-6/-7 and for Asp at P+5 similarly indicate conserved residues for which mutations decreased binding to PKCs. Note that the two basic residues with highest impact on binding, P-4 and P-5, as well as the Ser/Thr residue at P-6/-7 are conserved in novel PKC pseudosubstrates, while absent from classical PKC sequences, consistent with the lack of interaction with PKCβ (Fig.6D). The last row presents an EpCAM juxtamembrane consensus sequence based on sequence conservation. Symbols: +, basic; -, acidic, ζ, hydrophilic; Φ, hydrophobic. Note that sequences from fish EpCAMs lack several residues conserved in all other vertebrate species, explaining the weaker binding to human PKCs (supplementary Fig.S5).

Supplementary Table 3.S2. Related to figure 3.6 and 3.7.

Plasmon plasmon resonance measurement of EpCAM-PKC affinities.

Low-density PKC surfaces were captured to perform kinetic titrations in single-cycle mode (i.e. minimal assay time to maximize the stability of captured PKC surfaces). For example, dose-dependent binding of wild type xJM (and most other EpCAM fusions) to PKCδ was characterized by slow-on, slow-off kinetics, whereas equimolar binding of xJM to PKCη was characterized by faster-on, faster-off kinetics. For PKCδ PS binding to PKCδ, a similar dissociation rate but faster association rate was detected relative to xJM. Despite the increased or reduced binding capacities in the fixed-concentration multi-cycle screening, the single-cycle titrations indicated that there were no significant differences in overall affinity between the EpCAM fusions and pseudo substrates (i.e. all low nM K_D values). While fitting of the single-cycle data deviated from the "1:1 Titration" model (i.e. Chi^2 values > 1), the estimates indicate that EpCAM fusions interacted with PKCδ in the following kinetic range (on average): association, k_a ~2 x 10^5 $M^{-1}s^{-1}$; dissociation, k_d ~7 x 10^{-3} $M^{-1}s^{-1}$; K_D ~40 nM. On the other hand, the estimates indicate that wild type EpCAM interacted with PKCη in the following kinetic range (on average): faster association, k_a ~4 x 10^5 $M^{-1}s^{-1}$; faster dissociation, k_d ~1 x 10^{-2} $M^{-1}s^{-1}$; K_D ~30 nM. In the single-cycle titrations, such apparent differences likely explain why low concentrations of the wild type Xenopus fusion generated larger binding responses with PKCη (K_D ~31 nM) as compared to PKCδ (K_D ~54 nM).

Supplementary Table 3.S3. Related to figure 3.7

Proteome search for PKC-binding juxtamembrane domains.

A 41 residue-long profile for a PKC-binding JM domain (i.e. immediately preceded by a transmembrane domain), constructed based on the alignment of EpCAM JM homologous sequences (supplementary Table S2), was used to search the entire human proteome. The first 36 candidates issued from this search are presented ranked according to their relative score.

The three candidate tested by *in vitro* pull down are highlighted in yellow (EphA4, NrCAM and ICAM-1). Annotations in the second column refer to the following functional categories: CAM, cell adhesion molecules; (CAM), predicted cell adhesion molecules, based either on sequence homology, or on their ability to form direct homophilic/heterophilic bonds; "adhes/repuls", Eph receptors, which have an established dual role in adhesion and repulsion; guidance, proteins characterized by their role in neuronal guidance. In a few cases the candidates or their homologues are reported to participate to non-classical cell-cell junctions (Matrix-remodeling-associated protein 8, uromodulin) via homophilic interactions. TM7S4 is involved in cell to cell fusion, again via homophilic interaction. ADAM7 is a metalloprotease but also reported to interact with the actin cytoskeleton (cytosk).

The last column presents the 41 residue sequence of each candidate, with includes the transmembrane domains (grey and italic) and the JM motif (basic residues and tyrosine typical of the EpCAM JM are in blue and in bold, respectively). The number before each sequence indicates the position in the protein. Several sequences contain serines or threonines. Since the consensus PKC substrates remain imperfectly defined and may accommodate some variability (e.g. in spacing between key basic residues), one cannot exclude that some of these sequences may be substrates rather than pseudosubstrates. We have conservatively underlined all those serines and threonines that were either closely surrounded by at least one basic residue on each side in positions -2 and +2, or preceded by a basic cluster. Ser/Thr distant less than 6 residues from the transmembrane domain were not included, since, based on our molecular model, steric hindrance is likely to prevent positioning of these residues in the catalytic site. Note that a search through phospho-protein

data bases (Kinexus and Phosida) revealed only one case of reported phosphorylation among the underlined Ser/Thr, i.e. serine 1152 of L1CAM/VCAM (red underlined). And even in this case, phosphorylation was due to Rsk, not PKC (Wong et al., 1996). There is thus a fair chance that none of these candidates is an actual PKC substrate. Note that occludin is a reported substrate for PKCη, but the targeted residues are quite distant from the JM (Suzuki et al., 2009).

Figure 3.1

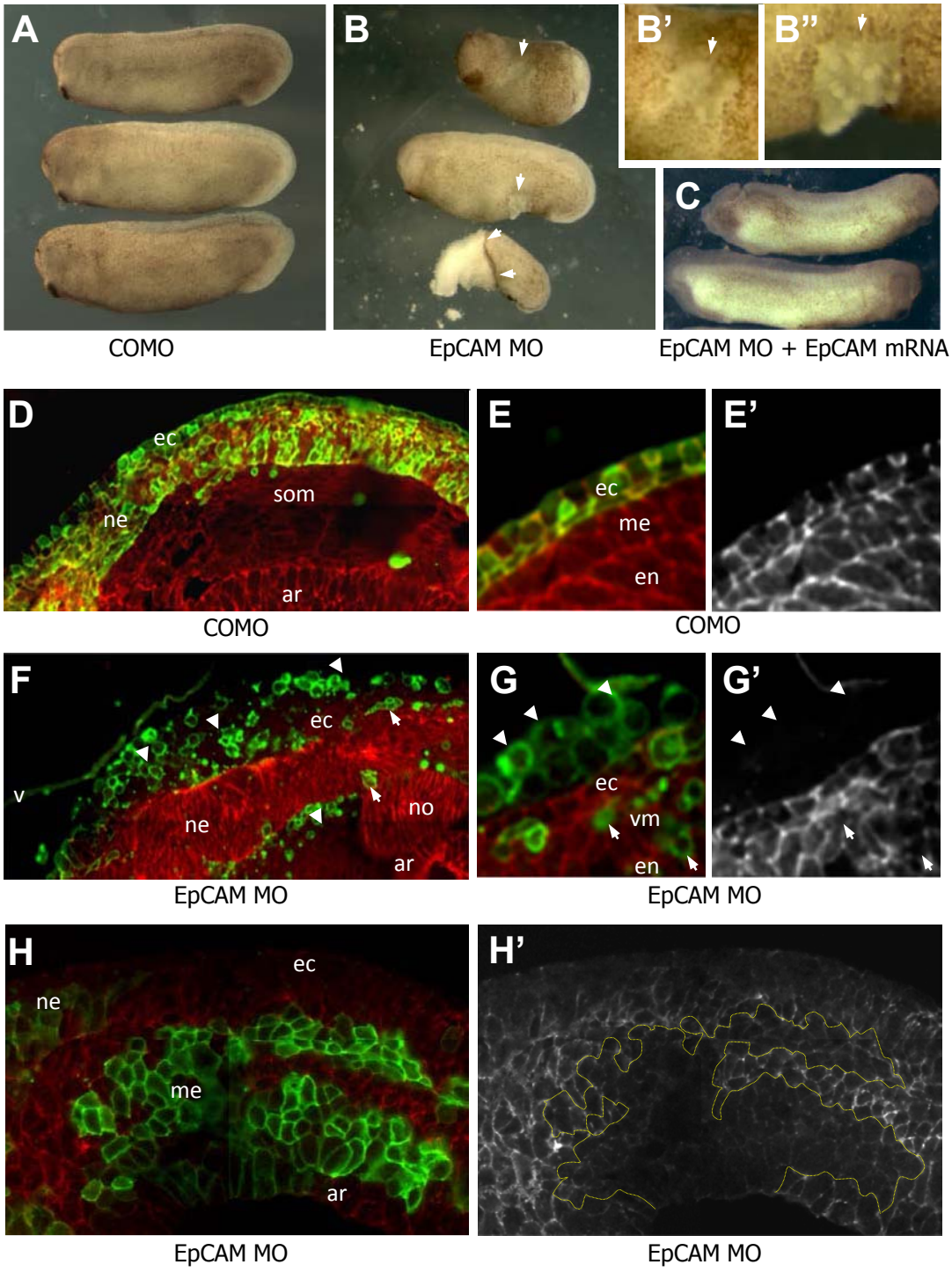
A
B
B'
B''
C
COMO
EpCAM MO
EpCAM MO + EpCAM mRNA
D
ec
som
ne
ar
COMO
E
ec
me
en
E'
COMO
F
ec
v
ne
no
ar
EpCAM MO
G
ec
vm
en
G'
EpCAM MO
H
ec
ne
me
ar
EpCAM MO
H'
EpCAM MO

Figure 3.2

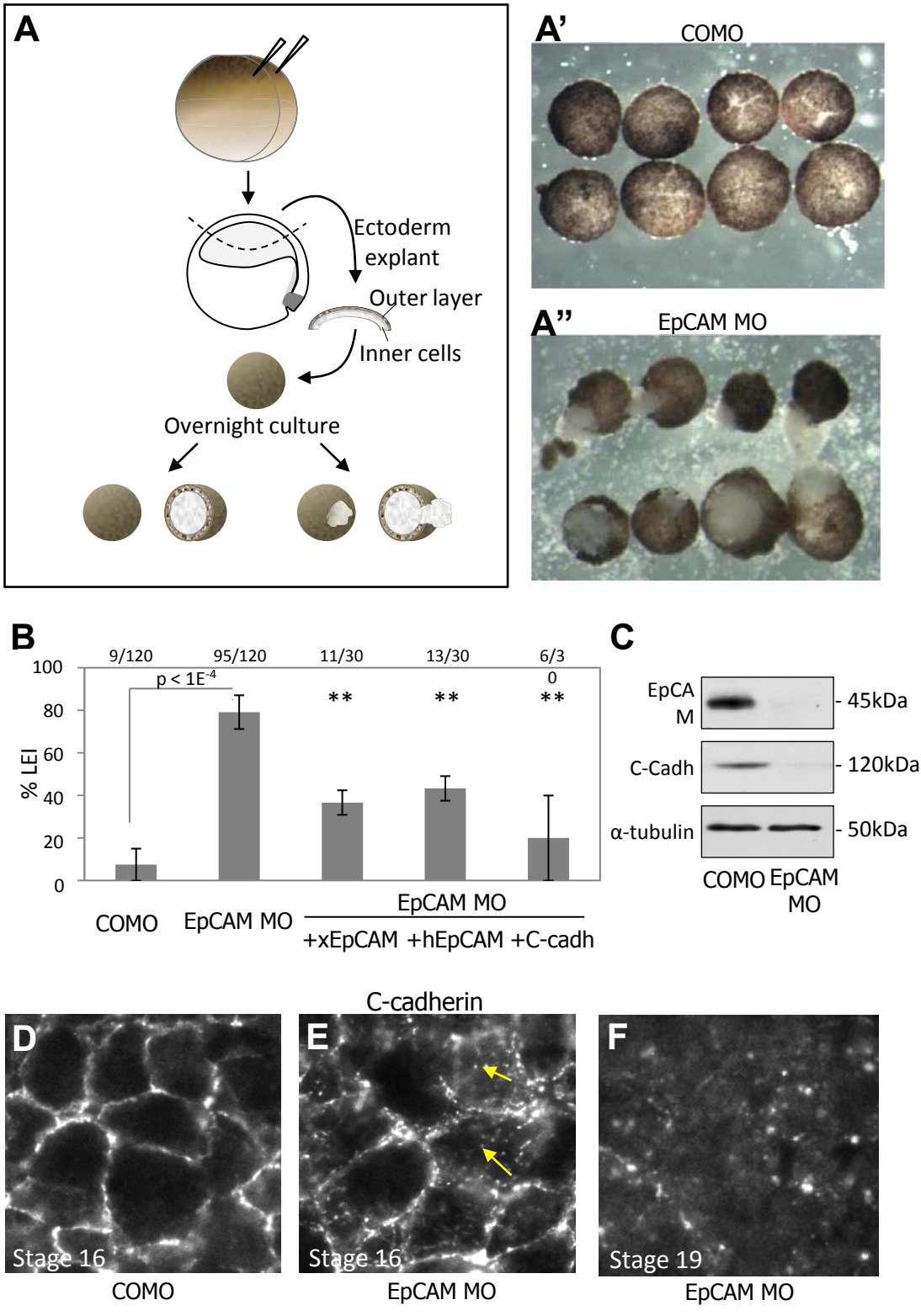
A
Ectoderm explant
Outer layer
Inner cells
Overnight culture
A'
COMO
A"
EpCAM MO
B
9/120
95/120
11/30
13/30
6/3
0
p < 1E-4
**
**
**
% LEI
100
80
60
40
20
0
COMO
EpCAM MO
EpCAM MO
+xEpCAM
+hEpCAM
+C-cadh
C
EpCAM
C-Cadh
α-tubulin
- 45kDa
- 120kDa
- 50kDa
COMO
EpCAM MO
C-cadherin
D
Stage 16
COMO
E
Stage 16
EpCAM MO
F
Stage 19
EpCAM MO

Figure 3.3

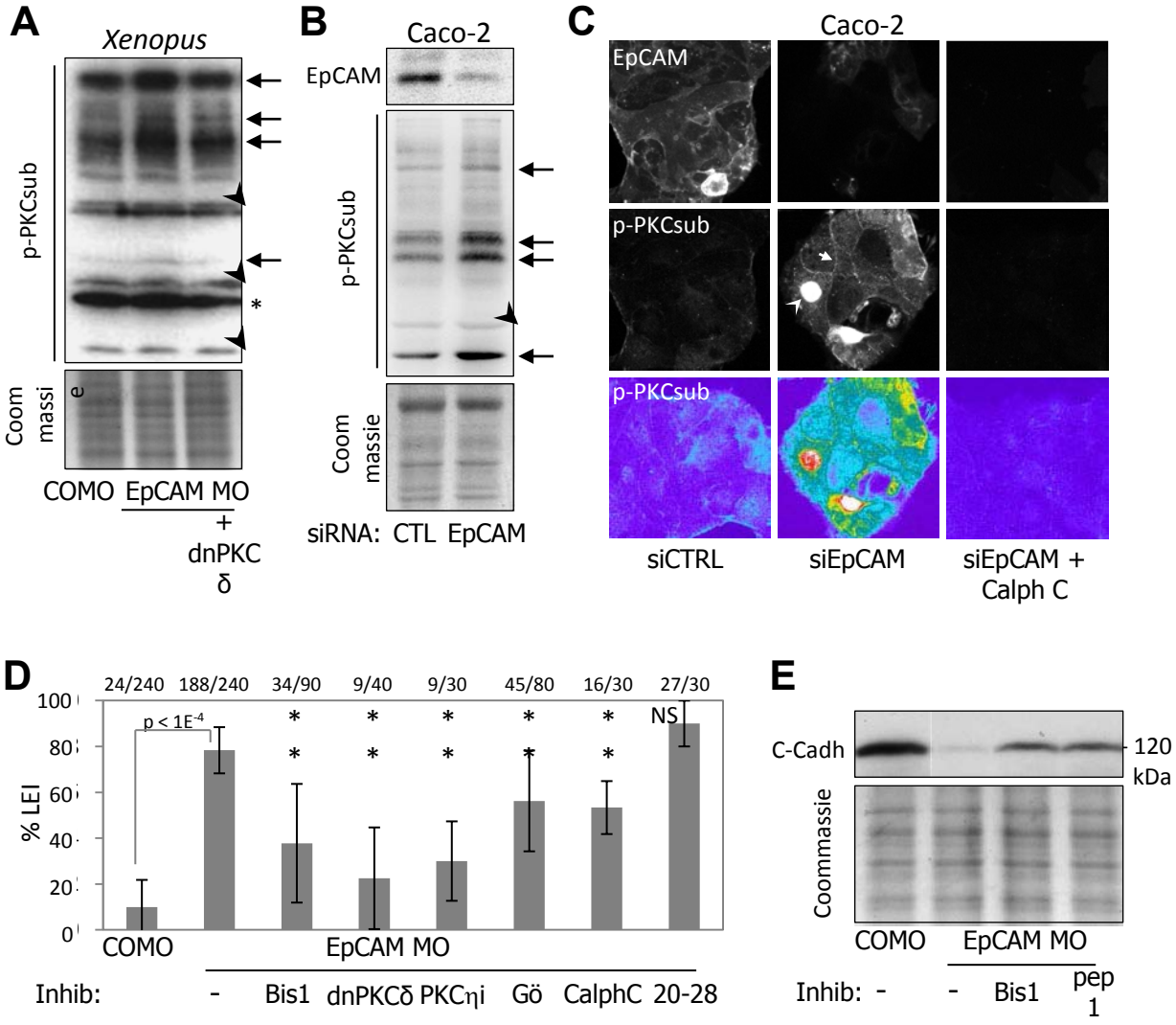
A
Xenopus
p-PKCsub
Coom massie
COMO
EpCAM MO + dnPKC δ
B
Caco-2
EpCAM
p-PKCsub
Coom massie
siRNA: CTL EpCAM
C
Caco-2
EpCAM
p-PKCsub
p-PKCsub
siCTRL
siEpCAM
siEpCAM + Calph C
D
24/240 188/240 34/90 9/40 9/30 45/80 16/30 27/30
p < 1E-4
NS
% LEI
COMO
EpCAM MO
Inhib: - Bis1 dnPKCδ PKCηi Gö CalphC 20-28
E
C-Cadh
120 kDa
Coommassie
COMO
EpCAM MO
Inhib: - - Bis1 pep 1

Figure 3.4

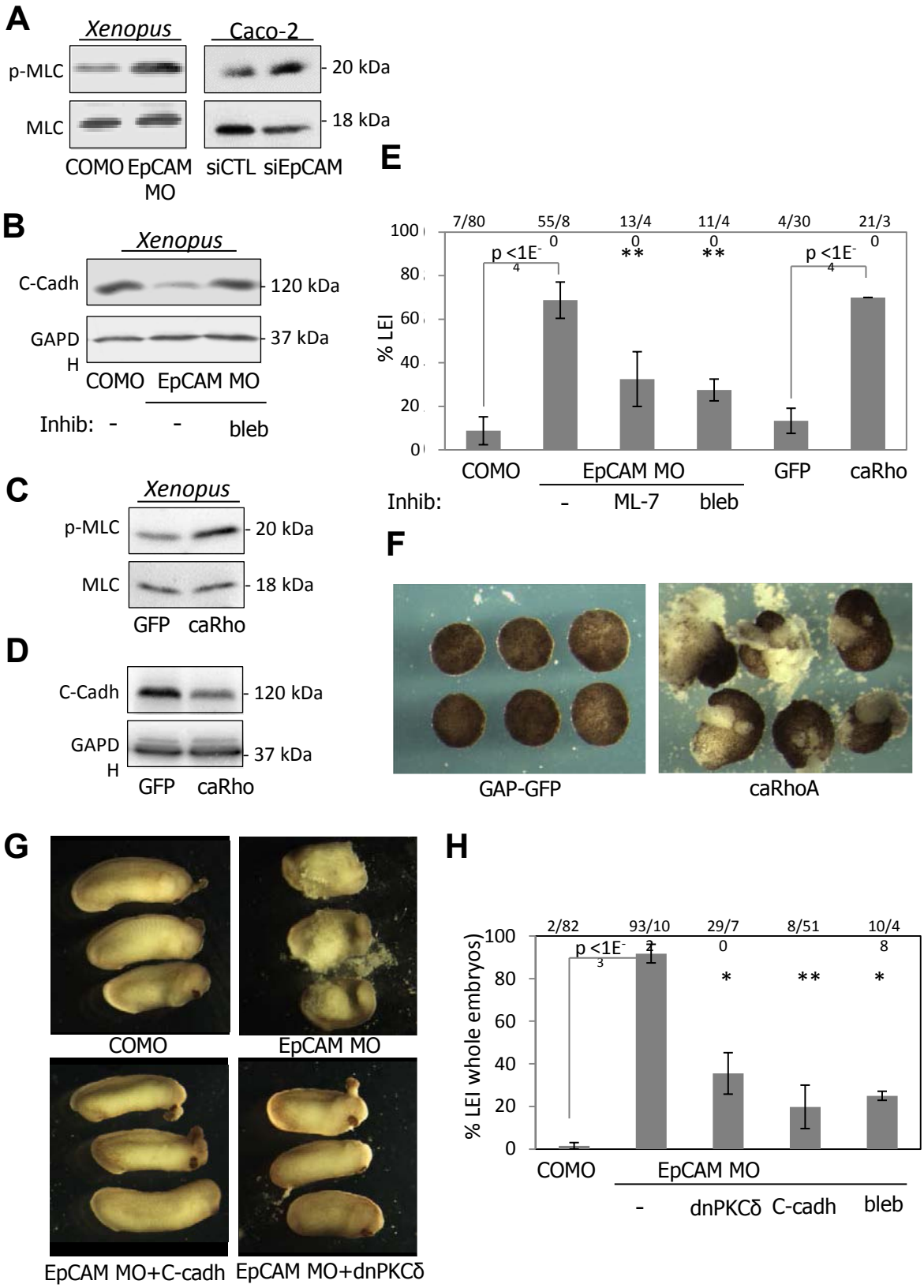
A
Xenopus
Caco-2
p-MLC
MLC
20 kDa
18 kDa
COMO
EpCAM MO
siCTL
siEpCAM
B
Xenopus
C-Cadh
GAPDH
120 kDa
37 kDa
COMO
EpCAM MO
Inhib: - - bleb
C
Xenopus
p-MLC
MLC
20 kDa
18 kDa
GFP
caRho
D
C-Cadh
GAPDH
120 kDa
37 kDa
GFP
caRho
E
7/80
55/8
13/4
11/4
4/30
21/3
p <1E-4
**
**
p <1E-4
% LEI
COMO
EpCAM MO
GFP
caRho
Inhib: - ML-7 bleb
F
GAP-GFP
caRhoA
G
COMO
EpCAM MO
EpCAM MO+C-cadh
EpCAM MO+dnPKCδ
H
2/82
93/10
29/7
8/51
10/4
p <1E-3
*
**
*
% LEI whole embryos)
COMO
EpCAM MO
- dnPKCδ C-cadh bleb

Figure 3.5

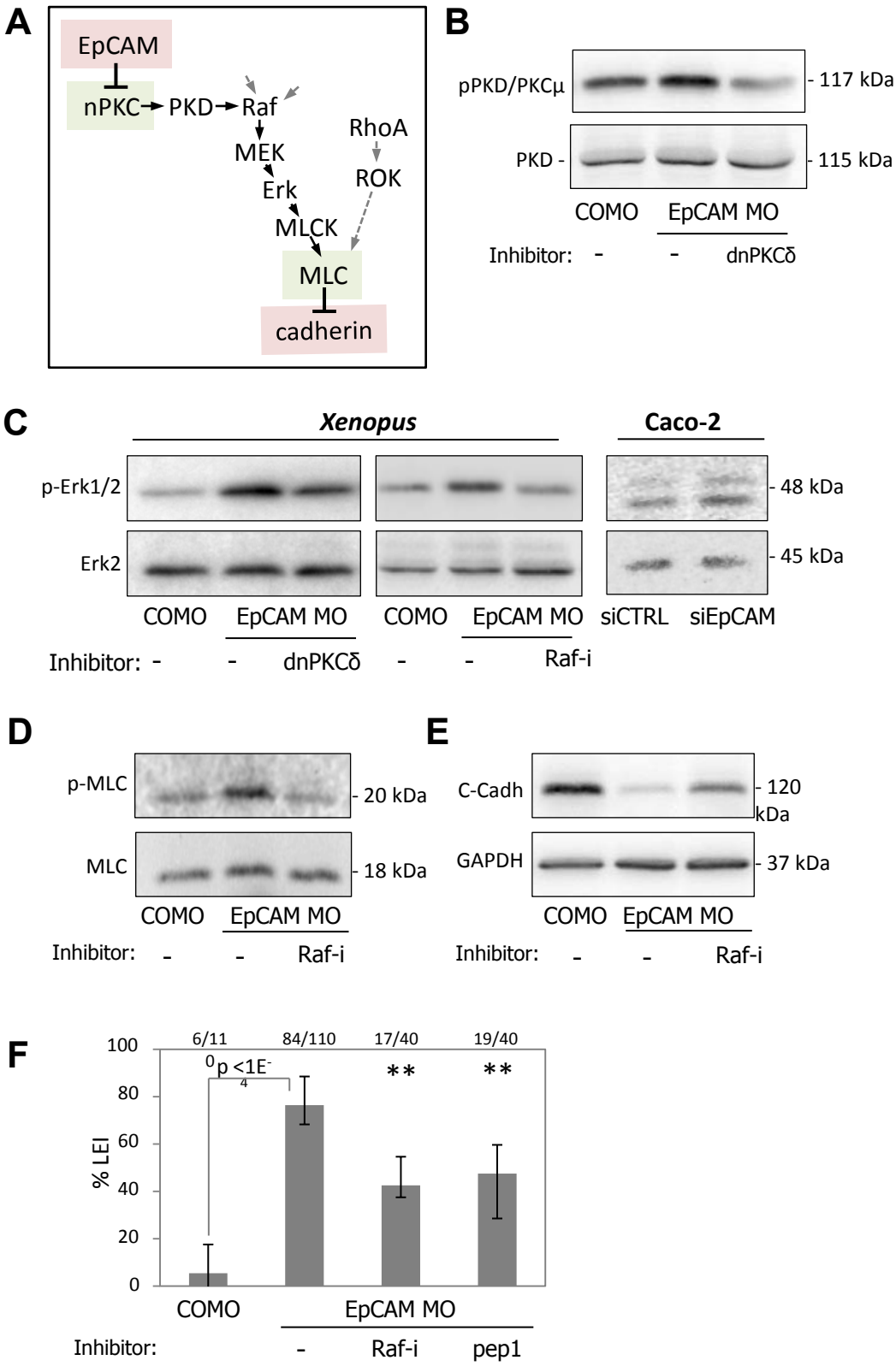
A
EpCAM
nPKC
PKD
Raf
RhoA
MEK
ROK
Erk
MLCK
MLC
cadherin
B
pPKD/PKCμ
117 kDa
PKD
115 kDa
COMO
EpCAM MO
Inhibitor: - - dnPKCδ
C
Xenopus
Caco-2
p-Erk1/2
48 kDa
Erk2
45 kDa
COMO
EpCAM MO
COMO
EpCAM MO
siCTRL
siEpCAM
Inhibitor: - - dnPKCδ - - Raf-i
D
p-MLC
20 kDa
MLC
18 kDa
COMO
EpCAM MO
Inhibitor: - - Raf-i
E
C-Cadh
120 kDa
GAPDH
37 kDa
COMO
EpCAM MO
Inhibitor: - - Raf-i
F
6/11
84/110
17/40
19/40
p <1E-4
**
**
100
80
60
40
20
0
% LEI
COMO
EpCAM MO
Inhibitor: - Raf-i pep1

Figure 3.6

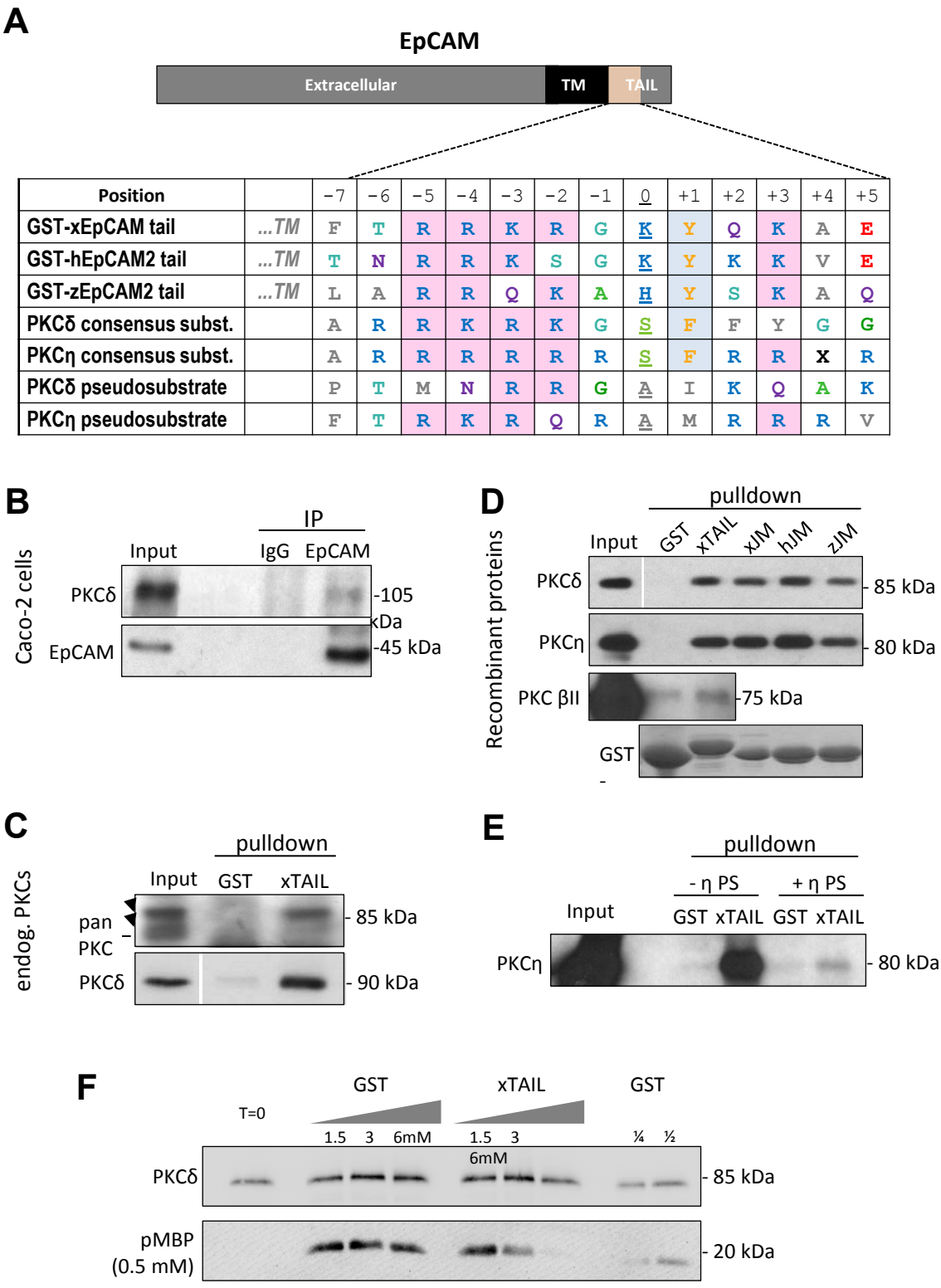

Position		−7	−6	−5	−4	−3	−2	−1	0	+1	+2	+3	+4	+5
GST-xEpCAM tail	...TM	F	T	R	R	K	R	G	K	Y	Q	K	A	E
GST-hEpCAM2 tail	...TM	T	N	R	R	K	S	G	K	Y	K	K	V	E
GST-zEpCAM2 tail	...TM	L	A	R	R	Q	K	A	H	Y	S	K	A	Q
PKCδ consensus subst.		A	R	R	K	R	K	G	S	F	F	Y	G	G
PKCη consensus subst.		A	R	R	R	R	R	R	S	F	R	R	X	R
PKCδ pseudosubstrate		P	T	M	N	R	R	G	A	I	K	Q	A	K
PKCη pseudosubstrate		F	T	R	K	R	Q	R	A	M	R	R	R	V

Figure 3.7

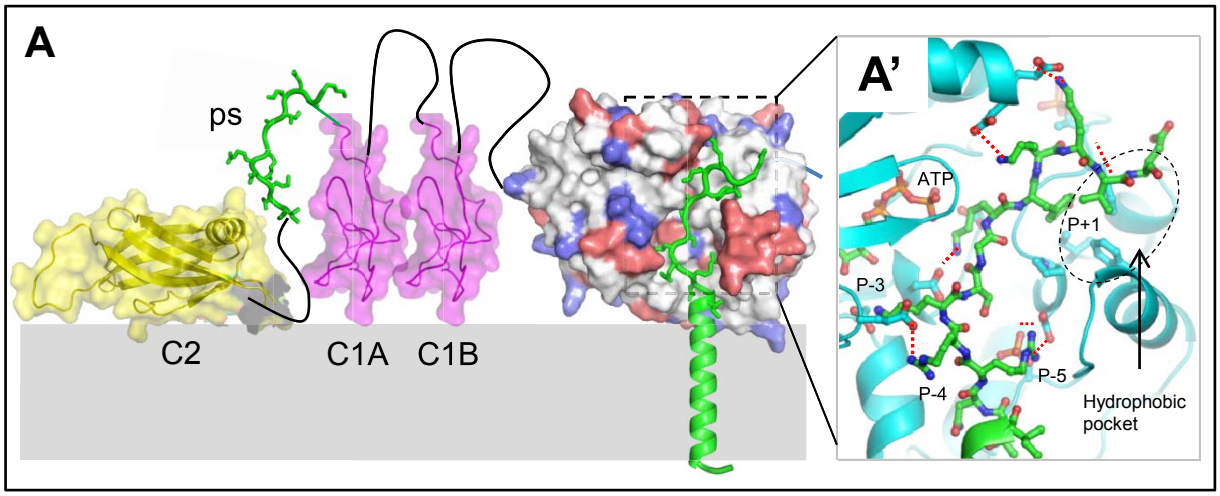

B

Position		−7	−6	−5	−4	−3	−2	−1	0	+1	+2	+3	+4	+5	+6
Main resid cons δ/η			+	+	+	+	+	X	S	F					
xEpCAM	...TM	F	T	R	R	K	R	G	K	Y	Q	K	A	E	M
hEpCAM2	...TM	T	N	R	R	K	S	G	K	Y	K	K	V	E	I
EphA4	...TM	I	S	R	R	R	S	-	K	Y	S	K	A	K	Q
NrCAM	...TM	I	R	R	N	K	G	G	K	Y	P	V	K	E	K
ICAM	...TM	N	R	Q	R	K	I	K	K	Y	R	L	Q	E	A

C

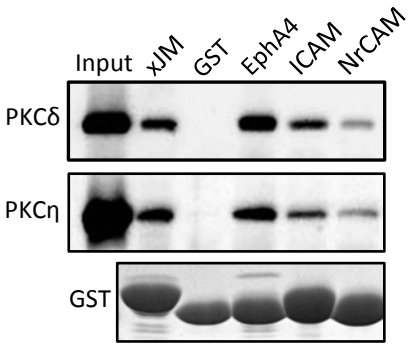

Figure 3.S1

Related to figure 3.1

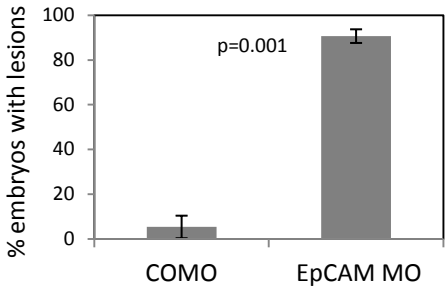

Figure 3.S2

Related to figure 3.2

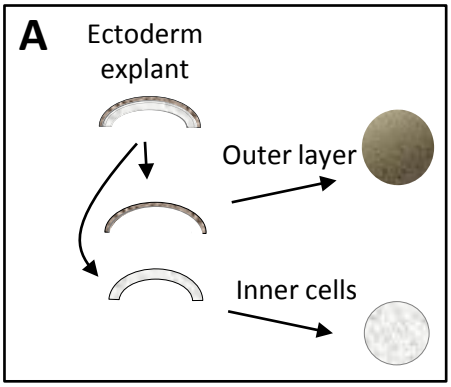

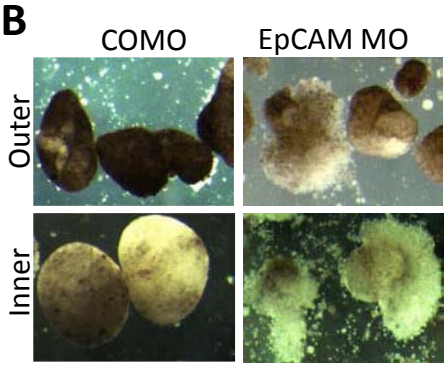

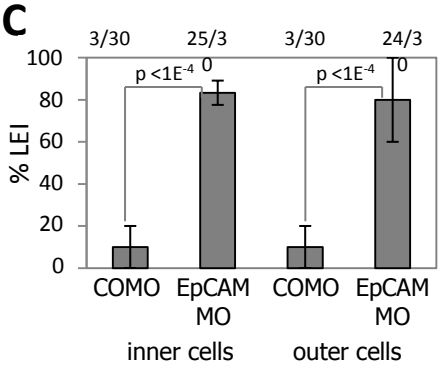

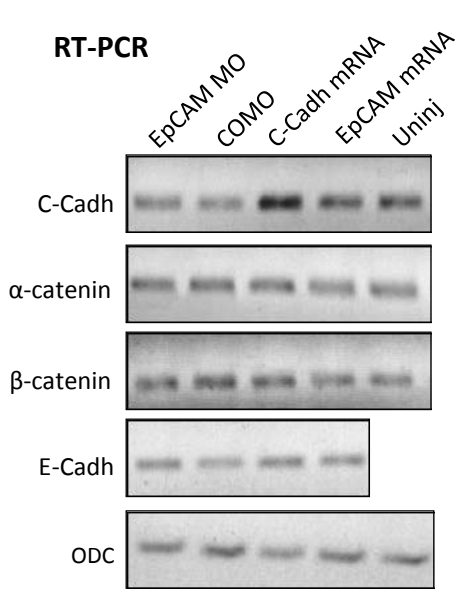

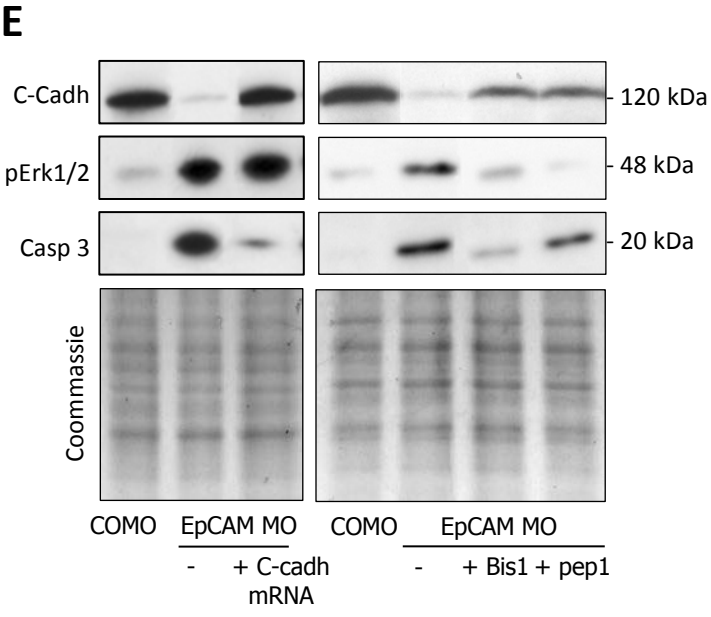

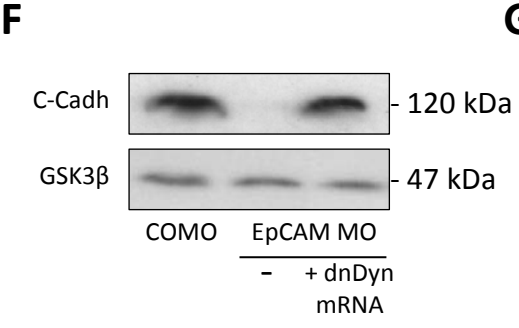

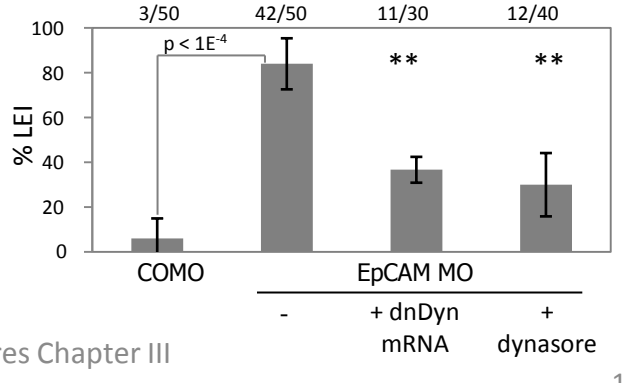

Figure 3.S3

Related to figure 3.3

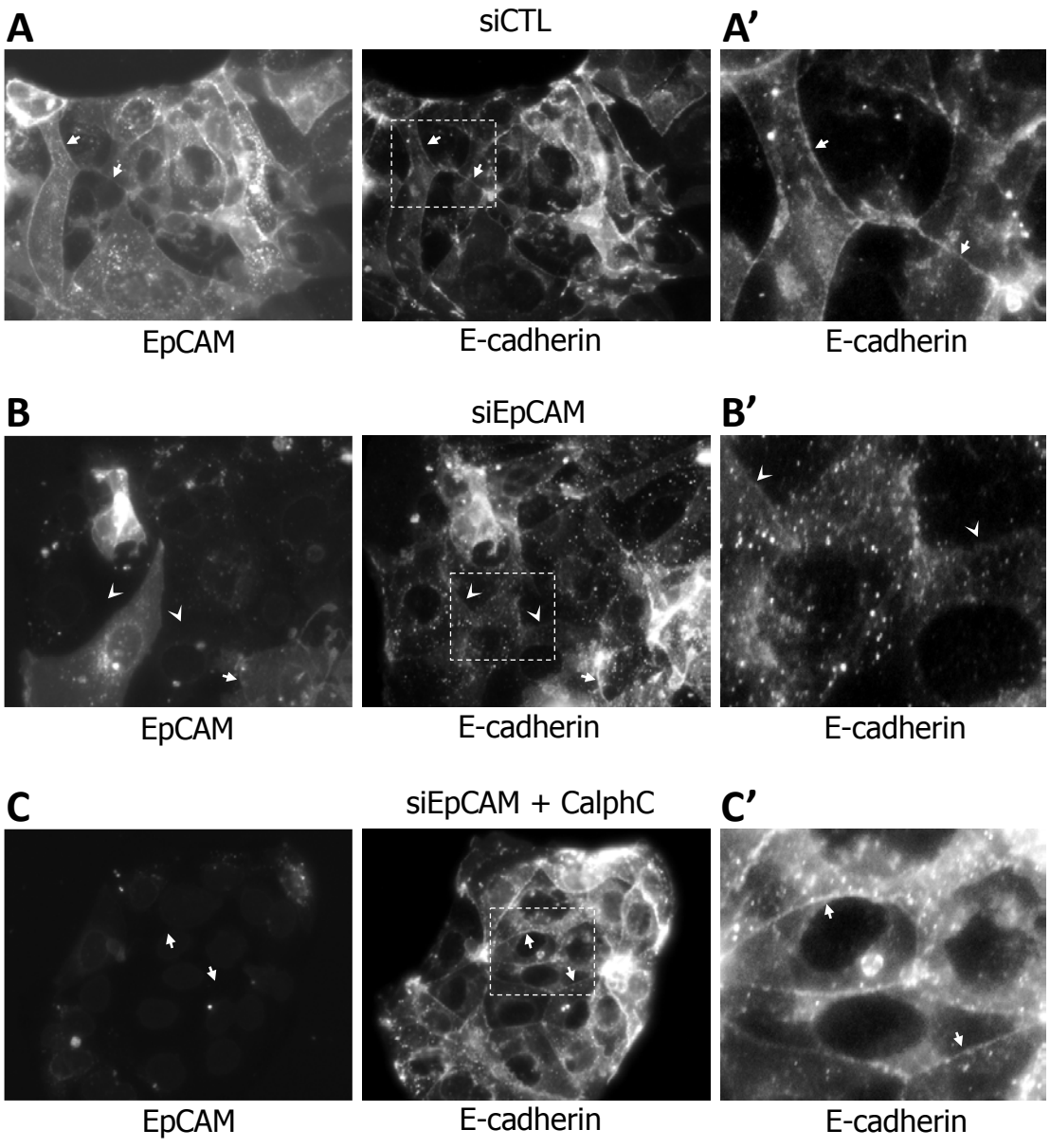

Figure 3.S4

Related to figure 3.4

A

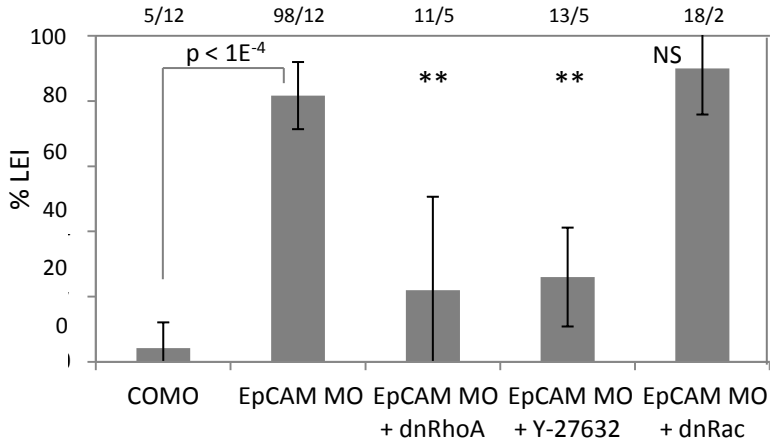

B

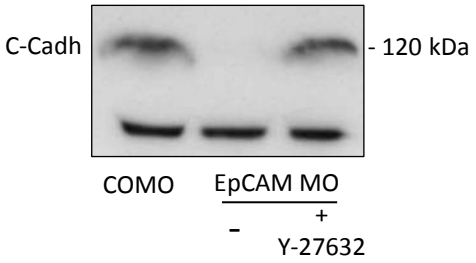

Figure 3.S5

Related to figure 3.5

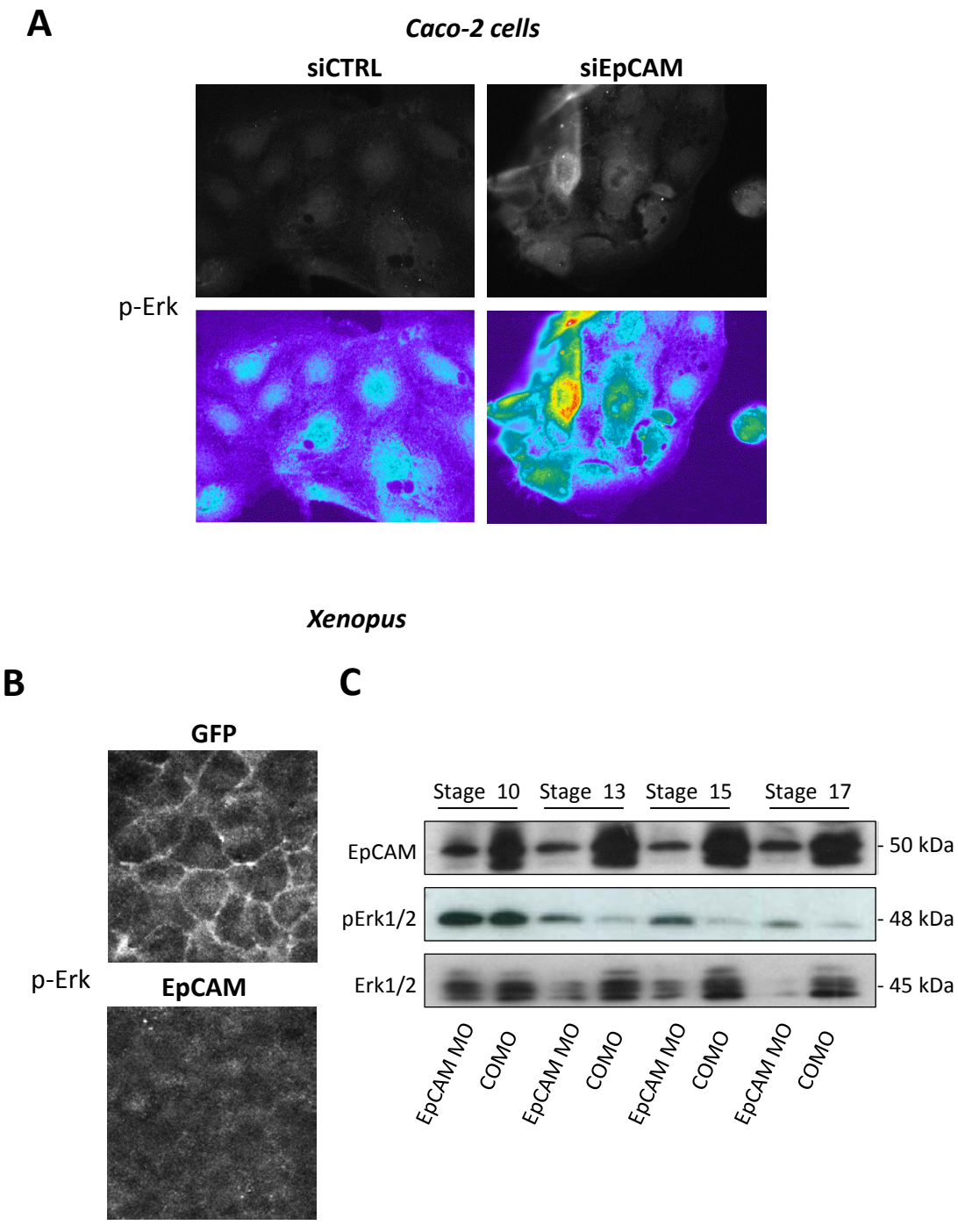

Figure 3.S6

A Related to figure 3.6 and 3.7

																binding	
Position	TM	−7	−6	−5	−4	−3	−2	−1	**0**	+1	+2	+3	+4	+5	+6	δ	η
Main resid cons δ/η			+	+	+	+	+	x	S	F							
GST-xEpCAM tail		S	T	R	R	K	R	G	K	Y	Q	K	A	E	M	++	++
GST-hEpCAM2 JM	I	T	N	R	R	K	S	G	K	Y	K	K	V	E	M	++	++
GST-zEpCAM2 JM	I	L	A	R	R	Q	K	A	H	Y	S	K	A	Q	I	+	+
GST-xEpCAM JM		S	T	R	R	K	R	G	K	Y	Q	K	A	E	I	++	++
GST- JM(T-6A)		S	A	R	R	K	R	G	K	Y	Q	K	A	E	I	++	+/−
GST- JM(R-5S)		S	T	S	R	K	R	G	K	Y	Q	K	A	E	I	+	−
GST- JM(R-4Q)		S	T	R	Q	K	R	G	K	Y	Q	K	A	E	I	+/−	−
GST- JM(K-3Q)		S	T	R	R	Q	R	G	K	Y	Q	K	A	E	I	+	+
GST- JM(R-2Q)		S	T	R	R	K	Q	G	K	Y	Q	K	A	E	I	+	+/−
GST- JM(G-1L)		S	T	R	R	K	R	L	K	Y	Q	K	A	E	I	++	++
GST- JM(K0Q)		S	T	R	R	K	R	G	Q	Y	Q	K	A	E	I	++	++
GST- JM(K0A)		S	T	R	R	K	R	G	A	Y	Q	K	A	E	I	+/−	+
GST- JM(Y+1F)		S	T	R	R	K	R	G	K	F	Q	K	A	E	I	+	+/−
GST- JM(Y+1N)		S	T	R	R	K	R	G	K	N	Q	K	A	E	I	++	++
GST- JM(Q+2A)		S	T	R	R	K	R	G	K	Y	A	K	A	E	I	++	+
GST- JM(K+3Q)		S	T	R	R	K	R	G	K	Y	Q	Q	A	E	I	+	+
GST- JM(A+4N)		S	T	R	R	K	R	G	K	Y	Q	K	N	E	I	++	+
GST- JM(E+5Q)		S	T	R	R	K	R	G	K	Y	Q	K	A	Q	I	+	+
GST- JM(-Δ2)		S	T	R	R	K	-	G	K	Y	Q	K	A	E	I	++	+
GST-PKCδ PS	P		T	M	N	R	R	G	A	I	K	Q	A	K		+/−	++
GST-PKCη PS	F		T	R	K	R	Q	R	A	M	R	R	R	V		+++	++
GST-PKCη PSY	F		T	R	K	R	Q	R	A	Y	R	R	R	V		+++	+++
Consensus (conservation)			S T	+	+	+	+	x	+	Y	ζ	+	A V	E	Φ		
Consensus (pulldown)			ζ	+	+	+	+	x	ζ	?	ζ	+	Φ	−	nd		

B

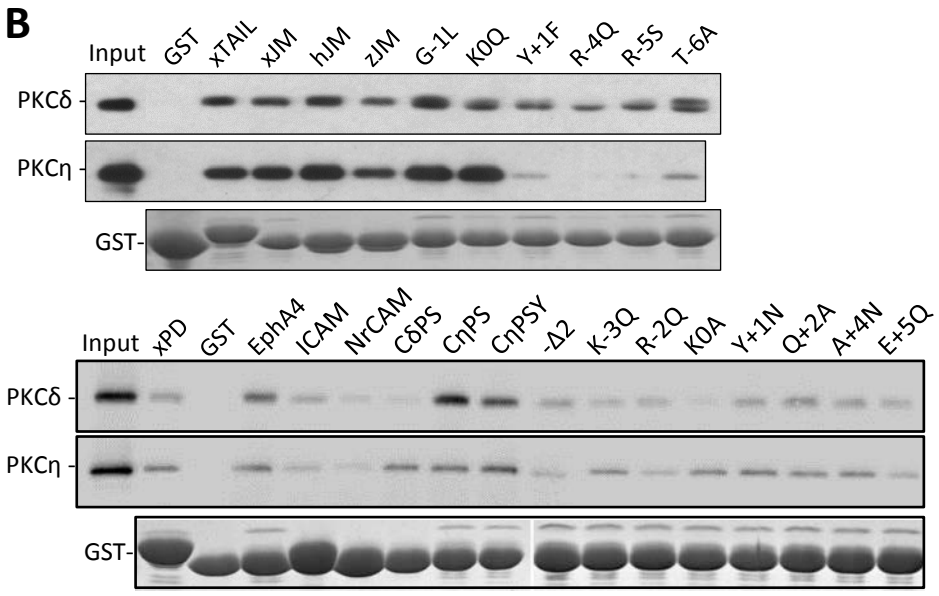

Figure 3.S7

Related to figure 3.6 and 3.7

A

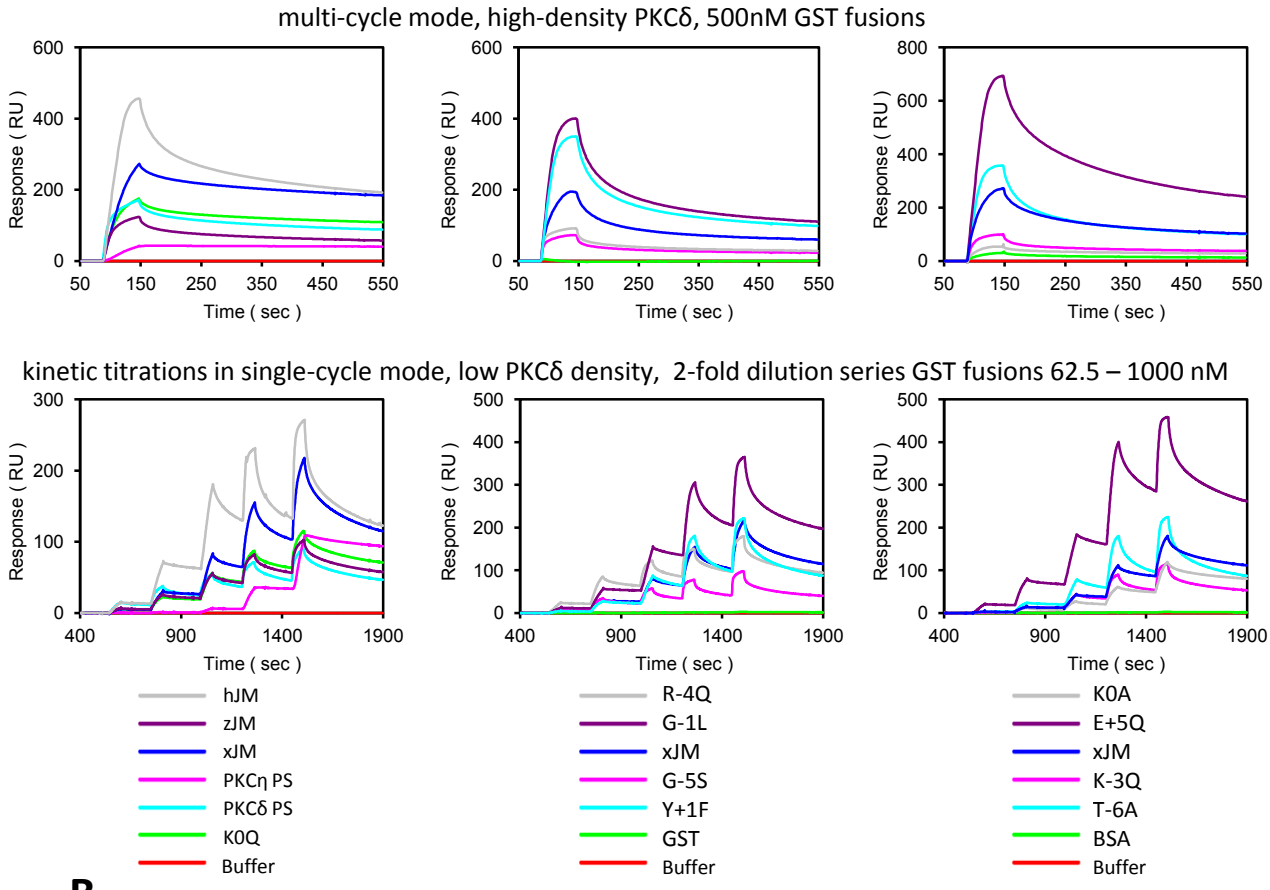

B

Captured PKC	EpCAM WT / mut.	K_D +/- SE (nM)	k_d +/- SE (s^{-1})	Relat. bind. capacity	Pulldown
δ	xJM	54 +/- 2	2.12 +/- 0.02 x 10^{-3}	1	++
δ	hJM	40 +/- 4	2.39 +/- 0.01 x 10^{-3}	1.7	++(+)
δ	zJM	62 +/- 6	1.68 +/- 0.03 x 10^{-3}	0.3	+
δ	PKCδ PS	62 +/- 1	1.99 +/- 0.04 x 10^{-3}	0.5	+/-
δ	PKCη PS	ND	5.79 +/- 0.20 x 10^{-4}	0.1	+++
δ	T-6A	45 +/- 6	3.09 +/- 0.03 x 10^{-3}	1.2	++
δ	R-5S	74 +/- 6	2.42 +/- 0.06 x 10^{-3}	0.3	+
δ	R-4Q	26 +/- 3	1.71 +/- 0.03 x 10^{-3}	0.2	-
δ	K-3Q	37 +/- 3	2.09 +/- 0.05 x 10^{-3}	0.2	+
δ	G-1L	38 +/- 9	2.10 +/- 0.01 x 10^{-3}	2.1	++
δ	K0Q	44 +/- 4	1.47 +/- 0.03 x 10^{-3}	0.5	++
δ	K0A	24 +/- 2	1.25 +/- 0.04 x 10^{-3}	0.1	+/-
δ	Y+1F	52 +/- 6	3.07 +/- 0.03 x 10^{-3}	1.9	+
δ	E+5Q	21 +/- 6	1.77 +/- 0.01 x 10^{-3}	2.8	+

Table 3.S1

Related to figure 3.6

Position		−7	−6	−5	−4	−3	−2	−1	0	+1	+2	+3	+4	+5
PKCα substr. cons.		R	R	R	R	R	K	G	S	F	R	R	K	A
PKCβ substr. cons.		F	K	L	K	R	K	G	S	F	K	K	F	A
PKCβ2 substr. cons.		Y	K	L	K	R	K	G	S	F	K	K	K	A
PKCγ substr. cons.		R	R	R	R	R	K	G	S	F	K	R	K	A
PKCδ substr. cons.		A	R	R	K	R	K	G	S	F	F	Y	G	G
PKCε substr. cons.		Y	Y	X	R	R	K	M	S	F	F	E	F	F
PKCη substr. cons.		A	R	R	R	R	R	R	S	F	R	R	X	R
PKCι substr. cons.		R	R	F	K	R	Q	G	S	F	F	Y	F	F
hPKCα pseudosubst.		N	R	F	A	R	K	G	A	L	R	Q	K	N
xPKCα pseudosubst.		Q	R	F	A	R	K	G	A	L	R	Q	K	N
hPKCβ pseudosubst.		V	R	F	A	R	K	G	A	L	R	Q	K	N
xPKCβ pseudosubst.		T	R	F	A	R	K	G	A	L	R	Q	K	N
hPKCβ2 pseudosubst.		V	R	F	A	R	K	G	A	L	R	Q	K	N
hPKCγ pseudosubst.		P	L	F	C	R	K	G	A	L	R	Q	K	V
xPKCγ pseudosubst.		P	L	F	C	R	K	G	A	L	R	R	W	R
hPKCδ pseudosubst.		P	T	M	N	R	R	G	A	I	K	Q	A	K
xPKCδ pseudosubst.		T	I	N	K	R	R	G	A	I	K	Q	A	K
hPKCε pseudosubst.		R	P	R	K	R	Q	G	A	V	R	R	R	V
hPKCη pseudosubst.		F	T	R	K	R	Q	R	A	M	R	R	R	V
xPKCη pseudosubst.		F	T	R	K	R	Q	R	A	M	R	R	R	V
hPKCι pseudosubst.		K	S	I	Y	R	R	G	A	R	R	W	R	K
xPKCι pseudosubst.		K	S	I	Y	R	R	G	A	R	R	W	R	K
Human EpCAM1	I	S	R	K	K	R	M	A	K	Y	E	K	A	E
Human EpCAM2	I	T	N	R	R	K	S	G	K	Y	K	K	V	E
Mouse EpCAM1	I	S	T	R	K	K	S	A	K	Y	E	K	A	E
Mouse EpCAM2	V	T	K	R	R	K	S	G	K	Y	K	K	V	E
Pig EpCAM	I	S	T	K	K	R	R	A	K	Y	E	K	A	E
Opossum EpCAM	V	S	K	R	K	R	R	T	K	Y	V	K	A	E
Chicken EpCAM		L	S	R	R	R	K	G	K	Y	V	K	A	E
Anolis EpCAM		F	N	R	W	R	K	T	K	Y	E	K	V	E
Xenopus EpCAM		F	T	R	R	K	R	G	K	Y	Q	K	A	E
Zebrafish EpCAM1	F	L	A	R	R	Q	K	A	H	Y	S	K	A	Q
Zebrafish EpCAM2	F	L	A	R	R	Q	K	A	Q	Y	S	K	A	Q
Tetraodon EpCAM	F	L	R	K	R	D	K	K	R	Y	N	K	T	Q
Consensus (conservation)			S T	+	+	+	+	x	+	Y	ζ	+	A V	E

Table 3.S2

Related to figure 3.7

score	UniProt #	Name	Annotations	SEQUENCE
11.68	TACD2	EpCAM-2/TACST2	CAM	272 RLTAGLIAVIVVVVVALVAGMAVLVI TNRRKSGKYKKVEI
10.9	EPCAM	EpCAM-1/TACST1	CAM	263 GLKAGVIAVIVVVVIAVVAGIVVLVI SRKKRMAKYEKAEI
8.17	EphA4	EphA4	adhes/repuls	542 DGANSTVLLVSVSGSVVLVVILIAAFVI SRRRSKYSKAKQ
6.82	OCLN	Occludin	CAM (Tight Jct)	240 DPQEAIAIVLGFMIIVAFALIIFFAV KTRRKMDRYDKSNI
6.38	MXRA8	Matrix-remodeling-associated protein 8	Jct	335 RAHFFQQLGYVLATLLLFILLLVTVLLAA RRRRGGYEYSDQ
6.15	EPHA7	EphA7	adhes/repuls	551 EQNPVIIIAVVAVAGTIILVFMVFGFII GRRHCGYSKADQ
6.03	MUC12	Mucin-12	CAM	5377 SLVYGIVGAVMAVLLLALIILIILFSL SQRKRHREQYDVPQE
6.03	PCDH7	Protocadherin-7	CAM	877 RLSIVIGVVAGIMTVILIILIVVMA RYCRSKNKNGYEAGKK
5.94	MUC17	Mucin-17	CAM	4389 SLVYGLVGAGVVLMLIILVALLMLVF RSKREVKRQKYRLSQL
5.91	NRCAM	Neuronal cell adhesion molecule	CAM	1163 DIATQGWFIGLMCAVALLILILLIVCFI RRNKGGKYPVKEK
5.82	DPCR1	Diffuse panbronchiolitis crit. region prot. 1		446 AWAIVIVVLVAVILLLVFLGLIFLV SYMMRTRRTLTQNTQYNDAED
5.81	PLXD1	Plexin-D1	Guidance	1268 SETAIIVSIVICSVLLLLSVVALFVFC TKSRRAERYWQKTL
5.71	TM7S4	Transmembrane 7 superfamily member 4	cell fusion	380 LSVILLILVMLGLLSSILM QLKILVSASFYPSVERKRIQYLHAKL
5.66	NFASC	Neurofascin	CAM	1211 DIATQGWFIGLMCAIALLVLILLIVCFI KRSRGGKYPVREK
5.68	HFE	Hereditary hemochromatosis protein		304 TLVIGVISGIAVFVVILFIGILFIIL RKRQGSRGAMGHYVLAER
5.64	UROL1	Uromodulin-like 1	"Barrier" (CAM)	1267 GLGAGYVVLIVVAIFVLVAGTATLLIV RYQRMNGRYNFKIQ
5.61	LR37B	Leucine-rich repeat-containing protein 37B	(guidance?)	901 DYKNKLIFAISVTVILIILIIFCLIEVN SHKRASEKYKDNP
5.59	MPZL3	Myelin protein zero-like protein 3	CAM	157 SSVALLSILVFVPSAVVVALLLV RMGRKAAGLKKRSRSGYKKSSI
5.56	SLIK6	SLIT and NTRK-like protein 6	Guidance	600SLTDAVPLSVLILGLLIMFITIVFCAAGIVVLVL HRRRRYKKKQV
5.56	ITB5	Integrin beta-5	CAM	722 TILLAVVGSILLVGLALLAIW KLLVTIHDRREFAKFQSERSRARYEMASN
5.46	CSF1R	Macrophage colony-stimul. factor 1 recept.		512 EFLFTPVVVACMSIMALLLLLLLLLLY KYKQKPKYQVRWK
5.46	ITA3	Integrin alpha-3	CAM	989 EIELWLVLVAVGAGLLLLGLIILLLW KCGFFKRARTRALYEAKRQ
5.43	CHL1	Neural cell adhesion mol. L1-like prot.	CAM	1076 DISTQGWFIGLMCAIALLTLLLLTVCFV KRNRGGKYSVKEK
5.39	PTPRT	Protein tyrosine phosphatase, recpt. type, T	(CAM)	740 QVDNTVKMAGVIAGLLMFIIILLGVMLTI KRRRNAYSYSYY
5.38	HBEGF	Proheparin-binding EGF-like growth factor		158 DHTTILAVVAVVLSSVCLLVIVGLLMF RYHRRGGYDVENE
5.35	E9PGC5	Receptor-type tyrosine-prot. phosphatase κ	(CAM)	740 QVDNTVKMAGVIAGLLMFIIILLGVMLTI KRRRNAYSYSYY
5.34	ADAM7	ADAM7	(cytosk)	663 TLHVTNITILVVVLVLVIVGIGVLILLV RYRKCIKLKQVQ
5.33	DCC	Netrin receptor DCC	Guidance	1095 NSNLLVIIVVTVGVITVLVVVIVAVIC TRRSSAQQRKKRA
5.31	PGFRB	Platelet-derived growth factor receptor β		527 SLPFKVVVISAILALVVLTIISLIILIML WQKKPRYEIRWK
5.28	NETO1	Neuropilin and tolloid-like protein 1		337 QLTNTSGTVIGVTSCIVIILIIISVIVQI KQPRKKYVQRKS
5.27	EPHB6	EphB6	adhes/repuls	592 RLSLVIGSILGALAFLLLAAITVLAVVF QRKRRGTGYTEQLQ
5.25	ICAM1	Intercellular adhesion molecule 1	CAM	478 RYEIVIITVVAAAVIMGTAGLSTYLY NRQRKIKKYRLQQA
5.2	L1CAM	Neural cell adhesion molecule L1/VCAM	CAM	1117 FATEGWFIGFVSAIILLLLVLLILCFI KRSKGGKYSVKDK
5.16	NEO1	Neogenin	CAM	1101 DSNMLLVIIVSVGVITIVVVVIIAVF CTRRTTSHQKKKRA
5.13	PVRL4	Poliovirus receptor-related protein 4	(CAM)	344 DLVSASVVVVGVIAALLFCLLVVVVVLM SRYHRRKAQQMTQKYEEELT
5.1	ERBB2	Receptor tyrosine-protein kinase erbB-2		650 PLTSIISAVVGILLVVVLGVVFGILI KRRQQKIRKYTMRRL
5.04	MUC1	Mucin-1	CAM	1155 GVPGWGIALLVLVCVLVALAIVYLIALAV CQCRRKNYGQLDI
5.04	DCBD1	Discoidin, CUB and LCCL domain cont. 1		455 NITTVAIPLVLLVVLVFAGMGIFAAF RKKKKKGSPYGSAEA
5.03	CAD20	Cadherin-20	CAM	616 SLSRGALIAILACIFVLLVLVLLIL SMRRHRKQPYIIDDE
5.02	MANS1	MANSC domain-containing protein 1		380 PFEKWLLIGSLLFGVLFLVIGLVLLGRIL SESLRRKRYSRLDY

Bridge to Chapter IV

This short chapter serves as an addendum to Chapter II. In Chapter II, I showed that during gastrulation, EpCAM is ubiquitously expressed in all tissues where its levels affect cell movements within tissues. EpCAM depletion in gastrula ectoderm impaired cell rearrangements required for epiboly. In Chapter IV, I show that 1) EpCAM remains ubiquitously expressed in all tissues up until the tailbud stage where its expression becomes restricted to the epithelium and notochord, and 2) similar to gastrula tissues (Chapter II), loss of EpCAM leads to cell rearrangement defects in the notochord. These data suggest that EpCAM promotes cell motility in the notochord, and that its expression is required for proper patterning and elongation of the tissue.

CHAPTER IV (addendum to Chapter II)

EpCAM is required for notochord morphogenesis

Introduction

EpCAM expression pattern during embryonic development

In mammalian systems, embryonic expression of EpCAM is observed in the initial phases of development, from the fertilized oocyte to the morula. In this early developmental window, EpCAM expression is not restricted to epithelial precursor cells but is also present in undifferentiated stem cells that are not yet assigned to a specific cell fate (Trzpis et al., 2007). In later stages of mammalian and zebrafish development, EpCAM expression becomes strictly epithelial-specific and terminally differentiated cells stop expressing EpCAM (Slanchev et al., 2009).

In the second chapter of this thesis, EpCAM was shown to be ubiquitously expressed in gastrulating *Xenopus* embryos, including in the mesoderm and endoderm tissues. At this stage, EpCAM levels affect the separation of the ectoderm and mesoderm at the Brachet's cleft and regulate intercalation movements of ectoderm cells during epiboly. Then, in the third chapter of this thesis, I discussed the role of EpCAM as a regulator of cell-cell adhesion in the neurula ectoderm and showed the whole embryo phenotype of EpCAM morphant tailbuds. Interestingly, at the neureula stage, EpCAM expression was still strong in all embryonic tissues including mesoderm-derived tissues. This addendum to Chapter II focuses on 1) describing the expression pattern of EpCAM at later developmental stages in the frog embryo and 2) characterizing the phenotype resulting from EpCAM depletion in the dorsal mesoderm.

Morphogenesis of axial mesoderm in amphibians

Perhaps one of the most spectacular morphogenetic processes taking place during neureulation is the formation, patterning and elongation of the notochord. The notochord is a defining structure of chordates that plays essential roles in development. It simultaneously acts as a major structural axis and a source of midline signals that pattern surrounding tissues. From its central position spanning the anterior to posterior (AP) axis, the notochord provides position and fate information

by secreting factors to surrounding tissues. By doing so, it plays key roles in specifying ventral fates of the central nervous system, controlling left-right asymmetry, inducing pancreatic fates and controlling arterial/venous identities. Structurally, the notochord serves as an axial skeleton in embryos until the formation of vertebrae. Where some vertebrate clades like primitive fishes keep the notochord at adult stages, the notochord of higher vertebrates exists only transiently, during embryonic and larval free-swimming stages, where it provides structural support necessary for locomotion (Stemple, 2005).

The notochord emerges from the dorsal organiser (Spemann's organizer), which in frogs corresponds to the dorsal lip of the blastopore. The development of the notochord starts in the early gastrula, when the chordamesoderm (direct antecedent of the notochord) becomes morphologically and molecularly distinct from the somatic mesoderm with which it forms a boundary. Later in gastrulation and throughout neureulation, the notochord extends and elongates via intercalation of its cells, which causes convergence (narrowing toward the dorsal midline) and extension (lengthening along the AP axis) of the chordamesoderm tissue. The convergent extension movements, driven by active intercalation of cells between one another, lead to the formation of a longer and narrower array of cells in a cylindrical "stack-of-coins" configuration. Mechanistically, intercalation movements involve cells at the surface of the notochord that become typically polarized with their apices stabilized and immobilized on the lateral surface and their inner ends protruding inward. These cells invasively exert traction on their neighbors which reduces the number of rows, thus yielding the "stack-of-coins" configuration of cells along the dorso-ventral (DV) axis (Keller et al., 1989). The notochord is therefore elongated exclusively via cell rearrangements independently of cell proliferation, and its elongation is required for proper embryonic elongation. In the following section, I show that EpCAM expression is detected in the notochord of *Xenopus* neureula and tailbud embryos, where it seems to be required for proper patterning and elongation of the notochord.

Results

EpCAM expression in late neureula and tailbud developmental stages

As observed in gastrulating embryos, immunofluorescence staining of late neureula embryos (stage 18) reveals a ubiquitous and graded expression of EpCAM. At this stage, strongest EpCAM expression is detected in the epithelium, followed by the neural ectoderm, the notochord and somatic mesoderm, the circumblastoporal collar, the forebrain, the archenteron roof, the endoderm and the ventral mesoderm (Fig. 4.1). At this developmental stage, the graded distribution seen in the neureula reflects zygotic EpCAM expression. In accordance with mouse and zebrafish data, EpCAM seems to be enriched basolaterally in the epithelium (Fig 4.1B'). However, unlike all studies of EpCAM in developing embryos, the expression of EpCAM is clear in mesoderm tissues as well as in other ectoderm-derived epithelia (Fig. 4.1B). By the mid-late tailbud stage (stage 26-30), total levels of embryonic EpCAM seem to drop significantly in all tissues, and some tissues, such as the endoderm, lose EpCAM expression altogether, but EpCAM staining was still retained in the epithelium and in somites (Fig. 4.2A). Surprisingly, the strongest EpCAM expression at this stage was seen in the notochord (Fig. 4.1A, B). This observation raised the possibility that similarly to its role in regulating epiboly movements in gastrulating ectoderm, EpCAM is also involved in regulating chordamesoderm cell intercalation movements that shape and elongate the notochord.

EpCAM loss of function disrupts notochord architecture

To test whether EpCAM expression in the notochord is required for its patterning, we knocked down EpCAM in the notochord by targeted injection of EpCAM MO and asked whether loss of EpCAM disrupts the notochord patterning or the elongation. Saggital sections of early tailbud stained with C-cadh antibody to visualize cell shapes showed the expected "stack-of-coins" configuration of COMO-injected notochord cells, which was strongly disrupted by EpCAM knock down (Fig. 4.3A-B'). COMO-injected notochords are circular and each cross-sectional plane is

occupied by a small number of extended cells that have become shaped like pizza slices in contrast to EpCAM MO-injected notochords that have a greater number of cells per plane with various shapes and sizes (Fig. 4.3D-E' arrows). EpCAM depleted notochords were also thicker (along the DV axis) and shorter (along the AP axis) compared to wild-type embryos (Fig. 4.4A-F, arrows). The wild-type morphology of notochord cells along the AP and the dorso-ventral (DV) axes, as well as the thinness of notochord, were restored upon co-injection of EpCAM mRNA with EpCAM MO, thus indicating that the disruption of notochord architecture is specifically due to EpCAM downregulation (Fig. 4.3C, C', F, F'). EpCAM-depleted notochords still formed and separated from somitic mesoderm via a boundary (Fig. 4.3E arrowheads), suggesting that the initial steps of notochord specification are unaffected by EpCAM downregulation. Rather, the higher number of randomly shaped smaller cells and the thicker notochords observed in EpCAM depleted embryos are most likely due to defective intercalation movements of notochord cells that are required for proper elongation and thinning of the notochord. Given that cell division has never been observed in the notochord (Keller et al., 1989), and that EpCAM depleted tailbud notochords are shorter than that of wild-type notochords at the same stage, the increase in cell number upon EpCAM depletion is not likely to be a consequence of overproliferation.

C-cadherin is downregulated in EpCAM depleted notochords

While staining with the cell membrane marker C-cadherin (C-cadh) antibody to visualize cell shapes, we found another interesting difference between COMO and EpCAM MO-injected notochords: C-cadh staining was strongly reduced in EpCAM-depleted notochords compared to wild-type COMO-injected notochords (Fig. 4.4A, B, D, and E). The reduction of C-cadh signal was rescued by co-injection of EpCAM mRNA with EpCAM MO (Fig. 4.4C, F). This result is consistent with the ectoderm EpCAM LOF phenotype discussed in chapter 3, where, by the late neureula stage, EpCAM depleted embryos had completely lost C-cadh expression. However, in contrast to the C-cadh decrease observed in the neureula ectoderm (by WB and IF), these preliminary results are not sufficient to confidently state that C-cadh levels are regulated by EpCAM levels in the notochord. More work needs to be done in order

to determine whether EpCAM has a similar regulatory role on C-cadh in the notochord mesoderm and whether this regulation accounts for the disruption of notochord tissue architecture observed upon loss of EpCAM function.

Discussion

EpCAM is required for proper notochord formation and elongation of Xenopus embryos

The results presented in this chapter reveal new aspects of EpCAM function in development. On one hand, they show for the first time that EpCAM expression is not restricted to epithelial tissues in developing embryos, even in late post-gastrulation stages. These results also suggest that EpCAM plays a crucial role in chordamesoderm cell intercalation movements required for proper patterning and elongation of the notochord. Interestingly, in addition to appearances of epithelial lesions on their surface, EpCAM morphant tailbuds failed to elongate properly and were smaller than wild-type controls (Fig. 3.1A, B). Since notochord elongation is required for proper elongation of the embryo, it is possible that EpCAM is required in the notochord to ensure proper cell intercalation movements, which drive its patterning and elongation as well as the elongation of the embryo post-neureulation. In the absence of EpCAM, embryos fail to elongate properly possibly because the elongation of the notochord is hampered.

During convergent extension movements and thinning of notochord, cells at the surface have their lateral sides anchored and their inner ends protruding inward where they invasively exert traction on their neighbors, which results in movement of cells along the AP axis and compaction of the notochord. To accomplish these movements, mesoderm cells need proper cell-cell adhesion for anchorage and traction as well as a dynamic actin cytoskeleton capable of driving protrusions, contracting and eventually supporting the final "stretched" conformation of "pizza slice"-shaped cells. In chapters 2 and 3, I showed that EpCAM regulates both cell movements and cadherin-mediated cell-cell adhesion by controlling the contractile state of the acto-myosin network. It is tempting to speculate that EpCAM functions in a similar fashion in the notochord mesoderm where its expression levels regulate

cell movements and cadherin-mediated cell adhesion. Similar to the gastrula ectoderm, the knockdown of EpCAM in the notochord might, via a PKC-dependent MLC activation, makes the cortical acto-myosin network too tense and rigid such that notochord cells fail to send out protrusions inward and, consequently, fail to move. A sustained increase of acto-myosin contractility in those cells (from the late gastrula to the late neureula) may consequently destabilize C-cadh adhesion thereby causing the observed downregulation of C-cadh levels (Fig. 4.4). Alternatively, it is possible that EpCAM directly regulates convergent extension movements of notochord cells by providing enough adhesion for anchorage and traction of cells that are needed for cell motility. EpCAM might provide adhesion either directly, via homophilic mediated adhesion, or indirectly by promoting C-cadherin-mediated adhesion, or both. EpCAM-depleted notochord cells with low EpCAM and C-cadh levels might become too "slippery" and unable to pull on one another, which might result in a "juvenile" notochord capable of separating from somites but incapable of thinning and extending properly.

Additional experiments are required to test these hypotheses. First, high resolution live imaging of explanted notochords should reveal how cells behave at the membrane. Labelling actin would allow testing whether there are differences in cortical actin dynamics in wild-type versus EpCAM-depleted notochords. Overexpressing C-cadherin in EpCAM depleted embryos should, in principle, restore cell movements and rescue the notochord phenotype if the latter is due to "slippery" cells. Second, it would be interesting to test whether PKC activity is increased in EpCAM-depleted notochords compared to wild-type controls, and if so, whether it activates acto-myosin contraction in this tissue. Then, I would test if inhibitions of PKC or myosin activities in EpCAM MO-injected notochords are sufficient to rescue the notochord phenotype in order to determine whether the notochord phenotype is due to increased acto-myosin tension. To determine if C-cadh downregulation occurs downstream of PKC and myosin, I would ask whether notochord C-cadh levels can be rescued by PKC or MLC inhibitions. These experiments will be more technically challenging than the ectoderm explants used to characterize EpCAM's function in the neureula ectoderm since it is more difficult to

target notochords, dissect and isolate them for biochemical and phenotypic rescue assays.

EpCAM expression is ubiquitous during most stages of Xenopus development

The results presented in this chapter reveal for the first time that EpCAM embryonic expression is not restricted to epithelial tissues. In the late neureula, EpCAM expression was even detected in tissues fated to produce non-epithelial cells like the notochord, the posterior mesoderm and the endoderm (Fig. 4.1A). This result is surprising given the fact that embryonic EpCAM expression was previously reported to be strictly epithelial-specific in both mammalian and zebrafish embryos (Slanchev et al., 2009; Trzpis et al., 2007). It is conceivable that embryonic EpCAM expression is ubiquitous in early vertebrates, where it is needed to regulate diverse morphogenetic events and then gets restricted to epithelial tissues in higher vertebrates, where alternate mechanisms have evolved to regulate morphogenesis of non-epithelial tissues. However, the fact that EpCAM was suggested to be expressed in zebrafish embryonic epithelial tissues specifically is puzzling and raises the possibility that the ubiquitous expression of EpCAM observed in *Xenopus* is specific to amphibians. While this interpretation may be valid, it is important to note that the authors of the only study suggesting an "epithelial-specific" expression of EpCAM in zebrafish had based their interpretation solely on mRNA *in situ* hybridization observations. They were not able to observe endogenous EpCAM protein levels in the embryo due to a lack of antibody suitable for zebrafish EpCAM protein detection (Slanchev et al., 2009). Therefore, it is possible that zebrafish embryonic EpCAM expression is broader and more ubiquitous than appreciated by mRNA hybridization experiments. Indeed, RT-PCR experiments in *Xenopus* embryos show that the abundance of total EpCAM mRNA transcripts progressively drops after gastrulation as it is the case for C-cadh mRNAs (data not shown), but in both cases, EpCAM and C-cadh proteins are still significantly expressed at detectable levels in embryonic tissues. In conclusion, additional work will be needed in other vertebrate model systems to better characterize the expression patterns of EpCAM in development.

Materials and Methods

Embryo manipulations

Embryos were obtained and cultured as described in "Embryo manipulations" part of Chapter 2's Materials and Methods section. Embryos were injected equatorially at the 4-cell stage (once in each dorsal blastomere) for notochord targeting. Embryonic staging was performed as described in "Embryo manipulations" part of Chapter 2's Materials and Methods section.

mRNAs and oligonucleotides

The sequences of Control MO (COMO) and EpCAM MO as well as cloning and transcription details for full-length EpCAM mRNA production (used for co-injection with EpCAM MO in Fig. 4 and 5) are all described in Chapter 2's Materials and Methods section.

Antibodies

Antibodies used in this study were rabbit anti-EpCAM ab (raised against the cytoplasmic tail of EpCAM fused to GST) and mouse anti-C-cadherin mAb 5G5 (generous gift of B.M. Gumbiner, University of Virginia).

Immunofluorescence

Cryosectioning, immunofluorescence, image acquisition and processing were performed as described in Chapter 2's Materials and Methods section.

References

Keller, R., Cooper, M.S., Danilchik, M., Tibbetts, P., and Wilson, P.A. (1989). Cell intercalation during notochord development in Xenopus laevis. The Journal of experimental zoology *251*, 134-154.

Slanchev, K., Carney, T.J., Stemmler, M.P., Koschorz, B., Amsterdam, A., Schwarz, H., and Hammerschmidt, M. (2009). The epithelial cell adhesion molecule EpCAM is required for epithelial morphogenesis and integrity during zebrafish epiboly and skin development. PLoS genetics *5*, e1000563.

Stemple, D.L. (2005). Structure and function of the notochord: an essential organ for chordate development. Development *132*, 2503-2512.

Trzpis, M., McLaughlin, P.M., de Leij, L.M., and Harmsen, M.C. (2007). Epithelial cell adhesion molecule: more than a carcinoma marker and adhesion molecule. The American journal of pathology *171*, 386-395.

Figure legends

Figure 1. EpCAM expression is ubiquitous in the *Xenopus laevis* neureula. **(A)** Sagittal section of stage 18 wild-type neureula stained with anti-EpCAM antibody showing ubiquitous expression of endogenous EpCAM in all tissues, the epithelial layer of neurectoderm (ep), notochord (no), somitogenic mesoderm (sm), sensorial layer of neural ectoderm (ne), circumblastoporal collar (cc), forebrain (fb), archenteron roof (ar), ventral mesoderm (vm) and endoderm (en). **(B)** Closer view of the dorsal region showing details of EpCAM staining in the epithelium, neuroderm (ne) notochord and archenteron, staining being strongest in the epithelium. **(B')** Zoom on the epithelium where EpCAM staining is enriched baso-laterally (arrows).

Figure 2. EpCAM is expressed in the notochord and epithelium of *Xenopus laevis* tailbuds. (A) Sagittal section of stage 26 wild-type tailbud stained with anti-EpCAM antibody. Arrows point to tissues where EpCAM expression is still detected including, the epithelium (ep), somites (so), notochord (no) and the roof of spinal chord (sc). No EpCAM expression was detected in the endoderm (en) at this stage. **(B)** Closer view of the notochord at this stage showing strong cell surface EpCAM staining in notochord and wall of spinal chord cells (sc).

Figure 3. EpCAM depletion disrupts the architecture of the notochord. (A, A') Sagittal sections of early tailbud COMO-injected embryos (~stage 23) stained with anti-C-cadh mAb 5G5 to visualize cell shapes. Yellow dotted lines in A' were drawn over plasma membrane C-cadh staining to clearly outline cell surfaces, and reveal the "stack-of-coins" configuration of cells normally seen at this stage. "D" and "V" indicate the dorsal and ventral sides respectively **(B, B')** same as (A, A') except using EpCAM MO injected embryo sections. "Stack-of-coins" morphology is strongly disrupted as individual cells fail to elongate along the dorso-ventral axis. **(C, C')** Co-injection of EpCAM MO with mRNA coding for full-length EpCAM but lacking 5'UTR recognized by the morpholinos restores the "stack-of-coins" morphology of cells. **(D, D')** Cross-sections of early tailbud COMO-injected embryos (~stage 23) reveal the "Pizza slice" morphology of cells (arrows) that have their apices at the surface and their basal sides extending towards the center of the notochord. Roughly all cell membranes meet at the center of the notochord. **(E, E')** "Pizza slice" morphology of cells is completely disrupted by EpCAM depletion; cross section view reveals the presence of at least twice more cells per plane compared to wild-type COMO-injected notochords (A'). Cells are also smaller than and not as extended as COMO cells. Note that exposure has been increased for EpCAM MO compared to COMO (D, D'). For proper comparison of C-cadherin levels, see figure 4. **(F, F')** Co-injection of EpCAM MO with EpCAM mRNA restores the "Pizza slice" morphology of cells.

Figure 4. EpCAM depletion leads to thicker notochords with weaker C-cadh staining. (A-C) Sagittal sections of (A) COMO, (B) EpCAM MO and (C) EpCAM MO + EpCAM-injected notochords stained with anti-C-cadh mAb 5G5 with arrows indicating the thickness of the notochord along the DV axis. EpCAM depletion causes a strong thickening of the notochord (compare B to A) which is rescued by restoring EpCAM (C). EpCAM depletion also causes a strong decrease of C-cadh membrane signal which is also rescued by restoring EpCAM (compare B to A and C to B). **(D-F)** Same as (A-C), except with cross-sections. Left "L" and right "R" arrows indicate notochord thickness across the left-right axis.

Figure 4.1

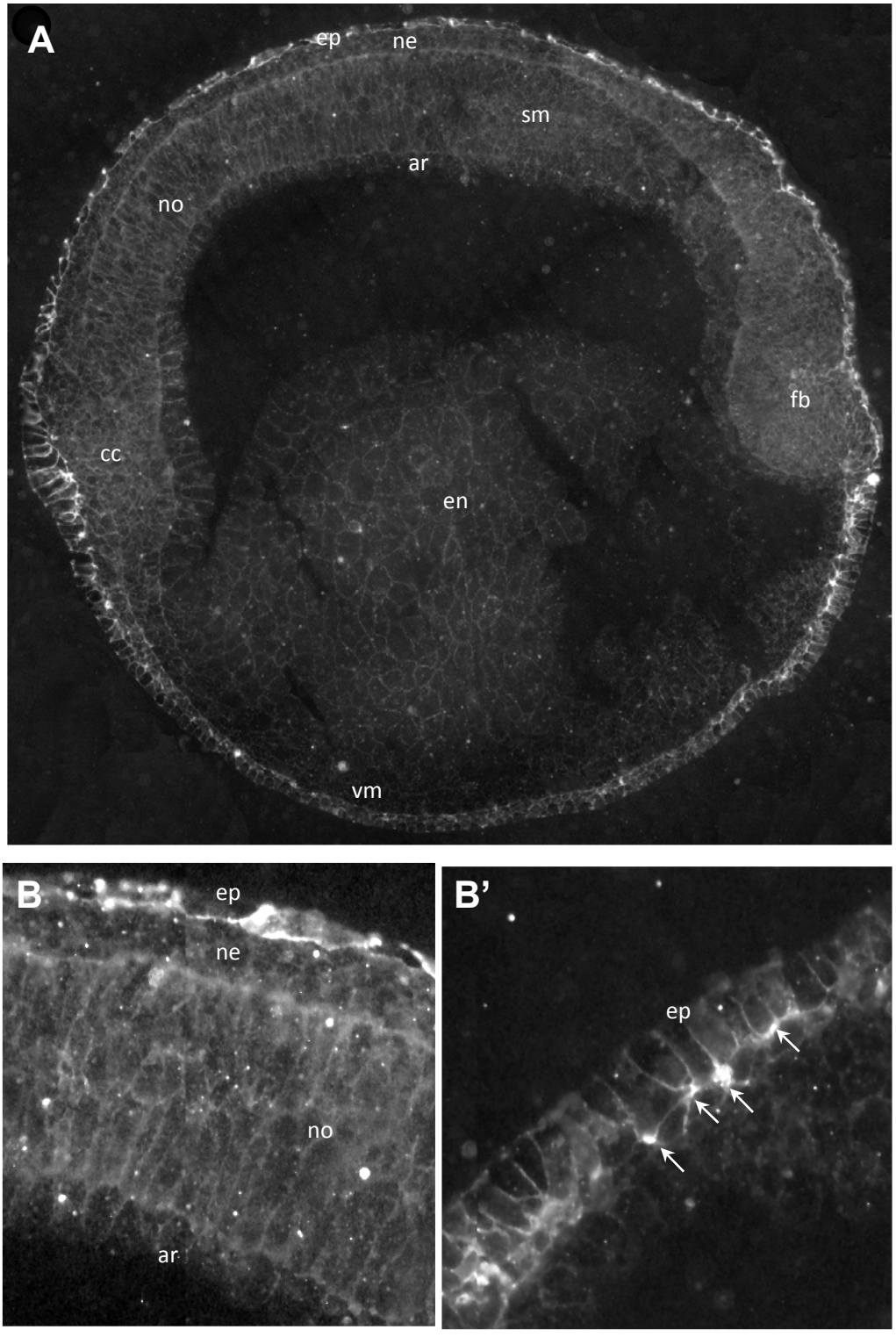

Figure 4.2

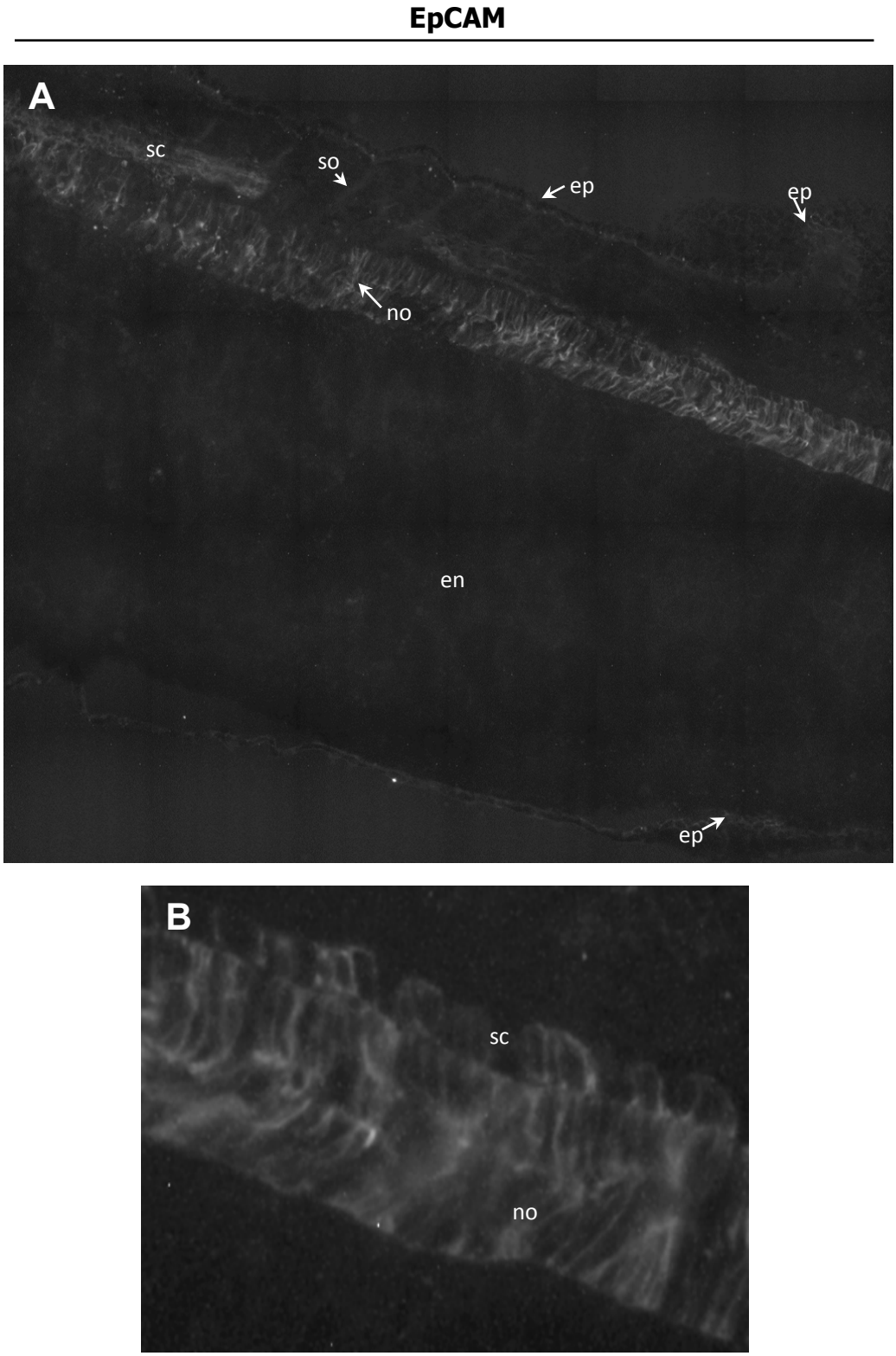

Figure 4.3

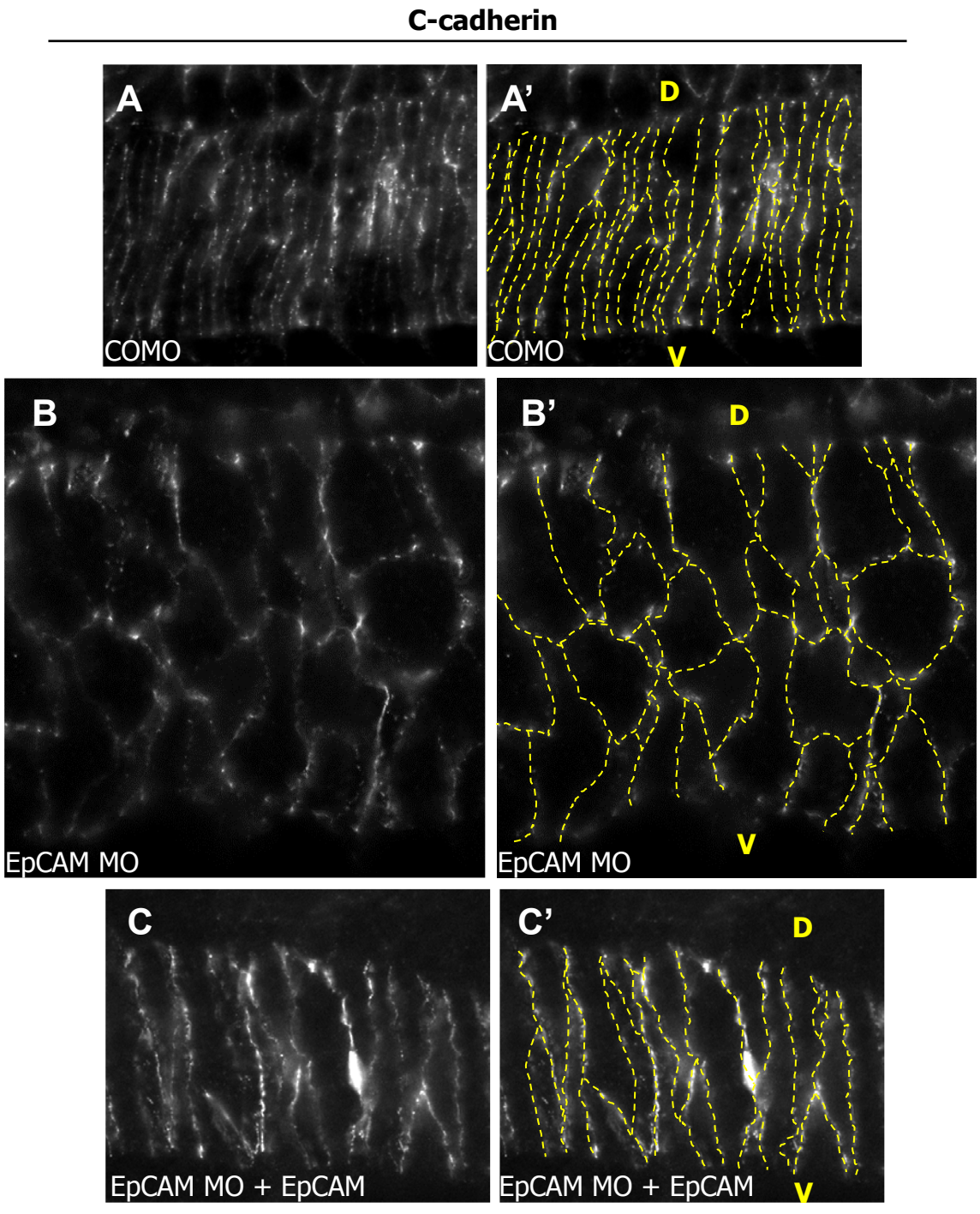
C-cadherin
A
COMO
A'
D
COMO
V
B
EpCAM MO
B'
D
EpCAM MO
V
C
EpCAM MO + EpCAM
C'
D
EpCAM MO + EpCAM
V

Figure 4.3 (continued)

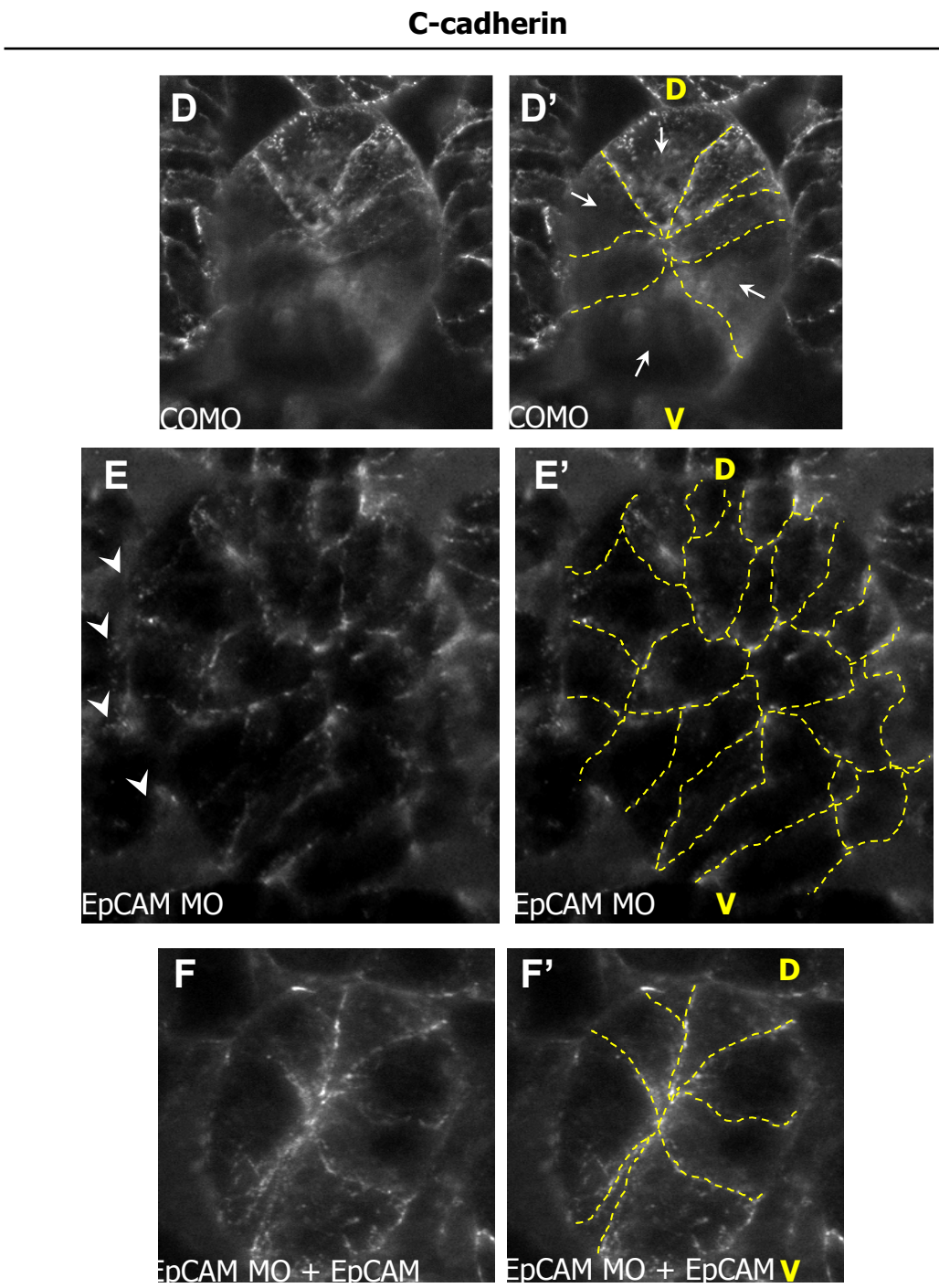

Figure 4.4

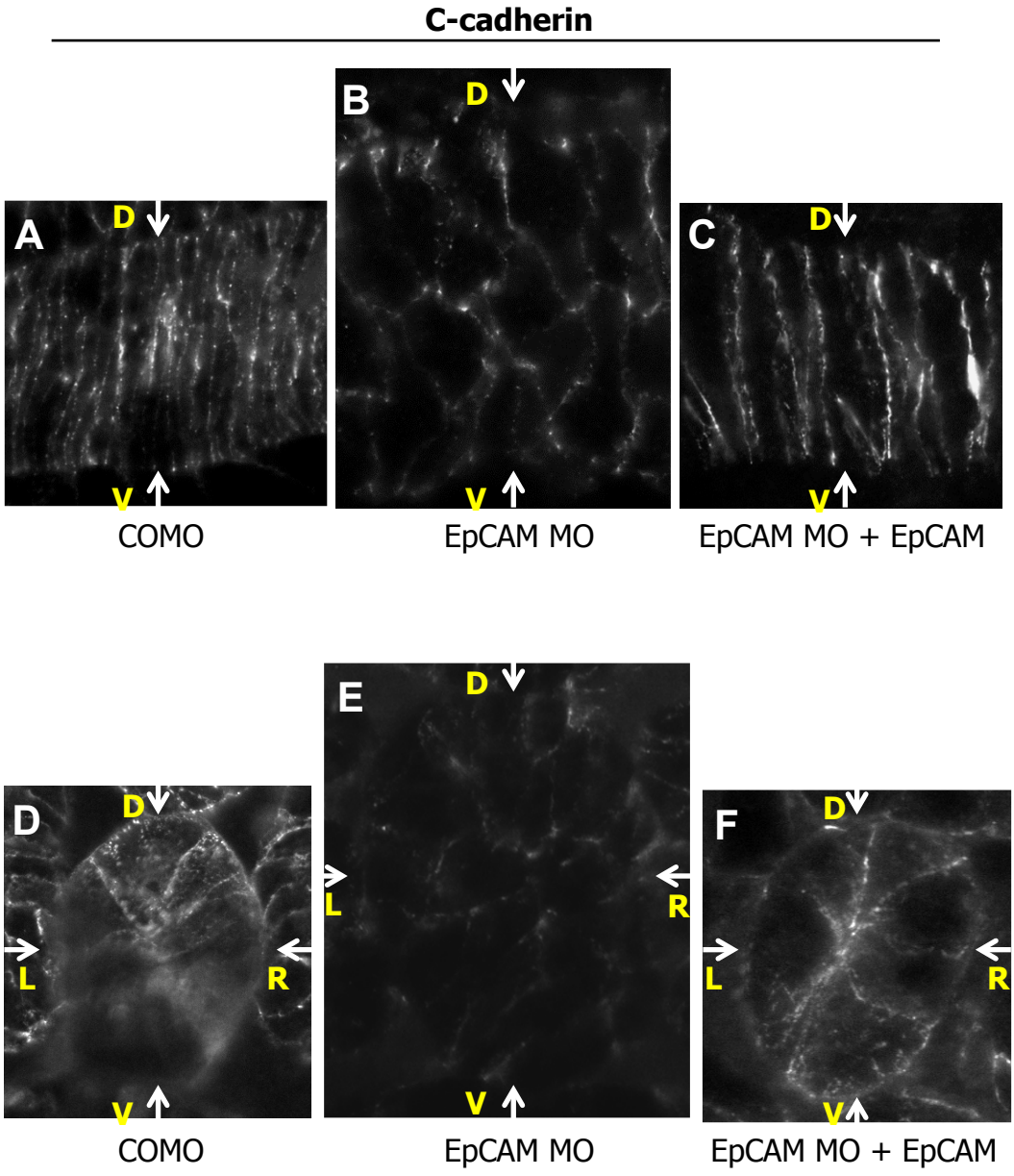
C-cadherin
A
B
C
D
E
F
D
V
L
R
COMO
EpCAM MO
EpCAM MO + EpCAM
COMO
EpCAM MO
EpCAM MO + EpCAM

CHAPTER V

Final Discussion

Discussion

The work presented in this thesis proposes a previously unknown molecular mechanism that accounts for the function of EpCAM in promoting cell motility and cell-cell adhesion, as well as a new mode of PKC inhibition at the membrane. In this section, I summarize the key findings presented in this thesis and discuss how these findings fit with data from other EpCAM studies.

Summary of contributions

Investigating EpCAM function in *Xenopus laevis* development has led me to discover an important molecular mechanism through which EpCAM affects cell motility and cell-cell adhesion: EpCAM reduces actomyosin contractility by downregulating Erk signaling through direct inhibition of nPKC activity. This molecular mechanism was validated in human carcinoma cell lines suggesting that the function of EpCAM as a negative regulator of PKC/Erk/MLC is conserved. This function satisfactorily accounts for the changes in motile behavior of cells upon EpCAM overexpression or depletion in the gastrula, as well as loss of cell-cell adhesion resulting from EpCAM depletion in the neureula. Alterations in the motile behavior of cells were due to modulations of PKC-mediated actomyosin contractility (Chapter II). On the other hand, the amount of MLC stimulation resulting from EpCAM depletion was sufficient to destabilize cadherins and to cause tissue dissociation in *Xenopus* ectoderm, consistent with the idea that high cortical contractility negatively affects adhesion (Chapter III). Based on data presented in this thesis, EpCAM emerges as an important regulator of cell motility and adhesion that is capable of stimulating cell movement while insuring tissue coherence at the same time by regulating actomyosin contractility via PKC inhibition. This ability of EpCAM to regulate both processes simultaneously makes it a key molecule in dynamic tissues during morphogenesis and cancer.

Another crucial contribution of this thesis is that it provides a detailed mechanism of PKC inhibition by EpCAM: EpTail directly binds and inhibits nPKC activity by mimicking a nPKC pseudosubstrate (PS) domain. This novel mechanism

of negative PKC regulation at the membrane is not unique to EpCAM, but rather appears to be shared by a small family of transmembrane proteins containing a PKC PS-mimicking motif in their membrane proximal cytoplasmic domains. Judging by the strength of nPKC inhibition by EpTail in embryonic ectoderm and in Caco-2 cells, as well as the severity of phenotypes resulting from EpCAM depletion, EpCAM-mediated nPKC inhibition appears to be a major function of EpCAM.

Reconciling EpCAM functions

In this section, I discuss how my findings account for previous hypotheses and observations made by other EpCAM studies.

EpCAM levels affect cell motility

During *Xenopus* gastrulation, EpCAM depletion disrupted epiboly movements of ectoderm cells (Chapter II), consistent with data from a zebrafish study showing that epiboly was defective in EpCAM null mutants (Slanchev et al., 2009). In the ectoderm of both *Xenopus* and zebrafish, cells that failed to undergo epiboly movements had less cortical actin protrusions. In zebrafish, ruffle-like actin-based protrusions in wild-type embryos were lost in EpCAM mutants, similar to the partial loss of basal actin protrusions in *Xenopus* EpCAM-depleted ectoderm cells (Fig. 2.8E-F). Mechanistically, there is a difference in the interpretation of both epiboly phenotypes: While in zebrafish, EpCAM homophilic adhesion between the protruding cell and its neighbor is thought to be required for the protruding membrane to exert traction on the neighboring cell resulting in motion by pulling the cell forward. I show that EpCAM homophilic interactions are completely dispensable for epiboly movements. Rather, in EpCAM-depleted *Xenopus* ectoderm, the highly contractile state of the cortical actin cytoskeleton, caused by increased PKC activity, appears to hinder epiboly movements by rendering the cells too stiff and unable to rearrange. Also, the severity of the epiboly phenotype in *Xenopus* EpCAM morphants is more important than in zebrafish mutants. This may be due to the fact that in my system (pseudotetraploid *Xenopus laevis*), I strongly block all EpCAM translation by targeting each of the two EpCAM pseudoalleles with a

specific morpholino antisense sequence, thus resulting in a complete loss of EpCAM. In tetraploid zebrafish containing two EpCAM genes, only one EpCAM gene was mutated resulting in partial depletion of EpCAM. So far, this explanation may be plausible since EpCAM protein levels were not assessed in zebrafish due to a lack of suitable antibody for endogenous EpCAM detection in this system.

Aside from this thesis and the zebrafish study, very little is known about the role of EpCAM in regulating cell motility *in vivo*. Recently, a study in adult mice epidermis reported a role for EpCAM in promoting the motility of epithelial Langerhans cells, which are EpCAM-expressing dendritic cells that are found in stratified squamous epithelia like the skin (Gaiser et al., 2012). Activated epithelial Langerhans cells send out protrusions (dendritic processes) and intercalate between keratinocytes to reach lymph nodes as an immune response. The loss of EpCAM decreased the migratory ability of activated epithelial Langerhans cells that failed to leave the skin and migrate to lymph nodes. At the molecular level, Langerhans cell migration remains poorly understood. Thus, their failure to move in the absence of EpCAM raises the possibility that high PKC signaling hinders movement by increasing MLC phosphorylation and actomyosin contraction.

The role of EpCAM as a promoter of cell migration has been previously reported *in vitro* (Litvinov et al., 1997; Osta et al., 2004). The earliest model proposes that EpCAM overexpression increases the invasiveness of carcinoma cells by reducing E-cadherin-mediated cell-cell adhesion via interference with the α-catenin/F-actin-mediated cytoskeletal anchorage of E-cadherin. Interference with cadherin anchorage is thought to be a result of EpCAM binding and sequestering α-actinin away from junctional cadherin/actin complexes. This model clashes with my following *in vitro* and *in vivo* results: First, I was not able to reproduce the EpTail/α-actinin interaction neither *in vivo* (in *Xenopus* embryos) nor *in vitro* with purified GST-EpTail and α-actinin. Second, I never saw a colocalization of α-actinin with EpCAM *in vivo*, and third, instead of antagonizing cadherin-mediated adhesion, overexpression of EpCAM in *Xenopus* ectoderm led to an upregulation of C-cadherin (Fig. 2.3 A,B,E,F). Based on these observations, the α-actinin model is unlikely to account for the function of EpCAM in regulating cell motility *in vivo* and *in vitro*.

Rather, it will be interesting to determine whether EpCAM functions via the PKC/Erk/MLC molecular pathway to promote migration of carcinoma cells. While I have established that changes in EpCAM levels in Caco-2 human carcinoma cells trigger the same cascade of molecular events responsible for changes in cell motility and cell-cell adhesion in *Xenopus* embryos, the effects of these changes on cellular processes remain to be elucidated.

EpCAM levels affect cell-cell adhesion

The contribution of the homophilic EpCAM adhesive bond, initially characterized in L cells (Litvinov et al., 1994), to tissue cohesion *in vivo* remains to be determined (See Chapter I). Based on the data presented in this thesis, the predominant function of EpCAM in promoting cell-cell adhesion *in vivo* appears to occur by stabilization of cadherin levels via EpTail-mediated inhibition of PKC/Erk/MLC activities (Chapter III). The notion that EpCAM promotes adhesion *in vivo* by stabilizing cadherin is consistent with data from the zebrafish study showing that EpCAM dowregulation affects E-cadherin levels (Slanchev et al., 2009). However, the effect of EpCAM on cadherin stability appears to be much more important in my system: Whereas loss of EpCAM in *Xenopus* ectoderm is sufficient to cause a quasi-complete depletion of C-cadherin and strong tissue dissociation, loss of EpCAM in zebrafish only leads to a mild decrease in E-cadherin membrane expression and a double knockdown of EpCAM and E-cadherin is required to induce tissue disintegration (Slanchev et al., 2009). The authors of the zebrafish study argue that this is likely due to a functional overlap between EpCAM and cadherin function in promoting cell-cell adhesion, but based on my results, this interpretation is unlikely. Rather, the mild reduction in E-cadherin levels resulting from EpCAM depletion in zebrafish may be due to the presence of residual EpCAM produced by the non-mutated second copy of the EpCAM gene in tetraploid zebrafish (See epiboly discussion above). Alternatively, assuming a complete loss of EpCAM is achieved in the zebrafish mutant, EpCAM depletion may not be sufficient to cause embryo disintegration, possibly because PKC activation by other pathways is not as high as in *Xenopus*. Another possibility is that increased actomyosin contractility induced by high PKC activity is not high enough to destabilize cadherins because the basal cell contractility/rigidity of

zebrafish epidermal cells is intrinsically lower. Collectively, the effects of EpCAM on epiboly and cadherin-mediated adhesion presented in the zebrafish study can entirely be accounted for by the PKC-dependent molecular model proposed in this thesis.

In addition to the effect on cadherin-based cell-cell junctions, EpCAM levels have been reported to influence tight junction formation and maintenance *in vitro* and *in vivo* (Ladwein et al., 2005; Lei et al., 2012). The only *in vivo* study shows that in developing mouse embryos, EpCAM depletion caused malformations of cell-cell tight junctions in the intestinal epithelium by downregulating claudins, but the molecular mechanism leading to claudin downregulation has not been identified (Lei et al., 2012). Similar to the effect it has on cadherins, it is possible that actomyosin contraction resulting from high PKC activity in EpCAM depleted epithelia disrupts tight junctional proteins claudins, which require anchorage to the actin cytoskeleton for proper adhesion (Fanning et al., 1998; Shen and Turner, 2005).

Increased PKC activity and actomyosin in this system does not seem to be high enough to disrupt adherens junctions/E-cadherin levels, which were unaffected in the intestine of EpCAM depleted embryos, and strong loss of cell-cell adhesion was not observed. This may be due to a few reasons: 1) adherens junctions in late mouse intestinal epithelial might be more stable than junctions in *Xenopus* neureula ectoderm, 2) PKC activity in those cells is lower overall, which means that the increase in PKC activity following EpCAM depletion affects claudins/tight junctions but is not sufficient to destabilize cadherin junctions, or 3) the presence of EpCAM homolog Trop-2 protein product which may be functionally redundant with EpCAM (See Chapter I). In the latter case, it is conceivable that in mouse intestinal epithelium, EpCAM specialized in regulating tight junction stability via inhibition of PKC/actomyosin contractility, while Trop-2 is involved in regulation of E-cadherin/adherens junctions through the same molecular mechanism. If this hypothesis is correct, a double mutant of EpCAM and trop-2 would be expected to result in destabilization of both tight and adherens junctions, loss of cell-cell adhesion and tissue disintegration.

<u>EpCAM levels affect cell proliferation</u>

It has been shown that EpCAM overexpression promotes cancer progression by increasing proliferation rates of carcinoma cells via nuclear signaling of the EpTail/β-catenin complex that promotes oncogene transcription (Maetzel et al., 2009). While increased EpCAM motility induced by PKC inhibition was shown to be independent of nuclear β-catenin/Lef-1 signaling (Chapter II), I have not directly tested whether EpCAM levels affect cell proliferation in developing *Xenopus* embryos. Cell proliferation is minimal in wild type embryos during the developmental stages that I mostly worked on, where morphogenesis is largely driven by massive reorganization of pre-existing tissues/cells. Preliminary observations made during late stages of tailbud development suggest that cell proliferation of posterior tail mesoderm may be reduced in EpCAM depleted embryos, although this possibility remains to be experimentally verified. In cancer systems, it seems that EpCAM functions via two distinct pathways to promote tumor progression: On one hand, EpTail overexpression promotes cell motility via inhibition of nPKC-mediated actomyosin contraction (Chapter III), and on the other hand, EpTail overexpression increases cell proliferation by inducing transcription of oncogenes (Denzel et al., 2009; Maetzel et al., 2009). These two functions are mutually exclusive for a single EpCAM molecule since binding β-catenin would prevent direct interaction of EpTail with PKC, and vice versa. Therefore, a single EpCAM molecule can only undergo one of the two functions at a time. The fact that EpCAM can increase both cell proliferation and cell motility via these two functions may account for its potent tumor promoting effect seen in some cancers.

Whether EpCAM functions predominantly via nuclear signaling or nPKC binding/inhibition may depend on the composition of its immediate environment at a given point. For instance, high concentrations of proteases involved in the cleavage of EpTail might favor the nuclear signaling function of EpCAM. Furthermore, nuclear signaling is thought to increase with cell density and cell-cell contacts, possibly via homophilic aggregation of EpECD, which promotes EpCAM cleavage. Cleaved EpECD then acts as a soluble ligand that promotes cleavage of more EpTail and consequently increases nuclear signaling (Denzel et al., 2009; Maetzel et al., 2009). Alternatively, membrane localization of EpCAM in domains devoid of

proteases and enriched in active membrane-recruited PKCs might favor cell motility induced by inhibition of PKC activity.

My preliminary data in Caco-2 cancer cells suggest that EpCAM-depleted cells proliferated less than control cells expressing EpCAM, and that this reduction in proliferation could be rescued by nPKC inhibition. This result raises the possibility that the positive effect EpCAM has on cell proliferation in tumors may be partly due to its PKC inhibitory function. In support of this possibility, activation of PKCδ was shown to inhibit growth of Caco-2 cells (Cerda et al., 2006). Therefore, in addition to proliferation induced by EpTail-mediated nuclear signaling, EpCAM may promote proliferation in carcinoma cells by inhibiting PKC activity.

Concluding remarks

The work presented in this thesis has a two-fold impact. First, the characterization of EpCAM in *Xenopus laevis* development has unravelled a major function of EpCAM through which the molecule controls important processes such as cell motility and cell-cell adhesion. Second, dissecting the molecular mechanism of EpCAM function has led to the discovery of a previously unknown mode of PKC regulation at the plasma membrane that may be highly important in cellular processes involving PKC signaling.

Discovery of an important signaling CAM in morphogenesis

Perhaps one of the most important findings of this thesis is the discovery of EpCAM as a crucial molecule in development. EpCAM emerges as a major regulator of morphogenetic movements, a promoter of ectoderm tissue cohesion and a vital protein in *Xenopus laevis* development. Unexpectedly, the role for EpCAM in morphogenesis relies predominantly on a signaling property of its cytoplasmic domain EpTail that regulates actin contractility and cadherin stability. As such, EpCAM function in morphogenesis resembles that of other CAMs identified as "non-adhesive" morphoregulators. A good example is the paraxial protocadherin PAPC that has been shown to 1) regulate ectoderm/mesoderm tissue separation via association with Frizzled-7 (Fz7) (Medina et al., 2004), and 2) mediate activin-

induced downregulation of C-cadherin adhesion activity and convergent extension movements in the *Xenopus* embryo (Chen and Gumbiner, 2006). Similar to EpCAM, the cytoplasmic domain of PAPC is required for its tissue separation function, presumably by signaling and/or modulating signals by Fz7. However, unlike EpCAM, PAPC regulates C-cadherin adhesion independently of its cytoplasmic domain. In the latter case, PAPC forms a complex with FLRT3 and C-cadherin, where it limits the disruptive effect that FLRT3 has on cadherins by preventing the recruitment of GTPase Rnd1 to the cytoplasmic domain of FLRT3, which is necessary for FLRT3-mediated inhibition of cell adhesion (Chen et al., 2009). Another example of a "non-adhesive" CAM morphoregulator is Echinoid (Ed), which has been mostly studied in *Drosophila* development. Recently, Ed was found to regulate tissue growth and oocyte polarity in *Drosophila* by impinging on Hippo signaling via its cytoplasmic domain (Yue et al., 2012). Similar to the EpCAM-PKC interaction, Ed regulates Hippo pathway signaling by physically interacting with Hippo pathway components via its cytoplasmic domain.

It is possible to speculate that some of the CAMs identified in Chapter III as potential PS-containing PKC regulators play important roles in morphogenesis since the regulation of PKC activity in development appears to be crucial (Chapter III). Some of these CAMs and "CAM-like" molecules have already been demonstrated to act as morphoregulators independently of their potential PKC regulatory property, e.g. EphA4 (Bisson et al., 2007), DCC (Bernadskaya et al., 2012), and plexin (Dalpe et al., 2005). It will be interesting to determine whether these molecules also play important roles in morphogenesis by inhibiting PKC activity similar to EpCAM.

Impact on the EpCAM field

The findings presented here are valuable for researchers studying EpCAM function because they provide a first detailed molecular mechanism of EpCAM function. The control that EpCAM has over PKC and Erk signaling, as well as myosin contraction and cadherin stability in development appears to be conserved amongst vertebrates and human carcinoma cells, making these results particularly valuable for researchers investigating EpCAM function in cancers. Indeed, the loss of EpCAM in human Caco-2 cells triggered the same molecular events as those caused by loss of EpCAM

function in *Xenopus* embryos. While the effects of these molecular changes were well characterized in *Xenopus* morphogenesis, it will be important to determine whether EpCAM promotes tumor progression by impinging on PKC/Erk signaling and modulating actomyosin contraction and E-cadherin adhesion. Similar to its effect on ectoderm gastrulating cells (Chapter II), EpCAM overexpression might promote the "invasive" behavior of tumor cells by reducing actomyosin contractility thus enabling cells to send out protrusion required for migration. Additionally, my preliminary data mentioned earlier point towards a role for PKC in mediating the effect of EpCAM on carcinoma cell proliferation. It is conceivable that via PKC/MLC signaling, EpCAM overexpression optimizes anchorage/spreading conditions which allows cells to strongly proliferate. Thus, addressing these possibilities should help improve EpCAM-based therapeutic methods by specifically targeting other key molecules through which EpCAM may promote tumor progression (e.g. PKC, Erk, and MLC).

Impact on the PKC signaling field

While dissecting the molecular mechanism by which EpCAM tames PKC activity, we discovered a potential new mode of PKC regulation at the membrane. Based on our model, EpCAM interacts with membrane-bound fully active PKC molecules that have their catalytic sites exposed. Because full activation and membrane recruitment of PKCs require membrane bound lipid co-activators/anchors, it is possible that EpCAM interacts with and inhibits PKCs in membrane domains enriched in lipid cofactors required for PKC activation. If it is the case, the distribution of PKCs might affect EpCAM localization by recruiting the latter to specific sites on the plasma membrane. Consistent with this idea, EpCAM accumulation has been detected in glycolipid-enriched membrane microdomains (Schmidt et al., 2004); whether active PKCs are also enriched in such domains and whether they are responsible for EpCAM recruitment remain to be established. Another interesting point to address in the future is to determine what becomes of PKC after its inhibitory interaction with EpTail is over. Presumably, the PS-mimicking nature of the EpTail-PKC catalytic domain interaction is not expected to result in de-activation of the kinase per se, which could therefore be released in its active "membrane-bound" form. However, it is possible that the duration of the interaction is long

enough to allow the loss of PKC lipid anchors or the recruitment of inhibitory PKC factors (e.g. sphingosines), which would result in the release of inactivated PKCs. This latter possibility is consistent with the observed massive repression that EpCAM seems to have on PKC activity in *Xenopus* and Caco-2 cells (Chapters II and III).

The identification of other PS-mimicking CAM molecules that can potentially regulate PKC activity opens up a very interesting avenue to explore. First it will be crucial to determine whether these candidates can bind and inhibit PKC activity *in vivo,* and whether this potential inhibition is physiologically relevant. Then, it would be interesting to ask whether these candidates are overexpressed in cancers, as seen with EpCAM. Interestingly, data from other studies have already implicated EphA4 and ICAM in cancer progression: EphA4 is typically known as a receptor tyrosine kinase that mediates repulsion upon binding its ephrin ligand in axon growth cones and embryonic boundaries (Bisson et al., 2007). It is expressed in prostate and colon cancers, and is up-regulated in lung carcinomas (Surawska et al., 2004). Furthermore, similar to EpCAM, in invasive breast carcinomas, Eph receptors are reliable molecular markers used for diagnostic and prognostic purposes (Fox and Kandpal, 2004). Likewise, the expression of ICAM, an endothelial and leukocyte-associated protein known for stabilizing cell-cell interactions and facilitating leukocyte endothelial transmigration, determines the metastatic potential of cancers of endothelial origin (Roland et al., 2007).

In conclusion, the body of work presented in this thesis furthers our understanding of EpCAM biology and proposes a new mechanism of PKC regulation, which will be important to fully characterize. The discovery of PKC regulation by EpCAM presents new avenues to explore that should help elucidate the exact impact of EpCAM levels on cancer progression, and design new therapeutic strategies.

References

Bernadskaya, Y.Y., Wallace, A., Nguyen, J., Mohler, W.A., and Soto, M.C. (2012). UNC-40/DCC, SAX-3/Robo, and VAB-1/Eph Polarize F-Actin during Embryonic Morphogenesis by Regulating the WAVE/SCAR Actin Nucleation Complex. PLoS genetics *8*, e1002863.

Bisson, N., Poitras, L., Mikryukov, A., Tremblay, M., and Moss, T. (2007). EphA4 signaling regulates blastomere adhesion in the Xenopus embryo by recruiting Pak1 to suppress Cdc42 function. Molecular biology of the cell *18*, 1030-1043.

Cerda, S.R., Mustafi, R., Little, H., Cohen, G., Khare, S., Moore, C., Majumder, P., and Bissonnette, M. (2006). Protein kinase C delta inhibits Caco-2 cell proliferation by selective changes in cell cycle and cell death regulators. Oncogene *25*, 3123-3138.

Chen, X., and Gumbiner, B.M. (2006). Paraxial protocadherin mediates cell sorting and tissue morphogenesis by regulating C-cadherin adhesion activity. The Journal of cell biology *174*, 301-313.

Chen, X., Koh, E., Yoder, M., and Gumbiner, B.M. (2009). A protocadherin-cadherin-FLRT3 complex controls cell adhesion and morphogenesis. PloS one *4*, e8411.

Dalpe, G., Brown, L., and Culotti, J.G. (2005). Vulva morphogenesis involves attraction of plexin 1-expressing primordial vulva cells to semaphorin 1a sequentially expressed at the vulva midline. Development *132*, 1387-1400.

Denzel, S., Maetzel, D., Mack, B., Eggert, C., Barr, G., and Gires, O. (2009). Initial activation of EpCAM cleavage via cell-to-cell contact. BMC cancer *9*, 402.

Fanning, A.S., Jameson, B.J., Jesaitis, L.A., and Anderson, J.M. (1998). The tight junction protein ZO-1 establishes a link between the transmembrane protein occludin and the actin cytoskeleton. The Journal of biological chemistry *273*, 29745-29753.

Fox, B.P., and Kandpal, R.P. (2004). Invasiveness of breast carcinoma cells and transcript profile: Eph receptors and ephrin ligands as molecular markers of potential diagnostic and prognostic application. Biochemical and biophysical research communications *318*, 882-892.

Gaiser, M.R., Lammermann, T., Feng, X., Igyarto, B.Z., Kaplan, D.H., Tessarollo, L., Germain, R.N., and Udey, M.C. (2012). Cancer-associated epithelial cell adhesion molecule (EpCAM; CD326) enables epidermal Langerhans cell motility and migration in vivo. Proceedings of the National Academy of Sciences of the United States of America *109*, E889-897.

Ladwein, M., Pape, U.F., Schmidt, D.S., Schnolzer, M., Fiedler, S., Langbein, L., Franke, W.W., Moldenhauer, G., and Zoller, M. (2005). The cell-cell adhesion molecule EpCAM interacts directly with the tight junction protein claudin-7. Experimental cell research *309*, 345-357.

Lei, Z., Maeda, T., Tamura, A., Nakamura, T., Yamazaki, Y., Shiratori, H., Yashiro, K., Tsukita, S., and Hamada, H. (2012). EpCAM contributes to formation of functional tight junction in the intestinal epithelium by recruiting claudin proteins. Developmental biology.

Litvinov, S.V., Balzar, M., Winter, M.J., Bakker, H.A., Briaire-de Bruijn, I.H., Prins, F., Fleuren, G.J., and Warnaar, S.O. (1997). Epithelial cell adhesion molecule (Ep-CAM) modulates cell-cell interactions mediated by classic cadherins. The Journal of cell biology *139*, 1337-1348.

Litvinov, S.V., Velders, M.P., Bakker, H.A., Fleuren, G.J., and Warnaar, S.O. (1994). Ep-CAM: a human epithelial antigen is a homophilic cell-cell adhesion molecule. The Journal of cell biology *125*, 437-446.

Maetzel, D., Denzel, S., Mack, B., Canis, M., Went, P., Benk, M., Kieu, C., Papior, P., Baeuerle, P.A., Munz, M.*, et al.* (2009). Nuclear signalling by tumour-associated antigen EpCAM. Nature cell biology *11*, 162-171.

Medina, A., Swain, R.K., Kuerner, K.M., and Steinbeisser, H. (2004). Xenopus paraxial protocadherin has signaling functions and is involved in tissue separation. The EMBO journal *23*, 3249-3258.

Osta, W.A., Chen, Y., Mikhitarian, K., Mitas, M., Salem, M., Hannun, Y.A., Cole, D.J., and Gillanders, W.E. (2004). EpCAM is overexpressed in breast cancer and is a potential target for breast cancer gene therapy. Cancer research *64*, 5818-5824.

Roland, C.L., Harken, A.H., Sarr, M.G., and Barnett, C.C., Jr. (2007). ICAM-1 expression determines malignant potential of cancer. Surgery *141*, 705-707.

Schmidt, D.S., Klingbeil, P., Schnolzer, M., and Zoller, M. (2004). CD44 variant isoforms associate with tetraspanins and EpCAM. Experimental cell research *297*, 329-347.

Shen, L., and Turner, J.R. (2005). Actin depolymerization disrupts tight junctions via caveolae-mediated endocytosis. Molecular biology of the cell *16*, 3919-3936.

Slanchev, K., Carney, T.J., Stemmler, M.P., Koschorz, B., Amsterdam, A., Schwarz, H., and Hammerschmidt, M. (2009). The epithelial cell adhesion molecule EpCAM is required for epithelial morphogenesis and integrity during zebrafish epiboly and skin development. PLoS genetics *5*, e1000563.

Surawska, H., Ma, P.C., and Salgia, R. (2004). The role of ephrins and Eph receptors in cancer. Cytokine & growth factor reviews *15*, 419-433.

Yue, T., Tian, A., and Jiang, J. (2012). The cell adhesion molecule echinoid functions as a tumor suppressor and upstream regulator of the Hippo signaling pathway. Developmental cell *22*, 255-267.